

**EFFECTS OF SEASONAL WEATHERING ON DEWATERING OF  
POLYMER AMENDED TAILINGS**

by

Umme Salma Rima

A thesis submitted in partial fulfillment of the requirements for the degree of

Doctor of Philosophy

in

Geoenvironmental Engineering

Department of Civil and Environmental Engineering  
University of Alberta

© Umme Salma Rima, 2022

## ABSTRACT

This study investigated the mechanisms driving the dewatering and strength behaviour of polymer amended treated (centrifuged and in-line thickened tailings/ILTT) deep tailings deposits undergoing seasonal weathering dominated by a) multiple freeze-thaw cycles and b) alternating freeze-thaw and drying-wetting cycles. A one-dimensional closed system freeze-thaw test was developed in the laboratory to simulate freeze-thaw cycles at three different freezing temperature gradients. The alternate/single evaporation and subsequent rainfall infiltration were simulated through multiple/single drying-wetting cycles to depict the atmospheric drying-wetting. The laboratory testing results of ILTT samples were further compared to the ILTT field deposit, while a coupled numerical approach was developed to simulate the laboratory testing performed on the centrifuged tailings samples. For coupled numerical simulation, the components of seasonal weathering (freeze-thaw, consolidation and evaporation) were coupled by incorporating freeze-thaw cycles into FSConsol consolidation model and drying-wetting cycles into UNSATCON model.

The laboratory results suggested that the surface of the treated tailings samples subjected to five freeze-thaw cycles resulted in an order of magnitude higher shear strength compared to their initial values. When evaporation/drying cycles were incorporated, the drying phase further improved the surficial strength by an order of magnitude higher than the strength obtained from multiple freeze-thaw cycles. The laboratory results also indicated that freezing temperature gradient, number of seasonal cycles and physico-chemical interactions among the tailings particles had the largest effect on dewatering and subsequent strength improvement. Lower freezing temperature gradient overall contributed to higher dewatering and subsequent strength gain. An increase in number of

seasonal cycles were also found to increase dewatering and strength performance. However, after a specified number of seasonal cycles, all these tailings samples exhibited a threshold strength when moisture content approached to the plastic limit. These threshold values were confirmed through the cessation of rainfall effects on strength. Further, when the effects of physico-chemical interactions between two different treated tailings were compared under similar boundary conditions, the difference in treatment process, solids mineralogy and pore water chemistry were found to affect the dewatering and strength behaviour.

Given the similar ranges of thermal boundary conditions in the field, the findings of these small-scale laboratory tests were capable to predict the field dewatering and strength behaviour, that can be utilized for design scenarios of the future field deposits incorporating seasonal weathering. Laboratory testing results were also able to validate the proposed coupled modeling approach. The coupled modeling reasonably predicted the water content profiles within a difference of 0-12%, as compared to the laboratory profiles. Overall, the findings of this thesis demonstrated that seasonal weathering has a potential to transform the slurry like surface into a desiccated one, regardless of the variations in initial water content, grain size distribution, solids mineralogy and pore water chemistry. Therefore, ensuring good surface drainage in the field is paramount to utilize the most benefits of this seasonal weathering process.

## ACKNOWLEDGEMENT

The opportunity to execute and complete this study would not have been possible without the guidance, continual support and encouragement of my supervisor, Dr. Nicholas Beier. Thank you for the patience, kindness and enthusiasm for research; some great qualities that I finally started learning from you. Thank you, Dr. Ward Wilson for always appreciating me, not always for the research, but for how I am as an individual. A great thanks to both of you for your understanding when I was going through a personal crisis in my life.

I would also like to thank Christine Hereygers and Dr. Louis Kabwe for their technical help with the laboratory component of this research project. A special thanks to Louis Kabwe who always cheered me up, provided constant encouragement and taught me how to say “Superb” in difficult times to boost up confidence. I cannot thank Dr. Ahlam Abdalnabi enough for her constant assistance with insight and advice related to research work and paper writing. Thank you, Vivian Giang and Jennifer Stogowski for the continuous support with scholarships assistance and all sorts of administrative works, which made my journey at the University of Alberta smoother.

I would also to thank the Natural Sciences and Engineering Research Council of Canada (NSERC), Canada’s Oil Sands Innovation Alliance (COSIA), Alberta Innovates Energy and Environmental Solutions (AIEES), and the University of Alberta for financial support, which made this research possible. Thankyou Syncrude Canada for access to reports and field data.

Shuvo, Shovon, Haley, Hilary and Sebastian, words will fall short to express my gratitude towards each of you. Edmonton will always be a special place because of you guys whom I met here. Thank you for always being there for me when I need someone to listen, someone to laugh with, someone to care or someone to lean on. Thank you should be an understatement for all of you.

I would not have made it this point in my career without the love of my parents. To my mother, father and sister Toma: Thank you for always supporting me through your prayers and love. Thank

you for all your sacrifices to provide me with a better education and making me a mentally strong and independent girl.

## PREFACE

This dissertation has been written in manuscript style with an Introduction (along with brief literature review covered in this section) preceding a total of five manuscripts. Four of the manuscripts have either been accepted or published. The other one is intended for submission to a peer-reviewed journal. Typically, each manuscript follows the sequences of an abstract, introduction, background, material and methodology, results, discussions, acknowledgements followed by references. Since every journal has its own format and guidelines for the manuscripts, the general guidelines for the thesis formatting specified by the Faculty of Graduate Studies were adopted here to ensure the consistency of the thesis. The manuscripts in this thesis are listed as follows along with the contributions from each of the authors for the manuscripts:

1. Umme Salma Rima and Nicholas Beier. 2021. Effects of multiple freeze-thaw cycles on oil sands tailings behaviour. *Cold Regions Science and Technology*, 192:103404. <https://doi.org/10.1016/j.coldregions.2021.103404>.

### **Authors Contributions:**

**Umme Salma Rima:** Conceptualization, methodology, validation, formal analysis, investigation, resources, data curation, writing-original draft and editing, and visualization

**Nicholas Beier:** Validation, resources, writing-review and editing, supervision, project administration and funding acquisition

2. Umme Salma Rima and Nicholas Beier. 2021. Effects of seasonal weathering on dewatering and strength of an oil sands tailings deposit. *Canadian Geotechnical Journal*, In press. <https://doi.org/10.1139/cgj-2020-0533>.

### **Authors Contributions:**

**Umme Salma Rima:** Conceptualization, methodology, validation, formal analysis, investigation, resources, data curation, writing-original draft and editing, and visualization

**Nicholas Beier:** Validation, resources, writing-review and editing, supervision, project administration and funding acquisition

3. Umme Salma Rima, Nicholas Beier and Adedeji Dunmola. Seasonal Weathering of Oil Sands Tailings Deposit: Comparison of Field and Laboratory Data. Prepared for submitting to a peer-reviewed journal

**Authors Contributions:**

**Umme Salma Rima:** Conceptualization, methodology, validation, formal analysis, investigation, resources, data curation, writing-original draft and editing, and visualization

**Nicholas Beier:** Validation, resources, writing-review and editing, supervision, project administration and funding acquisition

**Adedeji Dunmola:** Field data resources, funding resources, writing-review and editing, and validation

4. Umme Salma Rima and Nicholas Beier. Natural weathering as a surface crusting tool for tailings management. Accepted for the *20<sup>th</sup> International Conference on Soil Mechanics and Geotechnical Engineering*.

**Authors Contributions:**

**Umme Salma Rima:** Conceptualization, methodology, validation, formal analysis, investigation, resources, data curation, writing-original draft and editing, and visualization

**Nicholas Beier:** Validation, resources, writing-review and editing, supervision, project administration and funding acquisition

5. Umme Salma Rima, Nicholas Beier and Ahlam Abdulnabi. 2021. Modeling the effects of seasonal weathering on centrifuged oil sands tailings. *Processes*, 9 (11): 1906. <https://doi.org/10.3390/pr9111906>.

**Authors Contributions:**

**Umme Salma Rima:** Conceptualization, methodology, validation, formal analysis, investigation, resources, data curation, writing-original draft and editing, and visualization

**Nicholas Beier:** Validation, resources, writing-review and editing, supervision, project administration and funding acquisition

**Ahlam Abdalnabi:** Methodology, and writing-review and editing

The above five manuscripts are next followed by Summaries, Conclusion and Recommendation. A comprehensive list of references including the references used at each of the manuscripts is provided at the end, followed by Appendices.

# Table of Contents

<b>1</b>	<b>INTRODUCTION .....</b>	<b>1</b>
1.1	Problem Statement .....	1
1.2	Objectives.....	3
1.3	Scopes of the Research.....	4
1.4	Background .....	5
1.4.1	Oil Sands Overview .....	5
1.4.2	Tailings Management.....	6
1.4.3	Tailings Dewatering Technologies .....	7
1.4.4	Environmental Dewatering .....	9
1.4.5	Consolidation .....	9
1.4.6	Freeze-Thaw Mechanism.....	10
1.4.7	Factors affecting Freeze-Thaw Mechanism.....	13
1.4.8	Atmospheric Drying/Evaporation.....	20
1.4.9	Factors affecting Evaporation.....	20
1.4.10	Previous Works on Freeze-Thaw Dewatering .....	23
1.4.11	Previous Works on Evaporation/ Drying for Tailings .....	25
1.5	Thesis Outline .....	27
<b>2</b>	<b>EFFECTS OF MULTIPLE FREEZE-THAW CYCLES ON OIL SANDS TAILINGS BEHAVIOUR.....</b>	<b>29</b>
	Abstract .....	29
2.1	Introduction .....	29
2.2	Background .....	32
2.3	Laboratory Experiments.....	35

2.3.1	Test Materials.....	35
2.3.2	Test Equipment and Methodology.....	35
2.3.2.1	Characterization Testing .....	35
2.3.2.2	Cyclic Freeze-Thaw Test .....	36
2.3.2.3	Atmospheric Drying and Wetting Test .....	39
2.3.2.4	Sectional Analysis.....	39
2.4	Results .....	40
2.4.1	Characterization of Tailings.....	40
2.4.2	Cyclic Freeze-Thaw Test Results .....	42
2.4.3	Atmospheric Drying-Wetting Test Results.....	45
2.4.4	Sectional Analysis.....	49
2.5	Discussion .....	51
2.6	Conclusion.....	57
	Acknowledgements .....	58
	References .....	58
<b>3</b>	<b>EFFECTS OF SEASONAL WEATHERING ON DEWATERING AND STRENGTH OF AN OIL SANDS TAILINGS DEPOSIT.....</b>	<b>63</b>
	Abstract .....	63
3.1	Introduction .....	63
3.2	Background .....	65
3.3	Laboratory Experiments.....	68
3.3.1	Test Materials.....	68
3.3.2	Test Equipment and Methodology.....	69
3.3.2.1	Geotechnical Index Properties Tests .....	69
3.3.2.2	Geotechnical Index Properties Tests .....	69

3.3.2.3	Pore Water Chemistry Tests.....	70
3.3.2.4	Cyclic Freeze-Thaw Tests.....	70
3.3.2.5	Cyclic Drying-Wetting Tests .....	73
3.3.2.6	Sectional Analysis.....	73
3.4	Results .....	73
3.4.1	Characterization of Tailings.....	73
3.4.2	Dewatering Performance .....	75
3.5	Discussion .....	85
3.5.1	Effects of Initial Moisture Content .....	85
3.5.2	Effects of Temperature Gradient .....	85
3.5.3	Effects of Number of Seasonal Cycles .....	86
3.5.4	Effects of Rainfall/Wetting.....	87
3.5.5	Effects of Physico-chemical Properties .....	88
3.6	Limitations .....	88
3.7	Conclusion.....	89
	Acknowledgements.....	90
	References .....	90
<b>4</b>	<b>SEASONAL WEATHERING OF OIL SANDS TAILINGS DEPOSITS: COMPARISON OF FIELD AND LABORATORY DATA .....</b>	<b>96</b>
	Abstract .....	96
4.1	Introduction .....	96
4.2	Background .....	98
4.3	Laboratory Investigation .....	100
4.4	Results and Discussion.....	102
4.5	Conclusion.....	111

Acknowledgements .....	111
References .....	112
<b>5 NATURAL WEATHERING AS A SURFACE CRUSTING TOOL FOR TAILINGS MANAGEMENT .....</b>	<b>116</b>
Abstract .....	116
5.1 Introduction .....	116
5.2 Effects of Seasonal Weathering on Different Tailings Management Strategies .....	118
5.2.1 Oil Sands Tailings.....	118
5.2.2 Coal Tailings.....	119
5.2.3 Thickened Gold Tailings.....	120
5.2.4 Metal Mine Tailings.....	120
5.3 Materials and Methods.....	121
5.4 Results .....	121
5.5 Discussion .....	125
5.6 Conclusions .....	128
Acknowledgements .....	129
References .....	129
<b>6 MODELING THE EFFECTS OF SEASONAL WEATHERING ON CENTRIFUGED OIL SANDS TAILINGS .....</b>	<b>134</b>
Abstract .....	134
6.1 Introduction .....	134
6.2 Tailings Material and Characterization.....	137
6.3 Laboratory Setup .....	138
6.4 Coupled Modeling.....	140
6.4.1 Modeling Analysis Development .....	140
6.4.2 Numerical Model Parameters .....	144

6.5	Modeling Results.....	146
6.5.1	Numerical Simulation of First Phase Testing .....	146
6.5.2	Numerical Simulation of Second Phase Testing.....	147
6.5.3	Comparison between the Model and Laboratory Results.....	150
6.6	Discussion .....	156
6.7	Conclusion.....	159
	Acknowledgements .....	160
	References .....	160
<b>7</b>	<b>SUMMARY, CONCLUSIONS AND RECOMMENDATIONS.....</b>	<b>163</b>
7.1	Summary .....	163
7.1.1	Effects of Multiple Freeze-Thaw Cycles on Oil Sands Tailings Behaviour.....	163
7.1.2	Effects of Seasonal Weathering on Dewatering and Strength of Oil Sands Tailings Deposit.....	165
7.1.3	Seasonal Weathering of Oil Sands Tailings Deposit: Comparison of Field and Laboratory Data.....	167
7.1.4	Natural Weathering as a Surface Crusting Tool for Tailings Management.....	168
7.1.5	Modeling the Effects of Seasonal Weathering on Centrifuged Oil Sands Tailings.....	169
7.2	Conclusions .....	173
7.3	Recommendations .....	176
	<b>References.....</b>	<b>177</b>
	<b>Appendix A: Freeze-Thaw Tests Setup.....</b>	<b>189</b>
	<b>Appendix B: Grain Size Distribution (GSD).....</b>	<b>190</b>
	<b>Appendix C: Temperature Plot.....</b>	<b>191</b>
	<b>Appendix D: Thaw-Strain Diagram.....</b>	<b>213</b>
	<b>Appendix E: AE/PE Plot .....</b>	<b>214</b>

<b>Appendix F: Precisions of the Laboratory Measurements .....</b>	<b>227</b>
<b>Appendix G: Numerical Simulation Plots .....</b>	<b>228</b>

## List of Tables

Table 2.1: Summary of the laboratory testing information.....	37
Table 2.2: Summary of the index properties of the tailings.....	40
Table 2.3: Summary of the solids mineralogy of the tailings.....	41
Table 2.4: Summary of pore water chemistry results.....	42
Table 2.5: Comparisons between the final measured and calculated water content.....	49
Table 3.1: Summary of key properties of tailings.....	74
Table 3.2: Comparison between calculated and measured moisture content values at the near surface.....	82
Table 4.1: Summary of index properties of tailings.....	103
Table 4. 2: Summary of the solids mineralogy of the tailings.....	104
Table 4.3: Summary of pore water chemistry results.....	104
Table 5.1: Summary of key properties of tailings.....	122
Table 5.2: Sources of index properties and shear strength data.....	125
Table 6.1: Geotechnical properties of the centrifuged tailings.....	138
Table 6.2: Boundary conditions and summary of parameters for the FSConsol models.....	144
Table 6.3: Boundary conditions and summary of parameters for the UNSATCON models.....	145

## List of Figures

Figure 1.1: Relationship between tailings solids content by volume versus mass (after OSTC and COSIA, 2012).....	8
Figure 1.2: Effects of Crust Formation on the drainage conditions during freezing (Reproduced and modified after Andersland and Ladanyi, 2004).....	12
Figure 1.3: The change in final solids content in relation to initial solids content and freeze thaw cycles a) for the whole range of $s$ and b) for $s > 40\%$ (modified after Johnson et al., 1993).....	13
Figure 1.4: Development of ice lenses at different depth (modified after Konrad and Morgenstern, 1980).....	17
Figure 1.5: Temporal variation in relative evaporation from fresh water and saline tailings (after Newson and Fahey, 2003).....	21
Figure 2.1: Schematic diagram of the freeze- thaw test setup.....	38
Figure 2.2: Estimated water content (%) versus number of freeze-thaw cycles.....	43
Figure 2.3: Measured shear strength versus number of freeze–thaw cycles.....	44
Figure 2.4: Measured electrical conductivity vs the number of freeze-thaw cycles (measured at a depth of 15 mm from the surface).....	45
Figure 2.5: Water content and shear strength progression of the centrifuged tailings sample over time at a temperature gradient of $0.083^{\circ}\text{C}/\text{mm}$ .....	46
Figure 2.6: Water content and shear strength progression of the centrifuge tailings sample over time at a temperature gradient of $0.056^{\circ}\text{C}/\text{mm}$ .....	47
Figure 2.7: Water content and shear strength progression of the centrifuged tailings sample over time at a temperature gradient of $0.028^{\circ}\text{C}/\text{mm}$ .....	47
Figure 2.8: Water content and shear strength progression of the ILTT sample over time at a temperature gradient of $0.028^{\circ}\text{C}/\text{mm}$ .....	48
Figure 2.9: Photographs of drying-wetting test; 2.9a (left) shrinkage and cracking observed after drying test; and 2.9b (right) over-consolidated peds at the surface after wetting test.....	48
Figure 2.10: Measured water content profile at the end of the test.....	50
Figure 2.11: Measured electrical conductivity profile at the end of the test.....	50
Figure 2.12: Undrained shear strength vs liquidity index of the two investigated tailings.....	56
Figure 3.1: Schematic diagram of the freeze- thaw test setup.....	72

Figure 3.2: Estimated moisture content (%) versus number of seasonal cycles.....	76
Figure 3.3: Estimated moisture content and measured shear strength progression of centrifuged tailings over time at a temperature gradient of 0.083°C/mm.....	77
Figure 3.4: Estimated moisture content and measured shear strength progression of centrifuged tailings over time at a temperature gradient of 0.056°C/mm.....	78
Figure 3.5: Estimated moisture content and measured shear strength progression of centrifuged tailings over time at a temperature gradient of 0.028°C/mm.....	79
Figure 3.6: Estimated moisture content and measured shear strength progression of in-line thickened tailings sample over time at a temperature gradient of 0.028°C/mm.....	80
Figure 3.7: Crust layer formed at the surface of the centrifuged tailings subjected to a temperature gradient of 0.028°C/mm.....	80
Figure 3.8: The change in shear strength reduction (%) due to rainfall/ wetting event after each cycle.....	81
Figure 3.9: Measured moisture content (%) profile at the end of the test.....	82
Figure 3.10: Relationship between undrained shear strength and gravimetric moisture content (%).....	83
Figure 3.11: Undrained shear strength of treated tailings as a function of liquidity index.....	84
Figure 4.1: Comparison between the field and laboratory moisture content values after each cycle.....	105
Figure 4.2: Comparison between the field and laboratory moisture content profiles after seasonal cycles.....	107
Figure 4.3: Measured undrained shear strength values of field and laboratory samples versus the number of seasonal cycles (right Y axis-phase 2 test lab data, left Y axis-rest of the other data).....	108
Figure 4.4: Measured electrical conductivity values of field and laboratory samples versus the number of seasonal cycles.....	109
Figure 5.1: Effects of freeze-thaw cycles on the undrained shear strength of fine coal and oil sands tailings.....	123
Figure 5.2: The effects of evaporation/drying on treated oil sands tailings.....	123
Figure 5.3: The effects of natural weathering on the surficial strength of different tailings deposits around the world.....	124

Figure 6.1: Simplified diagram of the seasonal weathering cycles.....	137
Figure 6.2: Schematic diagram of the freeze-thaw test setup (After Rima and Beier, 2021a and 2021b).....	139
Figure 6.3: Flowchart diagram of coupling analysis.....	141
Figure 6.4: First and second phase laboratory testing and numerical simulation sequences.....	143
Figure 6.5: Water content profile simulation of centrifuged tailings at a temperature gradient of 0.083 °C /mm.....	146
Figure 6.6: Water content profile simulation of centrifuged tailings at a temperature gradient of 0.028 °C /mm.....	147
Figure 6.7: Water content profile of centrifuged tailings at a temperature gradient of 0.083 °C /mm.....	149
Figure 6.8: Water content profile of centrifuged tailings at a temperature gradient of 0.028 °C /mm.....	150
Figure 6.9: First phase testing comparisons: water content values per seasonal cycle for the centrifuged tailings samples under a temperature gradient of (a) 0.083°C /mm and (b) 0.028°C /mm.....	151
Figure 6.10: Second phase testing comparisons: water content values per seasonal cycle for the centrifuged tailings samples under a temperature gradient of (a) 0.083°C /mm and (b) 0.028°C /mm.....	152
Figure 6.11: Laboratory versus model water content profiles of centrifuged tailings at the end of the test under a temperature gradient of (a) 0.083°C /mm and (b) 0.028°C /mm.....	154
Figure 6.12: Liquidity index profiles of centrifuged tailings from coupled analysis.....	156
Figure 10.1: First phase testing results- correlation between laboratory and model predicted water content values.....	171
Figure 10.2: Second phase testing results- correlation between laboratory and model predicted water content values.....	172

## List of Symbols and Acronyms

AE	Actual Evaporation
AER	Alberta Energy Regulator
AFD	Atmospheric Fines Drying
CaO	Calcium Oxide (Quick-Lime)
CEC	Cation Exchange Capacity
CNRL	Canadian Natural Resources Ltd.
CNUL	Canadian Natural Upgrading Ltd.
COSIA	Canada's Oil Sands Innovation Alliance
CT	Composite Tailings
EC	Electrical Conductivity
FFT	Fluid Fine Tailings
GSD	Grain Size Distribution
H <sub>2</sub> SO <sub>4</sub>	Sulfuric Acid
ILTT	In-Line Thickened Tailings
LI	Liquidity Index
MBI	Methylene Blue Index
MFT	Mature Fine Tailings
NaOH	Sodium Hydroxide
NST	Non-Segregating Tailings
OSTC	Oil Sands Tailings Consortium
PE	Potential Evaporation
SAR	Sodium Adsorption Ratio
SFR	Sands to Fines Ratio
TFT	Thin Fine Tailings
TMF	Tailings Management Framework
TRO	Tailings Reduction Operation
TT	Thickened Tailings
XRD	X-ray diffraction

$e_o$	Initial Void ratio
$e$	Void Ratio
$\Delta e$	Change in Void Ratio
$G_s$	Specific Gravity
$H$	Total Frozen Height
$\Delta H$	Change in height
$k$	Permeability
$s$	Solids Content
$w$	Water Content
$w_l$	Liquid Limit
$w_p$	Plastic Limit
$\rho$	Bulk Density
$\rho_D$	Dry Density
$\varepsilon$	Thaw Strain
$\sigma'$	Effective Stress

# 1 INTRODUCTION

## 1.1 Problem Statement

The Athabasca oil sand deposits in northern Alberta, Canada, are considered to be the fourth largest proven reserve in the world that contain approximately 177 billion barrels of economically recovered crude oil (Government of Alberta, 2021a). In order to produce oil, bitumen extraction process generates approximately 0.25 m<sup>3</sup> of a fluid waste by product, known as tailings, per every barrel of recovered bitumen (Beier et al., 2016). Tailings, a mixture of sand, fines (clays and silts), residual bitumen and process affected water are disposed of by overboarding into the containment ponds, where the mixtures of coarse streams (primarily sand) form sand beaches near the deposition outlet and an aqueous slurry of fines and residual bitumen accumulates in the center termed as thin fine tailings (TFT) (Jeeravipoolvarn, 2010, OSTC and COSIA, 2012). When allowed to settle under quiescent conditions in the containment ponds, TFT forms a slurry with a solids content (mass of solids divided by the total mass of tailings including bitumen) of around 30-40% by mass referred to as mature fine tailings (MFT) (Spence et al., 2015). The collective term of TFT and MFT is known as fluid fine tailings (FFT) (Spence et al., 2015). Dewatering of fluid fine tailings, for recycling the released water and reducing the environmental footprint, is very slow as these materials are highly dispersed, resistant to consolidation and can remain in a soft, fluid state for decades (AER, 2020). Consequently, the inventory of tailings being stored in the pond has been steadily increasing over time and at present, the total volume of FFT stored in the pond already exceeded 1.3 billion m<sup>3</sup>(AER, 2020).

The continued accumulation of FFT led the Alberta Energy Regulator (AER) to introduce a new regulation under the Tailings Management Framework (TMF), Directive 085 which states that the land use must be returned to Albertans with sustainable ecosystem and minimal environmental effects after reclamation (AER, 2020). The TMF specifies site specific threshold for FFT volumes over the lifespan of an oil sands mine and are subjected to change upon further review of FFT volumes (AER, 2020). In addition to this, TMF requires to improve the existing reclamation strategy by ensuring that the FFT are ready to reclaim within 10 years of the end-of-mine life for

a given oil sands mining project (AER, 2020). Therefore, it is paramount to improve existing reclamation strategies in order to comply with the regulation. Hence, an efficient dewatering treatment technology is required to strengthen the tailings deposit so they can be reclaimed back to an acceptable condition. In order to meet the regulatory and closure commitments and to achieve the site-specific thresholds for FFT volumes implemented at each mine sites, different mechanical, physical and chemical methods are currently being employed including mechanical centrifuge, thickener, in-line flocculation, and chemical amendments. The resulting treated tailings with improved properties (lower moisture content and higher shear strength) from these treatment technologies are continuously deposited into on-site containment facilities/ in pit deposition areas, thus forming deep deposits (Cossey et al.,2021). Deep fine deposits follow single layered deep stacking depositional approaches where the deposited treated tailings are still considered to be soft, weak and non-trafficable, relying predominantly on self-weight consolidation for subsequent dewatering and development of strength (OSTC and COSIA, 2012). The strength inadequacy of the deep deposit surface prior to the placement of capping/soil cover necessitates an additional step to facilitate trafficable surface in order to meet the closure and regulatory requirements (OSTC and COSIA, 2012).

The strength of the deep fines deposit is known to increase over time due to the dissipation of pore pressures. Since self-weight consolidation is the predominant mechanism of dewatering, the upper few metres of the deep fines deposit would still remain soft and saturated until a surface crust can be developed through surface weathering (evaporative drying and freeze-thaw mechanism). Therefore, natural weathering effects due to freeze-thaw and evaporation can be considered a potential solution for the development of surface crust on a deep deposit. Since freeze thaw occurs naturally on a vast scale in Western Canada, this process along with evaporation is ideally suited to the geographical location of Northern Alberta as an alternative approach to reduce the reclamation cost and to stabilize the tailings surface area. Soft fine-grained tailings surface exposed to cyclic freeze-thaw actions works through the redistribution of moisture and solute in the tailings deposit, that results in the changes of macro and microstructure of the tailings and subsequent improved dewatering upon thaw. When evaporative drying is incorporated, the treated thawed tailings can further promote a significant amount of dewatering through cracking and desiccation, in turn, can develop desiccated surface crust (Pham and Segó, 2014). The formation of surface

crust may facilitate certain capping technologies or reduce the numbers of geotextiles, even if a free-standing trafficable deposit is not developed fully (OSTC and COSIA, 2012).

Overall, in an effort to provide a geotechnically stable landscape in a timely manner for colder climate like Western Canada, the components of seasonal weathering such as freeze-thaw and drying have the potential to further improve the dewatering rate of treated tailings. The present study aimed to evaluate the effect of natural/seasonal weathering conditions (repeated freeze-thaw cycles, summer drying and precipitation) on the dewatering and strength performance of existing treated tailings and fines enriched deep deposits waiting for reclamation. This research aimed to see whether the multiple cyclic freeze- thaw-atmospheric drying process is effective in forming a surface crust capable of gaining sufficient strength. Depending on the extent of stabilization and attained strength, it could be possible for equipment to start placing reclamation covers. This may potentially reduce the required amount of geosynthetics and result in savings of the reclamation cost.

## **1.2 Objectives**

The primary objective of this thesis is to evaluate the effect of the natural conditions (repeated freeze thaw cycles, summer drying and precipitation) on the strength of chemically amended deep tailings deposits following completion of deposition. The specific objectives of the research program are as follows:

1. To investigate the mechanisms driving the dewatering and strength behaviour of two types of treated deep tailings deposits (centrifuged tailings and in-line thickened tailings (ILTT)) undergoing seasonal weathering dominated by multiple freeze-thaw cycles using controlled laboratory experiments.
2. To investigate the mechanisms driving the dewatering and strength behaviour of two types of treated deep tailings deposits (centrifuge and ILTT) undergoing seasonal weathering through alternating freeze-thaw and drying-wetting cycles using controlled laboratory experiments.

3. To compare the near surface dewatering and strength behaviour of the field deposit (ILTT deposit) with laboratory experiments to evaluate whether the laboratory testing methodology can replicate the field behaviour and to further investigate into field behavior and mechanism driving the dewatering from seasonal weathering using controlled laboratory experimental conditions.
4. To evaluate the numerical approaches in order to simulate the laboratory results that investigated the effects of seasonal weathering on centrifuged tailings.

### **1.3 Scopes of the Research**

In order to accomplish the objectives, the following works were performed:

- Tailing characterization tests including Atterberg limits, specific gravity, grain size distribution (hydrometer tests), XRD (X-ray diffraction) analysis, Methylene Blue Index (MBI), and water chemistry.
- Simulation of seasonal weathering on two types of tailings (one of these belongs to commercially operated centrifuge technology and another one belongs to a pilot scale demonstration of in-line thickening process (ILTT)) in a small-scale freezing cell (diameter of 100mm and height of 220mm) laboratory setup under three different temperature gradients to carry out two different combinations of multiple freeze-thaw-drying-wetting cycle (one combination involves carrying out five freeze-thaw cycle tests followed by a single drying-wetting cycle and the other one involves alternate drying-wetting cycle between each freeze-thaw cycles to depict the combined seasonal weathering effects).
- Computation of dewatering properties (thaw strain, solids content/moisture content) through mass loss/gain on a daily basis and measurement of undrained shear strength near surface using benchtop vane shear apparatus upon completion of each cycle in order to investigate the dewatering and strength progress with multiple cycles over time.

- Measurement of physico-chemical properties at the near surface through the measurement of electrical conductivity (EC) at the end of each freeze-thaw cycles in order to investigate the effects of migration of solute transport.
- Sectioning the test samples into equal heights at the end of the tests in order to obtain solids content, moisture content and EC profiles varying with depth.
- A comparison of laboratory experimental data (moisture content/solids content, shear strength and EC) with the existing field data in order to replicate the expected field behaviour.
- Development of a coupled numerical analysis methodology (coupled FSConsol and UNSATCON model) in order to validate the laboratory experimental results

## **1.4 Background**

### ***1.4.1 Oil Sands Overview***

With a combined estimated reserve of 1.8 trillion barrels of in-place reserves of in-situ crude bitumen, the Athabasca, cold Lake, and Peace River deposits form a massive resource in Alberta, Canada. Of these regions, the Athabasca oil sand deposit is the largest and only one to be shallow enough to allow for surface mining. Alberta holds approximately 177 billion proven barrels of established reserves which can be economically extracted using current technologies (AER, 2016).

The oil sands deposits are predominantly composed of a quartz sand matrix surrounded by a thin film of water and fines while the remaining pores are filled with bitumen and gases. The bitumen (crude oil) ranges from 0 to 19 % by total mass with an average of 12%, water ranges from approximately 3 to 6% by total mass, and mineral predominantly quartz, sand, silts and clay vary approximately from 84 to 86% by total mass (Chalaturnyk et al., 2002). The bitumen that typically coats the mineral particles is extracted through the Clark hot water extraction process using sodium hydroxide. The mineral particles are broken down and get dispersed in the process water by the combined action of chemical additives, water, and mechanical energy. Using this process, the dispersed mineral particles form three streams: a predominantly coarse sand-water stream, a high-

water content fines stream and a bitumen froth (Jeeravipoolvarn, 2010). Around 88-95% of the bitumen present in the ore can be extracted through this extraction process (Masliyah et al., 2004), whereas, the coarse and fine mineral streams are formed as pumpable by-product waste stream known as tailings (Boratynec, 2003)

#### ***1.4.2 Tailings Management***

The resulting tailings slurry from the extraction process is composed of 10% to 30% fines along with residual bitumen and about three times more water than the produced oil (Xu et al., 2008). This sludge, referred to as whole tailings, is hydraulically discharged into on-site containment facilities/ tailings ponds where the fines (particle size of less than 0.044 mm) segregate from the sand and flow into the tailings ponds at around 90% fines and approximately a solids contents of 5% - 8%, known as thin fine tailings (TFT) (Chalaturnyk et al., 2002). After a few years of settling, the TFT forms a loose card-house structure of clay particles surrounded by water with a solids content of about 30-40% (corresponding to a moisture content of 150-230%), known as mature fine tailings (MFT) (Spence et al., 2015). Tailings streams that behave as fluids (TFT, MFT) are collectively referred to as fluid fine tailings (FFT) and these FFT will remain in this state for decades as they slowly dewater and consolidate. As a result, the inventory of tailings being stored in the pond has been steadily increasing over time and creates a unique challenge for the tailings management.

The Alberta Energy Regulator (AER) regulates oil sands mine and the associated management of FFT as part of its mandate to increase the rate of reclamation and enhance the reduction of the tailings ponds (AER, 2020). In an effort to introduce specific performance criteria for the reduction of the FFT and the formation of trafficable deposits, AER released the Tailings Management Framework for Mineable Athabasca Oil Sands (TMF), which in conjunction with Directive 085, focus on the site-specific thresholds for FFT volumes over the lifespan of an oil sands mine (AER, 2020). At present, each mine operators are required to annually report their actual tailings volume and to improve its existing reclamation strategies by ensuring that FFT are ready to reclaim within 10 years from the end of the mine life (AER, 2020).

### ***1.4.3 Tailings Dewatering Technologies***

In order to implement the regulations and promote the acceleration of dewatering, a large amount of time and efforts have been invested in researching different dewatering technologies through various chemical, mechanical and environmental processes. Of 550 treatment technologies as identified in the Oil Sands Tailings Technology Development Roadmap project, there are currently four dewatering methods being employed to promote dewatering (Beier et al., 2016; AER, 2018). These are described as below:

- **Thin lift drying:** This process involves injecting flocculant directly to FFT in the pipeline followed by deposition in thin layers over a larger area to promote atmospheric drying (freeze-thaw/ evaporation). The coupling of downward seepage and evaporation result in reduced moisture content and increased undrained shear strength of the deposit (AER, 2018). Upon a layer of drying, another layer/lift is added, and this process is repeated. It has been implemented commercially by Suncor Energy as part of its tailings reduction operation (TRO) and by Canadian Natural Upgrading Ltd. (CNUL) as Atmospheric Fines Drying (AFD) at their Muskeg River mine location (AER, 2020).
- **Thickened tailings (TT):** This process involves thickening the FFT in a mechanical/conventional thickener, where flocculants are added to promote rapid settling and sedimentation of suspended fines in tailings, thereby, creating thickened tailings (TT) (AER, 2018). The TT can be deposited in thin lifts or into deep deposits (>10 m deep). TT using mechanical thickener is being used at Imperial's Kearl and CNUL's Muskeg River and Jackpine mines (AER, 2020).
- **Composite tailings (CT) and Non-segregating tailings (NST):** Composite tailings (CT) technology involves blending FFT with sand slurry from the extraction plant using coagulant to prevent segregation (AER, 2018). Non-segregating tailings (NST) is formed when TT is mixed instead of FFT with sand slurry. This technology also requires the use of a thickener prior to deposition (AER, 2018). CT is currently being used at Syncrude's Aurora North and Mildred Lake mines and CNUL's Muskeg River Mine, whereas NST is being operated at Canadian Natural Resources Ltd. (CNRL) Horizon (AER, 2020).

- Centrifugation:** This technology involves adding flocculant and/or coagulant to the FFT prior to pumping into the centrifuge, where solids particles are separated from water under the action of centrifugal force (OSTC and COSIA, 2012). The separated water is further collected and recycled, whereas centrifuged tailings is deposited either in thin lifts or in deep deposits. Thin lift deposition occurs at a slower rate and this deposition relies on atmospheric drying and freeze-thaw process as the primary mechanism for dewatering. On the contrary, centrifuged tailings can be deposited continuously in deep deposits at a higher rate where the primary mechanism of dewatering occurs through the self-weight consolidation (OSTC and COSIA, 2012). At present, centrifuge is being used at Syncrude Mildred lake and CNUL Jackpine Mine (AER, 2020)

Figure 1.1 compares tailings solids content by mass versus the equivalent volume percentages. The figure shows that tailings (for example centrifuged tailings/cake) with a solids content of 55% by mass (corresponding to a moisture content of 82% by mass) holds 70% water by volume (30% of solids by volume), which is still below the range of the liquid limit.

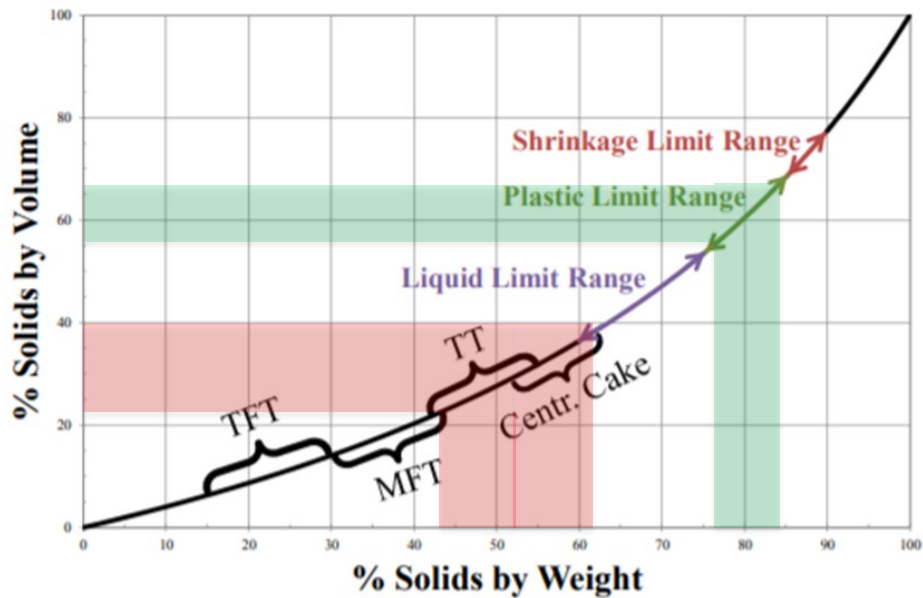


Figure 1.1: Relationship between tailings solids content by volume versus mass (after OSTC and COSIA, 2012)

In order to attain sufficient long-term strength and trafficability (within a range of 50-100 kPa), the centrifuged tailings must attain a solids content of over 75% by mass (corresponding to a

moisture content of 34% by mass) that would necessitate to reduce 48% of its water in the process, and thereby, reaching to the plastic limit range with a water content of 45% by volume. However, tailings need to further dewater as far as shrinkage limit to form unsaturated and dry stack tailings deposits (OSTC and COSIA, 2012).

Overall, the treated tailings (FFT that goes through different dewatering technologies) deposit, although exhibits higher strength and improved dewatering properties as compared to FFT, is still considered non-trafficable as it is essentially in the liquid state with minimal shear strength (Sorta et al., 2012). Hence, a capping layer made up of solid materials (ranging from half a meter to several meters of coarse sand tailings, coke or overburden materials) are required to place over these soft treated tailings deposit to increase the surface load in order to accelerate dewatering (OSTC and COSIA, 2012). Capping of soft deposits is capital intensive and hence, it can be advantageous to employ environmental dewatering process as an additional dewatering to assist surface strength development prior to/without the placement of capping.

#### ***1.4.4 Environmental Dewatering***

Environmental dewatering can occur through a combination of sedimentation, consolidation, evaporation, freeze-thaw and evapotranspiration processes. After deposition, tailings deposits will consolidate and may develop surface crust through these environmental effects (predominantly through evaporation and freeze-thaw process) (OSTC and COSIA, 2012). Once a sufficient crust has developed, the surface can be capped in order to further enhance the consolidation and trafficability for mobile equipment (OSTC and COSIA, 2012). Among all these environmental dewatering processes, freeze-thaw and evaporation have shown the most promising results as a method to reclaim high moisture content tailings (Proskin, 1998).

#### ***1.4.5 Consolidation***

Consolidation is a time dependent process by which soil decreases in volume through the dissipation of excess pore water pressure that results in a subsequent increase in effective stress. Self-weight consolidation of tailings has been used to naturally dewater the tailings for more than 50 years (BGC Engineering, 2010). In the context of geotechnical engineering, the classical one-

dimensional small strain consolidation theory, as proposed by Karl Terzaghi, is successfully used in predicting the consolidation of soils. 1-D consolidation theory assumes incompressible pore water and soil particles; linear time dependent relationship between void ratio and effective stress; small strain and stress increments; and constant compressibility and hydraulic conductivity during consolidation (Gibson et al., 1967). However, compressibility and hydraulic conductivity of oil sands tailings are highly non-linear that results in a large settlement and hence, the consolidation behaviour of soft tailings cannot be derived using Terzaghi's 1-D consolidation theory. Instead, a non-linear finite strain consolidation theory was proposed by Gibson, England and Hussey in 1967 that accounts for the large volume, hydraulic conductivity, and compressibility changes tailings undergo during consolidation.

The self-weight consolidation of oil sands tailings can be extremely slow and is expected to occur over decades, depending on the types and properties of the tailings including solids content, fines content and sands to fines ratio (SFR) (BGC Engineering, 2010). The higher the initial solids content, the faster is the consolidation rate. Therefore, treated FFT is expected to consolidate at a faster rate compared to the untreated FFT (Jeeravipoolvarn et al., 2009). Wilson et al. (2017) carried out large strain consolidation tests on untreated FFT (solids content of 46.1% by mass and fines content of 96% by dry mass) and TT samples (ranging from 49-55% solids content by mass and 51-67% fines content by dry mass) and the results indicate that the treatment process (higher solids content and lower fines content) resulted in faster consolidation compared to the untreated FFT. Similarly, SFR provides an indication of consolidation behaviour as mixing sand acts as an internal surcharge on FFT, which, in turn, accelerates the consolidation (Jeeravipoolvarn et al., 2009). Sorta et al. (2016) reported that mixing sand with FFT (fines content of 20% by dry mass and a clay content of 10% by dry mass) resulted in an order magnitude higher hydraulic conductivity and a lower compressibility than TT (fines content of 50-60% by dry mass and a clay content of 26-31% by dry mass), thus, indicating faster consolidation compared to TT.

#### ***1.4.6 Freeze-Thaw Mechanism***

When tailings slurries are subjected to below freezing temperatures, a freezing front advances into the tailings. The freezing of pore water develops an increase in ice pressure and a decrease in pore water pressure (Konrad and Morgenstern, 1980). Negative pore water pressures are eventually

generated due to the surface tension differences between unfrozen water surrounding the mineral particles and ice filling the voids. The difference in pressure causes water to migrate from the underlying unfrozen tailings towards the growing ice crystal/ ice lenses which eventually form a three-dimensional reticulate ice network surrounding the frozen pads of tailings (Dawson et al., 1999; Beier and Segó, 2009). The migration of water due to the large negative pore pressure also causes the formation of shrinkage cracks just below the freezing front. Since water flows from the tailings particles, the tailings mass is consolidated into blocks bounded by vertical and horizontal shrinkage cracks. These cracks are filled with water that freezes during freezing, known as ice lenses. Upon thawing, these ice lenses become conduit channels for upward water movement, thereby facilitating the settlement of heavier soil peds at the bottom and overall volume reduction (Rima and Beier, 2018). The extent of cracking is a function of the temperature gradient, overburden stress and the number of freeze thaw cycles (Proskin, 1998). The amount that is frozen and thawed is primarily dependent on the local climate and thermal properties of the deposited tailings (Pham and Segó, 2014).

The formation of ice lenses can be classified into two categories based on the external drainage condition during freezing: open and closed system freezing. Open system freezing refers to the freezing of in situ and additional moisture which migrates to the freezing front within the frozen soil. It allows additional water to move within the soil mass to the freezing front. On the contrary, closed system freezing refers to the freezing of only in situ moisture which migrates to the freezing front within the frozen soil. The difference between the open and closed system freezing is the presence of an unfrozen soil moisture reservoir. Impermeable boundary conditions, low permeability, higher freezing rates and lack of fissures in the unfrozen and frozen tailings are the factors that preclude the migration of moisture from outside the advancing front, thus, result in undrained freezing (Pham and Segó, 2014). However, re-distribution of in-situ moisture may occur during this process.

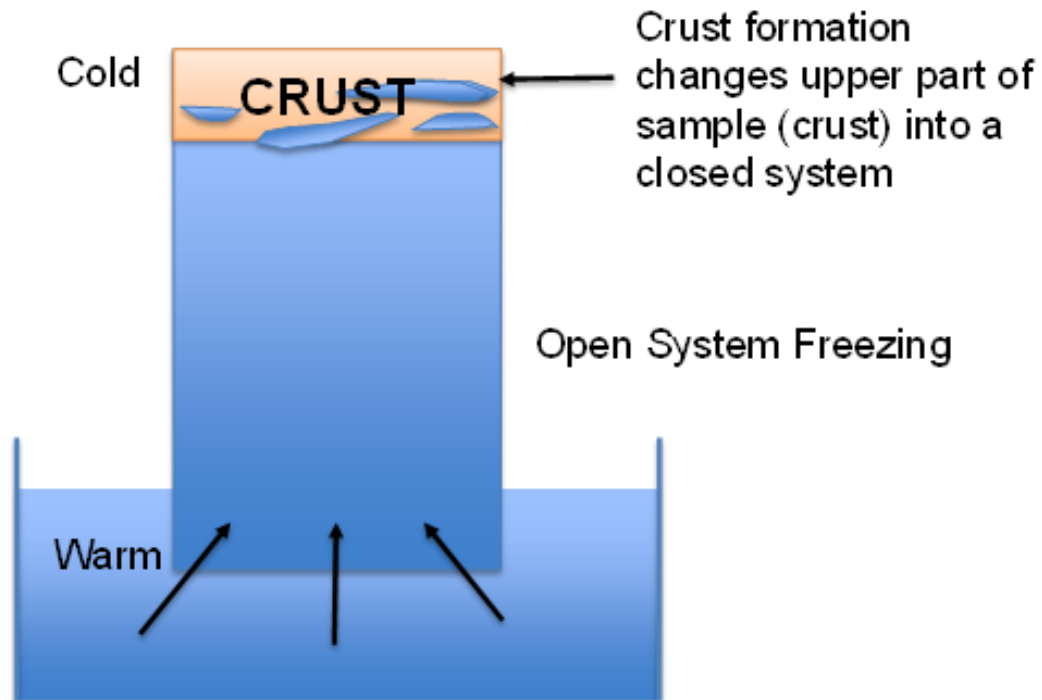


Figure 1.2: Effects of Crust Formation on the drainage conditions during freezing (Reproduced and modified after Andersland and Ladanyi, 2004)

In an open system freezing, which typically occurs in nature, the unsteady heat flow due to the freezing temperature develops formation of horizontal ice lenses just above the  $0^{\circ}\text{C}$  isotherm as water is drawn from the underlying unfrozen soil. Eventually, the heat flow becomes steady and during this process, a significant number of horizontal ice lenses form that develops a three-dimensional reticulate network of ice lenses surrounding the soil peds (Dawson et al., 1999). On the contrary, horizontal ice lenses are precluded in closed system freezing due to the restriction of external water migration towards the freezing front (Proskin et al., 2012). However, a 3D reticulate ice network is formed similar to the open system freezing which is responsible for dewatering (Dawson et al., 1999). Dawson and Segó (1993) conducted large scale multilayer closed system freeze-thaw tests on MFT samples and concluded that water from within the tailings is transported to the three-dimensional reticulate network of ice lenses surrounding the soil peds. The formation of soil peds at microscale and fissures at large scale result in the changes in soil structure and its mechanical behavior (Proskin et al., 2012).

Likewise, similar reticulate ice network was observed in field conditions where open system freeze-thaw conditions prevail (MacKay, 1974). Based on that, MacKay (1974) and Othman and Benson (1992, 1993) concluded that a reticulate ice network is developed irrespective of external drainage conditions that eventually releases water through a significant reduction in pore space. However, open system freezing test (shown in Figure 1.2) is more representative of tailings at the lower boundary of the crust (interactive layer between the frozen crust and underlying tailings) in the field conditions and it is expected to draw more water into the frozen tailings from the unfrozen tailings below, thereby, resulting in a higher number of ice lenses and eventually, a higher degree of dewatering. On the other hand, closed system freezing represents the upper part of the tailings deposit where lower thaw strain can be expected due to the restrictions of accessibility of water. Since the permeability for the tailings material is fairly low to provide any appreciable impact, similar results can be expected for both the testing procedure.

#### 1.4.7 Factors affecting Freeze-Thaw Mechanism

- Initial Solids Content:** The previous laboratory work carried out by Johnson et al. (1993) concluded that the final solids content of tailings sample is predominantly governed by its initial solids content and the subsequent cycles had an insignificant impact on it, particularly, for the samples with higher initial solids content (as shown in Figure 1.3a and Figure 1.3b).

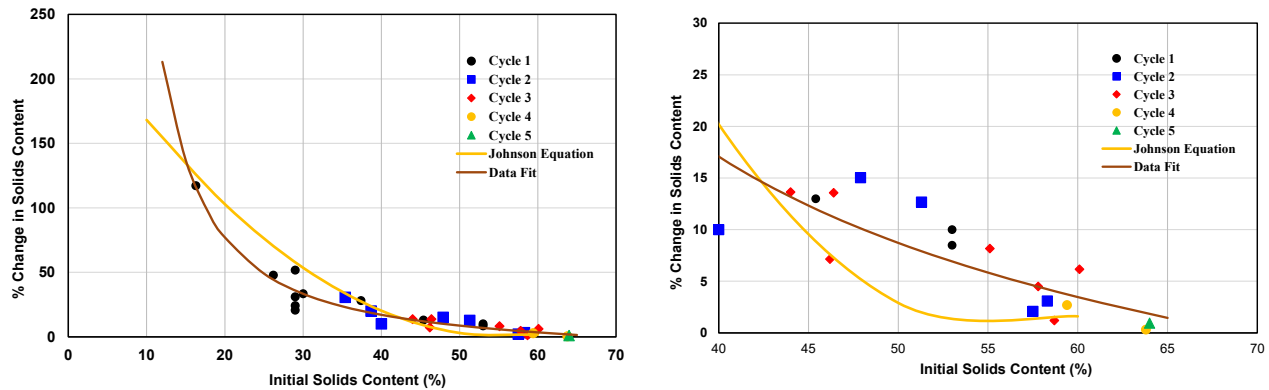


Figure 1.3: The change in final solids content in relation to initial solids content and freeze thaw cycles a) for the whole range of  $s$  and b) for  $s > 40\%$  (modified after Johnson et al., 1993)

Figure 1.3b shows the zoomed in visualization of Figure 1.3a to see the deviance between the two best fitted lines for the samples with higher initial solids content. Johnson et al. (1993) developed an exponential relationship that suggested a marginal increase in dewatering rate for the samples with higher initial solids content. However, based on the incorporated data from previous research studies and some initial laboratory test results from the present study, a best fitted line was plotted. that concluded that the changes in solids content are also affected by the number of freeze thaw cycles. Since the exponential decrease of Johnson's equation is independent of multiple freeze thaw cycle effects, the best fitted line predicts a higher final solids content compared to Johnson's equation. Therefore, it can be concluded that the changes in solids content are also affected by the number of freeze thaw cycles and thus, it cannot be predicted on the basis of the initial solids content solely.

- **Number of Freeze-Thaw Cycles:** In controlled laboratory incubations, multiple freeze thaw cycles ranging from three to nine were found effective to have an impact on natural soil, depending on moisture content (Oztas and Fayetorbay, 2003). However, the extent of the effects of cycles on oil sands tailings has not been investigated much. The optimum number of freeze thaw cycle required to alter the geotechnical properties still remains unclear. However, the highest amount of volume change or the highest volumetric strain will be always observed at the first cycle of freeze-thaw as the higher amount of moisture is available during this cycle prior to freezing and thawing (Eigenbrod et al., 1996). The volume changes are decreased significantly with subsequent cycles (Johnson et al. 1993; Othman and Benson, 1992) and eventually becomes insignificant once the water content reach the plastic limit (Eigenbrod et al., 1996). According to Beier and Segó (2009), five cycles of freeze-thaw led to an asymptotic strength gain on coal tailings with an initial solids content ranging from 50-55%. Similarly, freeze thaw cycles have been effective in increasing hydraulic conductivities of the tailings. As the number of freeze thaw cycles are increased, more ice lenses start to form, that, eventually increase the hydraulic conductivity (Othman and Benson, 1993). Proskin (1998) reported an increase in hydraulic conductivity of MFT up to three orders of magnitude higher than the never frozen MFT after multiple freeze thaw cycles, with the greatest increase (1.5 to 2 orders of magnitude higher) observed after first cycle. The increase in hydraulic conductivity was attributed to the vertical shrinkage cracks during freezing that gets reduced with subsequent cycles. The extent of cracking is a function of temperature gradient, overburden stress and the number of freeze-thaw cycles (Proskin, 1998).

However, the number of freeze thaw cycles applied on oil sands tailings is predominantly dependent on the researcher's judgement. Typically, one to three cycles are commonly used in the laboratory for oil sands tailings (Sanchez Sardon, 2013).

- **Temperature Gradient/ Freezing Rate:** The induced suction in the ice fringe is predominantly controlled by the temperature gradient (Rima and Beier, 2021a). Lower freezing rates and lower temperature gradient were found more effective for oil sands tailings sample (or high moisture content sample) in terms of dewatering (Proskin, 1998; Proskin et al., 2012; Pham and Sego, 2014). Lower temperature gradient allows the freezing front to advance slowly and draws more water to the frost front by suction, thereby, generating higher thaw strain and high solids content (Knutsson et al., 2016). Proskin (1998) investigated the effects of temperature gradient and boundary conditions on dewatering of Syncrude MFT samples. He conducted both single layer and multi-layer freeze- thaw tests and both of the results suggested a significantly higher increase in thawed solids content for lower temperature boundary conditions.

Eigenbrod et al. (1996) carried out a series of cyclic open system slow freezing and fast freezing tests on soft, normally consolidated clay specimens in the laboratory. Based on their laboratory results, they concluded that the volumetric strain during slow freezing tests were almost three times higher compared to the fast-freezing tests for the specimens with an initial liquidity index close to unity. They also concluded that the volumetric strains could approach to zero for a sample subjected to very fast freezing rates.

The thickness, frequency and spacing of ice lenses are primarily dependent on the temperature gradient and freezing rate (Othman and Benson, 1993). The very high freezing rate of a sample typically allows the frost front to advance faster such that water cannot be accumulated at a fixed place for growing ice lenses (Konrad and Morgenstern, 1980). The relatively higher freezing rate develops a larger number of smaller and thinner ice lenses, while the lower and slow freezing rate develops fewer and thicker ice lenses due to the longer time frame available for water accumulation at a fixed location (Othman and Benson, 1993). Since the freezing rates in the field are typically lower (Othman and Benson, 1993), it can be suggested that volumetric strains in the field can be reasonably predicted from laboratory tests, provided the reasonably similar boundary temperature conditions are applied (Eigenbrod et al., 1996). According to Sanchez Sardon (2013), the sample

volumes tested in the laboratory are typically smaller and a significant number of the samples are collected from the field at a depth of 10 to 20 cm from the surface, where temperature fluctuations are not greatly affected by the surface air temperature. Therefore, the similar boundary temperature conditions can lead to the faster rate of change in temperature through the small volume samples in the laboratory. This phenomenon can lead to the formation of numerous smaller ice lenses which might not represent the actual field conditions (Hobbs, 1974; Henry, 2007). According to Henry (2007), the effect of freeze-thaw cycles on soil/ tailings sample can be over-exaggerated and thus, a range of temperature gradients should be experimented in order to account for the variability in results.

- **Dimensionality of Freezing:** Eigenbrod et al. (1996) measured volume changes during one-dimensional (1D) and three-dimensional freezing tests on soft fine-grained soils and concluded that three dimensional/ all-round freezing test results in higher volumetric strain compared to 1D freezing tests. Since freezing in nature is one and unidirectional, 1D freezing test is recommended in the laboratory to simulate field conditions (Johnson et al., 1993; Proskin, 1998; and Dawson et al., 1999).

The testing sample usually tends to be smaller in the laboratory and hence, the negative boundary temperature applied on the sample can be quickly achieved in the laboratory that can cause the subsurface material exposed to an unrealistic negative temperature condition (Sanchez Sardon, 2013). This phenomenon is more intensified and critical for the samples subjected to three-dimensional freezing (Henry, 2007). However, hydraulic conductivities of the natural soils with lower moisture content were found comparable from these two 1D and 3D tests, although the sizes of the ice lenses were smaller in 3D freezing tests (Othman and Benson, 1993).

- **Sample Size:** Uni-directional freezing occurs in nature that allows a slow advance movement of the freezing front (Othman and Benson, 1993; and Eigenbrod et al., 1996). However, the freezing rate is not constant throughout the depth. Figure 1.4 shows the development of ice lenses throughout the sample depth.

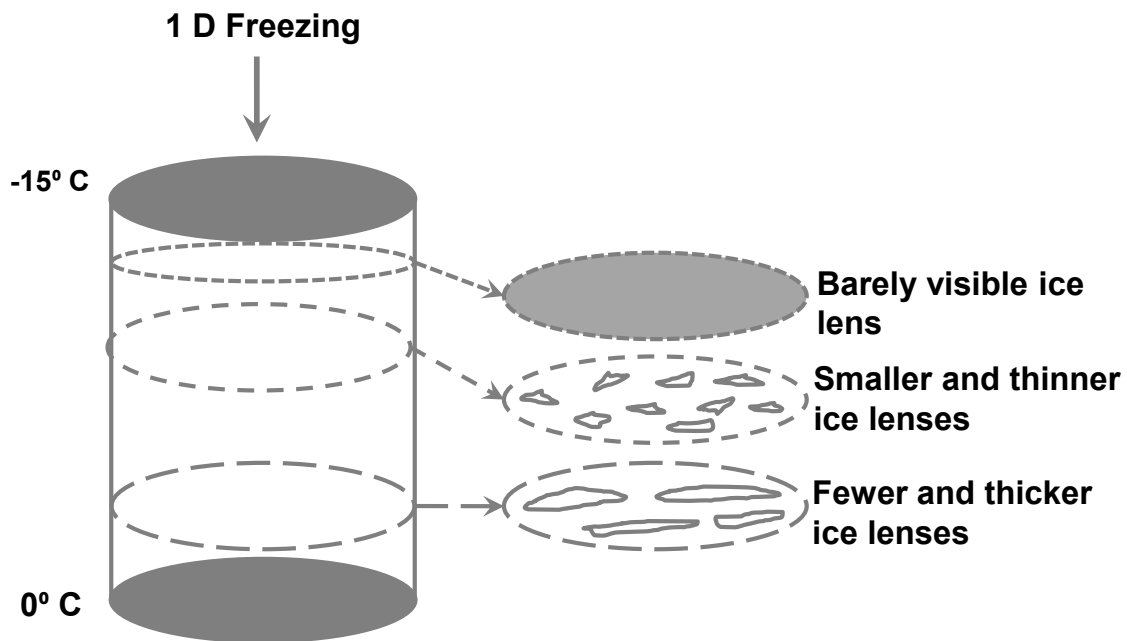


Figure 1.4: Development of ice lenses at different depth (modified after Konrad and Morgenstern, 1980)

One-directional freezing predicts a higher rate of change in temperature at the beginning of freezing that creates a frozen zone with increasing ice enrichment but no visible ice lenses near the surface (Konrad and Morgenstern, 1980). As the frost penetration advances and slows down, numerous thinner but barely visible ice lenses are formed. The temperature gradient is relatively higher during this stage. With time and at deeper depth, the freezing rate is reduced and hence, water is able to accumulate at a fixed location for a longer period of time to develop ice lenses (Othman and Benson, 1993). Therefore, ice lenses are more visible at deeper depth due to the greater thickness and larger spacing. The frozen fringe tends to reach to its maximum thickness once the steady state condition is achieved (Konrad and Morgenstern, 1980). Therefore, smaller and thinner ice lenses can be expected near the surface while fewer but thicker and visible ice lenses can be expected at the bottom of the frost depth (Othman and Benson, 1993). In small volume samples, higher rate of temperature gradient can lead to the formation of numerous small ice lenses instead of the variation of ice lenses at different depth (Henry, 2007). Hence, it is

paramount to select the rate and mode of freezing accordingly so that the smaller sample size in the laboratory can capture the different sizes and frequencies of ice lenses varying with depth.

- **Physicochemical Interactions:** Oil sands tailings have always been highly sensitive to the changes in physicochemical interactions (Proskin et al., 2012). A significant amount of research has been carried out in the previous years to establish a relationship between the oil sands tailings structures and the physicochemical properties like pH, electrical conductivity, dissolved ions and so on. However, the effect of physicochemical interactions on oil sands particles are still poorly understood due to its complexity (Mitchell and Soga, 2005).

Oil sands tailings particles can be viewed as a colloidal solution of clay particles and bitumen suspended in water. These clay particles (kaolinite as a dominant mineral in clay particles) exhibit highly negative electric charges in aqueous solution at neutral to high pH and the net negative charge is the primary factor in controlling clay dispersion (Kaminsky, 2008). A reduction in the net negative charges allows the particles to overcome the electrostatic repulsion and come close to each other resulting in flocculation. Flocculation of colloids is dependent on the thickness of the double layer. Therefore, the colloid- water interaction can be explained through the double layer theory. The thinner the electrical double layer, the stronger is the tendency for flocculation of particles (Mitchell and Soga, 2005). The net charge on these clay particles can be attributed to the changes in pH, ionic strength and cation type (Chorom and Rengasamy, 1995). Based on the diffuse double layer theory, the addition of NaOH causes the pH of the particles to increase, which, in turn is responsible to disperse the clay particles. On the contrary, lowering pH or increasing the opposite ion concentration causes developing positive charges along clay particle edges, which results in a change in the microfabric to edge to face flocculation of positive edges to negative surfaces (Dawson and Sego, 1993).

Freeze-thaw dewatering acts as a controlling mechanism for the re-distribution of water and solutes. The impact of freeze-thaw process on tailings dewatering can be interpreted on the basis of the changes in physicochemical interactions/pore water chemistry. Once the freezing starts, it is the free water that freezes first followed by the capillary water (Proskin et al., 2012). However, presence of solutes/ salt in tailings lowers the freezing temperatures below 0°C (Mitchell and Soga,

2005). Water is the transfer carrier of salt that migrates through the tailings particles from the unfrozen tailings towards the frozen front. The crystal lattice for ice is very sensitive as it only allows hydrogen and oxygen ions to form its regular lattice framework. Therefore, the foreign ions (salts) remain in the melt and the solutes/impurities are rejected by the growing ice crystals as water freezes. Overall, water volume decreases during freezing that, in turn, leads to the increase in electrolyte concentration within the remaining water (Proskin et al., 2012). Based on diffuse double layer theory, the increased concentration causes the adsorbed double layer thickness to decrease and thereby, flocculation of the particles occurs (Andersland and Ladanyi, 2004). Similarly, the addition of divalent ions can cause the double layer thickness to further decrease in addition to the increased electrolyte concentration, which, in turn, allows the particles to overcome the electrostatic repulsion and to facilitate flocculation (Proskin et al., 2012).

Treated tailings that goes through polymer addition/ adsorption, are even more susceptible to the changes in pH and ionic strength (Theng, 1982). The adsorption is promoted under acidic pH or at high ionic strength where the negative charges become neutralized due to  $H^+$  adsorption or by the presence of polyvalent cations that act as bridges between the polymer and negatively charged clay particles (Theng, 1982). Several studies show that long chain anionic high molecular weight polyacrylamides (PAM) flocculants work effectively for improved dewatering in oil sands tailings as it promotes the repulsion of the charged segments, extension of polymer chains, changes in conformation of polymers and the bridging capacity (Mpofu et al., 2003; Nasser et al., 2006). Having an ionic strength that is too high may weaken the bridging bonds and interfere with the adsorption of PAM to negatively charged clay particles (Tripathy et al., 2006). During freeze-thaw process, the polymer amended tailings can be subjected to high shear stress that may disrupt the stability of polymer and cause the rearrangement of adsorbed chains on the clay particle surface (King et al., 1969; Agarwal, 2002). Therefore, colloid (clay particles in tailings)-polymer-electrolytes (solutes/ions) interactions can affect the dispersion and flocculation behaviour of freeze-thaw process.

#### ***1.4.8 Atmospheric Drying/Evaporation***

Surface drying of sub aerial tailings is caused by evaporation at a rate which depends on the climatic condition of the tailings site. Evaporation is the process by which water is lost from the bare soil through a change from liquid to gaseous phase (Lal and Shukha, 2004). The driving force of evaporation is the difference in vapour pressure and temperature between the soil surface and its surrounding temperatures (Wilson et al., 1994). Evaporation from the tailings surface follow the classical conceptual model of evaporation (Simms et al., 2009) where the initial stage evaporation rate closely resembles the potential evaporation, defined by the theoretical maximum rate of evaporation from a pure water body under the given climatic conditions (Wilson et al., 1994). The initial stage is predominantly governed by the climatic and environmental conditions (Newson and Fahey, 2003). This stage is followed by the accelerated decrease in evaporation rate and this can be attributed to the decrease in vapour pressure gradient due to the higher suctions required to desaturate the pores (Innocent-Bernard, 2013). Climatic conditions and the tailings properties (like permeability) are the predominant controlling factor (Newson and Fahey, 2003). The last stage of evaporation involves gradual decrease in evaporation rate where the evaporation rate becomes effectively zero due to the discontinuous liquid-water phase for water migration towards the drying front (Hurtado, 2018).

#### ***1.4.9 Factors affecting Evaporation***

- **Pore Water Salinity:** Ionic composition of a tailings material is one of the controlling factor for evaporation from the tailings surface. Previous research studies (Newson and Fahey, 1997; Fujiyasu and Fahey, 2000; Dunmola and Simms, 2010; and Simms et al., 2017) on the pore water chemistry effects of the evaporation from mine tailings suggested that the that the presence of impurities/ salt concentration reduced the evaporation from the tailings.

Since oil sands tailings contain a significant amount of salt due to the origin of its ore and the addition of NaOH during extraction process, the solutes (salt) in the water migrates towards the drying front or at the surface as the evaporation progresses. Thus, a salt crust is gradually formed at the surface that can suppress the evaporation by the possible three mechanisms: osmotic suction, physical obstruction to moisture flow and the change in albedo (Hurtado, 2018). According to

Innocent-Bernard (2013), high salinity reduces evaporation, and this can be attributed to an increase in osmotic suction, that facilitates a decrease in vapour pressure and overall evaporation at the soil surface. In addition to that, the salt crust may induce lower hydraulic conductivity due to its occupancy in the soil pores, which, in turn, causes resistance to moisture flow. Finally, the accumulated salt crust at the surface may result in higher albedo by significantly reducing the net amount of radiation reaching the surface (Simms et al., 2017).

Figure 1.5 shows the effects of salinity on the tailings evaporation (Newson and Fahey, 2003).

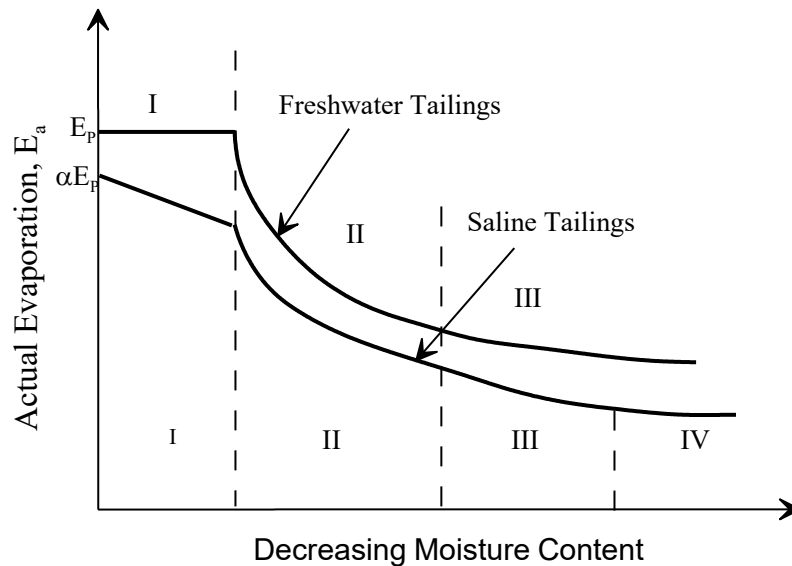


Figure 1.5: Temporal variation in relative evaporation from fresh water and saline tailings (after Newson and Fahey, 2003)

As shown in Figure 1.5, the rate of evaporation due to the presence of dissolved salts is always lower than the tailings with no salts. The authors also concluded that unlike natural soils and tailings with minimal salt content, tailings with a higher salt content are predominantly governed by the pore water salinity and hydraulic conductivity of the tailings (Newson and Fahey, 2003).

- **Crack formation and Desiccation:** Cracking facilitates surface evaporation/ drying through the exposure of underlying material with lower suctions. Therefore, the development of desiccated surface crust is anticipated in soft tailings disposal sites to provide sufficient undrained shear strength for the reclamation operations (Johnson et al., 1993). Cracks are formed due to the

soil/tailings volume reduction and during desiccation process. Desiccation is a process when the upward supply of water is lower than the evaporation from the surface. During desiccation, the degree of saturation of tailings decreases gradually (Innocent-Bernard, 2013), resulting in a reduction of moisture content in tailings. Decreasing moisture content with time facilitates consolidation under gradients induced by the evaporative water and hence, an increase in solids content is observed. Overall, desiccation significantly improves the trafficability of soft tailings deposits enabling reclamation effort. The main process affecting desiccation are evaporation, shrinkage, and the formation of desiccation cracks at the surface of tailings deposit and these properties can be characterized by soil water retention curve (Qiu, 2000).

Upon desiccation, suction is developed which creates tensile stress at the crack tip. Crack initiation will only occur once the total lateral tensile stress exceeds the tensile strength of the tailings (Pham and Seg0, 2014). The formation of surface cracks increases the surface area for evaporation and propagates downward, that eventually disrupts the sample integrity and accommodate rainfall (Innocent-Bernard, 2013). Concurrently, the tailings material above and near the cracks consolidate at a much faster rate compared to the parts of deposits without cracking Innocent Bernard (2013) investigated the effects of evaporation, cracking and salinity in a thickened oil sands tailings and he concluded that evaporation was never ceased during the formation of surface crust due to cracking, albeit it may have affected by the accumulation of salt at the surface.

Surface cracks and desiccation also helps to accelerate the freezing efficiency. The presence of desiccation cracks allows cold air to reach deeper sections of the tailings speeding up the freezing process of the next cycle (Sanchez Sardon, 2013).

- **Effects of Rainfall:** When rainfall reaches the surface of a soft fine- grained soil/ tailings, one part of the water infiltrates into the soil matrix where the other part of the rain water enters directly into the cracks and fills the void pore spaces. Water flows into the cracks when rainfall exceeds maximum infiltration rate of soil matrix. Surface runoff occurs once the cracks are closed by the rainfall. The amount of water infiltrating in the cracks can be attributed to the factors such as the rainfall intensity, maximum infiltration capacity of the soil/tailings and relative area of cracks (Bronswijk, 1988).

The induced wetting event/rainfall can cause the dissolution of salts, collapse of surface crust fully or partially and appearance of large number of new microcracks. As a result, soil surface may exhibit lower undrained shear strength compared to the before rainfall phase (Innocent Bernard, 2013).

#### ***1.4.10 Previous Works on Freeze-Thaw Dewatering***

The freeze thaw dewatering research on oil sands tailings started at the University of Alberta since 1990. The extensive research (Dawson and Segó, 1993; Johnson et al., 1993; Proskin, 1998) conducted at both laboratory and pilot scales showed that FFT subjected to multiple freeze thaw cycles experienced significant dewatering. However, the studies were predominantly limited to multiple/ thin layered MFT (untreated FFT) deposits. Thin layer/ multilayer freeze thaw dewatering approaches are allowed to freeze at a faster rate without access to water and also to dissipate the excess pore water pressure quicker compared to deep stack/ single layer deposit (Bale, 2007). However, freeze thaw dewatering in deep stack/single layer deposit can be more challenging as it is expected to result in smaller thaw strain compared to thin/ multi-layer.

Johnson et al. (1993) conducted small- and large-scale laboratory tests on un-amended sludge from a Syncrude tailings pond. The large-scale experiments were carried out with initial solids content of 15, 25, 35 and 45% at a temperature of -24°C. After three freeze-thaw cycles, the final solids content increased to 50, 53, 60 and 60.4%, respectively. Based on these results, the authors concluded that the final solids content is predominantly dependent on its initial solids content as the samples with higher solids content require less energy to freeze promptly compared to the samples with lower solids content.

Segó and Dawson (1992) investigated the effects of layer thickness, temperature gradient and boundary conditions on dewatering of Syncrude MFT samples. They conducted both single layer small scale and multi-layer large scale freeze-thaw tests and both of the results suggested a significantly higher increase in thawed solids content for the lower temperature boundary conditions. The single layer test showed that the sample subjected to a temperature of 0°C at top and -8°C at bottom showed significantly higher increase in solids content (16% increase) compared to -15°C and -8°C/-15°C single layer tests. Similarly, multi-layer large scale tests showed that the

sample which is fully frozen at  $-6^{\circ}\text{C}$  resulted in a 38% increase in solids content compared to the sample frozen at  $-25^{\circ}\text{C}$  temperature.

Sego (1992, cited by Proskin, 1998) reported the freeze-thaw laboratory test results of as received and chemically amended Suncor MFT. The closed system apparatus developed by Sego and Dawson (1992) was employed in that study where the sample was fully frozen with a top temperature of  $-8^{\circ}\text{C}$  and bottom temperature of  $-15^{\circ}\text{C}$  in order to simulate the field conditions. The solids content of the as received MFT resulted in a thawed solids content of 38, 44 and 48% after first, second and third freeze-thaw cycles, respectively, from an initial solids content of 30%. Proskin (1998) compared the effects of pore water chemistry on freeze thaw dewatering between Suncor MFT data (conducted by Sego, 1992) and OSLO cold water extraction (OCWE) process fine tailings data (conducted by Sego and Dawson, 1992). He reported that these two MFT samples are similar in terms of their mineral composition. However, OCWE process MFT dewaterers significantly higher compared to Suncor MFT. The difference in dewatering is attributed to the different extraction methods of OSLO tailings which does not employ the addition of NaOH in the bitumen extraction process.

The difference in pore water chemistry led to additional research for the authors to study the effect of chemical amendment on freeze-thaw dewatering of MFT (Proskin, 1998). The effect of chemical amendment on freeze thaw dewatering of MFT had been investigated by Sego (1992). The author observed an additional 18% increase in thawed solids content due to the addition of chemical amendment (sulfuric acid ( $\text{H}_2\text{SO}_4$ ) and quicklime ( $\text{CaO}$ )). Using the identical chemical additives, Proskin (1998) carried out thin layer freeze-thaw tests on Suncor MFT dewatering at a field scale. After a single year of freeze-thaw-drying process coupled with post thaw consolidation, surface drainage and surface drying, the solids content resulted in an increase from 28 to 69%. Among these, only freeze-thaw contributed to an increase in solids content to around 55%. The associated undrained vane shear strength was increased from 0.02 kPa to an average value of 3 kPa throughout the deposit. The second-year field test results suggested that once exposed to atmosphere for evaporation, a crust of 0.3 m was formed at the surface and the average solids content increased from 55 to around 70% with an associated average undrained shear strength of 7 kPa.

Dawson et al. (1999) also carried out field tests from a pilot plant located near Fort McMurray. He compared the initial and final solids content relationship post thawing for both laboratory and field tests. Based on the results, the author concluded that the field test performed better compared to laboratory test in terms of solids content enhancement. The authors also concluded that the thaw strain (volume change) becomes negligible once the initial solids content reaches 70%.

Overall, the tailings are expected to dewater and gain sufficient strength for reclamation activities to proceed within a reasonable time through freezing in winter, thawing in spring and desiccation during summer. However, the unfrozen water content distribution, pore water pressure dissipation and the location of the freezing front within the tailings are predominantly dependent on the selection of sample size, freezing rate, temperature gradient and number of freeze-thaw cycles (Proskin, 1998; and Dawson et al., 1999).

#### ***1.4.11 Previous Works on Evaporation/ Drying for Tailings***

A significant amount of research was carried out in the previous years to investigate the effects of atmospheric drying which confirmed that the evaporation drying, shrinkage and crack formation in the tailings contribute to the increase in evaporation rates while the migration of salts to the surface suppresses the evaporation rates due to the development of high osmotic suction (Simms et al., 2017; Innocent-Bernard, 2013; and Newson and Fahey, 2003). However, a very few numbers of field studies and laboratory experiments had been undertaken to investigate the desiccation cracks of tailings, much less for oil sands tailings to be specific.

Qiu (2000) conducted research on investigating the desiccation behaviour of tailings. He placed the tailings in thin layers and allowed to desiccate under climatic conditions. He concluded that CT dried the slowest compared to the other tailings (copper, gold and coal tailings) due to the presence of bitumen coating. After six weeks of drying in the lab, the surface moisture content of CT was found to decrease from 69 to 23% (solids content increased from 59 to 81%) and subsequently reached to an equilibrium of 1% moisture content after eight weeks of drying.

Heidarian (2012) studied the effects of initial moisture content (or initial solids content) and stress history on desiccation properties and water retention behaviour of oil sands tailings. His studies concluded that an increase in initial water content (or a decrease in initial solids content) results in an increase in air entry value. However, residual water content (the water content where a large suction is required to remove additional water from the tailings pore) in soil water characteristics curve was found not to be affected by the initial water content of MFT. High initial water content in oil sands tailings material also had no effect on shrinkage curve of the tailings. Overall, the tailings deposited at higher water contents tends to desaturate more at a given suction.

Innocent-Bernard (2013) investigated the effects of cracking, crust formation and salinity on the evaporation of oil sand thickened tailings. Her results concluded that the crust formation impedes water flow but allows the surfacing of fresh tailings through cracks. As drying continues, the surface crust along salt accumulation gets thicker, thus, suppressing evaporation from the surface. On the contrary, cracking contributes to the increase in surface area, thereby, exposing the underlying higher water content tailings and overall evaporation. Rozina (2015) compared the contribution of cracking to evaporation between his dry box polymer amended tailings at the laboratory scale and AFD tailings (atmospheric fines drying which consists of thin lift dewatering of in-line flocculated MFT) at the field scale, both dried to a solids content of approximately 60-70%. A noticeable change in cracking patterns, geometry and frequency were observed, where the AFD tailings in the field appeared to experience more shrinkage and seemed drier at the surface compared to the dry box tailings. However, the dry box tailings appeared to have similar dry surface once both the tailings surface reached to a solids content of 90%. Hurtado (2018) investigated the effects of cracking and salinity on centrifuged tailings. His investigation showed contrasting results from the similar experiments carried out by Innocent-Bernard (2013) and Rozina (2015). His analysis suggested that the contribution of the formation of cracks on the evaporation rate was minimal for the centrifuged tailings which was found the contributing factor for evaporation on the polymer amended and thickened tailings (experiments carried out by Innocent-Bernard, 2013; and Rozina, 2015). The difference in cracking influence was attributed to the differences in crack geometry that causes variations in the wind dynamics and in turn, influences the evaporation behaviour (Hurtado, 2018). However, the impact of salinity in suppressing the evaporation rate was found similar as observed by the above-mentioned authors.

## 1.5 Thesis Outline

The outline of this thesis is presented below:

Chapter One: This section provides the problem statement, objective and scope of the thesis followed by an overview of the background including a brief description of the oil sands tailings, different dewatering technologies, mechanism, factors and previous research works related to freeze-thaw and evaporation.

Chapter Two: This section accomplished objective 1 which provides the background, material, experimental methodology, results and discussions in order to evaluate the effects of multiple freeze-thaw cycles on dewatering and strength of treated tailings deep deposits. This section has been published in the journal of Cold Regions Science Technology.

Chapter Three: This section accomplished objective 2 which provides the background, material, experimental methodology, results and discussions in order to evaluate the effects of seasonal weathering (multiple freeze-thaw and alternate drying-wetting cycles) on dewatering and multiple strength of treated tailings deep deposits. This section has been accepted for publication in the Canadian Geotechnical journal.

Chapter Four: This section accomplished objective 3 which provides the background, laboratory investigation, comparative results with the field deposits and discussions in order to provide insights to predicting field behaviour. This section has been prepared for publication in future.

Chapter Five: This section briefly compares different mine tailings (oil sands tailings, coal tailings, gold tailings and metal mine tailings) and management approaches all over the world, where seasonal weathering has been employed to develop surface crust. This section has been accepted for the 20<sup>th</sup> International Conference on Soil Mechanics and Geotechnical Engineering 2022.

Chapter Six: This section accomplished objective 4 which develops a coupled analysis methodology (using FSConsol and UNSATCON) in order to investigate the effects of seasonal

weathering on treated tailings deposit by simulating laboratory results obtained from chapter one and two. This section has been published in the MDPI journal (Processes).

Chapter Seven: This section summarizes the conclusion from this research and provides recommendations for further research.

## 2 EFFECTS OF MULTIPLE FREEZE-THAW CYCLES ON OIL SANDS TAILINGS BEHAVIOUR

### Abstract

Continuous deposition of flocculated tailings into a deep containment facility (known as deep deposits) is gradually becoming widely acceptable as an alternative to multiple thin layered deposits, due to its reduced footprint and material handling requirements for tailings disposal. However, capping deep tailings deposits remains challenging due to the extremely slow self-weight consolidation, uncertainty in the prediction of consolidation and low surficial strength. Consequently, the resulting tailings deposits remain very soft and need to be desiccated at the surface to support capping for reclamation. This paper evaluated the effects of natural dewatering processes such as multiple freeze–thaw cycles and evaporative drying on surface crust formation for a deep oil sands tailings deposit. This paper also explored how changes in temperature gradient, initial solids content and initial water chemistry or a change in treatment process can influence the freeze–thaw dewatering process. The results suggested that the tailings samples subjected to a lower temperature gradient resulted in overall higher gravimetric solids contents and subsequent higher shear strengths at the surface after five freeze–thaw cycles. When coupled with evaporative drying, the combined freeze–thaw–drying processes further contributed to surface crust formation (strength at the surface >100 kPa). The electrical conductivity measured at each cycle and after the drying–wetting phase predicted that the upward migration of the solute contributed to the overall volume reduction during the freeze–thaw process due to osmotic and osmotically induced consolidation.

### 2.1 Introduction

Oil sands tailings are generated as by-products after extracting oil from oil sands ore and are composed of water, residual bitumen and solids (enriched in fine sands and clays). The management decisions related to the reclamation of these tailings deposits are usually complicated by high water content/ low solids content (water content refers to mass of water divided by the

mass of dry solids, where solids content refers to mass of dry solids divided by total wet mass) and subsequent low shear strength of the tailings surface. These fluid-like tailings streams, having an initial water content of approximately 230–560% (known as thin fine tailings or TFT) and settle with time to about 150–230% (known as mature fine tailings or MFT), are collectively referred to as fluid fine tailings or FFT (CTMC, 2012; Spence et al., 2015). The continued accumulation of FFT led the Alberta Energy Regulator (AER) to introduce new regulations to improve its existing reclamation strategy by ensuring that the FFT are ready to reclaim within 10 years of the end-of-mine life for a given oil sands mining project (AER, 2018). In response to AER, the oil sands industry has since focused on creating deep deposits of treated tailings to facilitate progressive reclamation, achieve a trafficable surface following the cessation of deposition and minimize the footprint of tailings deposits (CTMC, 2012; AER, 2018). Treated tailings are collectively referred to tailings that goes through different chemical, natural and/or mechanical dewatering treatment technologies in order to improve the mechanical properties of tailings (solids content and shear strength). Of 550 treatment technologies identified in the Oil Sands Tailings Technology Development Roadmap project, the commercially implemented dewatering technologies at present are 1. Thin lift drying that combines flocculant addition to FFT followed by deposition in thin layers over a larger area to facilitate atmospheric drying, 2. Thickened tailings combining flocculant with FFT and the use of thickener, 3. Composite tailings combining tailings sand and coagulant/ thickeners with FFT, and 4. Centrifugation combining flocculant and coagulant with FFT prior to feeding it into the centrifuge to separate water from the clay (Beier et al., 2016; AER, 2020). All these treated tailings are flocculated with polymers (water contents typically range from 60-120%) having high fines content. Despite their lower water contents, the treated tailings may still exhibit very low strengths (less than 1 kPa) that maybe challenging to support reclamation activities. On the other hand, deep deposits refer to in mined out pit deposits (typically >10-20 meters deep) that is formed by continuous discharge of treated FFT. The gradual shift from thin layer towards deep deposits offers an effective reclamation and depositional strategy by providing a better volume and area certainty with reduced land disturbance (OSTC and COSIA, 2012). However, deep deposits predominantly relying on self-weight consolidation for subsequent dewatering make it more challenging for the fines dominated treated tailings deposits that undergo very slow consolidation (OSTC and COSIA, 2012). Hence, these soft treated tailings deposits typically require the placement of a coarse-grained capping layer as a surcharge and/or a strong

geotextile as a soil reinforcement on the tailings surface to develop strength (OSTC and COSIA, 2012). The large volume of these caps/geotextiles has a direct impact on the production cost and profits of mining operations (Beier and Segó, 2009). Therefore, continuous improvement of existing technologies and management techniques in a tailings site is paramount for the successful management of fluid tailings (AER, 2017).

Freeze–thaw dewatering is considered an inexpensive technique for dewatering since it can use existing slurry transport facilities such as pipelines and tailings ponds. Additionally, it accommodates the logical climatic cycle in Western Canada where winter can be utilized conveniently for freezing (Johnson et al., 1993). Therefore, the effects of freeze–thaw can be evaluated to increase the dewatering and strength performance of current commercial tailings technologies for deep deposits employed at various oil sands operations. The tailings deposit subjected to the freeze-thaw process develops thaw strain which contributes to the increase in effective stress. The thawed tailings undergo post-thaw consolidation which further contributes to the change in void ratio and overall additional dewatering. Additionally, if the drying factor from evaporation is added, the environmental effects (freeze-thaw and evaporation) can potentially reduce the water content by passing through the liquid limit and, possibly, plastic limit. Depending on the extent of stabilization and attained strength, it is possible for the construction equipment to start placing reclamation covers that can potentially reduce the required amount of geosynthetics and result in reclamation cost savings.

The objective of the research reported in this paper was to evaluate the dewatering and strength performance of two different types of treated tailings deep deposit (one of these belongs to commercially operated centrifuge technology and another one belongs to a pilot scale demonstration of in-line thickening process) surfaces through consecutive freeze-thaw cycles followed by drying-wetting cycle under laboratory conditions. This paper also investigated the effects of physicochemical interactions on treated tailings deposits through a comparison of pore water chemistry results and migration of solute transport phenomena during freeze-thaw-drying-wetting process.

## 2.2 Background

Extensive research was carried out on the freeze-thaw process of soft fine-grained soils with water contents below/at the liquid limit and the results indicate volume changes, shear strength reduction and increased hydraulic conductivity after freeze-thaw (Benson and Othman, 1993; Eigenbrod, 1996). On the contrary, oil sands tailings deposited at water contents well above the liquid limits typically experience significant dewatering with subsequent increased shear strength as concluded by the extensive research (Dawson and Segó, 1993; Johnson et al., 1993; Proskin, 1998) conducted at both laboratory and pilot scale at the University of Alberta. However, the studies were predominantly limited to untreated MFT samples having water contents ranging from 150-230% (OSTC and COSIA, 2012). The shift from conventional untreated tailings disposal to treated tailings deposits may have a large impact on freeze-thaw dewatering since the freeze-thaw mechanism works through the re-distribution of available water in the tailings (Bing et al., 2015). As tailings undergo the freeze-thaw process, ice lenses surround the frozen tailings ped (tailings are consolidated into polygonal blocks) and develop a three-dimensional reticulate ice network structure which significantly changes the micro-structure of the tailings (Beier and Segó, 2009; Proskin et al., 2012). Upon thawing, these ice lenses become conduit channels for upward water movement, thereby facilitating the settlement of heavier soil ped at the bottom and overall volume reduction (Sanchez Sardon, 2016; Rima and Beier, 2018). The previous results suggest that a significant amount of dewatering could be achieved in MFT due to its extremely high-water content (around 230%) before initial freezing. On the contrary, freeze-thaw dewatering was proved to be marginal for the tailings samples with lower initial water content (around 120%) compared to MFT (Johnson et al., 1993). Therefore, the direct relationship between the initial water content and the degree of dewatering due to the freeze-thaw mechanism has contributed to an increased but challenging interest in the effects of freeze-thaw cycles on treated tailings.

Like initial water content, multiple freeze-thaw cycles are also believed to have a greater effect on dewatering from higher water content tailings than from tailings with a low water content (Johnson et al., 1993). The highest amount of volume change is usually observed after the first cycle of freeze-thaw, (Eigenbrod et al., 1996; Proskin et al., 2012). Afterwards, the volume changes decrease significantly with subsequent cycles (Johnson et al. 1993; Proskin et al., 2012) and

eventually becomes insignificant once the water content reaches the plastic limit (Eigenbrod et al., 1996). According to Beier and Segó (2009), five cycles of freeze–thaw led to an asymptotic strength gain on coal tailings with an initial water content ranging from 80 to 100%. However, the extent of the effects of freeze–thaw cycles on oil sands tailings like treated FFT has had little investigation. The optimum number of freeze–thaw cycles required to alter the geotechnical properties of oil sands tailings still remains unclear. Typically, one to three cycles are commonly used in the laboratory for oil sands tailings (Sanchez Sardon, 2016).

The efficiency of the freeze–thaw mechanism is controlled by the thickness, frequency and spacing of ice lenses, which in turn, are primarily dependent on the temperature gradient, boundary conditions and freezing rate (Othman and Benson, 1993). Proskin (1998) investigated the effects of temperature gradients and boundary conditions on the dewatering of Syncrude oil sands tailings samples. He conducted single and multiple layer freeze–thaw tests that emphasized the efficacy of lower freezing rates and lower temperature gradients on the dewatering and strength properties of oil sands tailings samples (Proskin, 1998). However, fluctuating upward-trending temperatures due to global warming and snow cover may limit the frost depth in the field, contributing to lower volumes of frozen tailings and overall lower dewatering properties. Hence, the contrasting effects of lower temperature gradients and thinner frost depth on the dewatering properties of tailings necessitate the experimentation of a range of temperature gradients in the laboratory to account for the variability in results. Given the prevalence of the number of freeze–thaw cycles, the temperature gradient and the freezing rate, there is a need to develop a fundamental understanding of the freeze–thaw effect on the stability of oil sands tailings surfaces.

Previous research (Segó, 1992; Proskin, 1998; Proskin et al., 2012) demonstrated that pore water chemistry plays a major role in the dewatering and strength properties of tailings, and this chemistry can be substantially variable due to changes in ore geology, the bitumen extraction process, the tailings depositional strategy and the tailings treatment process (Proskin et al., 2012). The treated tailings samples analyzed in this paper were both pre-treated with flocculants/polymer and hence, is expected to behave differently from the untreated tailings when exposed to freezing and thawing.

The research study in the present paper proceeded from earlier research works (as mentioned above) on oil sands tailings which were mostly limited to the freeze-thaw cycle effects on untreated FFT deposits, particularly MFT. Single and multiple thin layered MFT deposits were investigated in the past where the thin lifts placement overall provided better drainage and utilization of atmospheric drying (evaporation and freeze-thaw process) to facilitate higher dewatering. The present paper will investigate the challenges of the freeze-thaw process associated with the deep deposits of polymer amended treated tailings having low initial water contents. Since tailings particles are extremely sensitive to the changes in physico-chemical interactions, polymer amended treated tailings are hence, expected to respond differently to freeze-thaw process compared to the untreated MFT. Furthermore, as mentioned above, there was no basis of the extent of the number of freeze-thaw cycles in the laboratory and one to three cycles were typically carried out based on researchers' own judgement. This paper extended to five freeze-thaw cycles and continued with drying-wetting cycle afterwards to investigate the extent when wetting behaviour will have a minimal impact on strength reduction. To the authors' knowledge, multiple freeze-thaw cycles followed by drying-wetting cycles on polymer amended treated tailings deposits had never been investigated before. An in-depth understanding of the individual effects of multiple freeze thaw cycles and drying-wetting cycles can further be combined as multiple freeze-thaw-drying-wetting cycles simulating field conditions. Since the total frozen and thaw depth of the field deposit is predominantly dependent on the site climatic conditions, material thermal properties and thermal boundary conditions (Dawson et al., 1999), the site-specific thermal properties based on the water content (restricted to MFT mostly) are not applicable for the sites having lower water contents deposits. Therefore, given the similar ranges of thermal boundary conditions in the field, the outcomes of this small-scale laboratory tests can be utilized to calibrate the thermal properties to be used in thermal modeling in order to predict the treated tailings field behaviour over the longer period of time.

## **2.3 Laboratory Experiments**

### **2.3.1 Test Materials**

The materials tested at the University of Alberta Geotechnical Centre laboratories consisted of two types of treated tailings: centrifuged tailings and in-line thickened tailings. Both of the samples were collected from Syncrude's Mildred Lake Mine in Fort McMurray, Alberta.

Centrifuge tailings/cakes are the end products of commercial centrifuge plant having a capacity of producing more than 70 tonnes of cakes per hour (Spence et al., 2015). This process is implemented by injecting FFT with an anionic polyacrylamide flocculant and coagulating agent (gypsum) prior to feeding into the centrifuge that uses centrifugal force to separate water out of FFT (Mikula et al., 2008). Similarly, in-line thickened tailings (ILTT) is under pilot scale demonstration that implements in-line mixing of a flocculant (anionic Polyacrylamide) with FFT prior to deposition (Jeeravipoolvarn, 2010; CTMC, 2012). This method relies on having active water management by means of decant structures and mechanical channelling (rim ditching) to promote self-weight consolidation (OSTC and COSIA, 2012; Beier et al., 2013). The difference in centrifuge treatment process is the addition of a coagulant agent (gypsum) prior to centrifugation (Mikula et al., 2008; OSTC and COSIA, 2012) which is precluded in the investigated ILTT deposit. Upon receiving the sample and followed by thorough mixing, laboratory investigations including index properties, solids mineralogy and pore water chemistry were conducted and analysed using standard ASTM procedures and specialized test methods.

### **2.3.2 Test Equipment and Methodology**

#### **2.3.2.1 Characterization Testing**

Water content was determined according to the ASTM (2019) D2216 procedure for determining Water (Moisture) Content of Soil by which the sample was oven-dried at 105°C for 24 hours. Specific gravity ( $G_s$ ) was determined as outlined in ASTM (2014) standard D854 for determining the specific gravity of soil solids by water pycnometer. The liquid limit and plastic limit tests were performed according to the ASTM (2017) standard D4318 for the liquid limit, plastic limit and plasticity index for soils.

The solids mineralogy was determined using X-ray diffraction (XRD) on bitumen-free samples by using an ultrasonic bath and centrifuge followed by a glycol vapour bath for 24 hours. The Methylene Blue index to compute the clay fraction (MBI) was determined as per the ASTM (2019) standard C837-09 for the Methylene Blue index of clay. To correlate mineralogy with cation exchange, individual cations ( $\text{Na}^+$ ;  $\text{K}^+$ ,  $\text{Ca}^{2+}$  and  $\text{Mg}^{2+}$ ) were determined using the ammonium acetate method as suggested by Hendershot et al. (2008).

The water chemistry tests were conducted on the samples and pore water. The pH and electrical conductivity (EC) were measured using a benchtop pH/EC meter following the procedure outlined in ASTM (2019) standard D4972 for determining the pH of soils and ASTM (2014) standard D1125 for determining the electrical conductivity and resistivity of water, respectively. The concentrations of  $\text{Na}^+$ ,  $\text{K}^+$ ,  $\text{Mg}^{2+}$  and  $\text{Ca}^{2+}$  ions were determined by the inductively coupled plasma method as per Standard Methods (2017) 3125. Likewise, the Automated Ferricyanide Method using a Colorimetric Centripetal Analyzer determined the concentrations of  $\text{Cl}^-$  and  $\text{SO}_4^{2-}$  ions, and the ASTM (2017) standard D4327 for anions in water by suppressed ion chromatography was employed to determine the concentrations of  $\text{HCO}_3^-$  and  $\text{CO}_3^{2-}$  ions.

#### 2.3.2.2 *Cyclic Freeze-Thaw Test*

A one dimensional (1D) closed system top-down freezing test was conducted in the laboratory for five consecutive freeze–thaw cycles. The American Society for Testing and Materials guidelines on how to artificially freeze soil samples were followed including the provisions of one-dimensional freezing, good insulation chambers, thermistor placement and thermoelectric cooling plates (ASTM-STP 599, as reported in Baker (1976)). Since freezing in nature is one and unidirectional, the 1D top-down freezing test is recommended in the laboratory to simulate field conditions and to restrict upward heaving during freezing (Johnson et al., 1993; Proskin, 1998; and Dawson et al., 1999). Although open system freezing occurs in nature, closed system freezing was preferred in the laboratory to assess the freeze–thaw processes due to the internal water migration and re-distribution. As investigated by Othman and Benson (1993), Dawson and Sego (1993) and Dawson et al. (1999), a 3D reticulate ice network is formed in the closed system similar to the

open system freezing conditions in the field. Consequently, similar results can be expected irrespective of the external drainage conditions because the extremely low hydraulic conductivities of the tailings ( $1 \times 10^{-6}$  to  $1 \times 10^{-9}$  m/s as reported in Beier et al., 2016; Kabwe et al., 2017) will limit moisture transfer rates needed for open system freezing (MacKay, 1974; Proskin et al., 2012)

In past research, the number of cycles to capture the whole freeze–thaw effects are dependent on the researcher’s judgement (Sanchez Sardon, 2016). Beier and Segó (2009) applied five cycles on coal tailings, which led to an asymptotic dewatering and strength gain in the samples; thus, five cycles were initially selected to observe the seasonal dewatering impact on the tailings materials. Table 2.1 summarizes the total number and duration of tests performed on each sample.

Table 2.1: Summary of the laboratory testing information

Type of tailings	Total number of tests	Total number of cycles	Temperature gradient (°C/mm)	Total duration of test (days)
Centrifuged tailings	3	5 cycles of freeze-thaw	0.083	85
		1 cycle of drying-wetting		
		Same as above	0.056	85
In-line thickened tailings	1	Same as above	0.028	78
		Same as above	0.028	70

Figure 2.1 shows the schematic diagram of the freeze–thaw test setup for the tailings samples. Each sample was poured into a 100 mm diameter freezing cell at an initial height of 180 mm. The freezing cell was then transferred to a walk-in freezer where the temperature was maintained between 0 and 1°C. Freezing temperatures were applied to the freezing cells through two temperature baths to provide constant boundary connections. The bottom boundary temperature was set at 0°C, while the top boundary temperatures were set at -15, -10 and -5°C for three different samples of centrifuged tailings, thus resulting in temperature gradients of 0.083, 0.056 and

0.028°C/mm, respectively. These temperatures were selected based on the average historical weather data for Fort McMurray. Additionally, three thermistors were installed along the walls of the freezing cell at fixed distances of 40, 80 and 120 mm from the bottom cell plate to monitor temperatures within the tailings at different depths. Insulation was wrapped around the cell to ensure one dimensional vertical freezing.

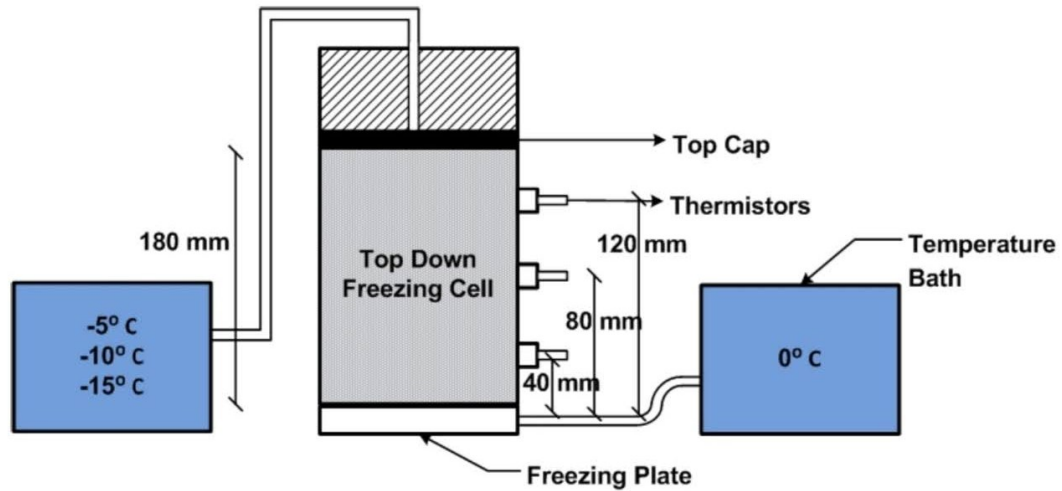


Figure 2.1: Schematic diagram of the freeze- thaw test setup

Samples were allowed to freeze for 72 hours until a constant equilibrium temperature was observed. Upon freezing, the cell was disconnected from the baths and allowed to thaw in the freezer ( $\sim 1^{\circ}\text{C}$ ) for 24 hours followed by another 48 hours under room temperature ( $\sim 20^{\circ}\text{C}$ ) in the laboratory. Upon complete thaw, the free water accumulated at the top was decanted to simulate surface drainage, and the change in height was recorded. The removal of water thus contributed to the increase in solids content of the tailings sample. Afterwards, the undrained shear strength was measured using a benchtop vane shear apparatus according to the ASTM (2016) standard D4648/S 4648M-16. A vane with a width and a height of 12.5 x 12.5 mm was inserted into the sample to their full length such that the top of the vane was level with the sample surface. The vane was rotated at a uniform rate of 60°/minute until the sample failed and the torsional force (further converted to strength) required to cause shearing was calculated using the calibration data provided with the vane device. Likewise, EC was measured at the near surface (measured at a depth of 15

mm from the surface) using a benchtop pH/EC meter. It is noteworthy to mention that the full profile was not measured to limit the sample disturbance. Once a cycle was completed, the whole procedure was repeated for another four cycles.

Given the limited time frame and resources, the ILTT sample was run for a single temperature gradient of  $0.028^{\circ}\text{C}/\text{mm}$  based on the overall improved performances (dewatering and strength) of centrifuged tailings under this temperature gradient compared to the other gradients. Also, the surface temperature profile of the ILTT field deposit varies from 0 to  $-8^{\circ}\text{C}$  with an average of  $-5^{\circ}\text{C}$  (a temperature gradient of  $0.028^{\circ}\text{C}/\text{mm}$ ) (BGC and O’kane, 2014).

#### 2.3.2.3 *Atmospheric Drying and Wetting Test*

After the five cycles of freeze–thaw tests were completed, each of the samples were subjected to atmospheric drying tests and measurement of near surface shear strength tests. The first phase of the drying test was carried out at room temperature ( $\sim 20^{\circ}\text{C}$ ) under which the weight loss due to evaporation/drying was recorded daily along with the subsequent shear strength measurements. The drying test continued for about a month (dried to a target actual evaporation/potential evaporation (AE/PE) ratio of 0.7 for each test) followed by a single wetting event to simulate rainfall. The volume of water evaporated during atmospheric drying was re-introduced as distilled water for the wetting test. Upon wetting, the second phase of the drying test was repeated for another twenty days to investigate the effects of rainfall on the strength of the tailings surface by examining the samples pre- and post-wetting. However, the laboratory test precludes the variation of daily temperature, wind speed and relative humidity (although the average monthly relative humidity was measured 47% in the laboratory while the field average monthly relative humidity varies from 40-51% in spring and summer as reported in weather statistics, Government of Canada) that may have an impact on field conditions.

#### 2.3.2.4 *Sectional Analysis*

After the cyclic freeze–thaw–drying–wetting tests were completed, each of the samples were sectioned into five equal parts (approximately 2 cm in height) for measuring the water content and EC distribution profiles.

## 2.4 Results

### 2.4.1 Characterization of Tailings

The index properties of the two tailings samples are summarized in Table 2.2. Water content, specific gravity and Atterberg limits (liquid limit and plastic limit) were all measured, while the solids content and densities were calculated. The measured water contents of the centrifuged tailings and ILTT samples were 89 and 122%, respectively. The presence of bitumen (specific gravity of 1.02) resulted in a low specific gravity ( $G_s$ ) for both of these tailings (2.24 for the centrifuged tailings and 2.45 for the ILTT sample), compared to typical sedimentary clays for which  $G_s$  ranges between 2.6 and 2.9 (Das, 1983). A marginally lower liquid limit value (provided in Table 2) for the centrifuged tailings sample is attributed to the higher sodium concentration (Miller et al., 2010) and indicates that these values are highly influenced by the combined effect of clay mineralogy, water chemistry and bitumen content (Scott et al., 1985).

Table 2.2: Summary of the index properties of the tailings

Property	Centrifuged tailings sample	ILTT sample
Water content, $w$ (%)	89	122
Solids content, $s$ (%) <sup>1</sup>	53	45
Specific gravity, $G_s$	2.24	2.45
Dry density, $\rho_D$ (gm/cm <sup>3</sup> ) <sup>2</sup>	0.75	0.61
Bulk density, $\rho$ (gm/cm <sup>3</sup> ) <sup>3</sup>	1.42	1.36
Liquid limit, $w_l$ (%)	57	62
Plastic limit, $w_p$ (%)	26	23

$$^1s = 1 / (1 + w)$$

$$^2\rho_D = \frac{G_s * \rho_w}{1 + w * G_s}, \text{ where } \rho_w = \text{density of water}$$

$$^3\rho = \rho_D (1 + w)$$

Table 2.3 gives a summary of the solids mineralogy of the two investigated tailings samples. The two tailings samples are characterized as predominantly clay minerals comprised mainly of kaolinite and illite, which is a reflection of the average clay mineralogy of the parent material, the oil bearing Cretaceous McMurray formation (Miller et al., 2010). However, one of the major differences between these two tailings samples is clay content.  $\text{Ca}^{2+}$  ion was found to be the major exchangeable cation for centrifuged tailings, whereas both  $\text{Ca}^{2+}$  and  $\text{Na}^{+}$  ions contributed equally as the major exchangeable cations accounting for more than half of the total CEC. These values are attributed to the presence of kaolinite (typically 3–15 meq/100g) and illite (typically 10–40 meq/100g) (Mitchell and Soga, 2005).

Table 2.3: Summary of the solids mineralogy of the tailings

Property	Centrifuged tailings sample	ILTT sample
Minerals (% weight)	Non-clay: Quartz (40); Siderite	Non-clay: Quartz (18); Siderite
Bulk and clay	(3); Potassium Feldspar (2); Pyrite (2); Dolomite (1)	(2); Potassium Feldspar (1); Plagioclase Feldspar (1)
	Clay: Kaolinite (36); Illite (15) = Total clay (52%)	Clay: Kaolinite (56); Illite (24) = Total clay (80%)
Clay fraction (%)	50	68
From MBI		
Exchangeable cations (cmol(+)/kg)	$\text{Ca}^{2+}$ (10); $\text{Na}^{+}$ (4.4); $\text{Mg}^{2+}$ (2.6); $\text{K}^{+}$ (0.4)	$\text{Ca}^{2+}$ (7.5); $\text{Na}^{+}$ (7.5); $\text{Mg}^{2+}$ (2.8); $\text{K}^{+}$ (0.5)
Total CEC (meq/100g)	17.4	18.3

Table 2.4 summarizes the pore water chemistry of the two investigated tailings. The dewatering properties of the tailings materials are predominantly governed by the complex physicochemical interactions at the solid-liquid phase boundaries (Scott et al., 1985). The pH measured 8.7 and 8.3 for the centrifuged tailings and ILTT sample, respectively, which is within the typically range (8.0–8.5) maintained in the extraction process to facilitate bitumen removal from the solid particles. The EC measured 3,560 and 2,800  $\mu\text{s}/\text{cm}$  for the centrifuged tailings and the ILTT sample, respectively, which is typical for fine grained soils (100–10,000  $\mu\text{s}/\text{cm}$ ), as reported by

Mitchell and Soga (2005). In addition to the enrichment of clay content, ILTT were found to contain lower concentrations of divalent cations ( $\text{Ca}^{2+}$ ,  $\text{Mg}^{2+}$ ) compared to the centrifuged tailings. However,  $\text{Na}^+$  and  $\text{HCO}_3^-$  were found to be the dominant ions for both of the tailings pore fluids. The presence of  $\text{Na}^+$  is attributed to the addition of NaOH during the extraction process and that of  $\text{HCO}_3^-$  is associated with  $\text{CO}_2$  adsorption during aeration for bitumen extraction (Jeeravipoolvarn, 2005).

Table 2.4: Summary of pore water chemistry results

Property	Centrifuged tailings sample	ILTT sample
pH	8.7	8.3
Electrical conductivity ( $\mu\text{s}/\text{cm}$ )	3,560	2,800
Dissolved ions (mg/L)	Cations: $\text{Na}^+$ (780); $\text{Ca}^{2+}$ (36.5); $\text{Mg}^{2+}$ (15.9); $\text{K}^+$ (14.6) Anions: $\text{HCO}_3^-$ (1,207); $\text{Cl}^-$ (446); $\text{PO}_4^{3-}$ (48); $\text{SO}_4^{2-}$ (17.7); $\text{CO}_3^{2-}$ (3.5); $\text{F}^-$ (2.47); $\text{Br}^-$ (0.53); $\text{NO}_3^-$ (0.26);	Cations: $\text{Na}^+$ (677); $\text{Ca}^{2+}$ (13); $\text{K}^+$ (8); $\text{Mg}^{2+}$ (6.6) Anions: $\text{HCO}_3^-$ (1,070); $\text{Cl}^-$ (631); $\text{SO}_4^{2-}$ (29); $\text{CO}_3^{2-}$ (<5); $\text{OH}^-$ (<5); $\text{F}^-$ (2.47); $\text{NO}_3^-$ (<0.5)
Total dissolved solids (mg/L)	2,573	1,890
Sodium adsorption ratio (SAR)	27.2	38.1

#### 2.4.2 Cyclic Freeze-Thaw Test Results

After each freeze–thaw cycle, the height change associated with freeze–thaw was measured and converted to a void ratio using the following equation:

$$\frac{\Delta H}{H} = \frac{\Delta e}{1+e_o} \quad [2.1]$$

where,  $\Delta H$  is the change in height after thawing,  $H$  is the total frozen height just before thawing,  $\Delta e$  is the change in void ratio, and  $e_o$  is the initial void ratio at the start of each freeze–thaw cycle.

Based on the change in void ratio, the corresponding water content was calculated for the entire sample using mass-volume relationship. The full profile of the water content distributions (including surface) could not be measured after each freeze-thaw cycle as sampling would disrupt the integrity of the sample while repeatability of each test would require a considerable amount of time within the limited resources. Hence, the water contents reported at each freeze-thaw cycle represent the estimated water content of the entire sample calculated based on the thaw strain. On the contrary, the shear strengths reported in this paper at each freeze-thaw cycle represent the measured shear strength at nominally 6 mm (centre of the vane to surface) below the surface only.

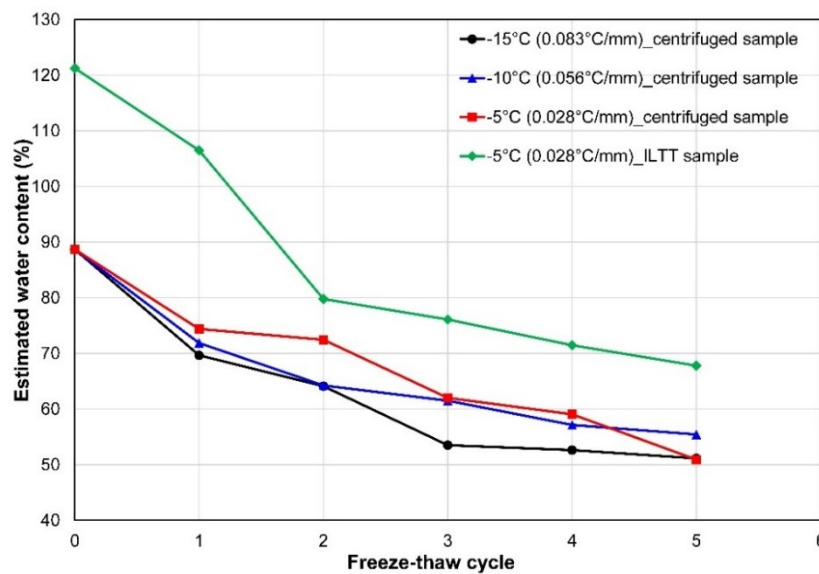


Figure 2.2: Estimated water content (%) versus number of freeze-thaw cycles

Figure 2.2 shows the cumulative reduction in estimated water content for the centrifuged tailings samples subjected to three temperature gradients of 0.083, 0.056 and 0.028°C/mm, and the ILTT sample subjected to a temperature gradient of 0.028°C/mm. The water content of the centrifuged tailings samples corresponding to the three temperature gradients of 0.083, 0.056 and 0.028°C/mm after five freeze–thaw cycles were calculated to be 51.1, 55.4 and 50.9%, respectively, from an initial value of 89%. Likewise, the final water content of the ILTT sample reduced to 68% from an initial water content value of 122%. As evident in the Figure 2.2, centrifuged tailings sample subjected to the temperature gradient of 0.028°C/mm exhibited an overall decreasing trend in water content at the end of five cyclic freeze-thaw, while the water contents of the other samples

gradually decreased with each freeze-thaw cycle followed by an asymptotic water content reduction at the end of five cycles.

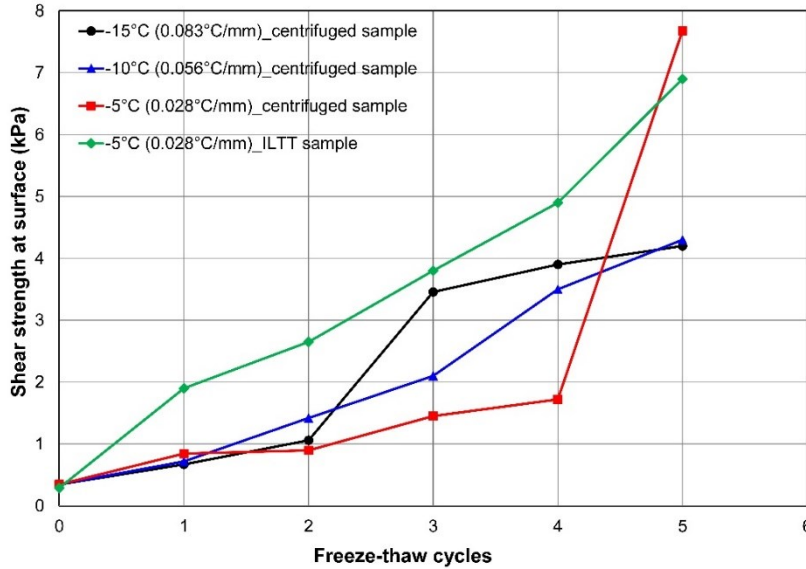


Figure 2.3: Measured shear strength versus number of freeze–thaw cycles

Figure 2.3 depicts the undrained shear strength measured at the near surface (A 12.5 mm vane was inserted until the top was level with the surface) after each freeze–thaw cycle. The strength continued to increase from values of 290–345 Pa to 4–8 kPa after five cycles of freeze–thaw. The highest shear strength was measured, on the lower temperature gradient centrifuged tailings sample, to be approximately 8 kPa after five freeze–thaw cycles. Likewise, the near surface shear strength was measured to be approximately 7 kPa for the ILTT sample subjected to the same temperature gradient, albeit the increase in strength was more gradual.

The exclusion of a coagulant/gypsum (divalent cation,  $\text{Ca}^{2+}$ ) in the ILTT treatment process is expected to influence the dewatering and physico-chemical properties of the tailings. To illustrate the impact of coagulant addition on freeze–thaw dewatering in an oil sands tailings deposit, the physico-chemical properties were assessed through EC measurements (Figure 2.4).

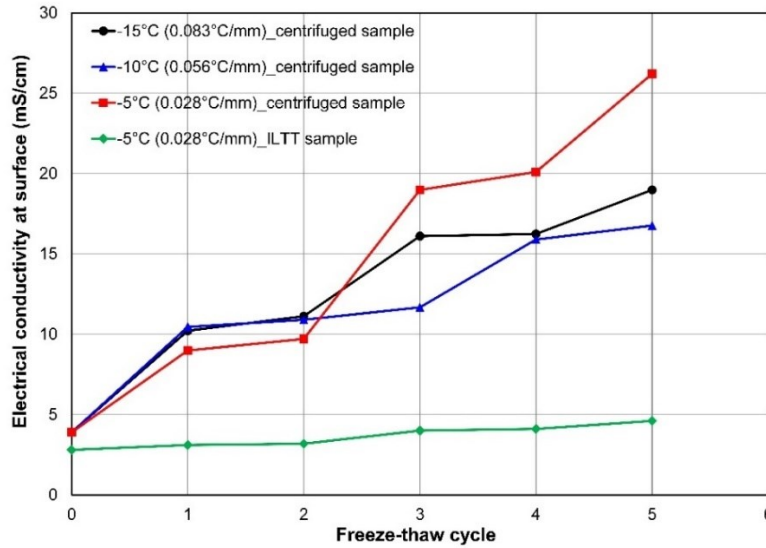


Figure 2.4: Measured electrical conductivity vs the number of freeze-thaw cycles (measured at a depth of 15 mm from the surface)

As evident in Figure 2.4, the increase in EC at the near surface with each freeze–thaw cycle was measured for the tailings samples under all the investigated temperature gradients. An increase in EC after each freeze–thaw cycle suggests an increase in ion concentration that can be related to the increase in osmotic suction, a component of the total suction (Innocent-Bernard, 2013). The increase in ion concentration is attributed to the migration of salts towards the surface along with unfrozen water due to the freeze–thaw mechanism. It is expected to increase the EC from its initial value, due to the reduction in water content through the cyclic freeze–thaw and drying–wetting phase (Innocent-Bernard, 2013). However, the increase in surface EC was significantly higher (4–7 times higher than the initial EC of 3.9 mS/cm) for the centrifuged tailings samples compared to the ILTT sample (approximately 1.6 times higher than its initial EC of 2.8 mS/cm). The highest EC value of 26.2 mS/cm was measured on the centrifuged tailings sample subjected to the lower temperature gradient.

### 2.4.3 Atmospheric Drying-Wetting Test Results

Figures 2.5 through 2.8 show the atmospheric drying–wetting test results for the samples subjected to different temperature gradients. Similar to the freeze-thaw tests, the water contents shown here

represent the estimated average water contents of the sample calculated based on the mass loss, while the shear strength refers to the measured one near the surface. As expected, surface drying can typically induce a crust layer of oil sands tailings through shrinkage, crack formation and desiccation (Figure 2.9a). However, the critical part is to see if the improved strength in the upper zone can be sustained throughout unpredictable environmental conditions. The centrifuged tailings samples subjected to temperature gradients of  $0.083$  and  $0.056^{\circ}\text{C}/\text{mm}$ , and the ILTT sample subjected to a temperature gradient of  $0.028^{\circ}\text{C}/\text{mm}$  collapsed upon wetting after a month of drying. The integrity of the samples was disrupted, sample heterogeneity was more intensified (Figure 2.9b) and the shear strength decreased from approximately  $40$  kPa (centrifuged tailings) and  $60$  kPa (ILTT sample) to non-significant values after the immediate simulated rainfall. Conversely, the centrifuged tailings sample with lower temperature gradient ( $0.028^{\circ}\text{C}/\text{mm}$ ) showed a comparably low water content ( $13\%$ ) and higher undrained shear strength ( $>100$  kPa) at the end of the atmospheric drying–wetting test.

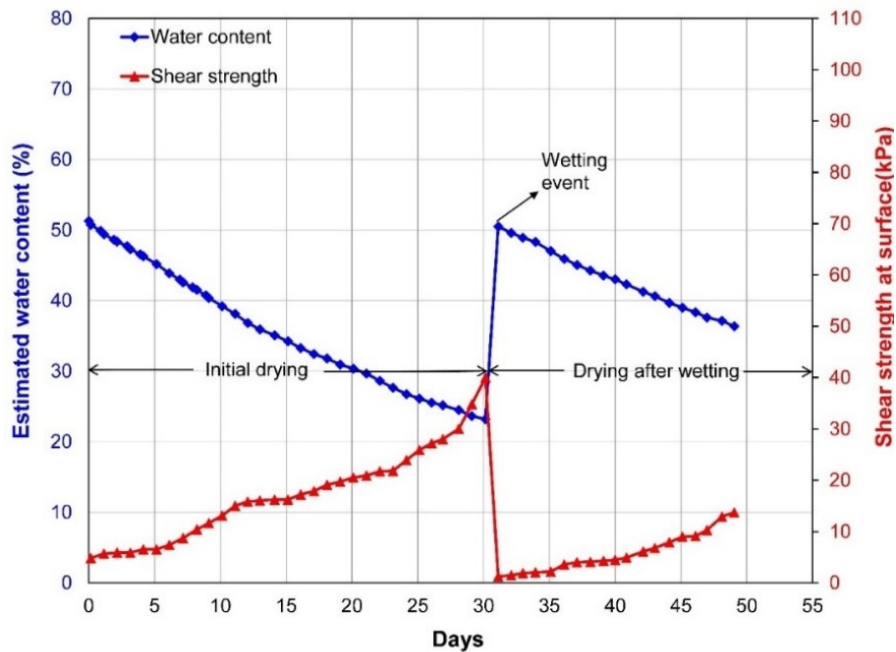


Figure 2.5: Water content and shear strength progression of the centrifuged tailings sample over time at a temperature gradient of  $0.083^{\circ}\text{C}/\text{mm}$

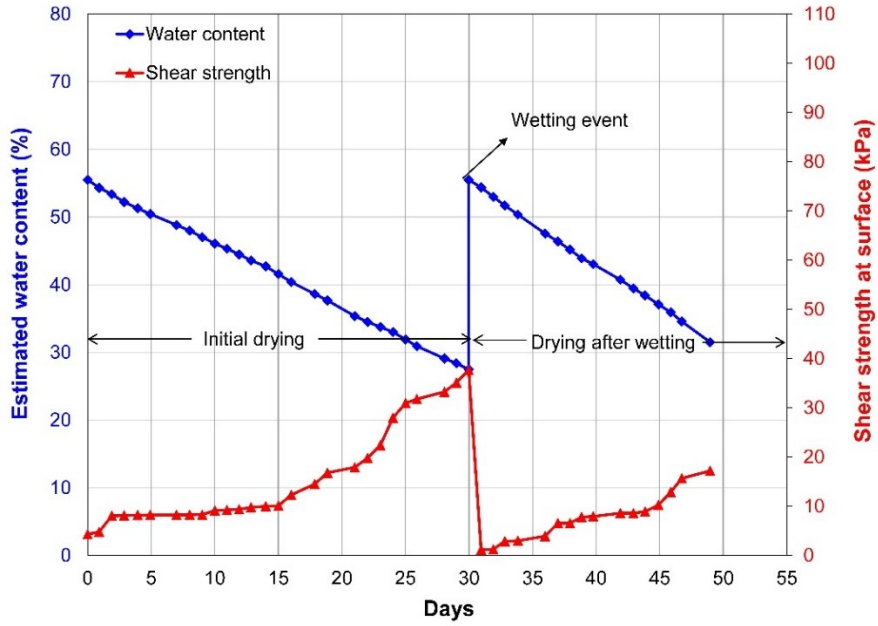


Figure 2.6: Water content and shear strength progression of the centrifuge tailings sample over time at a temperature gradient of  $0.056^{\circ}\text{C}/\text{mm}$

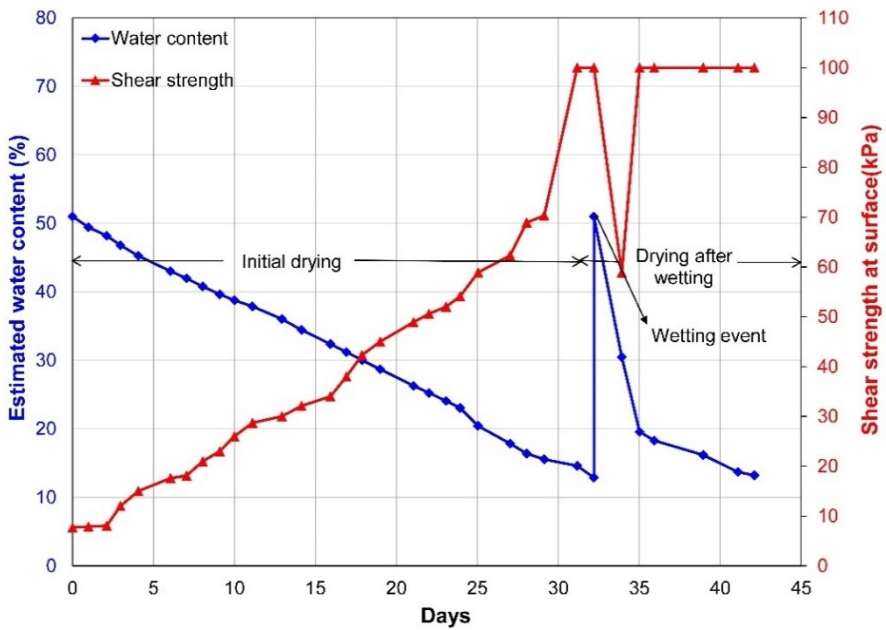


Figure 2.7: Water content and shear strength progression of the centrifuged tailings sample over time at a temperature gradient of  $0.028^{\circ}\text{C}/\text{mm}$

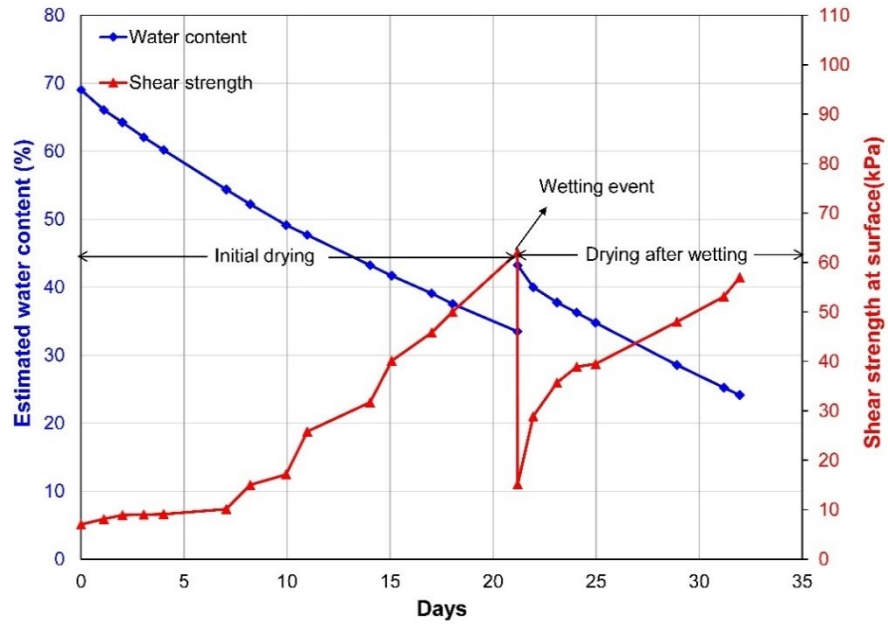


Figure 2.8: Water content and shear strength progression of the ILTT sample over time at a temperature gradient of  $0.028^{\circ}\text{C}/\text{mm}$



Figure 2.9: Photographs of drying-wetting test; 2.9a (left) shrinkage and cracking observed after drying test; and 2.9b (right) over-consolidated peds at the surface after wetting test

The second phase drying results (as shown in Figure 2.5 through 2.8) after the wetting event showed a reduction in shear strength compared to the initial drying phase. The centrifuged tailings samples subjected to temperature gradients of 0.083 and 0.056°C/mm reduced to shear strengths of 14 and 17 kPa, respectively. Due to the crust formed at the surface, the sample with lower temperature gradient was unaffected by the wetting event, and consequently, the shear strength remained unchanged (>100 kPa) after an initial drop in shear strength on the day of wetting. Though its shear strength significantly dropped immediately upon wetting, the ILTT sample subjected to the similar lower temperature gradient (0.028°C/mm) eventually was able to regain its initial drying phase shear strength (~60 kPa). However, a surface crust was not formed.

#### 2.4.4 Sectional Analysis

Figure 2.10 shows the sectional analysis results that depict the measured final water content profiles throughout the depth of the sample. The sectional analysis showed that the lowest water content was achieved at the surface of the investigated samples. As evident in Figure 2.10, both the centrifuged and ILTT tailings samples subjected to the lower temperature gradient resulted in lower water content followed by the centrifuged tailings samples with higher temperature gradients. At the end of the test, it was the centrifuged tailings sample of lower temperature gradient that developed a crust of 2 cm and achieved the lowest water content of 13% at the surface. Table 2.5 shows the comparisons between the final measured and estimated water content. The estimated water content based on the mass loss/thaw strain were found in good agreement with the water content measured at the surface after sectional analysis (through oven drying).

Table 2.5: Comparisons between the final measured and calculated water content

Water content (%)	Centrifuged tailings sample			ILTT sample
	0.083°C/mm	0.056°C/mm	0.028°C/mm	0.028°C/mm
Estimated	36.3	31.5	13	24
Measured (top sectional layer)	38.5	34.8	14	24.4

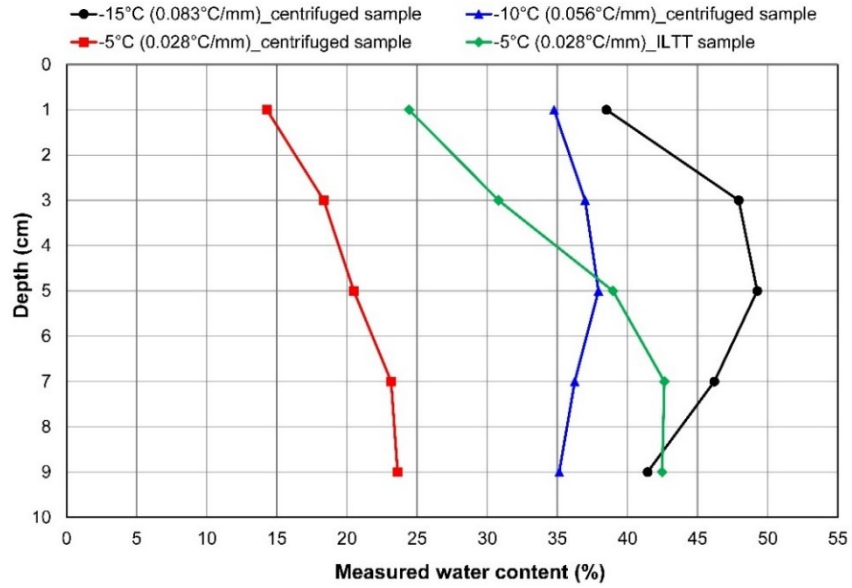


Figure 2.10: Measured water content profile at the end of the test

Figure 2.11 depicts the EC profiles throughout the depth of the investigated samples. The lower water content at the surface (as shown in Figure 2.10) resulted in a higher EC value followed by a gradual decrease with depth in the sample cell.

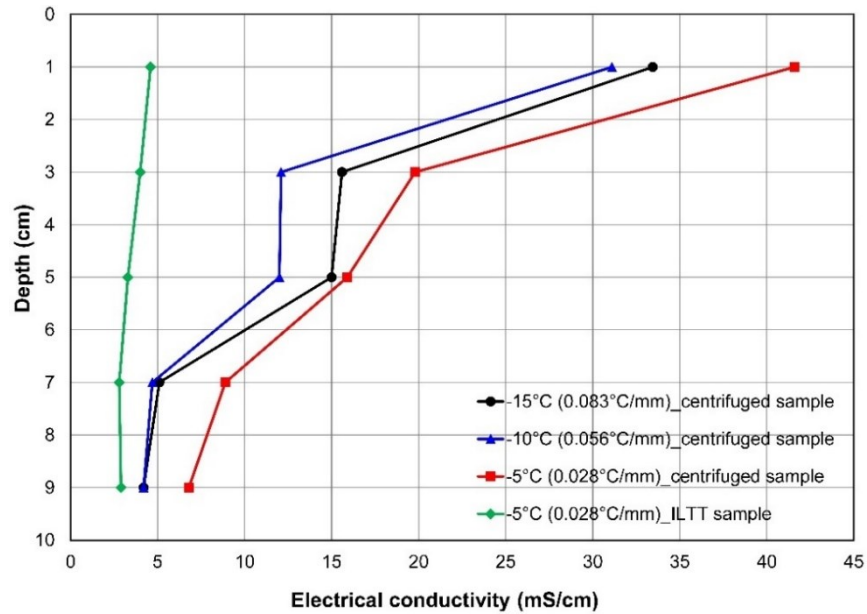


Figure 2.11: Measured electrical conductivity profile at the end of the test

## 2.5 Discussion

It is widely acknowledged that oil sands particles are highly negatively charged clay particles that are susceptible to changes in grain size distribution, clay content, solids mineralogy and pore fluid chemistry (Mitchell and Soga, 2005). Both of the investigated tailings samples were characterized as fine-grained materials consisting mainly of quartz, kaolinite and illite. However, the major difference is attributed to the difference in clay fraction. Because of the fairly high clay fraction (80% in the ILTT sample compared to 52% for the centrifuged tailings), in a basic solution (pH > 8) the ILTT sample predominated the negative charges at the particle edges with OH<sup>-</sup> serving as the potential determining ion (Prasanphan and Nuntiya, 2006). The net negative charge is the primary factor in controlling clay dispersion, and this can be attributed to the changes in pH, ionic strength and cation type (Chorom and Rengasamy, 1995; Kaminsky, 2008). The prevalence of Na<sup>+</sup> and HCO<sub>3</sub><sup>-</sup> ions in the pore water are responsible for facilitating the electrostatic repulsion in the dispersed card house structure of the kaolinite water system, as reported by Jeeravipoolvarn (2005). Based on the double layer theory, the increase in electrolyte concentration and ion valency can cause the clay particles to overcome the electrostatic repulsion, thereby resulting in the flocculation and re-orientation of the clay particles in response to the reduced repulsion (Mitchell and Soga, 2005; Proskin et al., 2012). Given the concentrations of Na<sup>+</sup>, Ca<sup>2+</sup> and Mg<sup>2+</sup> ions in Table 4, the calculated SAR values of the centrifuged and ILTT tailings samples were 27.2 and 38.1, respectively. According to Miller et al. (2010), SAR values higher than 20 indicates the likely dispersed structure. Though dispersed, the initial higher EC, presence of marginally higher divalent cations due to the coagulant and lower SAR value for the centrifuged tailings contributed to improved dewatering performance compared to the ILTT sample under similar testing conditions.

As evident in Figures 2.2 and 2.3, the estimated water content and measured shear strength properties of the investigated samples all improved through cyclic freeze–thaw dewatering. When the soft saturated fine-grained tailings are subjected to below freezing temperatures, a freezing front advances through the tailings that induces large suctions below the front due to the surface tension differences between the unfrozen water surrounding the mineral particles and ice filling the voids. The suction causes water to migrate from the underlying unfrozen tailings towards the growing ice lenses which eventually form a three dimensional reticulate ice network (although

these structures were not visually inspected in the laboratory since frozen core samples were not taken to limit the disturbance and taking photos of these ice lenses during testing was precluded to ensure proper insulation wrapping around the cell ) surrounding the frozen tailings peds (Dawson et al., 1999; Andersland and Ladanyi, 2004; Beier and Segó, 2009). Upon thawing, these ice lenses become conduit channels for upward water movement, thereby facilitating the settlement of heavier soil peds at the bottom and overall volume reduction (Rima and Beier, 2018).

Figures 2.2 through 2.4 show how samples tested under similar environmental conditions can be significantly affected by different temperature gradients. The thickness, frequency and spacing of ice lenses are predominantly controlled by the temperature gradient, and these ice lenses are the primary mechanism of freeze–thaw dewatering (Othman and Benson, 1993). The very high temperature gradient typically allows the frost front to advance faster such that water cannot be accumulated at a fixed place for growing ice lenses, while the lower temperature gradient draws more water to the frost front by suction, causing higher dewatering (Konrad and Morgenstern, 1980; Knutsson et al., 2016). This explanation supports the findings of this paper that was further supported by similar freeze–thaw experiment results conducted by Dawson et al. (1999), Eigenbrod et al. (1996) and Proskin (1998). Similar to the dewatering properties, the higher amount of free melt water accumulated at the surface of the sample subjected to the lower temperature gradient contributed to the higher shear strength. The soil peds at the microscale developed during freezing promotes internal attraction that results in the changes in soil structure and its mechanical behaviour (Beier and Segó, 2009; Proskin et al., 2012).

Figures 2.2 through 2.4 also illustrate the impact of pore water chemistry, flocculant/coagulant addition and the treatment process on strength gain in oil sands fine tailings. The addition of a coagulant significantly enhanced dewatering and the stability performance of centrifuged tailings compared to the ILTT sample under similar testing conditions. The shear strength gain at the surface (shown in Figure 2.3) with each freeze–thaw cycle was relatively higher in the initial cycles for the ILTT sample and somewhat similar (7-8 kPa) to the centrifuged tailings sample's strength at the end of the cyclic freeze–thaw testing. However, combining the other laboratory test results (drying–wetting test, final solids content profile and EC profile) and the overall performance of

the samples can provide insight to the further explanation of the differences between centrifuged tailings and ILTT sample.

It is widely acknowledged that the prevalence of negative charges at clay particle edges can be overcome by attracting a high concentration of cations at the clay boundary. This phenomenon results in greater electrical potential which causes clay particles to restrict the migration of electrically charged ions but allows electrically neutral water molecules to move freely (Witteveen et al., 2013). As shown in Figure 2.4, the increase in EC values for the centrifuged tailings samples after each freeze–thaw cycle is significantly higher compared to the ILTT sample. An increase in ion concentration results in a chemical concentration gradient that causes a volume reduction due to the combined influence of the processes of osmotic flow and osmotic compressibility. A higher chemical concentration gradient results in the migration of ions into the pores which reduces the inter-particle repulsive forces by forming particle assemblages. The formation of particle assemblages possibly leads to the suppression of the double layer and overall volume reduction (i.e. osmotic consolidation). Concurrently, clay particles, in response to osmotic gradients, cause osmotic flow to occur out of the sample that, in turn, develops negative pore water pressure/suction and an increase in effective stress, leading to an overall volume change (i.e. osmotically induced consolidation) (Barbour and Fredlund, 1989; Witteveen et al., 2013).

When tailings are subjected to below freezing temperatures, solutes/ions are re-distributed with water. The crystal lattice for ice is very sensitive as it only allows hydrogen and oxygen ions to form its regular lattice framework. Therefore, the solutes are expelled by the growing ice lenses as water freezes. The exclusion of solutes from the developing ice lenses with each cycle leads to the gradual increase in ion concentration within the remaining water (Proskin et al., 2012), as evident in Figure 2.4. Since increasing values of suction during freezing is responsible for attracting unfrozen water towards the freezing zone, salt/ion migration additionally facilitates the osmotic suction component that, overall, increases the total suction. Therefore, the improved dewatering properties of the centrifuged tailings can be attributed to the combined mechanism of volume changes due to freeze–thaw consolidation, osmotic consolidation and osmotically induced consolidation, while the ILTT sample dewatering is predominantly controlled by the freeze–thaw mechanism. Furthermore, the migration of salt is predominantly controlled by the temperature

gradient and the soil structure. The higher temperature gradient facilitates the fast movement of the freezing front, leading to ice occupying the transfer channel, thus restricting the migration of the salt concentration (Bing et al., 2015). This finding corroborated well with the results from Figure 4 where the highest EC value was recorded for the sample at a lower temperature gradient.

Figures 2.5 to 2.8 illustrate the atmospheric drying and wetting results that showed the progression of the water content and undrained shear strength at the surface with time. Like freezing, the driving force of evaporation/drying is suction. Instead of the liquid water/ice interface, suction occurs at the liquid water/gas interface due to the difference in vapour pressure and temperature between the soil and surrounding temperatures (Wilson et al., 1994). Surface drying/evaporation from the surface promotes volume shrinkage and cracking through the exposure of underlying material with lower suctions (as shown in Figure 2.9a). Therefore, the development of a desiccated surface crust is anticipated at soft tailings disposal sites to provide sufficient undrained shear strength for the reclamation operations (Johnson et al., 1993). Upon drying, the formation of surface cracks increased the surface area for evaporation that causes the degree of saturation to decrease, resulting in the overall volume change in the samples. The drying phase improved the strength properties by almost a magnitude higher than the freeze–thaw cycles for all of the investigated samples.

However, upon wetting, each of the samples responded differently. It is expected that an increase in water content will infiltrate into the underlying tailings through the cracks, thus lowering the shear strength. As seen in the centrifuged tailings samples with temperature gradients of 0.083 and 0.056°C/mm, both samples completely lost their strength due to the induced wetting event/rainfall. Conversely, the centrifuged tailings sample subjected to a gradient of 0.028°C/mm was almost unaffected by the wetting test, while the ILTT sample subjected to the same gradient was partially affected by rainfall (from 60 to 15 kPa). The atmospheric drying–wetting results corroborated well with the freeze–thaw results in terms of dewatering and strength properties, and this can be attributed to the formerly achieved water content just prior to the atmospheric drying test. Due to the crust formation at the surface, the centrifuged tailings sample with the lower temperature gradient achieved the lowest water content (<25% confirmed through the final water content profile shown in Figure 2.10) and possibly very high suction (although suctions were not measured

during the experiments). At higher solids content and very low water content, the suction can become so high that the suction loss due to hysteretic soil–water retention behaviour (Hen-Jones et al., 2017) induced by an alternate drying–wetting cycle may become insignificant in causing any impact on shear strength. In addition, the physico-chemical inter-particle forces govern the mechanical properties of cohesive soils at higher suction (Han and Vanapalli, 2016), which may resist the change in shear strength. Therefore, it can be concluded that the difference in pore water chemistry resulted in the differences in dewatering and strength properties between the centrifuged tailings and ILTT samples under similar boundary conditions.

Figure 2.10 shows the measured water content profile which is more of a confirmatory analysis along with Table 2.5 to support the accuracy of the estimated water content. The results confirmed the improvement of dewatering and subsequent strength due to the lower temperature gradient. Likewise, Figure 2.11 confirms the upward salt migration during freeze–thaw–drying testing, which is a contributing factor for an increase in ion concentration at the surface. The mechanism of water movement, controlled by the temperature gradient, determines, to a large extent, the mechanism of salt migration. Therefore, higher dewatering is also associated with a higher salt concentration at the surface. For the fine-grained tailings material, the salt migrated upward with unfrozen water towards the frozen zone due to convection followed by the exclusion of salt molecules from the growing ice lenses, thus leading to the increase in salt concentration at the surface (as shown in Figure 2.11). Once exposed to the atmosphere, evaporation/drying leaves behind the salt precipitates at the surface that further facilitates solute accumulation. In addition to the temperature gradient, salt migration is also influenced by the soil structure, moisture content and physico-chemical properties (Bing et al., 2015), which possibly shed light on the reason behind the significantly higher amount of salt accumulation for the centrifuged tailings (an order of magnitude higher than its initial value) compared to the ILTT sample with a similar boundary condition (twice its initial value). Hence, the employment of site-specific adaptive tailings management is paramount as each mine site, their treatment process and the inherent uncertainties associated with their target tailings volume generation are unique.

To preclude the effects of water content, clay content, solids mineralogy and pore water chemistry, the undrained shear strength of the two treated tailings are presented (Figure 2.12) with respect to

the liquidity index. The best fit line, as reported in Beier et al. (2013), establishes the relationship between the undrained shear strength and liquidity index for the typical MFT. As shown in Figure 2.12, both of the investigated treated tailings deposited at an initial water content much above their liquid limits (liquidity index of 1). With cyclic freeze–thaw, the samples achieved enhanced dewatering and shear strength gain by passing through the liquid limit. Further dewatering for densification and consolidation can be achieved if the drying/desiccation factor from evaporation is added (as shown in the rectangular area of the drying–wetting cycle effects in Figure 2.12). However, tailings had to be dried to an unsaturated state for getting to this stage which could be difficult to achieve in the field given the climate in northern Alberta. In addition to that, the influence of snow covers in winter and/or the prolonged/multiple wetting can also impact the expected field performance. Furthermore, the formation of surface crust cannot contribute to the trafficability in the field if the crust depth is limited and the underlying tailings are too soft. Hence, additional work is needed to evaluate how deep these natural processes will influence tailings under actual field conditions.

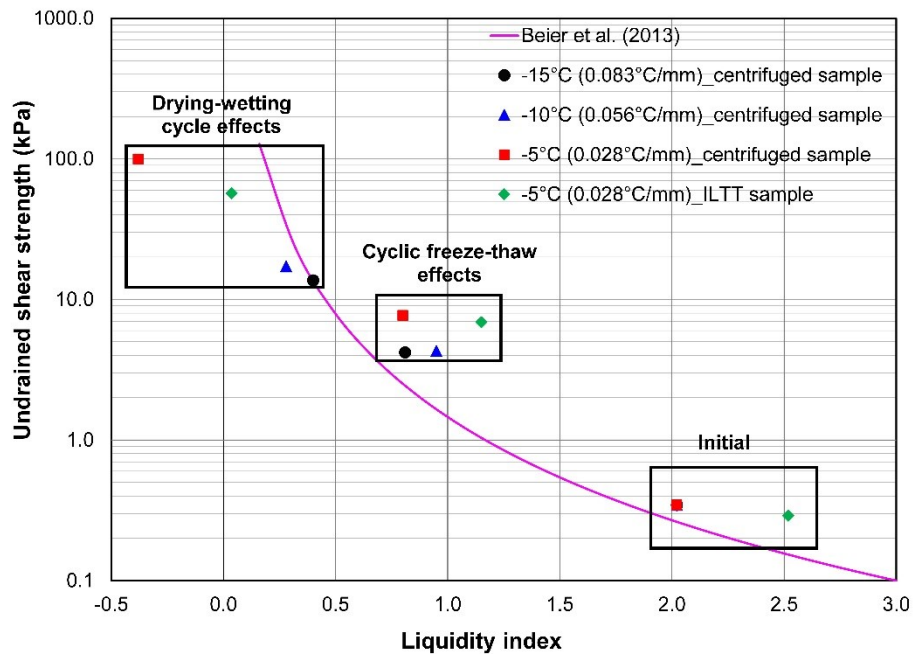


Figure 2.12: Undrained shear strength vs liquidity index of the two investigated tailings

## 2.6 Conclusion

The current approach for the mining industry is to use a single deep stacking depositional approach in order to minimize the required footprint for tailings management and to provide plans for efficient land use at the end of mine life with geotechnically secure containment of deposited tailings. This paper aimed to investigate different parameters that can affect the development of surface crust formation and suggests that a fundamental understanding and an appropriate prediction of tailings behaviour (dewatering and physico-chemical properties) combined with the monitoring performance of each treated tailings deposits are paramount to assess the long-term geotechnical behaviour of treated tailings deep deposits.

Two types of treated tailings were analyzed to evaluate the effects of freeze-thaw dewatering, evaporation/drying, rainfall and pore water chemistry. Based on the laboratory test results, the present paper revealed that the lower freezing temperature gradient contributed to higher freeze-thaw dewatering and subsequent higher undrained shear strength (~8 kPa for lower gradient sample vs 4 kPa for the other gradients samples). In addition, freeze-thaw dewatering coupled with evaporation/drying significantly increased the surficial strength of the tailings by an order of magnitude higher than multiple freeze-thaw cycles alone. The laboratory results also showed that the effects of rainfall had a minimal impact on the strength for the tailings samples with a very low water content (<25%) and possibly high suction. The impacts of pore water chemistry on dewatering and strength performance between centrifuged tailings and ILTT samples were evaluated by comparing the concentrations of divalent cations, EC values and salt migration phenomenon. An increase in ion concentration due to the probable higher osmotic suction component in conjunction with the higher concentration of divalent cations resulted in higher dewatering and enhanced strength for the centrifuged tailings. Overall, laboratory test approach can provide insights to predicting the mechanical properties of field deposits if the temperature gradients fall under the similar ranges in the field. The experimental results from the laboratory showed that the polymer amended treated tailings (centrifuged tailings and ILTT samples) will continue to dewater and gain sufficient strength for reclamation activities by incorporating a combination of consolidation, freeze-thaw dewatering and desiccation processes, provided adequate surface drainage is permitted. Hence, multiple freeze-thaw dewatering can be considered to facilitate surface strength for the deep deposits relying on self-weight consolidation.

## Acknowledgements

The authors would like to thank the Natural Sciences and Engineering Research Council of Canada (NSERC), Canada's Oil Sands Innovation Alliance (COSIA) and Alberta Innovates–Energy and Environment Solutions for their financial support. Thanks to Vivian Giang for proofreading and editing the paper.

## References

- Alberta Energy Regulator (AER), 2018. *State of Fluid Tailings Management for Mineable Oil Sands, 2017*. Report, Calgary, Alberta. See [https://static1.squarespace.com/static/52abb9b9e4b0cb06a591754d/t/5bcbdb777817f7df5097c309/1540086655594/Mineable\\_Oil\\_Sands\\_Fluid\\_Tailings\\_Status\\_Rpt\\_2017\\_Sept.28\\_Final.pdf](https://static1.squarespace.com/static/52abb9b9e4b0cb06a591754d/t/5bcbdb777817f7df5097c309/1540086655594/Mineable_Oil_Sands_Fluid_Tailings_Status_Rpt_2017_Sept.28_Final.pdf) (Accessed 04/04/2020)
- Alberta Energy Regulator (AER), 2020. *State of Fluid Tailings Management for Mineable Oil Sands, 2019*. Report, Calgary, Alberta. See <https://static.aer.ca/prd/2020-09/2019-State-Fluid-Tailings-Management-Mineable-OilSands.pdf> (Accessed 02/02/2021)
- Andersland, O.B. and Ladanyi, B. 2004. *Frozen Ground Engineering*, 2nd Edition, American Society of Civil Engineers & John Wiley & Sons Inc., Hoboken, New Jersey, USA.
- ASTM. 2014. Standard Test Methods for Electrical Conductivity and Resistivity of Water. *ASTM Standard D1125-14*. ASTM International, West Conshohocken, PA, 2014. DOI: 10.1520/D1125-14.
- ASTM. 2014. Standard Test Methods for Specific Gravity of Soil Solids by Water Pycnometer. *ASTM Standard D854-14*. ASTM International, West Conshohocken, PA, 2014. DOI: 10.1520/D0854-14.
- ASTM. 2016. Standard Test Methods for Laboratory Miniature Vane Shear Test for Saturated Fine-Grained Clayey Soil. *ASTM Standard D4648/ D4648M-16*. ASTM International, West Conshohocken, PA, 2016. DOI: 10.1520/D4648\_D4648M-16.
- ASTM. 2017. Standard Test Method for Anions in Water by Suppressed Ion Chromatography. *ASTM Standard D4327-17*. ASTM International, West Conshohocken, PA, 2017. DOI: 10.1520/D4327-17

- ASTM. 2017. Standard Test Methods for Liquid Limit, Plastic Limit, and Plasticity Index of Soils. *ASTM Standard D4318-17e1*. ASTM International, West Conshohocken, PA, 2017. DOI: [10.1520/D4318-17E01](https://doi.org/10.1520/D4318-17E01).
- ASTM. 2019. Standard Test Methods for Laboratory Determination of Water (Moisture) Content of Soil and Rock by Mass. *ASTM D2216-19*. ASTM International, West Conshohocken, PA, 2019. DOI: [10.1520/D2216-19](https://doi.org/10.1520/D2216-19).
- ASTM. 2019. Standard Test Method for Methylene Blue Index of Clay. *ASTM C837-09*. ASTM International, West Conshohocken, PA, 2019. DOI: [10.1520/C0837-09R19](https://doi.org/10.1520/C0837-09R19).
- ASTM. 2019. Standard Test Methods for pH of Soils. *ASTM D4972-19*. ASTM International, West Conshohocken, PA, 2019. DOI: [10.1520/D4972-19](https://doi.org/10.1520/D4972-19).
- Baker, T. 1976. Transportation, Preparation, and Storage of Freezing Soil Samples for Laboratory Testing, in Sangrey, D., and Mitchell, R. (Eds.), *Soil Specimen Preparation for Laboratory Testing*. ASTM STP 599, ASTM International, West Conshohocken, PA, pp. 88-112. <https://doi.org/10.1520/STP39077S>.
- Barbour, S.L. and Fredlund, D.G. 1989. Mechanism of osmotic flow and volume change in clay soils. *Canadian Geotechnical Journal*, 26 (4):551-562. <https://doi.org/10.1139/t89-068>.
- Beier, N. A. and Segó, D.C. 2009. Cyclic Freeze-Thaw to Enhance the Stability of Coal Tailings. *Cold Regions Science and Technology*, 55 (3): 278-285. <https://doi.org/10.1016/j.coldregions.2008.08.006>.
- Beier, N. A., Wilson, W., Dunmola, A., & Segó, D., 2013. Impact of flocculation-based dewatering on the shear strength of oil sands fine tailings. *Canadian Geotechnical Journal*, 50 (9):1001-1007. <https://doi.org/10.1139/cgj-2012-0262>.
- Beier, N.A., Kabwe, L.K., Scott, J.D., Pham, N.H., and Wilson, G.W. 2016. Modeling the Effect of Flocculation and Desiccation on Oil Sands Tailings. *Geo-Chicago 2016*, August 14-16, 2016, Chicago, Illinois, USA. <https://doi.org/10.1061/9780784480137.032>.
- BGC Engineering and O’Kane Consultants, 2014. *Perimeter Ditch Pilot 1 Trial, 2013 Performance Monitoring Update*, Report prepared for Syncrude Canada Ltd., Calgary, AB, Canada.
- Bing, H., He, P. and Zhang, Y. 2015. Cyclic Freeze-Thaw as a Mechanism for Water and Salt Migration in Soil. *Environmental Earth Sciences*, 74 (1): 675-681. <https://doi.org/10.1007/s12665-015-4072-9>.

- Chorom, M. and Rengasamy, P. 1995. Dispersion and zeta potential of pure clays as related to net particle charge under varying pH, electrolyte concentration and cation type. *European Journal of Soil Science*, 46 (4): 657-665. <https://doi.org/10.1111/j.1365-2389.1995.tb01362.x>.
- Consortium of Oil Sands Tailings Management Consultant (CTMC), 2012. *Oil Sands Tailings Technology Deployment Roadmap*. Project Report, Volume 2, Calgary, Alberta.
- Das, B.M. 1983. *Advanced Soil Mechanics*. Hemisphere Publishing Corp., New York, NY, USA.
- Dawson, R.F. and Segoo, D.C. 1993. Design Concepts for Thin Layered Freeze-Thaw Dewatering Systems, *Proceedings of the 46th Canadian Geotechnical Conference*, Saskatoon, SK, Canada: 283-288.
- Dawson, R.F., Segoo, D.C., and Pollock, G.W. 1999. Freeze-thaw dewatering of oil sands fine tails. *Canadian Geotechnical Journal*, 36: 587-598. <https://doi.org/10.1139/t99-028>.
- Eigenbrod, K.D. 1996. Effects of cyclic freezing and thawing on volume changes and permeabilities of soft fine-grained soils. *Canadian Geotechnical Journal*, 33(4): 529-537. <https://doi.org/10.1139/t96-079-301>.
- Government of Canada. 1981-2010 Canadian Climate Normal station data for Fort McMurray. [https://climate.weather.gc.ca/climate\\_normals/results\\_1981\\_2010\\_e.html?stnID=2519&autofwd=1](https://climate.weather.gc.ca/climate_normals/results_1981_2010_e.html?stnID=2519&autofwd=1) (accessed 13<sup>th</sup> January, 2021).
- Han, Z., and Vanapalli, S.K. 2016. Stiffness and shear strength of unsaturated soils in relation to soil- water characteristic curve. *Geotechnique*, 66 (8): 627-647. <https://doi.org/10.1680/jgeot.15.P.104>.
- Hendershot, W.H., Lalonde, H. and Duquette, M. 2008. Ion exchange and exchangeable cations, in: Carter, M.R. and Gregorich, E.G., ed. *Soil Sampling and Methods of Analysis*, 2nd edition, Canadian Society of Soil Science, CRC Press, Boca Raton, FL, pp. 197-206.
- Hen-Jones, R.M., Hughes, P.N., Stirling, R.A., Glendinning, S., Chambers, J.E., Gunn, D.A., and Cui, Y.J. 2017. Seasonal effects on geophysical–geotechnical relationships and their implications for electrical resistivity tomography monitoring of slopes. *Acta Geotechnica*, 12: 1159-1173. <https://doi.org/10.1007/s11440-017-0523-7>.
- Innocent-Bernard, T. 2013. *Evaporation, Cracking, and Salinity in a Thickened Oil Sands Tailings*. M.A.Sc. Thesis, Department of Civil and Environmental Engineering, Carleton University, Ottawa, ON, Canada.

- Jeeravipoolvarn, S. 2005. *Compression Behaviour of Thixotropic Oil Sands Tailings*. M.Sc. Thesis, University of Alberta, Edmonton, AB, Canada.
- Jeeravipoolvarn, S. 2010. *Geotechnical Behavior of In-Line Thickened Oil Sands Tailings*. PhD Thesis, University of Alberta, Edmonton, AB, Canada.
- Johnson, R.L., Pork, P., Allen E.A.D., James, W.H. and Koverny, L. 1993. *Oil Sands Sludge Dewatering by Freeze-Thaw and Evaporation*, Report-RRTAC 93-8, Alberta Conservation and Reclamation Council, AB, Canada.
- Kabwe, L.K, Wilson, G.W., Beier, N.A., and Scott, J.D. 2017. Effects of Atmospheric Drying and Consolidation of Flocculated Thickened Tailings and Centrifuged Cake on Near-Surface Shear Strength. *Second Pan-American Conference on Unsaturated Soils*, November 12-15, 2017, Dallas, Texas. <https://doi.org/10.1061/9780784481684.029>
- MacKay, J.R. 1974. Reticulate ice veins in permafrost, Northern Canada. *Canadian Geotechnical Journal*, 11(2): 230-237. <https://doi.org/10.1139/t74-019>.
- Mikula, R. J., Munoz, V. A. and Omotoso, O. 2008. Centrifuge options for production of “Dry stackable tailings” in surface mined oil sands tailings management. *Canadian International Petroleum Conference*, Calgary, AB, Canada.
- Miller, W.G., Scott, J.D., and Sego, D.C. 2010. Influence of the extraction process on the characteristics of oil sands fine tailings. *Journal of Canadian Institute of Mining, Metallurgy and Petroleum*, 1(2): 93-112.
- Mitchell, J.K. and Soga, K. 2005. *Fundamentals of Soil Behaviour*. 3rd ed., John Wiley and Sons, Inc., New York, NY, USA.
- Oil Sands Tailings Consortium (OSTC) and Canada’s Oil Sands Innovation Alliance (COSIA). 2012. *Technical Guide for Fluid Fine Tailings Management*, Report, Calgary, Alberta.
- Othman, M.A. and Benson, C.H. 1993. Effect of Freeze-Thaw on the Hydraulic Conductivity and Morphology of Compacted Clay. *Canadian Geotechnical Journal*, 30 (2): 236-246. <https://doi.org/10.1139/t93-020>.
- Prasanphan, S. and Nuntiya, A. 2006. Electrokinetic Properties of Kaolins, Sodium Feldspar and Quartz. *Chiang Mai Journal of Science*, 33(2): 183-190.
- Proskin, S.A. 1998. *A Geotechnical Investigation of Freeze-Thaw Dewatering of Oil Sands Fine Tailings*, PhD Thesis, Department of Civil and Environmental Engineering, University of Alberta, Edmonton, AB, Canada.

- Proskin, S., Segó, D. and Alostaz, M. 2012. Oil Sands MFT Properties and Freeze-Thaw Effects, *Journal of Cold Regions Engineering, ASCE*, 26 (2): 29-54. [https://doi.org/10.1061/\(ASCE\)CR.1943-5495.0000034](https://doi.org/10.1061/(ASCE)CR.1943-5495.0000034).
- Rima, U.S. and Beier, N. 2018. Evaluation of Temperature and Multiple Freeze-Thaw Effects on the Strength Properties of Centrifuged Tailings, *71st Canadian Geotechnical Conference*, Edmonton, Canada, September 23-26, 2018.
- Sanchez Sardon, M.A. 2016. *Combined Evaporation and Freeze-Thaw Effects in Polymer Amended Mature Fine Tailings*. MASc. Thesis, Department of Civil and Environmental Engineering, Carleton University, Ottawa, ON, Canada.
- Scott, J.D., Dusseault, M.B. and Carrier, W.D. 1985. Behaviour of the clay/bitumen/water sludge system from oil sands extraction plants. *Applied Clay Science*, 1(1-2): 207-218. [https://doi.org/10.1016/0169-1317\(85\)90574-5](https://doi.org/10.1016/0169-1317(85)90574-5).
- Segó, D.C. 1992. *Influence of pore fluid chemistry on freeze-thaw behaviour of Suncor Oil Sand Fine tails (Phase I)*, Report, submitted to Reclamation Research Technical Advisory Committee, Alberta Environment.
- Spence, J., Bara, B., Lorentz, J. and Mikula, R. 2015. Development of the Centrifuge Process for Fluid Fine Tailings Treatment at Syncrude Canada Ltd. *World Heavy Oil Congress 2015*, Edmonton, Alberta, 24-26 March, 2015.
- Standard Methods. 2017. 3125 Metals by Inductively Coupled Plasma-Mass Spectrometry. Standard Methods for the Examination of Water and Wastewater. <https://www.standardmethods.org/doi/abs/10.2105/SMWW.2882.048>.
- Wilson, G.W., Fredlund, D.G., and Barbour, S.L. 1994. Coupled soil-atmosphere modeling for soil evaporation. *Canadian Geotechnical Journal*, 31(2): 151-161. <https://doi.org/10.1139/t94-021>.
- Witteveen, P., Ferrari, A., and Laloui, L. 2013. An experimental and constitutive investigation on the chemo-mechanical behaviour of a clay. *Geotechnique*, 63 (3): 244-255. <https://doi.org/10.1680/bcmpge.60531.003>.

# **3 EFFECTS OF SEASONAL WEATHERING ON DEWATERING AND STRENGTH OF AN OIL SANDS TAILINGS DEPOSIT**

## **Abstract**

Considerable research has been conducted over the past decade by oil sands mining companies to improve the dewatering and strength properties of fluid fine tailings deposits in an effort to meet the regulatory and closure requirements. Commercially employed dewatering treatment technologies (inline flocculation, thickening, and centrifugation) may not be sufficient to develop the strength for the creation of trafficable landscape without the use of soft soil capping technologies. These treated tailings are continuously deposited creating soft and saturated deep deposits. Seasonal weathering may be an additional promising technology to further dewater the treated tailings and promote the development of shear strength at the surface. The effects of seasonal weathering on dewatering and strength were investigated in this paper by performing multiple cycles of freeze-thaw and alternate drying-wetting cycles on two types of treated tailings deposit. The results indicate that multiple cycles of seasonal weathering significantly increased the dewatering and strength properties. However, different parameters such as freezing gradient, number of seasonal cycles, and pore water chemistry play an influential role in changing the magnitude of the strength. The results also suggest that a minimum threshold strength value is required where the effects of rainfall rewetting had a minimal impact on strength reduction (the strength corresponding to the moisture content approaching the plastic limit).

## **3.1 Introduction**

The Athabasca oil sand deposits in northern Alberta, Canada, are considered to be the fourth largest proven reserve in the world that contain approximately 177 billion barrels of economically recovered crude oil (Government of Alberta, 2021a). In order to produce oil, bitumen extraction process generates approximately 0.25 m<sup>3</sup> of a fluid waste by product, known as fluid fine tailings (FFT), per every barrel of recovered bitumen (Beier et al., 2016). FFT is considered to be a low-

density tailings composed of fines (less than 44 micron) and water with a solids content (by mass) greater than 2%, but less than the solids content corresponding to the liquid limit (OSTC and COSIA, 2012). Therefore, the growing volume of FFT with slow settling rate has become a serious liability for the oil sands industry with respect to storage capacity and water recycling in the containment facilities. In order to meet the regulatory and closure commitments and to achieve the site-specific thresholds for FFT volumes implemented at each mine sites, different mechanical, physical and chemical methods are currently being employed including mechanical centrifuge, thickener, in-line flocculation, and chemical amendments. The resulting treated tailings with improved properties (lower moisture content and higher shear strength) from these treatment technologies are continuously deposited into on-site containment facilities/ in pit deposition areas, thus forming deep deposits (OSTC and COSIA, 2012). These treated tailings deposited in deep deposits are still considered to be soft, weak and non-trafficable, relying predominantly on self-weight consolidation for subsequent dewatering and development of strength (OSTC and COSIA, 2012). Hence, the strength inadequacy of the deep deposit surface prior to the placement of capping/soil cover necessitates an additional step to meet the closure and regulatory requirements in order to promote trafficable surface (OSTC and COSIA, 2012).

Environmental dewatering process such as freeze-thaw dewatering, evaporation, and desiccation investigated by Johnson et al. (1993); Proskin (1998); and Dawson et al. (1999) have the potential for further dewatering of the surface of the deep tailings deposits to comply with the directives of Alberta Energy Regulator (AER), although most of these works were focused on thin layers FFT deposit and not on deep deposits. One such process, cyclic freeze-thaw, works as a controlling mechanism for redistributing moisture and solute in the tailings deposit that results in the changes of macro and microstructure of the tailings and subsequent improved dewatering upon thaw (Proskin et al., 2012). The thawed tailings further promote a significant amount of dewatering through cracking and desiccation if evaporation is sufficient during summer, which, in turn, can develop desiccated surface crust (an over-consolidated layer at the surface developed from weathering and desiccation that has higher density and strength, and poor infiltration than the soil/tailings immediately beneath it (Park et al, 2010)) (Pham and Seg0, 2014). However, predicting the volume change behavior of the tailings deposits exposed to surficial seasonal weathering is quite challenging, provided that drying associated with surface cracking can vary

due to the degree of uncertainty associated with climate and weather. Overall, cyclic freeze-thaw-drying process can be evaluated as an effective dewatering tool as the desiccated surface will retain less water resulting in an increase in solids content at the surface, provided surface water is adequately decanted (Proskin, 1998). Hence, the tailings deposit will be able to consolidate at a substantial higher rate under self-weight (Proskin, 1998). The objective of this paper was to gain an in-depth understanding of dewatering and strength performance of two different types of treated tailings representing the surface of deep tailings deposits through alternate freeze-thaw and drying-wetting cycles in the laboratory. This paper investigated the effects of moisture content, temperature gradient, and pore water chemistry of tailings deposit subjected to seasonal weathering (repeated multiple cyclic freeze-thaw-drying-wetting cycles).

### **3.2 Background**

FFT collectively refers to thin fine tailings (TFT) that is generated during surface mining of oil sands deposits with an initial moisture content ( $w$ ) of approximately 230–560%, and mature fine tailings (MFT) that typically achieve moisture content of about 150-230% within a couple of years after deposition in the containment pond (CTMC, 2012). Additional dewatering of these FFT is extremely difficult and time consuming due to its card house microstructure with large pore spaces entrapping bulk of the process water and tortuous drainage path resulting in extremely low permeability at a high void ratio (Tang, 1997). In order to reclaim the tailings pond back to the stable land use equivalent to the original landscape, FFT needs to be sufficiently dewatered to develop strength at the surface. Different dewatering methods that employ mechanical, physical and chemical amendments or different types of co-disposal and co-mixing technologies or the combination of two or all of them result in the formation of different types of tailings: thickened tailings, non-segregating tailings (NST), in-line thickened tailings (ILTT), and centrifuged tailings. All these treated tailings comprise improved gravimetric moisture content ranges from 80% to 120% (gravimetric solids content ranges from 45% to 65%) with an improved strength properties (OSTC and COSIA, 2012). However, the attained strength is not sufficient enough to develop a trafficable landscape in order to support equipment and allow reclamation to occur (OSTC and COSIA, 2012). Hence, treated tailings deep deposits at the completion of deposition can be further

dewatered by employing environmental dewatering process such as freeze-thaw dewatering and desiccation due to evaporation.

Soft, fine grained tailings surfaces exposed to cyclic freeze-thaw actions are expected to experience volume reduction because of the development of high negative pore water pressures during freezing (Eigenbrod et al., 1996). However, the volume changes subsequent to freezing and thawing are predominantly dependent on the initial moisture content of the tailings, freezing properties (freezing rate, temperature gradient, number of freeze-thaw cycles) and the physicochemical interactions among the tailings particles, water and solutes (Proskin, 1998; Proskin et al., 2012). Since freeze thaw mechanism works through the re-distribution of moisture in the tailings, tailings with a higher initial moisture content are susceptible to a greater extent of dewatering due to a higher magnitude of volume changes compared to the lower moisture content tailings (Johnson et al., 1993). Hence, treated tailings deposits with a significantly lower initial moisture content (compared to FFT as investigated by Johnson et al., 1993; Proskin et al., 2012 etc.) need to be evaluated for the effectiveness of freeze-thaw consolidation. It is worth mentioning that limited research on freeze-thaw dewatering had been conducted on treated tailings (Wilson et al. 2018).

The extensive research (Dawson and Segó, 1993; Johnson et al., 1993; Proskin, 1998) conducted at both laboratory and pilot scale showed that the non-flocculated/untreated FFT samples subjected to multiple freeze thaw cycles experienced significant dewatering. The number of freeze thaw cycles applied on oil sands tailings is predominantly dependent on the researcher's judgement since the volume changes subjected to freeze-thaw are decreased significantly with subsequent cycles (Johnson et al. 1993; Othman and Benson, 1992), and eventually, stabilized once the moisture content reaches the plastic limit (Eigenbrod et al., 1996). So, depending on the initial moisture content and the availability of water prior to freeze-thaw, these numbers can vary significantly. Typically, one to three cycles are commonly used in the laboratory for oil sands tailings (Sanchez Sardon, 2013). However, these studies were predominantly limited to consecutive multiple freeze-thaw cycles (Dawson and Segó, 1993; Johnson et al., 1993; Proskin, 1998; Beier and Segó, 2009) in the laboratory that does not fully represent the field conditions. Under field conditions, freeze-thaw cycle in a single year is followed by alternate drying and

wetting cycles due to evaporation and subsequent rainfall infiltration during the summer. Drying/evaporation cycles during summer facilitates cracking and volume shrinkage that allows the exposure of underlying material with lower suction. As a result, the moisture content in tailings reduces with time which facilitates consolidation under gradients induced by the evaporative water and hence, an increase in solids content is observed (Qiu, 2000). Therefore, the development of desiccated surface crust is anticipated in soft tailings disposal sites to provide sufficient undrained shear strength for the reclamation operations (Johnson et al., 1993). Additionally, the desiccation cracks formed in the previous drying cycle, close upon rainfall resulting an increase in the moisture content and a significant rearrangement of particles and modification of pore network (Tang et al., 2011). Therefore, the re-distribution of moisture in the tailings due to the consecutive multiple freeze-thaw cycles will be substantially different than the combined multiple freeze-thaw-drying-wetting cycles. In addition to this, the shrinkage and/or cracks developed during previous drying-wetting cycles facilitate the advancing ice front to penetrate easily during the subsequent freezing period and draw more unfrozen water towards the ice lens from the underneath unfrozen tailings (Sanchez Sardon, 2013). The combined effect of drying-wetting cycle between each freeze-thaw cycle have not been investigated yet for flocculated tailings samples.

Apart from the number of freeze-thaw cycles, the volume changes subsequent to freeze-thaw depend primarily on the rate of freezing and the temperature gradient (Eigenbrod et al., 1996). Previous research (Johnson et al., 1993; Proskin, 1998; and Dawson et al., 1999) conducted at the laboratory to investigate the effects of temperature gradients on oil sands tailings samples suggested that lower freezing rates and lower temperature gradient resulted in higher dewatering and improved strength performance compared to the samples subjected to high temperature gradient for freezing. Since the freezing rates in the field are typically lower (Othman and Benson, 1993), it can be suggested that volumetric strains in the field can be reasonably predicted from laboratory tests, provided the reasonably similar boundary temperature conditions are applied (Eigenbrod et al., 1996). However, the sample volumes tested in the lab are typically smaller and a significant number of the samples are collected from the field at a depth of 10 to 20 cm from the surface where temperature fluctuations are not greatly affected by the surface air temperature. Therefore, the similar boundary temperature conditions can lead to the faster rate of change in temperature through the small volume samples in the lab. This phenomenon can lead to the

formation of numerous smaller ice lenses which might not represent the actual field conditions (Hobbs, 1974; Henry, 2007). According to Henry (2007), the effect of freeze-thaw cycles on soil/tailings sample can be over-exaggerated and thus, a range of temperature gradients should be experimented in order to account for the variability in results.

Previous research (Sego, 1992; Proskin, 1998; Dawson et al., 1999) also indicates that the physicochemical properties play one of the dominant roles to influence the fabric and structure of the tailings. The type of cation/ electrolytes adsorbed at the clay mineral surface can significantly affect the mobility of unfrozen water through freezing soil/tailings (Darrow et al., 2020). Overall, the present research study proceeded from earlier work which was mostly restricted to freeze-thaw dewatering effects on untreated single/multiple thin layered deposits of FFT. This paper also investigated the extent of number of seasonal cycles required to meet the strength when moisture content approaches the plastic limit. Past research efforts to determine the number of cycles were mostly based on the researchers' own judgement. Furthermore, to the best of the authors' knowledge, there is currently no literature available that accounts for the multiple freeze-thaw and alternate drying-wetting cycle effects on the polymer amended treated tailings deep deposit surface and also closely represents the seasonal cycle in nature. Thus, the central objective of this research is to advance current knowledge with the aim of bridging the gaps, so that the mechanical behaviour of polymer amended treated tailings deep deposits can be predicted and optimized in future and used for further planning purposes.

### **3.3 Laboratory Experiments**

#### ***3.3.1 Test Materials***

The experiments were carried out on two types of polymer amended treated tailings: centrifuged tailings (also known as centrifuge cake) and in-line thickened tailings (ILTT). Centrifugation is commercially operated technology that employs dilution and flocculation of FFT with flocculating agent (anionic polyacrylamide) and coagulant (such as gypsum), followed by centrifugation prior to deposition (Mikula et al., 2008; OSTC and COSIA, 2012; Spence et al., 2015). Similarly, in – line thickening employs injecting polymer flocculant (branched polyacrylamide) into the transfer pipeline that contains dredged FFT followed by deposition into a containment area where

substantial dewatering is promoted via perimeter rim ditching, settlement, seepage and environmental dewatering (CanmetENERGY, 2009; OSTC and COSIA, 2012; Beier et al., 2013). This depositional technique has been piloted at the Syncrude mining operation since 2009 and is commercially known as in-line thickening with accelerated dewatering (O’Kane Consultants, 2017).

Both the treated samples were received at the University of Alberta laboratory in a 200L barrel. Upon arrival, the drums were thoroughly mixed with a mixer, samples were kept in different buckets for the ease of handling and test samples were obtained from the mid-height of the bucket using a scoop sampler. Afterwards, laboratory investigations including index properties, solids mineralogy and pore water chemistry were conducted and analysed using standard ASTM procedures and specialized test methods.

### ***3.3.2 Test Equipment and Methodology***

#### *3.3.2.1 Geotechnical Index Properties Tests*

Initial moisture content for each of the samples was determined according to the ASTM (2019) D2216 procedure for determining Water (Moisture) Content of Soil by which the sample was oven-dried at 105°C for 24 hours. Likewise, specific gravity ( $G_s$ ) was determined according to the ASTM (2014) standard D854 for determining the specific gravity of soil solids by water pycnometer. Based on the specific gravities of the bitumen (1.03) and tailings samples, geotechnical bitumen contents (mass of bitumen/mass of total solids) were calculated and also shown in Table 1. The tailings underwent the liquid limit and plastic limit tests following the procedure outlined in ASTM (2017) standard D4318 for the liquid limit, plastic limit and plasticity index for soils. The fines content (<0.04 mm) and clay content (<0.002 mm) were determined by performing hydrometer tests as per the ASTM (2017) Standard D7928 for particle-size analysis of fine-grained soils.

#### *3.3.2.2 Geotechnical Index Properties Tests*

X-ray diffraction (XRD) analysis was conducted using bitumen free samples. The sample was treated in a toluene vapor bath at 110°C for 24 hours to preclude hydrocarbons from the insoluble solids. For X-ray diffraction (XRD) analysis, the sample was treated in an ultrasonic bath using a deflocculating agent. Upon treatment, the bitumen free over dried sample went through centrifugation at different accelerations, which contributes to the separation of clay fraction from the bulk material. Methylene Blue Index (MBI) was determined as per the ASTM (2019) standard C837-09 for the Methylene Blue index of clay.

### 3.3.2.3 *Pore Water Chemistry Tests*

The pH and electrical conductivity (EC) were measured using a benchtop pH/EC meter as per the ASTM (2019) standard D4972 for determining the pH of soils and ASTM (2014) standard D1125 for determining the electrical conductivity and resistivity of water, respectively. Prior to testing, the instrument was calibrated with a known solution for both pH and EC. The concentrations of Na<sup>+</sup>, K<sup>+</sup>, Mg<sup>2+</sup> and Ca<sup>2+</sup> ions were determined by the Inductively Coupled Plasma method according to the Standard Methods (2017) 3125.

### 3.3.2.4 *Cyclic Freeze-Thaw Tests*

The combined freeze-thaw-drying wetting cycles were initially targeted at conducting at least five cycles as per Beier and Segro (2009), where five freeze-thaw cycles were required for fine grained coal tailings sample to have an asymptotic dewatering and strength gain. The focus of these experiments was to investigate the impact of seasonal weathering on the dewatering and strength of investigated two tailings-centrifuged tailings and ILTT sample. The guidelines on how to artificially freeze soil samples were followed according to the American Society for Testing and Materials (ASTM-STP 599, as reported in Baker, 1976). A one- dimensional top-down freezing test was carried out in the lab as per the guidelines to represent the nature and, also to restrict the upward heaving during freezing. All the guideline suggestions such as having provisions for insulation wraps, thermoelectric cooling plate and thermistors were taken into considerations for designing the freeze-thaw test setup. However, having access to free water from the non- freezing end of the sample, as suggested by the guideline, was precluded and instead, closed system freezing was preferred to measure the contribution from the freeze-thaw process due to the internal moisture

distribution only. Tailings having extremely low permeability can hold greater amounts of water due to higher specific areas of the particles. Low permeability, steep temperature gradients and lack of fissures in the unfrozen and frozen tailings contribute to the reduction of water flow from the external water source to the ice lenses, and hence, a reticulate soil-ice structure is developed irrespective of the external drainage conditions for the fine-grained materials like tailings (Proskin et al., 2012). The similar soil-ice structure resulting from the comparisons between open and closed system freezing tests (as conducted by MacKay (1974); Othman and Benson (1992, 1993); Dawson and Segó (1993)) indicates that the external drainage conditions do not significantly influence the results. As mentioned above, the number of cycles was chosen to be at least five and the test stopped when the strength approached 80-110 kPa (the limit of vane apparatus is 110 kPa) and/or the moisture content reached the plastic limit.

Figure 3.1 shows the schematic diagram of the freeze thaw test setup for the tailings samples. A special experimental apparatus was developed following the similar apparatus and testing procedure developed by Proskin (1998); Xia et al. (2005); Xia (2006); and Proskin et al. (2010). Each of the sample was poured into the cylindrical freezing cell of 100 mm diameter with an initial height of 180 mm. The wall of the freezing cell was made of 20 mm thick plexiglass (which has lower thermal conductivity) to ensure vertical heat flow. The test was carried out inside a walk-in freezer and the temperature was maintained between 0 to 1°C to minimize the air temperature around the cell. Two temperature baths were connected to the freezing cell through its base cooling plate at the bottom as per the guideline, and an attached cap at the top. The temperatures were applied to the freezing cells through these temperature baths to provide constant boundary conditions. The Fort McMurray climate data (1981-2014) shows that the freezing period is approximately six months having an average temperature varies from -8 to -17°C (Government of Canada). Taken these values into consideration, the bottom boundary temperature was set at 0°C, while the top boundary freezing temperatures were chosen to be -15, -10 and -5°C for three different samples of centrifuged tailings. These temperatures, hence, result in temperature gradients of 0.083, 0.056 and 0.028°C/mm, respectively. Additionally, three thermistors, as per guidelines, were installed along the walls of the freezing cell at fixed distances of 40, 80 and 120 mm from the bottom cell plate to record the temperatures within the tailings at different depths.

As recommended by ASTM-SPT 599 (Baker, 1976), insulation was wrapped around the cell and at the top to ensure one dimensional vertical freezing.

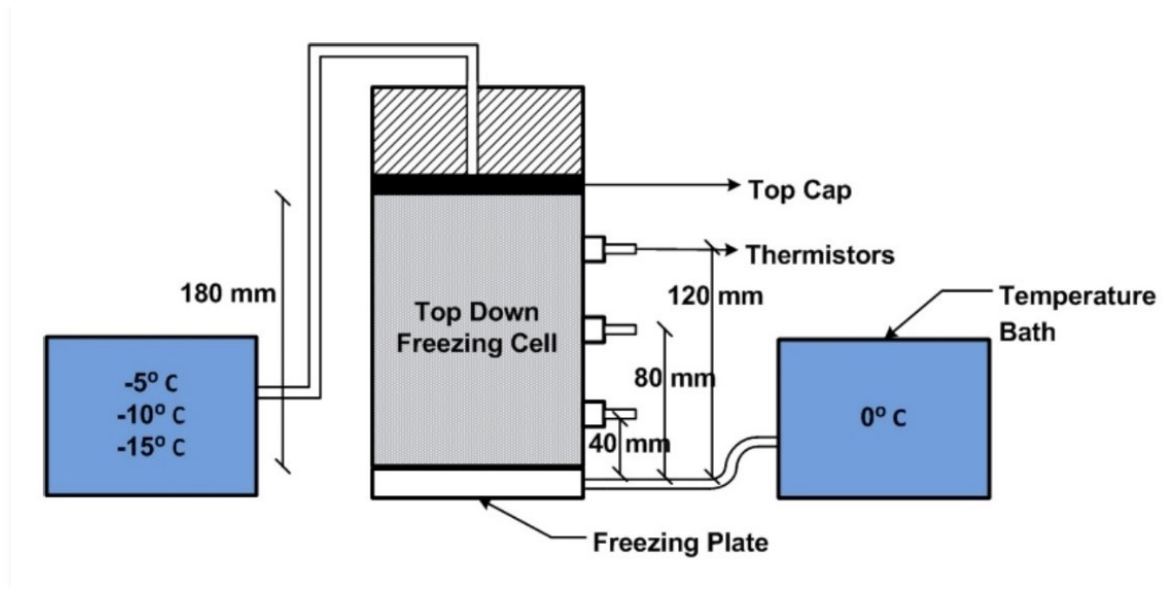


Figure 3.1: Schematic diagram of the freeze- thaw test setup

Once the setup was complete, the freezing phase commenced and was continued for 72 hours followed by thawing at the room temperature of the freezer for 24 hours by disconnecting the cell from the temperature baths. Afterwards, the sample was taken out of the freezer and allowed to thaw for another 48 hours under the room ( $\sim 20^{\circ}\text{C}$ ) temperature. Upon complete thaw, the free water accumulated at the top was decanted to simulate surface drainage and the associated change in height due to freeze-thaw was recorded. Removal of water facilitates an increase in solids content of the tailings sample. Afterwards, undrained shear strength and electrical conductivity were measured at the near surface (measured at the depth of 12.5 mm from the surface) using a manual vane shear apparatus and benchtop pH/EC meter.

For the ILTT sample, the test was run for a single temperature gradient of  $0.028^{\circ}\text{C}/\text{mm}$  ( $-5^{\circ}\text{C}$  at top and  $0^{\circ}\text{C}$  at bottom) to validate the proposed lab testing procedure, given that the field data from the same deposit suggests having the temperatures in winter varying from 0 to  $-8^{\circ}\text{C}$  with an average of  $-5^{\circ}\text{C}$  (O’Kane Consultants, 2017).

### 3.3.2.5 *Cyclic Drying-Wetting Tests*

After the first cycle of freeze-thaw test was completed, each of the samples were exposed to the atmospheric drying tests. The drying cycle was continued for a week at the room temperature (~20°C) where the changes in mass loss due to evaporation/drying were recorded on a daily basis along with the subsequent shear strength measurements. The drying test was followed by a single wetting event to simulate the rainfall where the volume of water evaporated during atmospheric drying was re-introduced as distilled water. Upon wetting, each of the samples underwent another ambient drying cycle for a week to understand the behaviour of the tailings prior to and after a rainfall event. The entire process was repeated for at least five cycles of freeze-thaw-drying-wetting tests per sample with each experiment requiring about four months to complete. It is noteworthy to mention that duplicate samples were not tested due to limited resources and long-time scale of experiments.

### 3.3.2.6 *Sectional Analysis*

After the cyclic freeze-thaw-drying-wetting tests were completed, each of the samples were sectioned into five equal parts of approximately 2 cm in height to perform gravimetric moisture content/ solids content profile throughout the depth.

## 3.4 **Results**

### 3.4.1 *Characterization of Tailings*

Table 3.1 summarizes the key material properties and water chemistry of the investigated two tailings. The moisture content for the centrifuged tailings and accelerated dewatered tailings samples were measured to be 89 and 122% respectively, corresponding to the solids content of 53 and 45%, respectively. The lower moisture content for the centrifuged tailings sample is attributed to the combined flocculants and centrifugation process resulting in higher densification (Mikula et al., 2008) compared to the ILTT sample relying predominantly on flocculants for initial dewatering (Beier et al., 2013; CTMC, 2012). The fines contents were measured 87 and 93%, respectively, for centrifuge tailings and ILTT sample indicating fine grained nature of the two investigated

tailings samples. However, the predominance of clay sized fractions (confirmed through hydrometer test, XRD and MBI analyses as shown in Table 3.1) with potentially higher negative charges for ILTT sample are less susceptible to adsorbed cations/electrolytes indicating overall dispersed structure (Darrow et al., 2020) compared to the centrifuged tailings. These highly negative charges may have a lower impact of surface charge neutralization to form flocculated structure due to the presence of lower divalent cations (Darrow et al., 2020). Given the values of  $\text{Na}^+$ ,  $\text{Ca}^{2+}$ , and  $\text{Mg}^{2+}$  cations, SAR (sodium adsorption ratio) values calculated to be 27 and 38.1, respectively for centrifuged tailings and ILTT samples, suggesting a likely dispersed structure (Miller et al., 2010).

Table 3.1: Summary of key properties of tailings

Property	Centrifuged Tailings	ILTT Sample
Moisture content, w (%)	89	122
Solids content, s (%) <sup>*</sup>	53	45
Bitumen content (%) <sup>†</sup>	5.7	2
Specific gravity ( $G_s$ )	2.24	2.45
Material finer than 0.044 mm (%)	87	93
Material finer than 0.002 mm (%)	52	70
Liquid limit (%)	57	62
Plastic limit (%)	26	23
Clay fraction (%) from XRD diffraction	52	80
Clay fraction (%) from MBI	52	68
Dissolved cations (mg/L)	$\text{Na}^+$	780
	$\text{K}^+$	14.6
	$\text{Ca}^{2+}$	36.5
	$\text{Mg}^{2+}$	15.9
Total dissolved solids, TDS (mg/L)	2,573	1,890
Sodium adsorption ratio (SAR) <sup>‡</sup>	27	38.1

**Note.** <sup>\*</sup>  $s = 1 / (1 + w)$

<sup>†</sup>Bitumen content = mass of bitumen divided by the total mass of the tailings

$$\ddagger\text{SAR} = \frac{[\text{Na}^+]}{\sqrt{\frac{[\text{Ca}^{2+} + \text{Mg}^{2+}]}{2}}}$$

### 3.4.2 Dewatering Performance

Figure 3.2 illustrates the cumulative decrease in estimated moisture content for the investigated two treated tailings samples after each seasonal cycle where centrifuged tailings samples are subjected to three temperature gradients of 0.083, 0.056 and 0.028°C/mm, and ILTT sample is subjected to a temperature gradient of 0.028°C/mm, respectively. Each of the seasonal cycles is divided into alternate freeze-thaw (written as F/T on graph) and drying wetting cycles (written as D/W on graph) to distinguish the contribution of freeze-thaw dewatering from evaporation/drying phase.

The change in moisture content associated to freeze-thaw dewatering was calculated on the basis of change in height ( $\Delta H$ ) prior to and after thawing divided by the total frozen height ( $H$ ) in each cycle. The change was calculated from the following equation:

$$\frac{\Delta H}{H} = \frac{\Delta e}{1 + e_0} \quad [3.1]$$

where,  $H$  is the measured total frozen height just before thaw,  $\Delta H$  is the change in measured height prior to and after thawing,  $\Delta e$  is the change in void ratio due to freeze-thaw and  $e_0$  is the initial void ratio at the start of each freeze-thaw cycle. Based on the change in void ratio, the corresponding moisture content of the entire sample was computed from the following equation:

$$w (\%) = \frac{100e}{G_s} \quad [3.2]$$

where,  $e$  is the new void ratio after thaw for each freeze-thaw cycle,  $w$  is the corresponding calculated moisture content and  $G_s$  is the specific gravity of the tailings sample. Likewise, the moisture content after each drying-wetting cycle was calculated on the basis of the daily changes in weight loss during drying phase and daily changes in weight gain during rainfall event divided by the initial mass of dry soil.

The estimated moisture content of the centrifuged tailings samples corresponding to the three gradients of 0.083, 0.056 and 0.028°C/mm and after five freeze thaw cycles were computed to be 27, 21.6 and 13.6%, respectively from an initial value of 89%. Likewise, the estimated moisture content of the ILTT sample decreased from an initial value of 121% to a value of 25%. As evident in the figure, the lowest moisture content was computed, on the lower temperature gradient (0.028°C/mm) centrifuged tailings, to be 13.6% after five cyclic freeze-thaw and drying-wetting cycles. However, the overall total amount of dewatering is higher in ILTT sample (a cumulative 96% decrease in moisture content from the initial value) compared to the centrifuged tailings sample (a cumulative 75% decrease in moisture content from the initial value) at similar temperature gradient.

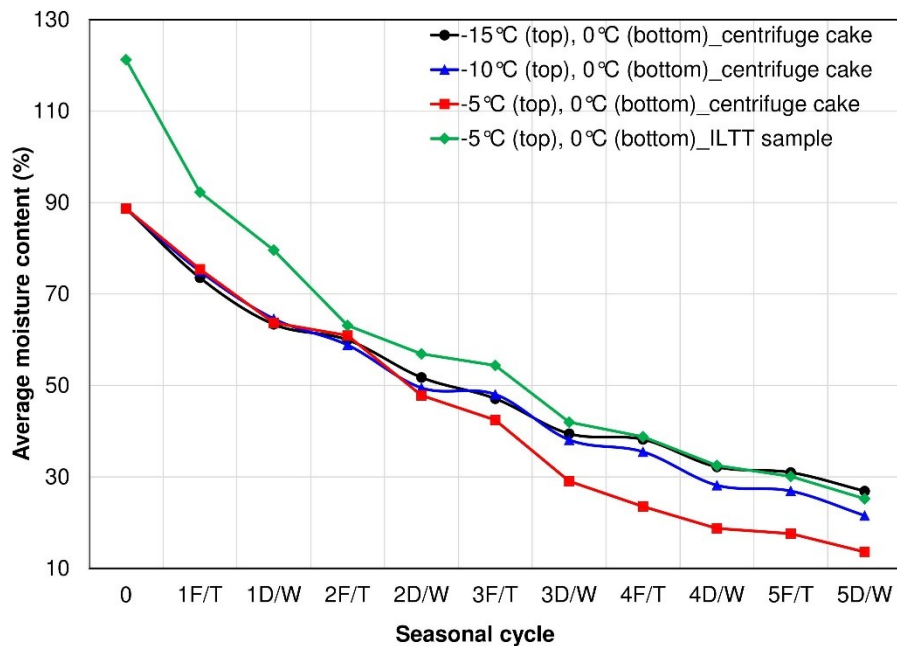


Figure 3.2: Estimated moisture content (%) versus number of seasonal cycles

Figures 3.3 through 3.6 show the estimated moisture content and measured shear strength (measured at 12.5 mm from the surface) progression over time for the investigated centrifuged and ILTT samples. Each of the seasonal cycles is divided into freeze-thaw cycles (denoted as F/T in the figures), drying cycles (denoted as D) and drying cycles after wetting event (D/W in the figures). A full strength and moisture content profiles were not measured in order to limit sample

disturbance between cycles. The combined analysis shows that the centrifuged tailings sample with lower temperature gradient reached to a lowest moisture content (13.6%, as shown in Figure 3.5) after five cyclic freeze-thaw and drying-wetting cycles while the similar temperature gradient under similar cycles resulted in a moisture content of around 25.2% (as shown in Figure 3.6) for the ILTT sample. The surficial strength (>110 kPa for centrifuged tailings and 84 kPa for ILTT sample) suggests a consistency of stiff soil for both of these samples, provided the moisture content (13.6%) of the centrifuge tailings passed through the plastic limit (26%) while the moisture content (25.2%) for the ILTT sample almost reached to its plastic limit (23%).

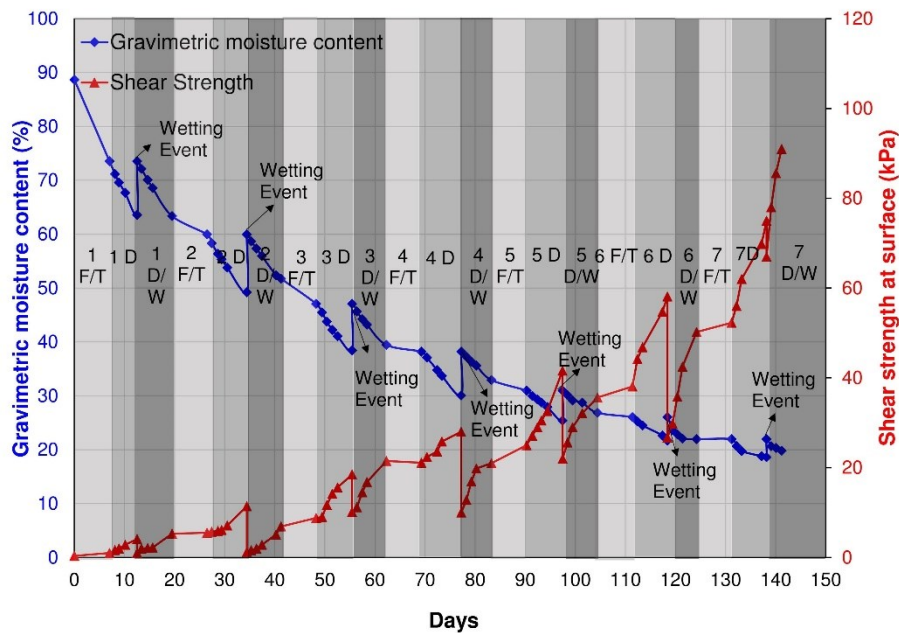


Figure 3.3: Estimated moisture content and measured shear strength progression of centrifuged tailings over time at a temperature gradient of  $0.083^{\circ}\text{C}/\text{mm}$

Additionally, surface drying induced a distinguishable crust layer at the very top of 2 cm (as shown in Figure 3.7) of the centrifuged tailings sample under this lower gradient. This thin denser layer (compared to the tailings underneath) was formed at the surface as a result of the exposure to the atmosphere due to the physical weathering processes such as desiccation (due to alternating drying-wetting cycles) combined with the frost action (alternating freeze-thaw cycles) (Lutenegger, 1995; Park et al., 2010). The surface of a soft tailings deposit is susceptible to drying out when the upward supply of water is less than the water evaporated from the surface which, in

turn, results in the development of negative pore water pressures/suction and pre-consolidation stresses (Luteneggar, 1995). An increase in pre-consolidation stress resulting from an increase in capillary suction (due to drying and/or a decrease in temperature during freezing process) can cause jointing/fissures, that develops desiccated surface crust over time and with multiple cycles of alternating drying-wetting and/or alternate freeze-thaw (Chamberlain, 1981; Luteneqgar, 1995).

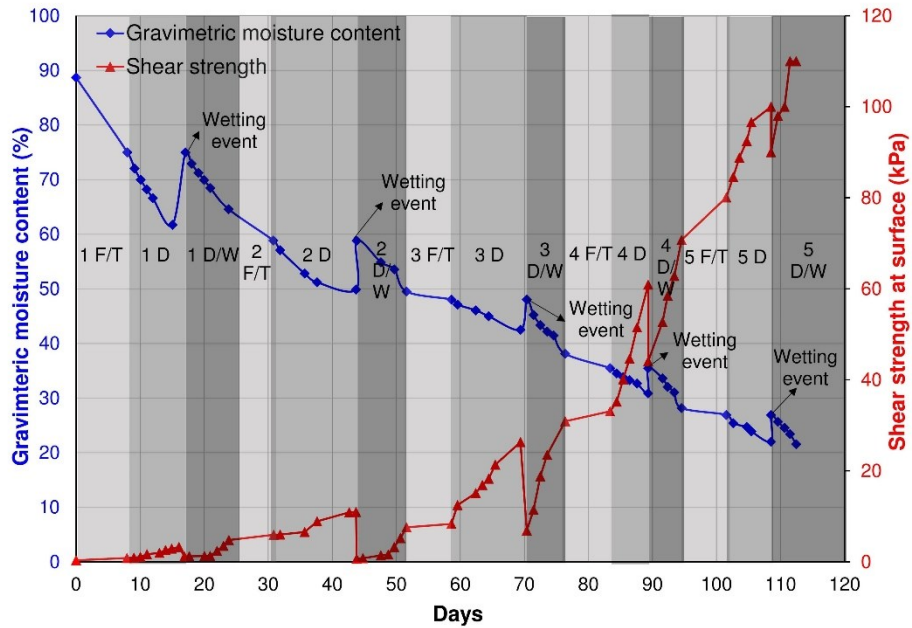


Figure 3.4: Estimated moisture content and measured shear strength progression of centrifuged tailings over time at a temperature gradient of  $0.056^{\circ}\text{C}/\text{mm}$

The moisture content of the crust layer exceeded plastic and shrinkage limit of the sample (shrinkage limit is 21% for the investigated sample). The shear strength could not be measured following the formation of crusts due to the inability of the vane to push into the extremely stiff surface to the required depth and hence, constant shear strength was reported.

However, the difference in treatment process had a considerable impact on the development of crust under similar temperature gradient and similar number of seasonal cycles. The ILTT sample did not develop any distinguishable surface crust (moisture content could not exceed its plastic limit) like the centrifuged tailings sample. Next, the centrifuged tailings with a temperature gradient of  $0.056^{\circ}\text{C}/\text{mm}$  (as shown in Figure 3.4) exceeded the plastic limit at its fifth cycle with

an associated undrained shear strength exceeding 110 kPa. On the contrary, the estimated moisture content for the highest gradient sample (as shown in Figure 3.3) was computed to be 29% with an associated undrained shear strength of 35 kPa after five cycles of freeze thaw and drying-wetting phase. It took seven seasonal cycles for this sample to reach the plastic limit without any distinguishable crust and yet, the near surface strength could not exceed 100 kPa.

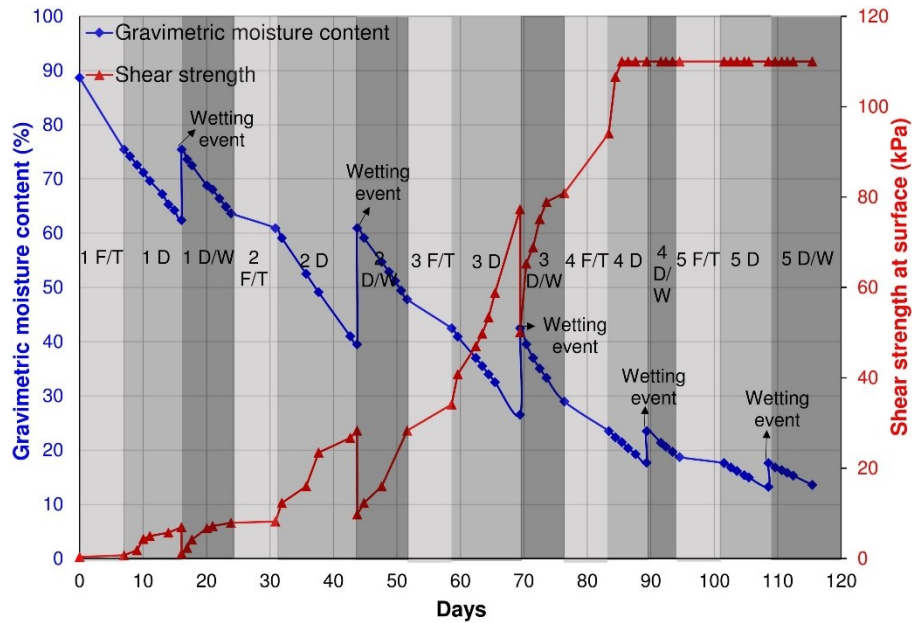


Figure 3.5: Estimated moisture content and measured shear strength progression of centrifuged tailings over time at a temperature gradient of  $0.028^{\circ}\text{C}/\text{mm}$

While it is expected to improve the dewatering and strength performance through multiple freeze-thaw and drying cycles, samples subjected to wetting event are expected to increase the moisture content with an associated shear strength reduction, as evident in Figures 3.3 through 3.6. Upon re-introduction of the evaporated water to simulate the rainfall event after each drying phase, each of the samples underwent significant strength and stability reduction. However, with a reduction in moisture content with each cycle, the effects of wetting event/rainfall had lower impact on the strength. The results suggest that once these samples reached to a very high solids content (or moisture content exceeding the plastic limit), the reduction in near surface shear strength of the sample due to rainfall became insignificant.

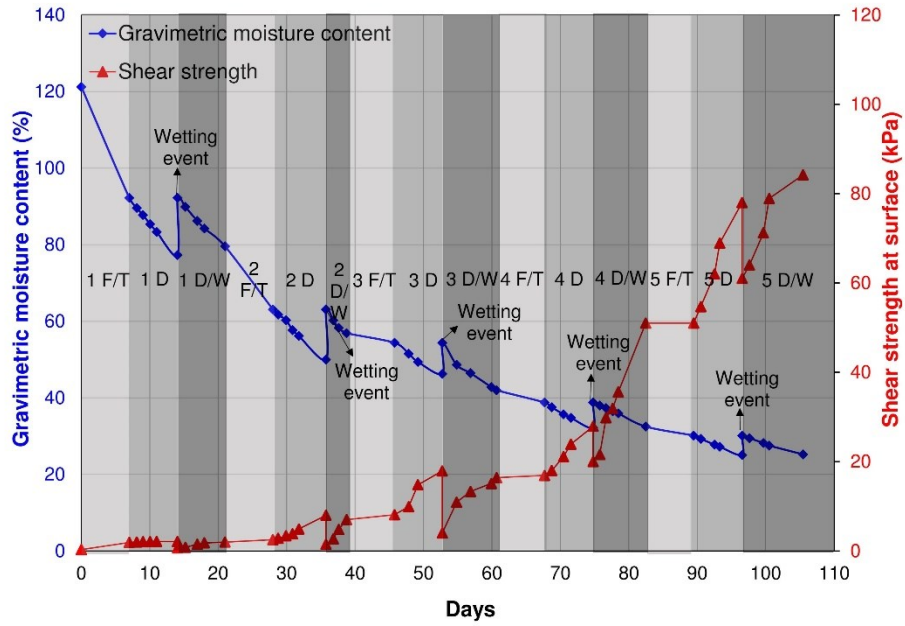


Figure 3.6: Estimated moisture content and measured shear strength progression of in-line thickened tailings sample over time at a temperature gradient of  $0.028^{\circ}\text{C}/\text{mm}$



Figure 3.7: Crust layer formed at the surface of the centrifuged tailings subjected to a temperature gradient of  $0.028^{\circ}\text{C}/\text{mm}$

Figure 3.8 shows the % change in shear strength prior to and after wetting event at each cycle. The shear strength reduction was reported as a change in shear strength just prior to and after rainfall divided by the initial strength just prior to rainfall at each cycle. As shown in the Figure 3.8, the effects of rainfall on the strength reduction are most significant and continued beyond 5 cycles for the centrifuged tailings subjected to the highest temperature gradient. A decrease in temperature gradient along with an increase in cycle results in cessation of rainfall effects on strength.

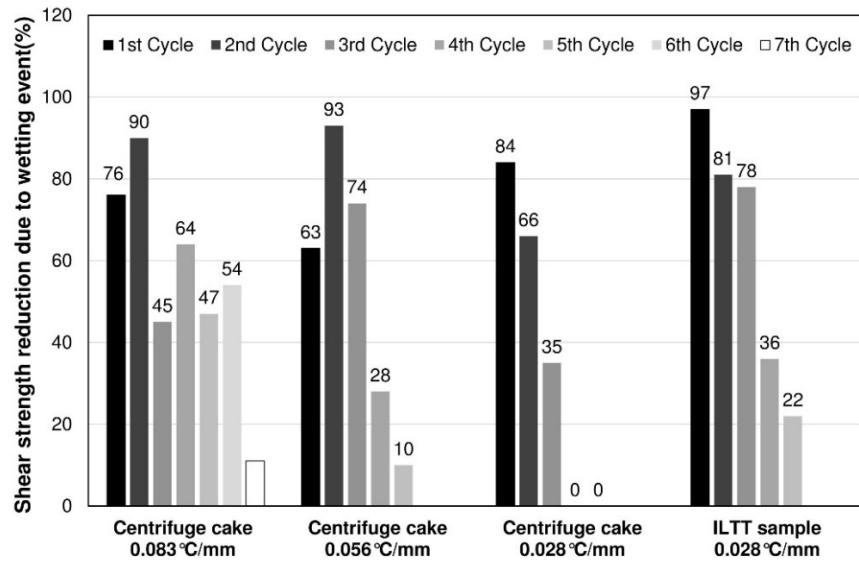


Figure 3.8: The change in shear strength reduction (%) due to rainfall/ wetting event after each cycle

Figure 3.9 shows the measured final moisture content profiles throughout the depth of the samples after sectional analysis at the end of the test. This figure coupled with Figure 3.7 confirm the formation of the crust layer on the centrifuged tailings sample subjected to the lowest temperature gradient (0.028°C/mm). Two layers were formed: a surface crust layer at the very top 2 cm where the lowest moisture content (=12%) was recorded exceeding the shrinkage limit (=21%) and the underlying tailings below the crust where the moisture content was at or very close to the shrinkage limit of the sample. On the contrary, the ILTT sample subjected to the identical temperature gradient (0.028°C/mm) resulted in an overall moisture content (30.4%) close to the plastic limit with the lowest value recorded at the surface (=25.8%). The centrifuged tailings samples subjected to temperature gradients of 0.056 and 0.083°C/mm resulted in the final moisture content of 20.5

and 24.2% at the surface, respectively. Both of these samples exceeded the plastic limit but not sufficient enough to create a desiccated distinguishable surface crust.

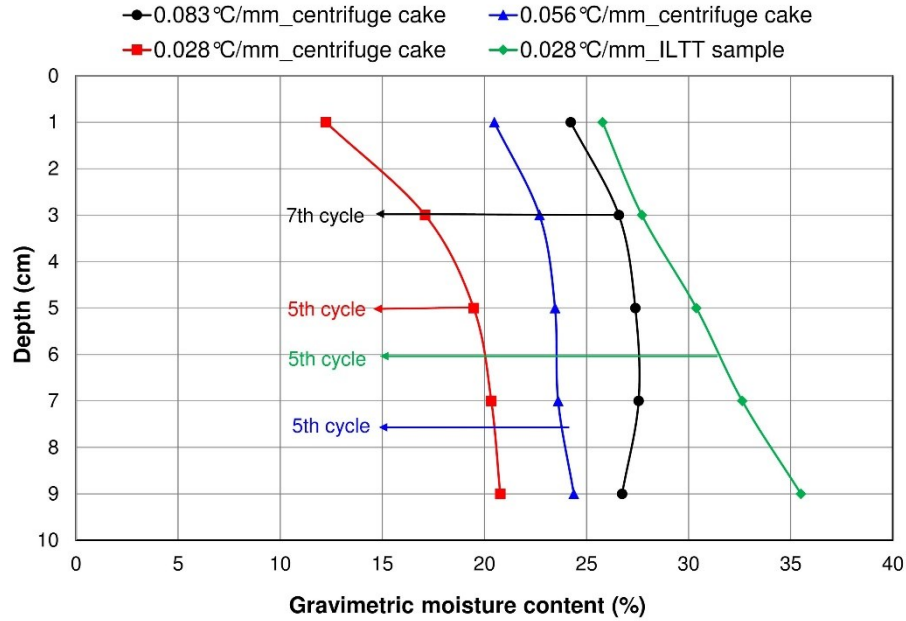


Figure 3.9: Measured moisture content (%) profile at the end of the test

Table 3.2: Comparison between calculated and measured moisture content values at the near surface

Types of samples	Moisture content (%) (measured value at the top sectional layer)	Moisture content (%) (estimated value)
Centrifuged tailings (0.083°C/mm)	24.2	19.8
Centrifuge tailings (0.056°C/mm)	20.5	21.5
Centrifuge tailings (0.028°C/mm)	12.2	13.6
ILTT sample (0.028°C/mm)	25.8	25.2

Table 3.2 compares the calculated moisture content values (as shown in Figures 3.2 to 3.6) to the measured ones (as shown in Figure 3.9). The measured values at the end of the cycles were found in agreement with the estimated values calculated from the loss of moisture. The experimental error varies from 2.3 to 18%, thereby, indicating the efficacious mass balance for the laboratory experiment.

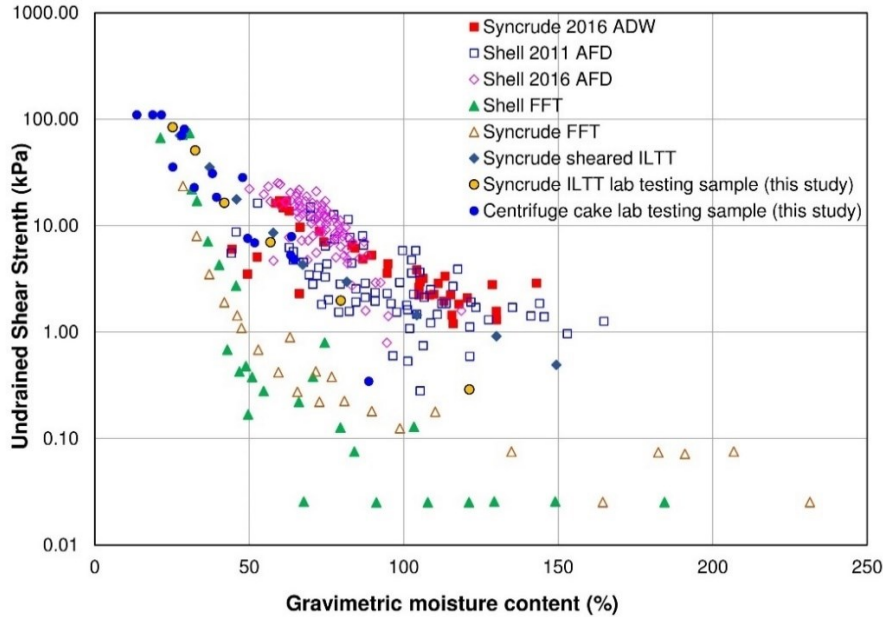


Figure 3.10: Relationship between undrained shear strength and gravimetric moisture content (%)

Figure 3.10 illustrates the impact of physical and natural dewatering processes with chemical addition on the strength gain in oil sands fine tailings by comparing untreated FFT deposits data (Shell and Syncrude FFT) with flocculated fine tailings deposits field (Shell ‘Atmospheric Fines drying’ or AFD which is a commercial scale demonstration of ILTT facilitated with a combination of consolidation, seepage and environmental dewatering, Syncrude sheared ILTT and Syncrude ILTT) and laboratory data (centrifuged tailings and ILTT sample). As evident in the Figure 3.10, the addition of dewatering technologies (physical/mechanical methods in combination with flocculant addition and natural weathering) significantly enhanced the shear strength at higher moisture content. The commercially operated dewatering technologies (Shell AFD and Syncrude

ILTT) could achieve a shear strength of 5-15 kPa at moisture content ranging from 65-100% which is 10-100 times higher than the strength of untreated FFT at same moisture content. Overall, the laboratory results from the current study (centrifuged tailings and Syncrude ILTT) suggest that seasonal weathering of these treated deposits has a potential to further promote dewatering by reducing moisture content as low as 40% with an associated shear strength greater than 50 kPa.

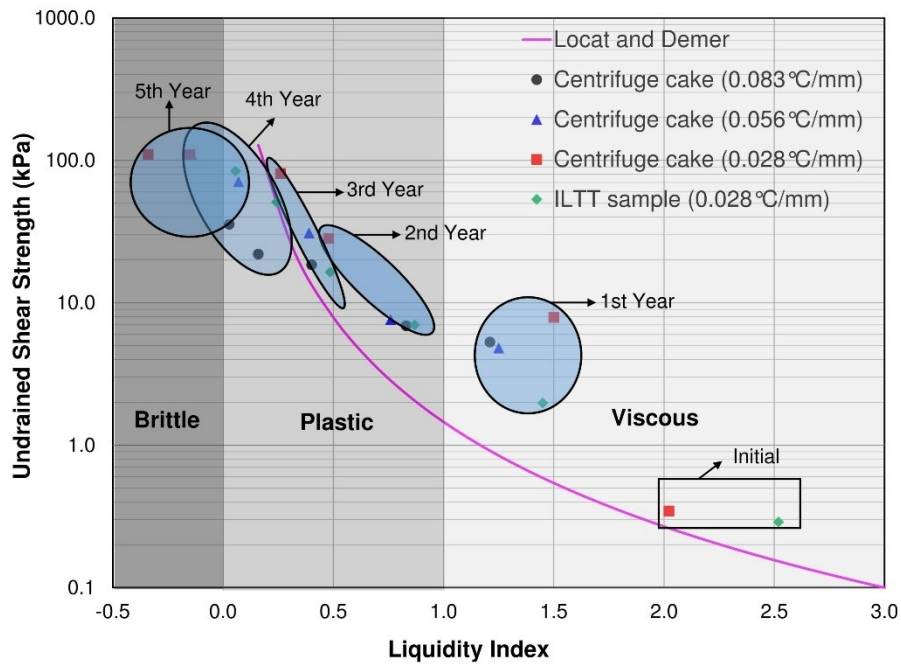


Figure 3.11: Undrained shear strength of treated tailings as a function of liquidity index

To preclude the effects of moisture content, clay content, solids mineralogy and pore water chemistry, the undrained shear strength of two investigated tailings are also presented (Figure 3.11) as a function of liquidity index (LI). It is to be noted that the moisture content (for estimating LI) denotes the average moisture content of the sample while the shear strength is measured at the near surface. The figure shows that the surficial strength of these deposits with multiple seasonal cycles can behave like natural clay slurries and can be converged towards Locat and Demers (1988) line at higher strength. Locat and Demers (1988) proposed this line for sensitive natural clay soils which provided a good overall fit for typical MFT (Beier et al 2013). The graph suggests that the tailings deposited at an initial moisture content over liquid limit can undergo through a transition

from slurry phase to solid state, passing through the liquid limit and plastic limit by simply exposing to seasonal weathering for multiple years.

### **3.5 Discussion**

#### ***3.5.1 Effects of Initial Moisture Content***

Tailings subjected to below freezing temperatures develop high negative pore water pressures/suction that causes water migration toward the freezing front, resulting in ice lens formation (Andersland and Ladanyi, 2004). Since ice layer growth is limited by the available water contained in the voids of saturated tailings under closed system freezing (Andersland and Ladanyi, 2004), the available moisture is expected to have an impact in volume changes subsequent to freezing and thawing (Eigenbrod et al. 1996). The investigated two treated tailings did not have a significant difference in their initial moisture content (89% moisture content for centrifuged tailings and 122% moisture content for the ILTT sample). However, a sharp decrease in moisture content from the initial value (Figure 3.2) and overall higher amount of dewatering (a cumulative 96% decrease in moisture content from the initial value in contrast to an overall 75% reduction in moisture content for centrifuged tailings) for the ILTT sample suggest that lower solids content/higher moisture content of the never frozen soft tailings sample contributes to higher magnitude of the volume changes subsequent to freeze-thaw dewatering.

#### ***3.5.2 Effects of Temperature Gradient***

The differences in dewatering and strength behaviours among centrifuged tailings samples were predominantly attributed to the variations in temperature gradient. Based on the laboratory results (as shown in Figures 3.2 through 3.9), the centrifuged tailings sample subjected to a lower temperature gradient during freezing contributed to an overall lowest moisture content (18% at the surface and 12% on an average throughout the sample depth) and subsequent higher shear strength (greater than 110 kPa). The results of this paper were found consistent with the earlier findings (Dawson et al., 1993; Othman and Benson, 1993; Eigenbrod et al., 1996; Proskin, 1998; Dawson et al., 1999; and Knutsson et al., 2016).

The formation of ice lenses during freezing contributes to dewatering to a larger extent by creating water migration channels upon thaw (Proskin et al., 2012; Rima and Beier, 2018). Ice lenses will always be formed during freezing, regardless of the freezing rate/temperature gradient (Tang, 1997). Earlier findings suggest that the frequency and thickness of ice lenses are one of the predominant factors to influence the dewatering and stability performance (Othman and Benson 1993), although frozen samples were not sectioned to examine ice lenses in this experiment. The higher temperature gradient allows the freezing front to move faster which creates numerous smaller ice lenses (Othman and Benson 1993). However, the growth of these ice lenses is not sufficiently larger enough to push the clay particles altogether, thereby, resulting in a little impact on the tailings structure (Tang, 1997). In contrast to this, the slow temperature gradient draws more water to the suction front and transform this water into larger sized ice lenses due to the longer time frame available for water accumulation at a fixed location (Othman and Benson, 1993; Knuttson et al., 2016). Since the freezing rates in the field are typically lower (Othman and Benson, 1993), it can be suggested that the volume changes in the field can be reasonably predicted from laboratory tests, provided the reasonably similar boundary temperature conditions are applied (Eigenbrod et al., 1996).

### ***3.5.3 Effects of Number of Seasonal Cycles***

As the number of freeze-thaw cycles increases, more ice lenses are expected to form (Othman and Benson, 1993) that eventually contributes to higher dewatering and subsequent higher strength gain. However, the volume changes subsequent to freezing and thawing is always higher in its first cycle and decrease with subsequent cycles (Eigenbrod et al., 1996; and Andersland and Ladanyi, 2004). This finding is, however, limited to multiple consecutive freeze-thaw cycles. The combined freeze-thaw and alternate drying-wetting cycles (as shown in Figures 3.2 through 3.6) suggest that the subsequent cycles had lower impact on volume changes due to freeze-thaw dewatering, not on evaporation/drying. Evaporation/drying continued to facilitate dewatering at each cycle through the development of suction at liquid water/gas interface and crack propagation (Innocent-Bernard, 2013). However, laboratory testing confirmed the adequacy of running five seasonal cycles in the lab. The wetting behavior when moisture content approaches the plastic limit confirmed that seasonal dewatering has minimal impact on strength gain (>100 kPa) after five cycles of freeze-thaw and drying-wetting.

The differences in shear strength behaviour between Syncrude perimeter ditch pilot deposit (denoted as Syncrude 2016 ILTT in Figure 3.10) and the laboratory results from the same deposit (denoted as Syncrude ILTT lab testing sample) can possibly be attributed to the higher number of seasonal cycles for the field deposit. The pilot deposit in the field, being exposed to seven seasonal cycles (from 2009 to 2016) resulted in higher strength gain at high moisture content compared to the laboratory sample running for five cycles. However, the depth (several meters deep field deposits versus tens of centimeters deep laboratory samples), scale and boundary conditions (controlled laboratory versus uncontrolled field freezing and evaporative boundaries) for the similar tailings under field and laboratory are substantially different and hence, can have an influential impact on dewatering and strength performances.

Figure 3.11 also confirms that the increase in seasonal cycles has a potential to transform the slurry like surface into a desiccated one, regardless of the variations in moisture/solids content, clay content and mineralogy, and water chemistry. According to Eigenbrod (1996), the volume changes of the soft fine-grained soil subjected to multiple freeze-thaw cycles become insignificant once the soil reaches to its plastic limit. The overlapping circles (as shown in Figure 3.11) towards the plastic limit also suggest that environmental dewatering for densification and strength gain associated with the number of seasonal cycles seem to stabilize around its plastic limit.

#### ***3.5.4 Effects of Rainfall/Wetting***

The laboratory testing results suggest that the centrifuged tailings sample subjected to lower temperature gradient becomes unaffected by wetting (as shown in Figure 3.8, indicated by the no change in shear strength from 4<sup>th</sup> cycle) once the sample exceeds its plastic limit (as shown in Figure 3.5). Due to the crust formation at the surface (as shown in Figure 3.7), the sample achieved a very high solids content/very low moisture content (as shown in Figure 3.9) and possibly very high suction (although suctions were not measured during the experiments). At higher solids content, it is therefore inferred that the suction can become so high that the suction loss due to hysteretic soil-water retention behaviour (Hen-Jones et al., 2017) induced by alternate drying-wetting cycle may become insignificant to cause any impact on shear strength. Hence, the

desiccated crust layer formed during drying cycle was not collapsed upon wetting. Consequently, the centrifuged tailings sample of lower temperature gradient retained relatively lower moisture content (12% at the surface) and the strength remained unchanged ( $>110$  kPa). On the contrary, the strength of the other investigated tailings samples due to relatively higher moisture content (and possibly with lower suction) continued to be affected by wetting (as shown in Figure 3.8), although the effects started to diminish with subsequent later cycles. As a result, a potential reduction of stability was observed for all of these samples.

### ***3.5.5 Effects of Physico-chemical Properties***

The differences in dewatering and strength behaviour between centrifuged tailings and ILTT samples at similar temperature gradient ( $0.028^{\circ}\text{C}/\text{mm}$ ) are attributed to the variations in treatment process, solids mineralogy and pore water chemistry between these samples. The prevalence of divalent cations ( $\text{Ca}^{2+}$  and  $\text{Mg}^{2+}$ ) combined with lower clay content for centrifuged tailings can facilitate higher charge neutralization compared to ILTT sample, hence, resulting in double layer compression (Mitchell and Soga, 2005; Darrow et al., 2020). The double layer compression allows Van-der Waals attraction force to dominate over electrostatic repulsion force that causes flocculation (Mitchell and Soga, 2005) and overall moisture content reduction and strength gain. Furthermore, the physico-chemical inter-particle forces govern the mechanical properties of cohesive soils at higher suction (Han and Vanapalli, 2016). Wetting behaviour at high suction seem to suggest that two deposits with different deposition technique and physico-chemical properties can exhibit different dewatering and strength behaviour under the similar environmental conditions.

## **3.6 Limitations**

Repeatability of the test could not be carried out in the present study to account for the variation of the effects of the studied parameters on the results due to the limited resources and longer time frames of the experiment. The laboratory approach presented in this paper is based on several assumptions such as closed system was preferred in the laboratory while open system exists in the field conditions, although the external drainage conditions have minimal impacts on the extremely low permeable fine-grained tailings deposits. The laboratory results can be expected to predict the

field response if the temperature gradients are in the same range and the depth of snow covers is minimal. Also, ponded water management is imperative to utilize the full potential of seasonal weathering in the field. The laboratory testing methodology presented in here employed a sequence of freeze-thaw-drying-wetting cycles. Prolonged wetting or drying period, multiple wetting events or the other changes to this sequence could have impacted the results.

While seasonal dewatering has been shown to increase the strength of the small lab samples under controlled laboratory conditions, further work is needed to evaluate how deep this seasonal weathering will influence tailings under actual field conditions. Numerical modeling of the field deep deposits subjected to seasonal weathering in order to predict whether the materials can meet the minimum strength threshold in a specified amount of time is beyond the scope of this paper. Previous modeling work conducted by Wilson et al. (2018) suggested that seasonal weathering (freeze-thaw cycles) increased the shear strength compared to treated tailings/ FFT deposits with increasing effective stresses at depth. Hence, the effective stresses or the extent of depth required to achieve the threshold strength for reclamation activities are needed to investigate as the next step to meeting the closure and regulatory requirements.

### **3.7 Conclusion**

Technological advances over the past decade have improved oil sand tailings management practices regarding conversion of FFT into semi solid deposits capable of capping for terrestrial reclamation (CTMC, 2012). Nevertheless, the mining industry still faces challenges to reduce the legacy volumes of fluid tailings in order to meet the regulatory and closure requirements. In response to the AER's Directive 085, the oil sands industry currently has focused on creating deep deposits of flocculated tailings. In these deposits, seasonal weathering may be employed to promote self-weight consolidation and substantial dewatering (OSTC and COSIA, 2012).

The present paper investigated the use of natural weathering as a dewatering process for treated tailings deep deposits requiring a reclamation cap. The results suggest that the surficial strength can be potentially enhanced to form a cappable deposit, provided adequate surface water management is implemented to ensure seasonal freezing and drying of the tailings. However, the

current study of this paper implies that the dewatering and strength properties can be significantly influenced by the type of tailings, different mineralogy and pore water chemistry, freezing temperature gradient, number of seasonal cycles and the effect of rainfall. When comparing shear strengths and dewatering as a function of freezing gradient within the same tailings deposit, the sample subjected to lower temperature gradient overall achieved lower moisture content and a subsequent higher shear strength. To compare the shear strengths and dewatering performance of different tailings deposits, however, it is imperative to consider the differences of solids mineralogy and pore water chemistry among these different types of tailings. Based on the laboratory testing results, both the investigated tailings required approximately five seasonal cycles to meet a threshold strength ( $> 80$  kPa) when moisture content approaches to the plastic limit. These threshold values were confirmed through the wetting behaviour when strength reduction due to rainfall became insignificant. Overall, this paper summarizes different parameters of seasonal weathering and how incorporating them with the flocculation and/thickening process can facilitate improved dewatering and shear strength properties.

### **Acknowledgements**

The authors would like to thank Natural Sciences and Engineering Research Council of Canada (NSERC), Canada's Oil Sands Innovation Alliance (COSIA) and Alberta Innovates – Energy and Environment Solutions for their financial support.

### **References**

- AER. 2016. Alberta's Energy Reserves 2015 & Supply/Demand Outlook 2016-2025 (ST98-2016), Alberta Energy Regulator, Calgary, Alberta.
- Andersland, O.B. and Ladanyi, B. 2004. *Frozen Ground Engineering*. 2nd Edition, American Society of Civil Engineers & John Wiley & Sons Inc., Hoboken, New Jersey, USA.
- ASTM. 2014. Standard Test Methods for Electrical Conductivity and Resistivity of Water. *ASTM Standard D1125-14*. ASTM International, West Conshohocken, PA, 2014. doi: 10.1520/D1125-14.

- ASTM. 2014. Standard Test Methods for Specific Gravity of Soil Solids by Water Pycnometer. *ASTM Standard D854-14*. ASTM International, West Conshohocken, PA, 2014. doi: 10.1520/D0854-14.
- ASTM. 2017. Standard Test Methods for Liquid Limit, Plastic Limit, and Plasticity Index of Soils. *ASTM Standard D4318-17e1*. ASTM International, West Conshohocken, PA, 2017. doi: 10.1520/D4318-17E01.
- ASTM. 2017. Standard Test Methods for Particle Size Distribution (Gradation) of Fine-Grained Soils Using the Sedimentation (Hydrometer) Analysis. *ASTM Standard D7928-17*. DOI: 10.1520/D7928-17.
- ASTM. 2019. Standard Test Methods for Laboratory Determination of Water (Moisture) Content of Soil and Rock by Mass. ASTM D2216-19. ASTM International, West Conshohocken, PA, 2019. doi: 10.1520/D2216-19.
- ASTM. 2019. Standard Test Method for Methylene Blue Index of Clay. *ASTM C837-09*. ASTM International, West Conshohocken, PA, 2019. doi: 10.1520/C0837-09R19.
- ASTM. 2019. Standard Test Methods for pH of Soils. *ASTM D4972-19*. ASTM International, West Conshohocken, PA, 2019. doi: 10.1520/D4972-19.
- Baker, T. 1976. Transportation, Preparation, and Storage of Freezing Soil Samples for Laboratory Testing. In *Soil Specimen Preparation for Laboratory Testing*. Edited by D. Sangrey and R. Mitchell. ASTM STP 599, ASTM International, West Conshohocken, PA, pp. 88-112.
- Barbour, S.L. and Fredlund, D.G. 1989. Mechanism of osmotic flow and volume change in clay soils. *Canadian Geotechnical Journal*, 26 (4):551-562. doi: 10.1139/t89-068
- Barr Engineering Co. (Barr) and O’Kane Consultants (OKC). 2016. *Atmospheric Fines Dryng (AFD) Deposition Optimization: Multi-lift versus Deep Stacking*. Final Report prepared for Shell Canada Energy, Calgary, AB, Canada.
- Beier, N. A and Segó, D.C. 2009. Cyclic Freeze-Thaw to Enhance the Stability of Coal Tailings. *Cold Regions Science and Technology*, 55 (3): 278-285. doi: 10.1016/j.coldregions.2008.08.006
- Beier, N., Wilson, W., Dunmola, A., & Segó, D., 2013. Impact of flocculation-based dewatering on the shear strength of oil sands fine tailings. *Canadian Geotechnical Journal*, 50 (9):1001-1007. doi: 10.1139/cgj-2012-0262.

- Beier, N., Kabwe, L.K., Scott, J.D., Pham, N.H., and Wilson, G.W. 2016. Modeling the effect of flocculation and desiccation on oil sands tailings. *Geo-Chicago*, Chicago, Illinois, USA, August 14-18, 2016.
- CanmetENERGY, 2009. *Rim ditch dewatering pilot test*. Division Report, Devon 09-80, Alberta.
- Chamberlain, E.J. 1981. Overconsolidation effects of ground freezing, *Engineering Geology*, 18 (1-4): 97-110. doi:10.1016/0013-7952(81)90050-8.
- Consortium of Oil Sands Tailings Management Consultant (CTMC), 2012. *Oil Sands Tailings Technology Deployment Roadmap*. Project Report, Volume 2, Calgary, Alberta.
- Cowie, B.R., James, B., and Mayer, B. 2105. Distribution of total dissolved solids in McMurray Formation water in the Athabasca oil sands region, Alberta, Canada: Implications for regional hydrogeology and resource development, *AAPG Bulletin*, 99(1): 77-90.
- Darrow, M.M., Guo, R. and Trainor, T.P. 2020. Zeta potential of cation treated soils and its implication on unfrozen water mobility. *Cold Regions Science and Technology*, 173:103029. doi: 10.1016/j.coldregions.2020.103029.
- Dawson, R.F. and Segó, D.C. 1993. Design Concepts for Thin Layered Freeze-Thaw Dewatering Systems. In *Proceedings of the 46th Canadian Geotechnical Conference*, Saskatoon, SK, Canada: 283-288.
- Dawson, R.F., Segó, D.C., and Pollock, G.W. 1999. Freeze-thaw dewatering of oil sands fine tails. *Canadian Geotechnical Journal*, 36: 587-598. doi: 10.1139/t99-028.
- Eigenbrod, K.D. 1996. Effects of cyclic freezing and thawing on volume changes and permeabilities of soft fine-grained soils. *Canadian Geotechnical Journal*, 33(4): 529-537. doi: 10.1139/t96-079-301.
- Government of Canada. Historical weather data for Fort McMurray. Available from [https://climate.weather.gc.ca/historical\\_data/search\\_historic\\_data\\_e.html](https://climate.weather.gc.ca/historical_data/search_historic_data_e.html) (accessed 28 July, 2020).
- Han, Z., and Vanapalli, S.K. 2016. Stiffness and shear strength of unsaturated soils in relation to soil- water characteristic curve. *Geotechnique*, 66 (8): 627-647. doi: 10.1680/jgeot.15.P.104.
- Hen-Jones, R.M., Hughes, P.N., Stirling, R.A., Glendinning, S., Chambers, J.E., Gunn, D.A., and Cui, Y.J. 2017. Seasonal effects on geophysical-geotechnical relationships and their implications for electrical resistivity tomography monitoring of slopes. *Acta Geotechnica*, 12: 1159-1173. doi: 10.1007/s11440-017-0523-7.

- Henry, H. 2007. Soil freeze–thaw cycle experiments: Trends, methodological weaknesses and suggested improvements. *Soil Biology and Biochemistry*, 39: 977-986. doi: 10.1016/j.soilbio.2006.11.017.
- Hobbs, P. 1974. *Ice Physics*, Oxford, UK: Clarendon Press.
- Innocent-Bernard, T. 2013. *Evaporation, Cracking, and Salinity in a Thickened Oil Sands Tailings*, MAsc. Thesis. Department of Civil and Environmental Engineering, Carleton University, Ottawa, ON, Canada.
- Johnson, R.L., Pork, P., Allen E.A.D., James, W.H. and Koverny, L. 1993. *Oil Sands Sludge Dewatering by Freeze-Thaw and Evaporation*. Report-RRTAC 93-8, Alberta Conservation and Reclamation Council, AB, Canada.
- Knutsson, R., Viklander, P. and Knutsson, S. 2016. Stability Considerations for Thickened Tailings due to Freezing and Thawing. *In Proceedings of the 19th International Seminar on Paste and Thickened Tailings*, Santiago, Chile, pp. 567-577.
- Locat, J. and Demers, D. 1988. Viscosity, yield stress, remolded strength, and liquidity index relationships for sensitive clays. *Canadian Geotechnical Journal*, 25 (4): 799-806. doi: 10.1139/t88-088.
- Luteneggar, A.J. 1995. *Geotechnical Behavior of Over-consolidated Surficial Clay Crusts*. Transportation Research Board, No. 1479, pp 61-74.
- MacKay, J.R. 1974. Reticulate ice veins in permafrost, Northern Canada. *Canadian Geotechnical Journal*, 11(2): 230-237. doi: 10.1139/t74-019.
- Mikula, R. J., Munoz, V. A. and Omotoso, O. 2008. Centrifuge options for production of “Dry stackable tailings” in surface mined oil sands tailings management. *Canadian International Petroleum Conference*, Calgary, AB, Canada.
- Miller, W.G., Scott, J.D., and Sego, D.C. 2010. Influence of the extraction process on the characteristics of oil sands fine tailings. *Journal of Canadian Institute of Mining, Metallurgy and Petroleum*, 1(2): 93-112.
- Mitchell, J.K. and Soga, K. 2005. *Fundamentals of Soil Behaviour*. 3rd ed., John Wiley and Sons, Inc., New York, NY, USA.
- Oil Sands Tailings Consortium (OSTC) and Canada’s Oil Sands Innovation Alliance (COSIA). 2012. *Technical Guide for Fluid Fine Tailings Management*, Report, Calgary, Alberta.

- O’Kane Consultants, 2017. *Perimeter Ditch Pilot 1 Trial 2016 Performance Monitoring Update*, Report prepared for Syncrude Canada Ltd., Calgary, AB, Canada.
- Othman, M.A. and Benson, C.H. 1992. *Effect of Freeze-Thaw on the Hydraulic Conductivity of three Compacted Clays from Wisconsin*. Transportation Research Record, 1369: 118-129.
- Othman, M.A. and Benson, C.H. 1993. Effect of Freeze-Thaw on the Hydraulic Conductivity and Morphology of Compacted Clay. *Canadian Geotechnical Journal*, 30 (2): 236-246. doi: 10.1139/t93-020.
- Park, H., Lee, S.R., and Jee S.H. 2010. Bearing Capacity of Surface Footing on Soft Clay Underlying Stiff Nonhomogeneous *Desiccated Crust*. *International Journal of Offshore and Polar Engineering*, 20 (3): 224-232.
- Pham, N.H. and Segoo, D.C. 2014. Modeling Dewatering of Oil Sands Mature Fine Tailings using Freeze Thaw. *International Oil Sands Tailings Conference*, Lake Louise, AB, Canada, December 7-10, 2014.
- Proskin, S.A. 1998. *A Geotechnical Investigation of Freeze-Thaw Dewatering of Oil Sands Fine Tailings*, PhD Thesis. Department of Civil and Environmental Engineering, University of Alberta, Edmonton, AB, Canada.
- Proskin, S., Segoo, D. and Alostaz, M. 2010. Freeze-thaw and consolidation tests on Suncor mature fine tailings (MFT). *Journal of Cold Regions Science and Technology*, 63 (3): 110-120. doi: 10.1016/j.coldregions.2010.05.007.
- Proskin, S., Segoo, D. and Alostaz, M. 2012. Oil Sands MFT Properties and Freeze-Thaw Effects. *Journal of Cold Regions Engineering, ASCE*, 26 (2): 29-54. doi: 10.1061/(ASCE)CR.1943-5495.0000034.
- Qiu, Y. 2000. *Optimum Deposition for Sub-Aerial Tailings Disposal*. Ph.D. Thesis. University of Alberta, Edmonton, Alberta, Canada.
- Rima, U.S. and Beier, N. 2018. Evaluation of Temperature and Multiple Freeze-Thaw Effects on the Strength Properties of Centrifuged Tailings. *71st Canadian Geotechnical Conference*, Edmonton, Canada, September 23-26, 2018.
- Sanchez Sardon, M.A. 2013. *Combined Evaporation and Freeze-Thaw Effects in Polymer Amended Mature Fine Tailings*. MAsc. Thesis, Department of Civil and Environmental Engineering, Carleton University, Ottawa, ON, Canada.

- Sego, D.C. 1992. *Influence of pore fluid chemistry on freeze-thaw behaviour of Suncor Oil Sand Fine tails (Phase I)*. Report, submitted to Reclamation Research Technical Advisory Committee, Alberta Environment.
- Spence, J., Bara, B., Lorentz, J. and Mikula, R. 2015. Development of the Centrifuge Process for Fluid Fine Tailings Treatment at Syncrude Canada Ltd. In *World Heavy Oil Congress 2015*, Edmonton, Alberta, 24-26 March, 2015.
- Sorta, A.R., and Sego, D.C. 2010. Segregation related to use of Centrifuge in Oil Sands Tailings. In *Proceedings of the 13<sup>th</sup> International Conference on Tailings and Mine waste*, Banff, AB, Canada. pp. xvii-xli
- Standard Methods. 2017. 3125 *Metals by Inductively Coupled Plasma-Mass Spectrometry. Standard Methods for the Examination of Water and Wastewater*. doi: abs/10.2105/SMWW.2882.048.
- Tang, C.S., Cui, Y.J., Shi, B., Tang A.M., and Liu, C. 2011. Desiccation and Cracking Behaviour of Clay Layer from Slurry State under Wetting-Drying Cycles. *Geoderma*, 166 (1): 111-118. doi: 10.1016/j.geoderma.2011.07.018.
- Tang, J. 1997. *Fundamental Behaviour of Composite Tailings*. M.A.Sc. Thesis, Department of Civil and Environmental Engineering, University of Alberta, Edmonton, AB, Canada.
- Wilson, G.W., Kabwe, L.K., Beier, N.A., and Scott, J.D. 2018. Effect of various treatments on consolidation of oil sands fluid fine tailings. *Canadian Geotechnical Journal*, 55 (8): 1059-1066. doi: 10.1139/cgj-2017-0268.
- Xia, D; Arenson, L.U., Biggar, K.W., and Sego, D.C. 2005. Freezing process in Devon silt-using time lapse photography. In *Proceedings of the 58th Canadian Geotechnical Conference 2005*, September 18-21, Saskatoon, SK, Canada.
- Xia, D. 2006. *Frost Heave Studies using Photographic Technique*. M.A.Sc. Thesis, Department of Civil and Environmental Engineering, University of Alberta, Edmonton, AB, Canada.

# **4 SEASONAL WEATHERING OF OIL SANDS TAILINGS DEPOSITS: COMPARISON OF FIELD AND LABORATORY DATA**

## **Abstract**

This paper presents a comparative study on the effects of seasonal weathering on dewatering and strength behaviour of an oil sands in-line thickened tailings (ILTT) deposit. Laboratory results are compared to the field measurements from a field pilot ILTT deposit located at the Syncrude Canada Ltd.'s Mildred Lake mine site to evaluate if the laboratory testing could simulate the field observations. Good agreement between the field and laboratory results was obtained in terms of dewatering and strength gain at the near surface subjected to seasonal weathering (freeze-thaw and evaporation). After five seasonal cycles, the geotechnical moisture contents at the surface obtained from the laboratory experiments were 68% (represented by only freeze-thaw cycles with no summer drying condition) and 25% (represented by five freeze-thaw and five alternate drying-wetting cycles). This range of moisture contents was consistent with the values measured at three testhole locations of the field deposit (39, 45 and 43%, respectively). The laboratory results also indicate an undrained shear strength of 84 kPa at the surface that can be correlated to the surface crust observed in the field. Overall, the laboratory-based experiments were found to simulate the field conditions, provided that similar boundary conditions (thermal) can be achieved.

## **4.1 Introduction**

Extraction of bitumen from oil sands in a surface mining operation is a water-based process that generates a large volume of fine-grained slurry waste as by-products that are known as tailings. Tailings, a mixture of sand, fines (clays and silts), residual bitumen and process affected water, are disposed of by overboarding into the containment ponds, where these particles naturally undergo segregation. Upon deposition, the coarser fractions (sand) settle out to form beaches leaving the fines (particle size less than 0.044 mm) in suspension (Jeeravipoolvarn, 2010). Because of the water-based extraction process and slow consolidation behaviour, large amounts of water are trapped within the fine streams, which result in accumulation of fluid fine tailings (FFT) over

time (AER, 2017). At present, mine operators are required to improve their reclamation strategies by ensuring that FFT are ready to reclaim within 10 years from the end of the mine life (AER, 2018). Ready to reclaim implies the tailings can support a landform of similar topography to the pre-existing boreal forest (McKenna, 2017) which, would necessitate an undrained shear strength of a minimum 20 kPa (Hurtado, 2018) before reclamation activities could begin. In an effort to facilitate dewatering and promote trafficable surfaces for reclamation, oil sands mine operators employ different technologies to treat FFT (OSTC and COSIA, 2012). Of these technologies, one such method under investigation, adapted from Florida phosphate mining industry, is “accelerated dewatering/ perimeter ditching” where a combination of perimeter ditching and decant system was employed with the polymer treated FFT deposit to promote additional dewatering via surface drainage and self-weight consolidation (Lahaie et al., 2010).

A large-scale pilot test incorporating accelerated dewatering with in-line thickened tailings (ILTT) is underway at Syncrude Canada Ltd. (Syncrude) to evaluate the effectiveness of dewatering performance, strength development and overall reclamation strategies for deep (typically >10 meters or deeper) in-line thickened tailings deposit (BGC and OKC, 2014). Following the end of deposition, the test deposit was intended to be exposed to the atmosphere for five to ten years in order to monitor the effects of atmospheric drying (evaporation and freeze-thaw process) and surface dewatering system (perimeter ditching) on the ILTT (BGC and OKC, 2014). It should be mentioned that the construction of the perimeter ditching to collect and drain away surface water was completed annually, starting a year after the end of deposition. However, the performance of the pilot test deposit over the first 50 months after end of deposition showed that the dewatering rates less than what obtained in the clay slurry deposits of the Florida phosphate mines (BGC and OKC, 2014). Atmospheric drying due to freeze-thaw dewatering and evaporation was found to be the dominant dewatering mechanism (BGC and OKC, 2014). Hence, this paper compares the efficacy of the atmospheric drying process (freeze thaw and evaporation) achieved in the laboratory to the field behaviour.

The specific objective of this paper is to compare the near-surface dewatering and strength behaviour of the field deposit with results from a laboratory-developed methodology to evaluate whether the laboratory testing can replicate field behaviour. A one-dimensional closed system

freeze-thaw process coupled with drying and rewetting cycles was developed to simulate the seasonal weathering process of the in-line thickened tailings (ILTT) on a small laboratory scale (Rima and Beier, 2021a and 2021 b). Following each cycle of freeze-thaw, the samples were subjected to surface water removal prior to evaporation. Evaporation/ drying tests followed by a wetting event were undertaken to simulate the summer drying and rainfall in the field, respectively. However, dewatering by under-drainage was not considered for the laboratory testing.

## 4.2 Background

In-line flocculation of FFT coupled with perimeter ditching concept was piloted by Syncrude in the summer 2009 in a 10 m deep and approximately 60,000 m<sup>3</sup> tailings field deposit (Lahaie et al., 2010). ‘Perimeter ditching’ simply refers to digging a ditch around the perimeter of the flocculated FFT deposit, which is advanced deeper as the phreatic surface lowers in the deposit (Lahaie et al., 2010). In-line flocculation involves dredging FFT from the tailings pond, followed by injecting and mixing flocculant into the FFT (in-line), and then discharging the flocculated slurry over a large area with a gently sloped base (Thurber engineering, 2012). Following initial dewatering due to the flocculation, self-weight consolidation occurs at a very slow rate due to the long seepage path through the deep tailings deposit and a low hydraulic conductivity (Jeeravipoolvarn, 2010). Since self-weight consolidation is the predominant mechanism of dewatering for the deep deposits (OSTC and COSIA, 2012) and FFT consolidates slowly due to its low hydraulic conductivity, a combination of different technologies and deposit management strategies are required to promote further dewatering and development of shear strength. Hence, perimeter ditching coupled with subsequent dewatering by atmospheric effects (freeze-thaw dewatering and evaporation) was evaluated to promote densification and shear strength development (Thurber engineering, 2012). Additionally, drying (due to freeze-thaw and evaporation) causes the upper parts of the tailings to be unsaturated and therefore, the unit weight acting on the underlying tailings progressively starts to change from buoyant unit weight to effective unit weight (Lahaie et al., 2010). As a result, an increase in surcharge load is observed with an increase in effective stress and a decrease in pore pressures that speeds up the self-weight consolidation.

The oil sands deposits in Fort McMurray, Northern Alberta, experiences mean daily air temperatures ranging from -17°C in January to 17°C in July with an average temperature of -10°C

in winter and 14°C in summer (Environment Canada meteorological station at Fort McMurray, climate normal for 1981-2010). Thus, the colder temperature in Northern Alberta facilitates freeze-thaw dewatering as a potential cost-effective technology for further dewatering and shear strength development for oil sands tailings deposits. The mechanism of freeze-thaw dewatering involves the development of negative pore-water pressure/suction between the unfrozen water surrounding the tailings particles and the ice filling voids when slurries are subjected to below-freezing temperatures (Konrad and Morgenstern, 1980). The suction facilitates unfrozen water to migrate from the tailings towards the growing ice lenses, eventually forming a three-dimensional reticulate ice network surrounding the frozen consolidated blocks/peds of tailings (Dawson, et al., 1999; Beier and Seg0, 2009). Upon thawing, the ice matrix melts, leaving channels that promotes water to move upward to the surface resulting in overall volume reduction of the tailings deposit. Therefore, the new microstructure developed during freeze-thaw process retains less water which accounts for the increase in solids content (by weight) and development of shear strength (Proskin, 1998). The effectiveness of freeze-thaw dewatering is predominantly dependent on the initial solids content (Johnson et al., 1993; Lahaie et al., 2010), number of freeze-thaw cycles (Othman and Benson, 1993; Oztas and Fayetorbay, 2003), freezing rate (Proskin, 1998; Rima and Beier, 2021a and 2021b), dimensionality of freezing (one-dimensional vs. three-dimensional) (Eigenbrod, 1996; Johnson, et al., 1993), sample size (Konrad and Morgenstern, 1980; Henry, 2007), physicochemical interactions (Proskin et al., 2012; Mitchell and Soga, 2005), and the climate (air temperature and snow cover) contributing to the maximum seasonal depth of frost penetration (Lahaie et al., 2010).

The climate in the Fort McMurray area is such that it receives an average of 419 mm of precipitation annually, of which around 70% is contributed from rainfall (Environment Canada meteorological station at Fort McMurray, climate normal for 1981-2010). The area also experiences an average of 600 mm of potential evaporation (PE) annually (this value was calculated using the Penman method on the basis of climate data collected from various stations at the Mildred Lake mine site) (Lahaie et al., 2010). The higher amount of annual PE compared to the annual rainfall has a potential to facilitate surface drying and cracking. Therefore, the development of desiccated surface crust is anticipated in soft tailings disposal sites to contribute to increase in undrained shear strength that is required for reclamation operations (Johnson et al.,

1993). Additionally, the formation of surface cracks accelerates the efficiency of the freezing process (Sanchez Sardon, 2013) and accommodates deeper percolation of rainfall as well as an increase in surface area for evaporation of the underlying tailings (Innocent-Bernard, 2013). However, evaporation is a complex phenomenon predominantly governed by local climatic and environmental conditions such as solar radiation, wind speed, air temperature, ground temperature and relative humidity (Lahaie et al., 2010).

This paper aims to further investigate the field behaviour and mechanism driving the dewatering due to atmospheric drying and seasonal weathering using controlled laboratory experimental conditions. Two different sequences of freeze-thaw-drying-wetting cycles (one representing worst condition of multiple freeze-thaw cycles only and another representing both freeze-thaw and drying-wetting cycles) under field representative temperature gradient were evaluated. The impacts on the mechanical properties (such as solids content/ moisture content and shear strength) and salt migration was investigated in the laboratory and compared to the observed field behaviour.

### **4.3 Laboratory Investigation**

The ILTT samples were received from the pilot field deposit in three 20L pails. The samples were collected approximately 1m below the surficial crust. The materials, being collected 1 m below the surface, were not exposed to freeze-thaw cycle in the field and hence, thaw strain history for the samples was assumed to be negligible. The field samples were then tested in the laboratory by subjecting them to at least five seasonal cycles in order to compare to the available field data collected over five freeze-thaw seasons. Additionally, previous research (Rima and Beier, 2021a and 2021b) indicates that five seasonal cycles were adequate for a fine-grained cohesive tailings sample to approach the plastic limit or to gain an asymptotic shear strength (>100 kPa). For the laboratory freeze-thaw testing in this study, the tests were conducted in freezing cells within a walk-in freezer where the samples were frozen from top to down (one dimensional) to represent the field condition. A single thermal gradient of  $0.028^{\circ}\text{C}/\text{mm}$  ( $-5^{\circ}\text{C}$  at top and  $0^{\circ}\text{C}$  at bottom) was utilized in all experiments. These boundary conditions fall within the range of measured winter surface temperatures at the field location which varied from 0 to  $-10^{\circ}\text{C}$ , with an average of  $-5^{\circ}\text{C}$  (OKC, 2015). Closed system freezing was preferred to measure the contribution from freeze-thaw process due to the internal moisture distribution only as opposed to the open system freezing.

These two modes of freezing are differentiated according to the accessibility of an external supply of water. Open system freezing test is more representative of tailings deposit at the lower boundary of the crust (interactive layer between the frozen crust and underlying tailings) in the field and it is expected to draw more water into the frozen tailings from the unfrozen tailings below, thereby, resulting in a higher number of ice lenses and eventually, a higher degree of dewatering. On the contrary, closed system freezing would be more representative of the upper part of the tailings deposit where lower dewatering can be expected due to the restrictions of accessibility of water. Since the hydraulic conductivity for the tailings material is fairly low, lower conductivity along with the lack of fissures in the unfrozen and frozen tailings restrict water flow from the external water source (underlying unfrozen tailings in this case) to the ice lenses (Proskin et al., 2012). Hence, similar soil-ice reticulate structure can be expected for both the testing procedure irrespective of the external drainage conditions (Proskin et al., 2012; Sanchez Sardon, 2013). The installation of insulation wrap, thermoelectric cooling plate and thermistors were all applied for the freeze-thaw test setup, as suggested by the guidelines to artificially freeze soil samples (ASTM-STP 599, as documented in Baker, 1976). The detailed procedure is documented in Rima and Beier (2021a, 2021b).

The laboratory investigation was conducted in two phases: 1. first phase -five consecutive freeze-thaw cycles followed by a single cycle of drying-wetting-drying to investigate the contribution of freeze-thaw and drying-wetting cycles separately on the ILTT, and 2. second phase-five alternating freeze-thaw and drying-wetting cycles to better represent the natural seasonal weathering cycles. For each drying-wetting cycle, the samples were subjected to atmospheric drying under the ambient laboratory temperature ( $\sim 20^{\circ}\text{C}$ ) and the daily mass losses due to evaporation were recorded by means of weighing scale. No bottom drainage was permitted in these tests. In order to simulate rainfall, the volume of water evaporated during atmospheric drying was poured back by adding distilled water as a onetime event. The rationale for selecting the time frame of these tests in order to correlate to the annual cycle of the field deposit were as follows: 1. Each of the freeze-thaw cycles took approximately seven days to complete, and the freezing cycle was considered as complete when the temperature data (shown in Appendix-C) of the thermistors placed along the sample cells showed consistent values. 2. For the first phase of testing, the tailings sample was subjected to a month-long drying cycle followed by a single wetting event to simulate the rainfall.

After the wetting event, another drying cycle was continued until the AE/PE ratio declined to 0.7. The AE/PE ratio of the field deposit declined to 0.65-0.7 each year at the end of summer period (OKC, 2015) and 3. The second phase of testing included five drying–wetting cycles and hence, each of the drying cycles was run for a shorter duration (seven days) prior to a single wetting event. After the wetting event, the re-drying cycle was continued for another seven days to maintain time consistency in each cycle. However, even after such a shorter time duration, the AE/PE ratio at the end of the five cycles was found to be 0.40 (as shown in Figure E-8, Appendix-E). Therefore, this scenario can be represented as an upper boundary condition when higher evaporation/ prolonged summer period is expected and/or evaporation can be fully utilized in the field. However, the scale effects when increasing the sample volume tested from the laboratory to field scale (18 cm thick laboratory sample versus 10 m deep field deposit) were not considered for water contents and strength measurements as near surficial water contents and undrained shear strength were analysed in this paper. Also, the effects of seasonal weathering on the field deposits were expected to be limited to the top 1 m of the field deposit.

A manual desktop vane shear apparatus was used to measure the undrained shear strength of the 18 cm high (initial height) laboratory samples at the near surface (measured at a depth of 12.5 mm from the surface) after each of the cycle. Vane shear apparatus was chosen over other devices as the field undrained shear strength was also measured using field vane shear testing. Standard vane sizes and torque springs by the manufacturer were employed for the laboratory vane shear testing. However, for the ILTT samples with strength below 8 kPa, Brookfield DV3T Rheometer was used to measure the undrained shear strength. The detailed procedures of the first phase and the second phase testing are documented in Rima and Beier (2021a, 2021b).

#### **4.4 Results and Discussion**

A summary of the index properties, solids mineralogy and pore water chemistry results of the ILTT sample are included in Tables 4.1, 4.2 and 4.3. The measured geotechnical moisture contents,  $w$  (mass of water divided by the mass of dry solids including bitumen) of the laboratory sample was found to be 122%, corresponding to a solids content ( $s$ ) of 45%. Material finer than 0.044 mm and 0.002 mm was measured to be 93 and 70%, respectively, indicating the fine-grained nature of the tailings. Mineralogy analyses by X-ray diffraction indicates that the ILTT sample has about 80%

clay minerals comprising predominantly kaolinite (56%) and illite (24%). The predominance of clay-sized fractions in a basic (pH = 8.3) medium indicates the presence of higher negative charges in the solution where OH<sup>-</sup> serves as the potential determining ion (Prasanphan and Nuntiya, 2006). Clay dispersion is primarily affected by the net negative charges that was confirmed through the calculated sodium adsorption ratio value (38.1). This value indicates “a likely dispersed microstructure” of the tailings fabric, as suggested by Miller et al. (2010). Additionally, the presence of residual bitumen (2%) adds further sensitivity by promoting electrostatic repulsion and hence, result in an overall higher negative surface charge (Hogg, 2000).

Table 4.1: Summary of index properties of tailings

Property	Value
Moisture content, $w$ (%)	122
Solids content, $s$ (%) <sup>1</sup>	45
Bitumen content (%)	2
Specific gravity, $G_s$	2.45
Material finer than 0.044 mm (%)	93
Material finer than 0.002 mm (%)	70
Liquid limit, $w_l$ (%)	62
Plastic limit, $w_p$ (%)	23

**Note.** <sup>\*</sup> $s = 1 / (1 + w)$

In-situ sampling and strength testing of the field deposit were conducted at three testhole locations (designated as TH-03, TH-05 and TH-SB) on an annual basis since 2009 after the commencement of the pilot test program (BGC and OKC, 2014). Test hole TH-03, TH-05 and TH-SB represent 27, 42 and 31% of the total area of the deposit (OKC, 2015). A month after deposition, the average moisture content of the field deposit ranged between 108 and 212%, with an average of 138% (corresponding to an average  $s$  of 42%) due to initial dewatering caused by the in-line flocculation using a polymer (Lahaie et al., 2010). The measured field profiles of solids content and undrained shear strength were compared with the laboratory-tested samples, where each of the laboratory

samples was run for five cycles (to represent five years) and then, oven-dried to measure the solids content.

Table 4. 2: Summary of the solids mineralogy of the tailings

Property	Value
Minerals (% weight)	Non-clay: Quartz (18); Siderite (2); Potassium Feldspar (1); Plagioclase Feldspar (1)
Bulk and clay	
	Clay: Kaolinite (56); Illite (24) = Total clay (80%)
Clay fraction (%)	68
From MBI	
Exchangeable cations (cmol(+)/kg)	Ca <sup>2+</sup> (7.5); Na <sup>+</sup> (7.5); Mg <sup>2+</sup> (2.8); K <sup>+</sup> (0.5)
Total CEC (meq/100g)	18.3

Table 4.3: Summary of pore water chemistry results

Property	Value
pH	8.3
Electrical conductivity, EC (µs/cm)	2,800
Dissolved ions (mg/L)	Cations: Na <sup>+</sup> (677); Ca <sup>2+</sup> (13); K <sup>+</sup> (8); Mg <sup>2+</sup> (6.6)
	Anions: HCO <sub>3</sub> <sup>-</sup> (1,070); Cl <sup>-</sup> (631); SO <sub>4</sub> <sup>2-</sup> (29); CO <sub>3</sub> <sup>2-</sup> (<5); OH <sup>-</sup> (<5); F <sup>-</sup> (2.47); NO <sub>3</sub> <sup>-</sup> (<0.5)
Total dissolved solids (mg/L)	1,890
Sodium adsorption ratio (SAR)	38.1

Figure 4.1 compares the moisture content values of the 18 cm (initial height) laboratory samples to the field data obtained from three different testhole locations. The laboratory moisture content values were calculated based on the change in thaw strain after each freeze-thaw cycles and the change in mass loss/gain due to evaporation/wetting after each drying-wetting cycles. The field data shown were collected following spring melt and thawing (from April to June) at a depth

between 0 and 25 cm from the surface, as this zone is expected to be more closely represented by closed system freezing due to the presence of surface crust and its higher solids contents.

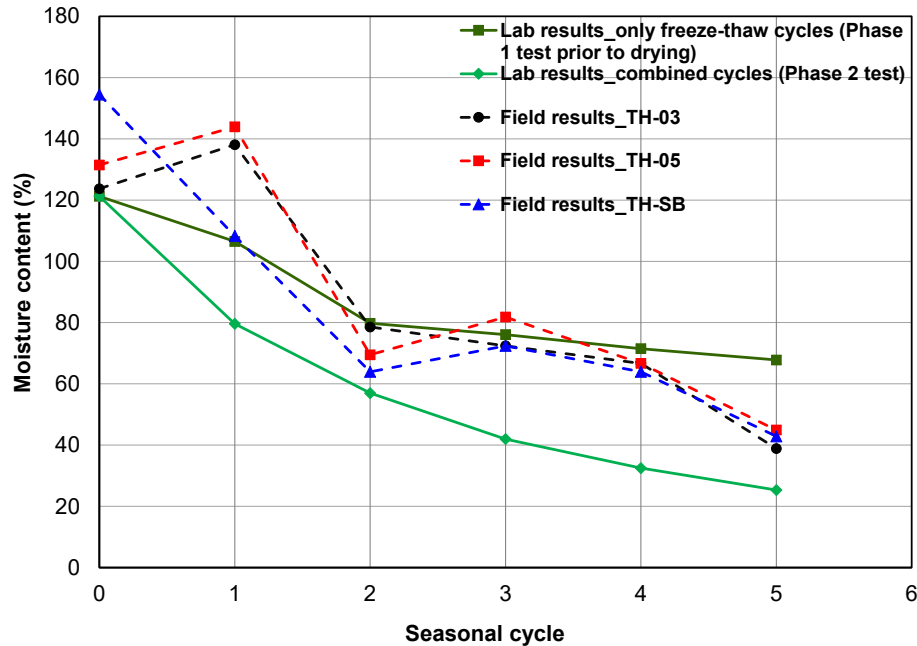


Figure 4.1: Comparison between the field and laboratory moisture content values after each cycle

Figure 4.1 shows that where only freeze-thaw cycles were applied (representative of extreme field condition with no evaporation/drying), a gradual decrease in moisture content from 122 to 68% was observed (corresponding to a solids content from 45 to 60%). This is in contrast to a case where combined freeze-thaw-drying-wetting cycles were applied, which resulted in a three-fold lower moisture content (final moisture content value was 25%), as compared to the only freeze-thaw cycles. For comparison, the field (at a depth of 0 to 25 cm) moisture contents at three testhole locations TH-03, TH-05 and TH-SB were found to be 39, 45 and 43%, respectively, five years after the end of deposition. Although an overall long-term downward trend in moisture contents was observed throughout the deposits, the seasonal fluctuating temperature in the upper couple of meters of the deposit along with the weathering of the surface crust resulted in the fluctuations in moisture retention and prevented the development of deep surface cracks (OKC, 2015). Colder winter season/ lower freezing temperatures typically results in deeper frost depth and hence, more dewatering. However, snow covers, surface relief and/or sub-surface drainage can significantly

affect the freeze-thaw dewatering process (Andersland and Ladanyi, 2004), thus, making it challenging to replicate the field behaviour in the laboratory. Figure 1 shows that the area bounded by a lower limit (representing the condition with no evaporation/drying component) and an upper limit (representing the combined effects of freeze-thaw-drying-wetting) for moisture content values under the controlled laboratory temperature condition can approximate the trends of dewatering observed in the field provided the temperature gradients are in the same range. It is worth mentioning that the frost depth of the field deposit reached a maximum of 50 cm at the 3rd and 4th seasonal cycles and 1.4 m at the 5th seasonal cycle (OKC, 2015). In these seasonal cycles, the temperature within the deposit ranges from -1 to -10°C with an average of -5°C and an average temperature gradient of 0.01°C/mm (OKC, 2015). The field frost penetration depths for the first two years were not available.

Figure 4.2 compares the measured oven-dried moisture content profiles of the laboratory samples to the field deposit (measured at three test hole locations) after five seasonal cycles. The moisture content values of the upper 10 cm of the field deposit were compared with the laboratory samples of 10 cm thicknesses (final height of the samples after five cycles). As expected, samples obtained from the laboratory and field deposit were subjected to the lowest moisture content at the surface, in which the laboratory samples subjected to the phase 1 testing and phase 2 testing resulted in the surface moisture content values of 24 (solids content of 80%) and 26% (solids content of 79.5%), respectively. The field deposit data at three testhole locations TH-03, TH-05 and TH-SB experienced moisture contents of 5, 15 and 22% (solids contents of 95, 87 and 82%), respectively. As a result of higher solids content at the surface, a 15 to 20 cm thick crust (an over-consolidated layer at the surface formed due to the weathering and desiccation which can also be differentiated by its higher density and shear strength compared to the underlying tailings) was developed in the field deposit (OKC, 2015). On the contrary, no distinguishable surface crust was observed in the laboratory investigation, thereby, contributing to the lower solids content compared to the field data. It should also be noted that atmospheric drying (freeze-thaw and evaporation) in the field contributed to approximately 72% of the total dewatering for 2014 monitoring year (OKC, 2015), while the laboratory investigation was entirely based on the contributions from seasonal weathering. Hence, lower solids content or higher moisture content in the laboratory was naturally expected. However, under-drainage, which was considered the second most dominant field

dewatering mechanism (20% of the total dewatering), limits the upward migration of water to the deposit surface (OKC, 2015). Therefore, contributions of under-drainage to the dewatering of the upper surface of the deposit can be considered minimal. Hence, the laboratory values generally represent a conservative result when compared to the field deposit.

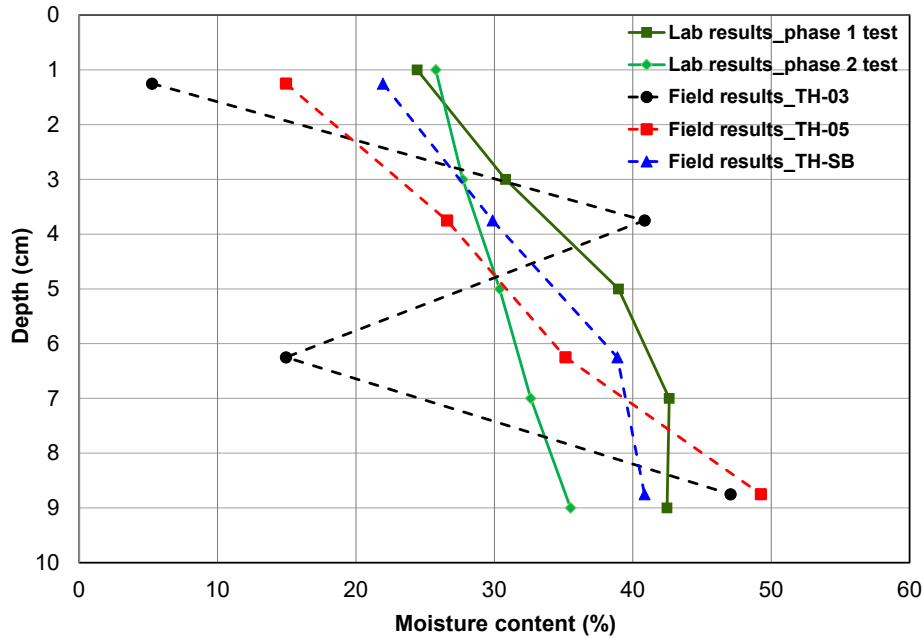


Figure 4.2: Comparison between the field and laboratory moisture content profiles after seasonal cycles

Figure 4.3 shows the measured undrained shear strength values of the laboratory samples and field deposit over five seasonal cycles. The combined freeze-thaw-drying-wetting cycles (second phase testing) conducted in the laboratory is only presented in right vertical axis so the smaller values (<10 kPa) obtained from the other samples (field deposit and laboratory sample subjected to only freeze-thaw cycle are on the left side axis) can be viewed easily. It is to be noted that the vane shear strength for the laboratory samples were measured at a depth of 12.5 mm from the surface whereas, the strength at the three testhole locations were measured at a depth of 50 cm from the surface and below the crust. For practical reasons, field shear strength testing was completed below the surface crust. The maximum depth of crust developed at the surface of the field deposit was 15-20 cm where lowest moisture content was measured (as per Figure 4.2). The upper and lower boundaries of the deposit were subjected to atmospheric drying and under-drainage, respectively,

which in turn, resulted in the significant gain in solids content and shear strength (OKC, 2015). On the contrary, shear strengths in the middle portion of the deposit remained almost unchanged due to the weathering of the deposit surface preventing further crack propagation and hence, minimizing the contributions of atmospheric drying at depths (OKC, 2015).

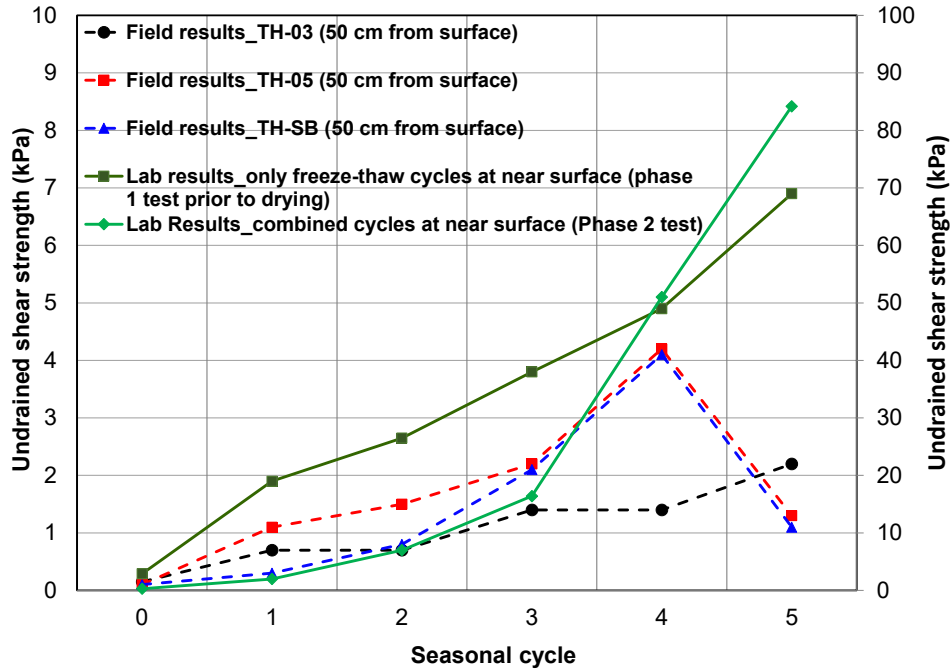


Figure 4.3: Measured undrained shear strength values of field and laboratory samples versus the number of seasonal cycles (right Y axis-phase 2 test lab data, left Y axis-rest of the other data)

As evident in Figure 4.2, all the three testhole locations showed an increase in moisture content within just a few centimetres from the surface and hence, lower shear strength at depths compared to the surface is expected. These findings are consistent with Figure 4.3 which clearly shows a difference in shear strength values between the field data (measured at a depth of 50 cm from the surface) and laboratory data (measured at near surface) where combined seasonal weathering (freeze-thaw-drying-wetting) was applied. Since the surficial shear strength data were not available for the field deposit, it would be inconsistent to compare the effects of seasonal weathering on the shear strength values between the field deposit and the laboratory samples at different depths. However, the temperature fluctuations at a greater depth for the field deposit are not significantly affected by the ambient temperature. The absence of deeper surface cracks in the

field deposit suggests that the contribution of atmospheric drying on shear strength gain is minimal at depths from the surface. Additionally, the depth of frost penetration reached a maximum of approximately 50 cm for the 3rd and 4th seasonal cycles (first two cycles were not reported). Only the winter in the 5th seasonal cycle resulted in a deeper frost depth (maximum frost depth was 1.4 m and overall greater than 50 cm) into the deposit. Therefore, freeze-thaw dewatering is likely not contributing to the gain in shear strength at depths greater than 50 cm from the surface (excluding 5th seasonal cycle).

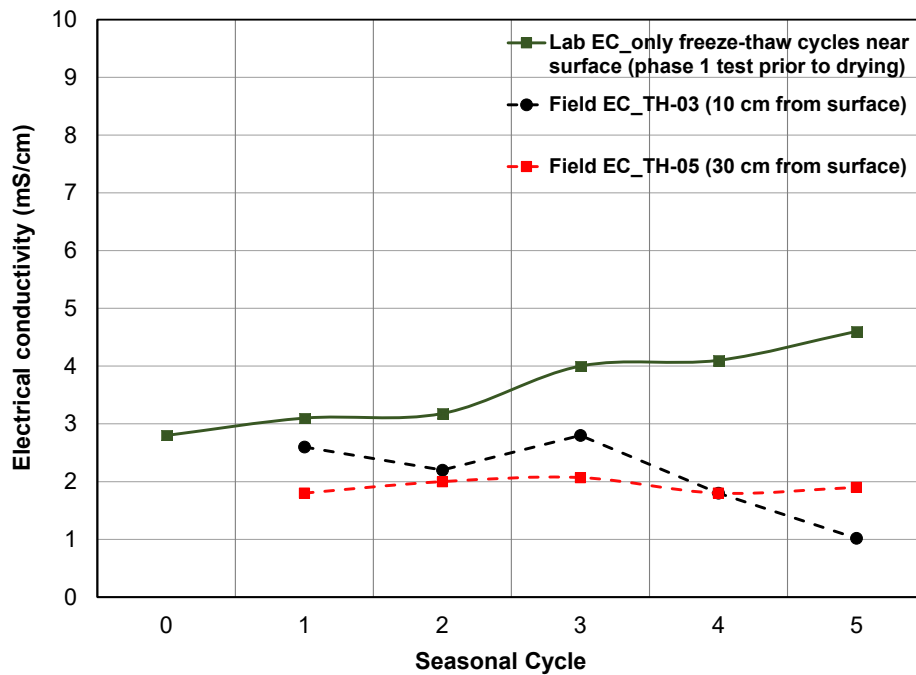


Figure 4.4: Measured electrical conductivity values of field and laboratory samples versus the number of seasonal cycles

Figure 4.4 shows the measured EC values of the laboratory and field samples over five years. Soil EC indicates the concentration of solute dissolved in the soil water phase that can correlate the freeze-thaw dewatering to the physico-chemical properties. For fine-grained materials like tailings, salt migration during freezing is considered the major contributor to an increase in ion concentration at the surface, thereby increasing that osmotic suction (Innocent-Bernard, 2013; Bing et al., 2015). Higher osmotic suction reduces the inter-particle repulsive forces by forming particle flocculation that possibly leads to the suppression of the double layer and increases overall

volume reduction (Barbour and Fredlund, 1989). Therefore, higher dewatering is associated with the higher ion/salt concentration at the surface. In the laboratory, EC values were measured at a depth of 15 mm from the surface using a benchtop pH/EC meter after the completion of each freeze-thaw cycle, whereas TDR (time domain reflectometry) sensors were used to measure the EC values for the field deposit. Like shear strength, no surficial / near surface EC data from the field deposit were available to allow for a precise comparison to the laboratory measured values. As shown in Figure 4.4, the laboratory EC values increased with each seasonal cycle (from 2.8 mS/cm at the beginning to 4.6 mS/cm after five freeze-thaw cycles). Unfrozen water volume is known to decrease during freezing due to the phase change from water to ice. The growth of ice lenses with increasing freeze-thaw cycles results in solute exclusion from the ice phase, thereby contributing to an increase in solute concentration within the remaining water (Proskin et al., 2012). The laboratory results support this theory. The pore-water EC for the laboratory sample (2.8 mS/cm) was found within the ranges observed in the field deposit (1.8 and 2.6 mS/cm for TH-03 and TH-05, respectively), albeit the field EC values showed an overall slight decrease with time. The decrease in EC was attributed to the gradual disappearance of salt crusts (reflecting upward salt migration observed during the first year after deposition) due to deposit weathering from wind-blown tailings sand, dust and granules replacing the salt crusts (BGC and OKC, 2014). In addition to this, the decrease in EC may be caused by surface run off washing off any surface salt precipitate into the decant/dewatering structure in the field (OKC, 2017). However, marginal changes in EC values after each freezing cycle from both the laboratory and field investigations suggest that the salt migration did not occur substantially for this deposit. Hence, salt migration/EC values cannot be correlated to particle flocculation and dewatering contributing to the observed increase in shear strength.

Given the similar ranges of thermal boundary conditions in the field, the findings of the current small-scale laboratory tests demonstrate the utility of such tests in simulating the freeze-thaw dewatering potential of treated tailings deposits for design scenarios incorporating seasonal weathering. Despite the controlled versus uncontrolled boundary conditions for the laboratory samples and field deposit, respectively, overall, this study demonstrates that given similar initial and thermal boundary conditions, the dewatering and shear strength performance of the ILTT deposit can be simulated.

## **4.5 Conclusion**

The present study developed a methodology to simulate the expected behaviour of a deep ILTT deposit. The thermal boundary conditions/ thermal gradients of the laboratory samples were in similar range as the field deposit. For the field deposit, seasonal weathering (atmospheric drying with freeze-thaw dewatering) facilitated the formation of a surface crust (15 to 20 cm thick). However, the shallow surface crust was insufficient to ensure a trafficable surface as the tailings just underneath the crust remained very soft. The maximum shear strength at 50 cm below the surface of the field deposit was 5 kPa. When compared to the field samples, the laboratory samples did not form any distinguishable surface crust at the surface. This can be attributed to the difference in the duration of testing (five years for the field deposit versus 3~4 months long laboratory testing to simulate five seasonal cycles) under field and laboratory conditions. The laboratory samples subjected to seasonal weathering generally correlated well with the field results in terms of dewatering and strength gain at the near surface. This implies that the laboratory approach has the potential to simulate the field behaviour if the initial and boundary conditions can be closely replicated. Also, it is paramount to ensure the provisions of adequate water management/good surface drainage in the field in order to fully utilize the benefits of the seasonal weathering effects in the laboratory. Overall, the laboratory test approach described in this paper can provide insights into the expected performance of future field deposits for the purpose of closure planning and design.

## **Acknowledgements**

The authors would like to thank Natural Sciences and Engineering Research Council of Canada (NSERC), Canada's Oil Sands Innovation Alliance (COSIA) and Alberta Innovates – Energy and Environment Solutions for their financial support and Syncrude Canada Ltd for sharing the field data with us.

## References

- Alberta Energy Regulator (AER). 2018 *State of Fluid Tailings Management for Mineable Oil Sands, 2017*. Report, Calgary, Alberta. Available online: [https://static1.squarespace.com/static/52abb9b9e4b0cb06a591754d/t/5bcbdb777817f7df5097c309/1540086655594/Mineable\\_Oil\\_Sands\\_Fluid\\_Tailings\\_Status\\_Rpt\\_2017\\_Sept.28\\_Final.pdf](https://static1.squarespace.com/static/52abb9b9e4b0cb06a591754d/t/5bcbdb777817f7df5097c309/1540086655594/Mineable_Oil_Sands_Fluid_Tailings_Status_Rpt_2017_Sept.28_Final.pdf) (accessed 25/08/2021).
- Andersland, O.B. and Ladanyi, B. 2004. *Frozen Ground Engineering*, 2nd Edition, American Society of Civil Engineers & John Wiley & Sons Inc., Hoboken, New Jersey, USA.
- Baker, T. 1976. Transportation, Preparation, and Storage of Freezing Soil Samples for Laboratory Testing, in Sangrey, D., and Mitchell, R. (Eds.), *Soil Specimen Preparation for Laboratory Testing*. ASTM STP 599, ASTM International, West Conshohocken, PA, pp. 88-112. <https://doi.org/10.1520/STP39077S>
- Barbour, S.L. and Fredlund, D.G. 1989. Mechanism of osmotic flow and volume change in clay soils. *Canadian Geotechnical Journal*, 26 (4):551-562. doi: 10.1139/t89-068.
- Beier, N. A. and Sego, D.C. 2009. Cyclic Freeze-Thaw to Enhance the Stability of Coal Tailings. *Cold Regions Science and Technology*, 55 (3): 278-285. <https://doi.org/10.1016/j.coldregions.2008.08.006>.
- BGC Engineering Inc. (BGC) and O’Kane Consultants Inc. (OKC). 2014. *Perimeter Ditch Pilot 1 Trial, 2013 Performance Monitoring Update*, Report prepared for Syncrude Canada Ltd., AB, Canada.
- Bing, H., He, P., and Zhang, Y. 2015. Cyclic Freeze-Thaw as a Mechanism for Water and Salt Migration in Soil. *Environmental Earth Sciences*, 74 (1): 675-681. <https://doi.org/10.1007/s12665-015-4072-9>.
- Dawson, R.F., Sego D.C., and Pollock G.W. 1999. Freeze-thaw dewatering of oil sands fine tails. *Canadian Geotechnical Journal*, 36: 587-598. <https://doi.org/10.1139/t99-028>.
- Eigenbrod, K.D. 1996. Effects of cyclic freezing and thawing on volume changes and permeabilities of soft fine-grained soils, *Canadian Geotechnical Journal*, 33(4): 529-537.
- Jeeravipoolvarn, S. 2010. *Geotechnical Behavior of In-Line Thickened Oil Sands Tailings*. PhD Thesis, University of Alberta, Edmonton, AB, Canada.

- Henry, H. 2007 Soil freeze–thaw cycle experiments: Trends, methodological weaknesses and suggested improvements. *Soil Biology and Biochemistry*, 39: 977-986. <https://doi.org/10.1016/j.soilbio.2006.11.017>.
- Hogg, R. 2000. Flocculation and Dewatering. *International Journal of Mineral Processing*, 58 (1-4): 223-236.
- Hurtado, O. 2018. *Desiccation and Consolidation in Centrifuge Cake Oil Sands Tailings*. MASC. Thesis, Carleton University, Ottawa, ON, Canada.
- Johnson, R.L., Pork, P., Allen E.A.D., James, W.H. and Koverny, L. 1993. *Oil Sands Sludge Dewatering by Freeze-Thaw and Evaporation*, Report-RRTAC 93-8, Alberta Conservation and Reclamation Council, AB, Canada.
- Innocent-Bernard, T. 2013. *Evaporation, Cracking, and Salinity in a Thickened Oil Sands Tailings*. MASC. Thesis. Department of Civil and Environmental Engineering, Carleton University, Ottawa, ON, Canada.
- Konrad, J. and Morgenstern, N.R. 1980. A mechanistic theory of ice lens formation in fine-grained soils, *Canadian Geotechnical Journal*, 17 (4): 473-486. <http://dx.doi.org/10.1139/t80-056>.
- Lahaie, R., Seto, J.T.C., Chapman, D., and Carrier III, W.D. 2010. Development of accelerated dewatering technology for managing oil sands fine fluid tailings. In *Proceedings of the 63<sup>rd</sup> Canadian Geotechnical Conference*, Calgary, AB, Canada, pp. 678-685.
- McKenna, G. 2017. Soft Tailings landform Design. *Tailings and Mine waste Conference*, 2017, Banff, Canada.
- Miller, W.G., Scott, J.D. and Sego, D.C. 2010. Influence of the extraction process on the characteristics of oil sands fine tailings. *Journal of Canadian Institute of Mining, Metallurgy and Petroleum*, 1(2): 93-112.
- Mitchell, J.K. and Soga, K. 2005. *Fundamentals of Soil Behaviour*. 3rd ed., John Wiley and Sons, Inc., New York, NY, USA.
- Norwest Corporation. 2018. *Fluid Fine Tailings Management Methods- An Analysis of Impacts on Mine Planning, Land, GHGs, Costs, Site Water Balances and Recycle Water Chloride Concentrations*, Report submitted to COSIA, AB, Canada. See [https://www.cosia.ca/sites/default/files/attachments/FFT%20Management%20June%202018\\_0.pdf](https://www.cosia.ca/sites/default/files/attachments/FFT%20Management%20June%202018_0.pdf) (accessed 10/05/2021).

- Oil Sands Tailings Consortium (OSTC) and Canada's Oil Sands Innovation Alliance (COSIA). 2012. Technical Guide for Fluid Fine Tailings Management, Report, Calgary, Alberta. See [https://www.cosia.ca/uploads/documents/id7/TechGuideFluidTailingsMgmt\\_Aug2012.pdf](https://www.cosia.ca/uploads/documents/id7/TechGuideFluidTailingsMgmt_Aug2012.pdf) (accessed 7/05/2021)
- O'Kane Consultants (OKC). 2015. *Perimeter Ditch Pilot 1 Trial 2014 Performance Monitoring Update*, Report No. 690/91-01, A Report prepared for Syncrude Canada Ltd., Calgary, AB, Canada.
- O'Kane Consultants (OKC). 2017. *Perimeter Ditch Pilot 1 Trial 2016 Performance Monitoring Update*, Report No. 690/128-01, A Report prepared for Syncrude Canada Ltd., Calgary, AB, Canada.
- Othman, M.A. and Benson, C.H. 1993. Effect of Freeze-Thaw on the Hydraulic Conductivity and Morphology of Compacted Clay. *Canadian Geotechnical Journal*, 30 (2): 236-246. <https://doi.org/10.1139/t93-020>.
- Oztas, T. and Fayetorbay, F. 2003. Effect of freezing and thawing processes on soil aggregate stability. *Catena*, 52 (1):1-8.
- Prasanphan, S. and Nuntiya, A. 2006. Electrokinetic Properties of Kaolins, Sodium Feldspar and Quartz. *Chiang Mai Journal of Science*, 33(2): 183-190.
- Proskin, S.A. 1998. *A Geotechnical Investigation of Freeze-Thaw Dewatering of Oil Sands Fine Tailings*, PhD Thesis. Department of Civil and Environmental Engineering, University of Alberta, Edmonton, AB, Canada.
- Proskin, S., Segoo, D. and Alostaz, M. 2012. Oil Sands MFT Properties and Freeze-Thaw Effects. *Journal of Cold Regions Engineering*, ASCE, 26 (2): 29-54. [http://dx.doi.org/10.1061/\(ASCE\)CR.1943-5495.0000034](http://dx.doi.org/10.1061/(ASCE)CR.1943-5495.0000034).
- Rima, U.S. and Beier, N. 2021a. Effects of seasonal weathering on dewatering and strength of an oil sands tailings deposit. *Canadian Geotechnical Journal*, In press. <https://doi.org/10.1139/cgj-2020-0533>.
- Rima, U.S. and Beier, N. 2021b. Effects of multiple freeze-thaw cycles on oil sands tailings behaviour. *Cold Regions Science and Technology*, 192:103404. <https://doi.org/10.1016/j.coldregions.2021.103404>.

- Sanchez Sardon, M.A. 2013. *Combined Evaporation and Freeze-Thaw Effects in Polymer Amended Mature Fine Tailings*. MAsc. Thesis, Department of Civil and Environmental Engineering, Carleton University, Ottawa, ON, Canada.
- Thurber Engineering Ltd. 2012. *Oil Sands Tailings Technology Deployment Roadmaps*, Project Report-Volume 1, Report prepared for Alberta Innovates-Energy and Environment Solutions, AB, Canada.
- Wilson, G.W., Fredlund, D.G. and Barbour, S.L. 1994. Coupled soil-atmosphere modelling for soil evaporation. *Canadian Geotechnical Journal*, 31(2):151-61. <https://doi.org/10.1139/t94-021>.

## **5 NATURAL WEATHERING AS A SURFACE CRUSTING TOOL FOR TAILINGS MANAGEMENT**

### **Abstract**

Canada's oil sands are one of the largest unconventional fossil reserves, constituting 81% of the world's total bitumen reserve and are considered world's third largest reserve after Saudi Arabia and Venezuela. Extracting bitumen from oil sands generates a waste slurry referred to as tailings. The abundant large volumes and the extremely low settling rates of tailings present a unique management concern for the mining industries. The objective of the research presented in this paper is to utilize freeze-thaw (Canadian weather) as a crusting tool in order to increase the surface strength of the tailings to support capping and reclamation. This paper also compares different tailings (oil sands, coal, and gold) management approach using seasonal weathering (multiple freeze-thaw cycles and evaporation) in order to understand the effects of seasonal weathering on the development of a surface crust. The results concluded that predicting the volume change behavior of the tailings deposits exposed to surficial seasonal weathering is quite challenging in Canada compared to Australian arid/semi-arid climate zone. However, the laboratory results also suggest that seasonal weathering in Canadian weather can facilitate surface crust for oil sands tailings deposits with an associated peak shear strength of more than 110 kPa, provided active water management is ensured.

### **5.1 Introduction**

The volume change and shear strength behavior of tailings slurries are a function of gravimetric moisture content. Lowering moisture content or dewatering the tailings deposits is paramount to improve the strength and stability of any deposit. Finding ways to densify the deposit and improve the strength performance are imperative for stabilization, capping and reclamation of soft tailings deposits. The surficial mine waste deposits in arid or semi-arid regions around the globe are naturally subjected to surface crusting and desiccation and in turn support the placement of capping layer. On the contrary, soft tailings deposits in Canada, particularly in Western Canada are subjected to freezing weather conditions where the benefits of surface crusting due to evaporation

are limited. Hence, finding cost effective, practical methods to manage the ever-growing soft tailings accumulation and promote reclamation through the development of shear strength have long been a challenge for the mining industry, particularly for the oil sands industry.

The Athabasca oil sand deposits in northern Alberta, Canada, are considered to be the third largest proven reserve in the world that contain approximately 177 billion barrels of economically recoverable crude oil (AER, 2016). The current water-based bitumen (crude oil) extraction process from the oil sands ore body generates about 1 m<sup>3</sup> of sand and 0.25 m<sup>3</sup> of a fluid waste byproduct, known as fluid fine tailings (FFT), per every barrel of recovered bitumen (Beier et al., 2016). The FFT, consisting of process affected water, sand, fines (particle size of less than 44 µm) and residual bitumen are typically stored in tailings impoundments/ponds because of the inability to release water out of these high-water content tailings on-site (OSTC and COSIA, 2012; Sorta et al., 2013). At current and predicted bitumen production rates, the inventory of the tailings ponds is expected to grow over the next decade as the total fluid tailings volumes increased from 1075 million cubic meters (Mm<sup>3</sup>) in 2014 to 1270 Mm<sup>3</sup> in 2019 (AER, 2020). The FFT deposited in the tailings ponds is considered non-trafficable with minimal shear strength (Sorta et al., 2012) that takes many decades to settle out due to extremely slow settling and consolidation rate. Hence, it is paramount to sufficiently dewater these FFT to gain shear strength and allow reclamation to occur (McKenna et al., 2016).

In order to address these issues, progress has been made to gradually shift from conventional tailings disposal to treated tailings discharge where different mechanical, physical and chemical methods have been implemented prior to disposal in order to improve the mechanical properties of the tailings (OSTC and COSIA, 2012). However, the treated tailings may not have the strength required to promote trafficable surfaces and hence, these tailings deposits are left to gain strength under self-weight consolidation and natural dewatering processes (OSTC and COSIA, 2012). Natural dewatering processes such as freeze-thaw, evaporation and desiccation have the potential to act as an additional dewatering step for tailings deposits where, freeze-thaw process promotes dewatering through the changes in macro and microstructure of the tailings fabric while evaporation promotes surface drying and cracking leading to surface desiccation (Proskin et al., 2012; Pham and Segó, 2014).

Since most of Canada experiences seasonal temperature variations leading to alternate freezing and thawing cycles, this paper will primarily evaluate the effectiveness of freeze-thaw dewatering as a crusting tool in tailings deposit surface. This paper will also compare different mine tailings and management approaches where seasonal weathering has been employed to develop surface crust.

## **5.2 Effects of Seasonal Weathering on Different Tailings Management Strategies**

### **5.2.1 *Oil Sands Tailings***

The extensive research (Johnson et al., 1993; Proskin, 1998; and Proskin et al., 2012) conducted at both laboratory and pilot scales showed that the FFT subjected to multiple freeze thaw cycles promotes dewatering. However, the studies were predominantly limited to untreated FFT. The clay dominant fine particles in the ore are typically dispersed as a result of water-based extraction process (Jeeravipoolvarn et al., 2005), thereby, contributing to the large volumes of FFT. The matrix of these high-water content-fine particle suspensions can be altered by freezing the slurry. Within the frozen zone, localized moisture migration develops a three-dimensional reticulate network of consolidated mineral pedes and ice lenses (Proskin et al., 2012). Upon thawing, the consolidated pedes formed during the freezing process and pure water from the thawed ice matrix develop a segregated profile where the pedes settle and pure water reports to the surface (Proskin et al., 2012).

Since the freeze-thaw process is controlled by moisture migration/re-distribution, treated tailings (centrifuged tailings, in-line thickened tailings and flocculated tailings) may be less impacted by the benefits of freeze-thaw process compared to FFT because of their lower initial moisture content (Johnson et al., 1993). Therefore, incorporation of atmospheric drying and active water management by means of mechanical channeling or decant structures may be required for subsequent dewatering (Beier et al., 2013). Certain tailings management strategies have incorporated evaporation in their commercial operation/ commercial scale demonstration in Canada, such as Suncor's tailings reduction operation (TRO) (Wells et al., 2011) and Shell's (known as Canadian Natural Upgrading Limited (CNUL) at present) atmospheric fines drying (AFD) (Dunmola et al., 2013) to promote subsequent additional dewatering from in-line thickened tailings (ILTT). The TRO process achieved dry landscape by employing thin lift drying (AER,

2018). Similarly, the AFD process employing three different tailings depositional approaches (thin lift deposit, thick lifts deposits and deep fines-dominated deposits) and exposed to environmental dewatering (freeze-thaw dewatering and evaporative drying) for two years achieved a strength gain of 5-25 kPa within the entire deposit, where evaporative drying and freeze-thaw dewatering contributed to a 22-23.5% and 4.5-8% gravimetric moisture content reduction (mass of water to the mass of solids in a given mass of soil/tailings) from its the initial treated FFT, respectively (Kolstad et al., 2016). Syncrude's large scale pilot test incorporating accelerated dewatering/ rim ditching with in-line flocculated FFT (known as ADW) is currently underway to investigate the effects of atmospheric drying (evaporation and freeze-thaw dewatering) and surface dewatering system (perimeter ditching/ lateral drain) (BGC and OKC, 2014). Overall, atmospheric drying through evaporation and freeze-thaw dewatering is currently considered an important component for the present and future oil sands fine tailings management, despite seasonal temperature fluctuations (BGC, 2010).

### **5.2.2 Coal Tailings**

Research (Beier and Segó, 2009; Stahl and Segó, 1995) carried out at the Coal Valley mine in Canada to investigate the effect of freeze-thaw dewatering on coal tailings indicates that this process has the potential to transform fine coal tails to a state of weak soil with a measurable shear strength. Freezing and subsequent thawing of the frozen tailings continued for four to five cycles in the laboratory resulted in 5 to 9 times increase in surficial shear strength compared to the never frozen tailings (Stahl and Segó, 1995), provided adequate drainage is incorporated. When coupled with evaporation, evapotranspiration and fibre reinforcement from plants, the seasonal weathering has a potential to overall provide sufficient stability to implement dry landscape reclamation (Stahl and Segó, 1995).

Stability assessments of other coal tailings deposits at New Acland Coal Mine and Ulan Coal Mine in Australia confirmed the formation of about 1 m of surface crust prior to the commencement of capping (Williams and King, 2016). The desiccation and surface crusting of these deposits are attributed to the contribution of solar and wind drying associated with the warm climate of Australia (Williams and King, 2016), although the number of years (it was mentioned as “some

years”) exposed to the seasonal weathering was not reported. The authors mentioned that the upper part of the tailings surface was well desiccated and the shear strength in the surface ranges from 15 kPa to 40 kPa ahead of capping.

### **5.2.3 Thickened Gold Tailings**

Extensive laboratory research, field trials and numerical predictions (Simms et al., 2017; Fisseha et al., 2010; Dunmola and Simms, 2010) were implemented to study the effects of evaporation from the thickened gold tailings at the Bulyanhulu gold mine in Tanzania. Gold tailings are predominantly sand and silt sized (Bussiere, 2007) and thus the particle sizes are relatively coarser compared to the coal and oil sands fine tailings. Promoting evaporation from the tailings for 15-20 days was found to improve densification and strength gain by reducing the gravimetric moisture content from 38% to 5-13% (Simms et al., 2017; Dunmola and Simms, 2010). Therefore, maximizing strength gain due to evaporation is of less concern for these tailings deposits. However, excess evaporation from this acid generating hypersaline thickened tailings deposit can have an adverse effect since desaturation can consequently increase the probability of acid generation along with densification (Simms et al., 2017). In addition to this, the accumulation of salts was found to suppress the evaporation and lower the shear strength gain (Dunmola and Simms, 2010). Therefore, predicting evaporation rate is considered one of the major parameters for the engineers to optimize deposition planning (Simms et al., 2017; Dunmola and Simms, 2010).

### **5.2.4 Metal Mine Tailings**

Evaporation/atmospheric drying greatly contributed to the desiccation of the Cannington Metal Mine (silver, lead and zinc) tailings located in Queensland, Australia, thus confirming that evaporation is a useful process for mining operation in order to dewater their tailings. The semi – arid climate zone results in a heavily desiccated tailings surface by exposing to atmosphere for four consecutive years (Williams et al., 2015). Similar to the gold tailings, the sandy silt to silty sand sized particles of this site also contributes to the desiccated surface crust and stability (Williams, 2016).

### 5.3 Materials and Methods

The current study presented in this paper utilized two types of treated oil sands tailings: a). centrifuged tailings (initial moisture content = 89%) generated from centrifuge after treating FFT with polymer flocculant and coagulant and b). ILTT (initial moisture content = 122%) generated from injecting polymer flocculants into the FFT containing transfer pipeline, which was deposited into the containment area for subsequent further self-weight dewatering.

The laboratory research in this study was conducted in two phases. First phase included subjecting the treated tailings to five consecutive freeze-thaw cycles followed by a single drying-wetting cycle. Second phase included five alternating freeze-thaw and drying-wetting cycles, where each freeze-thaw cycle was followed by ambient drying cycle prior to and after a rainfall event. For the freeze-thaw testing, one dimensional closed system freezing tests were carried out in freezing cells inside a walk-in freezer whereas, evaporation tests were undertaken under the ambient temperature (~20°C) of the laboratory. The undrained shear strength was measured using a benchtop vane shear apparatus according to the ASTM (2016) standard D4648/S 4648M-16. A vane (width and height of 12.5 x 12.5 mm) was inserted into the sample to their full length such that the top of the vane was level with the sample surface. The vane was rotated at a uniform rate of 60°/minute until the sample failed and the torsional force required to cause shearing was calculated using the calibration data provided with the vane device. The detailed procedure was documented in Rima and Beier (2021a and 2021b).

### 5.4 Results

Table 1 summarizes the index properties of different tailings deposits around the world. It shows different tailings deposits having different ranges of particle sizes and consistency limits that are expected to affect the dewatering and strength properties of these tailings. As shown in the Table, oil sands tailings are the finest grained materials with higher consistency limits followed by the coal tailings from the Coal valley mine, Canada. Coal tailings from the New Acland mine and the base metal mine tailings are relatively coarser grained materials (either silt or silty sand) with the lower consistency limits that indicate lower compressibility and lower water adsorption.

Table 5.1: Summary of key properties of tailings

Type	Name	LL <sup>1</sup>	PL <sup>2</sup>	Clay fraction <sup>3</sup> (%)	Fines fraction <sup>4</sup> (%)
	Shell AFD	NA <sup>5</sup>	NA <sup>5</sup>	21-22	90-100
Oil sands tailings	Syncrude centrifuge	57	26	52	92
	Syncrude ADW	62	23	70	96
Coal tailings	Coal Valley mine	54	31.5	45	98
	New Acland mine	41	17	0	12
Gold tailings	Bulyanhulu mine	23	20	5	45
Metal mine tailings	Cannington mine	14-16	Non- plastic	3-7	40-70

<sup>1</sup>LL = Liquid limit

<sup>2</sup>PL = Plastic limit

<sup>3</sup>Clay fraction = Particle sizes finer than 0.002 mm

<sup>4</sup>Fines fraction = Particle sizes finer than 0.075 mm

<sup>5</sup>NA = Not available

Figure 5.1 shows the effects of freeze-thaw cycles on the undrained shear strength at the near surface of coal tailings (initial moisture content ranges from 83 to 102%, as reported in Beier and Segó (2009)) and treated FFT (initial moisture content ranges from 89 to 122%). The peak undrained shear strength after four/five cycles increased from a negligible value to about 5 to 10.5 kPa at the surface.

Figure 5.2 depicts how evaporation can dominate over freeze-thaw dewatering process in treated oil sands tailings samples over time. The investigated treated tailings samples (centrifuged tailings and ILTT) subjected to different temperature gradients were only compared here since the identical tailings samples with and without evaporation component were unavailable in the previous published literature.

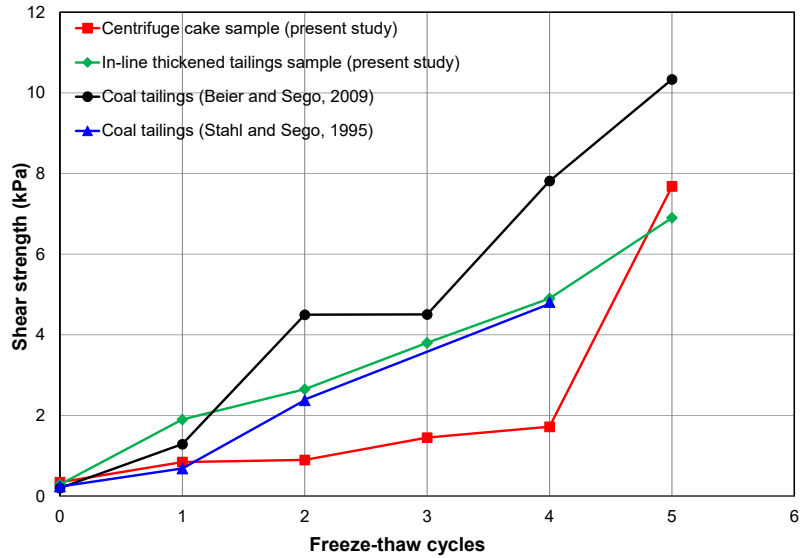


Figure 5.1: Effects of freeze-thaw cycles on the undrained shear strength of fine coal and oil sands tailings

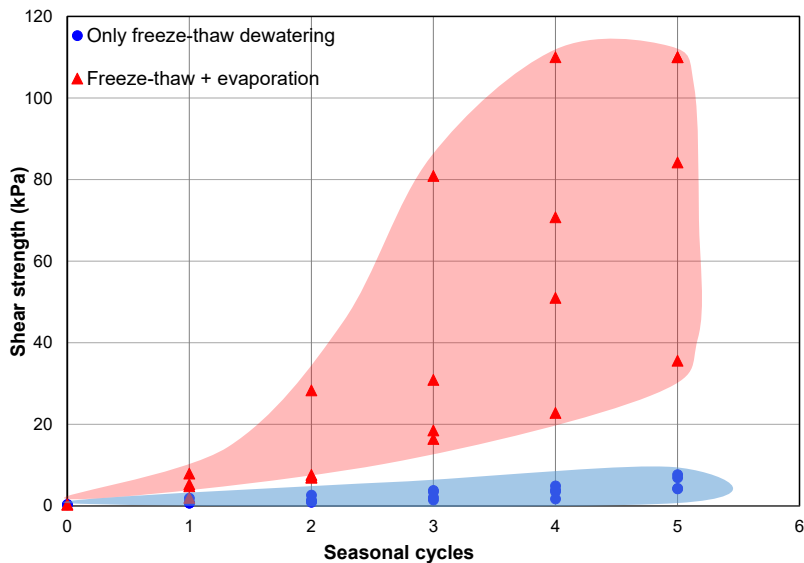


Figure 5.2: The effects of evaporation/drying on treated oil sands tailings

The result shows that the evaporation had profound impact on oil sands tailings sample. The volume changes subsequent to only freezing and thawing is minimal and hence, the shear strength ranges from 5-8 kPa at the surface (denoted by blue boundary). Conversely, the combined freeze-

thaw-drying cycles result in high volume changes and subsequent shear strengths of 35-110 kPa. The treated FFT sample that experienced the shear strength of >100 kPa developed a surface crust of about 2 cm. However, the underlying tailings below the surface crust was very soft and weak, although the shear strength below was not measured in the laboratory.

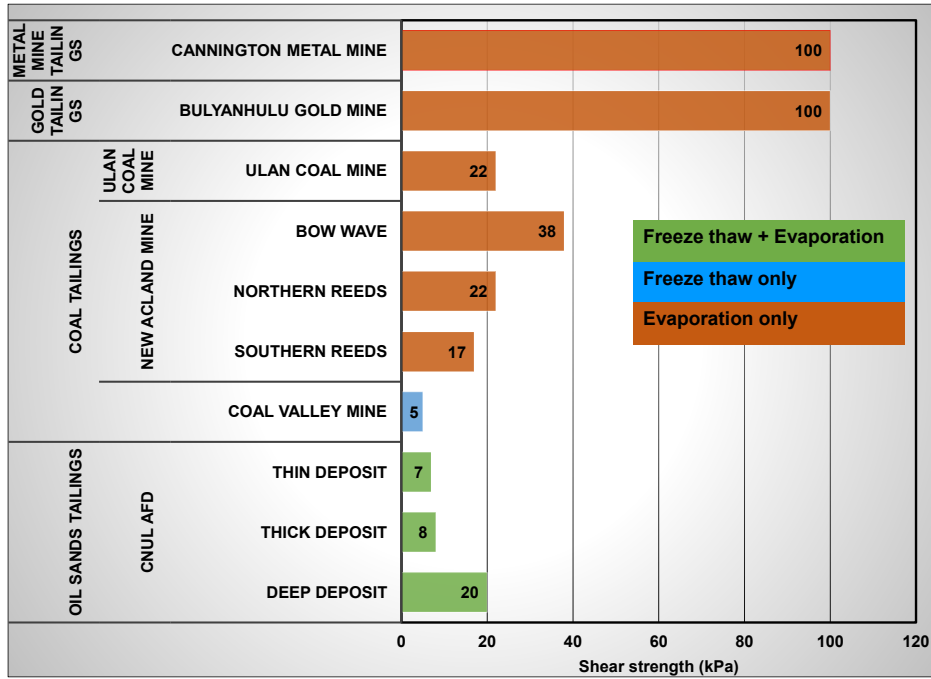


Figure 5.3: The effects of natural weathering on the surficial strength of different tailings deposits around the world

Figure 5.3 shows the contribution of seasonal weathering in strength gain of different tailings deposits at the surface around the world. The strengths of gold tailings at the Bulyanhulu mine and metal mine tailings (silver, lead and zinc) at Cannington Metal Mine were reported here as 100 kPa since these were reported as stiff and well-desiccated surface prior to capping (Simms et al., 2017; Williams et al. 2015). Simms et al (2017) reported that the thickened gold tailings surface subjected to 15/20 days of exposure of atmospheric drying resulted in moisture content from 38 (corresponding to a solids content of 72%) to 5-13% (corresponding to solids content of 88 to 95%). At such a high solids content, it is expected to achieve a well-desiccated surface and hence, the peak strength was reported here corresponding to a strength of 100 kPa. Similarly, Williams et al. (2015) reported that the vane shear strength data in the upper 4 m of Cannington mine site were

unavailable due to the difficulties in testing a stiff desiccated crust. Nevertheless, the tailings samples in the present study were not compared in this data chart. Only the field deposit strengths were shown here to have a better understanding of the impact of climate. The data sources are summarized in Table 5.2.

Table 5.2: Sources of index properties and shear strength data

Data	Source
Cannington metal mine, Australia	Williams et al., 2015
Bulyanhulu gold mine, Tanzania	Simms et al., 2017; Dunmola and Simms, 2010
Ulan coal mine, Australia	Williams and King, 2016
New Acland coal mine, Australia	Shokouhi et al., 2014; Williams and King, 2016
Coal Valley mine, Canada	Stahl and Segó, 1995; Beier and Segó, 2009
CNUL AFD, Canada	Kolstad et al., 2016
Syncrude centrifuge, Canada	Rima and Beier, 2021a and 2021b
Syncrude ADW, Canada	Present study

## 5.5 Discussion

Table 5.1 shows the index properties of all the different types of tailings discussed in this paper. Among all these tailings, oil sands tailings primarily consist of clay minerals that are highly negatively charged particles and highly affected by the changes in grain size distribution, clay content, solids mineralogy, and pore water chemistry (Mitchell and Soga, 2005). On the contrary, coal, gold and base metal tailings have either sand or silt as their predominant minerals (Williams et al., 2015; Bussiere, 2007). All these variables can substantially impact the shear strength of tailings (Mitchell and Soga, 2005).

Figure 5.1 shows the effects of freeze-thaw cycles on the surficial shear strength of three types of fine tailings: coal tailings and two types of oil sands tailings. The two types of treated oil sands tailings compared here were: centrifuged tailings and in-line thickened tailings. The clay fractions of these tailings (coal, centrifuged tailings and ILTT) were measured to be 45 (Beier and Segó, 2009), 52 and 70% by weight, respectively, which indicates that these tailings are fine grained. All

these fine-grained tailings subjected to below freezing temperatures develop high negative pore pressures/ suction that cause water migration towards the freezing front, feeding a growing ice lens (Andersland and Ladanyi, 2004). The warmer temperatures during the spring and summer result in thawing these frozen tailings and unlocking the benefits of thawed ice matrix developed during freezing by facilitating the settlement of heavier soil pedes and release of thawed water and overall dewatering and strength gain (Stahl and Segoo, 1995).

However, the magnitudes of dewatering (measured as “thaw strain” that refers to change in height after thaw divided by the frozen height of sample) and shear strength are predominantly governed by initial moisture/ solids contents (Johnson et al., 1993), mineral compositions, grain size distribution (Stahl and Segoo, 1995), pore water chemistry (Proskin et al., 2012), freezing rate (Proskin, 1998), and temperature boundary conditions (Proskin, 1998). Since oil sands particles are highly negatively charged clay particles and net negative charges are the primary factor in controlling clay dispersion, the prevalence of clay fractions compared to the coal fine tailings (predominantly silty sized fractions, as reported by Beier and Segoo (2009)) can have some impact on lower strength gain as evident in the Figure 5.1.

Figure 5.2 shows the effects of evaporation/ atmospheric drying on the investigated treated oil sands tailings samples. Centrifuged tailings samples subjected to three different temperature gradients (0.083, 0.056 and 0.028°C/mm) and ILTT sample subjected to a temperature gradient of 0.028°C/mm were studied for this purpose. All these samples were exposed to similar atmospheric drying conditions under ambient temperature of the laboratory (~20°C). As expected, incorporating evaporation greatly enhanced the shear strength (about 10 times compared to the freeze-thaw dewatering alone).

Evaporation is desirable in mining operation as it promotes surface cracking and desiccation through the exposure of underlying tailings with lower suction (Johnson et al., 1993). The extent of cracking is predominantly dependent on the initial moisture contents, mineralogy, pore water chemistry and physical boundary conditions (Vogel et al., 2005). Therefore, it is anticipated that the two investigated treated tailings having differences in moisture content, mineralogy and pore water chemistry will respond differently to evaporation/ atmospheric drying. The centrifuged

tailings resulted in a surficial strength of >100 kPa and developed a surface crust while the ILTT sample under similar freezing temperature gradient and similar atmospheric conditions resulted in a surficial strength of 84 kPa with no distinguishable crust. Although, the strength values of both of these samples suggest a consistency of stiff soil, the formation of a surface crack has a larger impact on tailings reclamation process. On the contrary, identical samples (centrifuged tailings in this case) under similar atmospheric drying conditions would be expected to behave similarly for gaining shear strength and developing surface crust. However, the interesting fact is the identical tailings samples can respond discordantly to the atmospheric drying if the boundary conditions in the previous freeze-thaw cycles are kept different. In the present study, centrifuged tailings subjected to three different freezing temperature gradients while freezing and prior to atmospheric drying, resulted in distinctive strength values. Samples subjected to lower temperature gradient (0.028°C/mm) resulted in a formation of a surface crust while higher gradient (0.083°C/mm) sample behaved like a slurry. The detailed results are documented in Rima and Beier (2021a and 2021b; also documented in the Chapter 2 and 3 of this thesis). Therefore, it can be implied that although the effects of freeze-thaw on strength gain can seem marginal, this process can help accelerate the strength gain during evaporation process. The cracks developed during previous drying cycles, or the shrinkage developed during previous freeze-thaw cycles contribute to the easier penetration of advancing ice front during the subsequent freezing period (Sanchez Sardon, 2013). As a result, more water is expected to be drawn from the underlying tailings causing relatively higher dewatering and strengthening.

Figure 5.3 shows the chart of undrained peak shear strength of various mine tailings deposits prior to capping. Evaporation depends on various local climatic and environmental factors such as solar radiation, wind speed, air temperature, ground temperature and relative humidity (Lahaie et al., 2010). Oil sands tailings deposits are typically discharged at water contents (water contents range between 90-130% for the investigated tailings) well above the liquid limits (liquidity index of 2~3). Coal tailings from the Coal Valley mine are also categorized as fine-grained tailings deposited at a liquidity index of 2.3 to 3 (moisture content varies between 83~102%, as reported in Beier and Segó (2009)). Both of these tailings create non-trafficable deposits and hence, evaporation can contribute to an enhanced dewatering. On the contrary, the metal mine and gold tailings were deposited into the impoundments at lower initial moisture contents of 54% (liquidity

index=3.6) and 40% (liquidity index=7) at the Cannington metal mine and Bulyanhulu gold mine, respectively (Simms et al., 2017; Williams et al., 2015). However, both of these tailings contain smaller amounts of clay/ no clay (as shown in Table 5.1) thus impacting liquidity index. Therefore, gaining strength and forming surface crusts in these tailings due to atmospheric drying are relatively less challenging compared to the fine tailings deposits. The semi-arid climate in Australia and Tanzania further facilitates desiccation and cracking for these tailings. However, an optimal rate of drying is paramount in order to ensure that contamination from mine effluent does not adversely affect the environment such as acid generation (Fisseha et al., 2010). Therefore, the thickness of the deposited layer and deposition approach are important for the tailings management.

On the contrary, fine-grained tailings such as coal and oil sands tailings (as shown in Figure 5.3) will lack strength adequacy without capping/ soil cover. Even in a semi-arid zone like Australia, the strength gain due to atmospheric drying was not adequate enough to allow for a trafficable deposit without capping. The New Acland and Ulan coal mines in Australia experienced surface desiccation but the depth and shear strength of the surface crust were limited because of the marginal effects of solar and wind drying below 1 m depth and some reversal in shear strength due to subsequent deposition of fresh tailings on the desiccated crust (Williams and King, 2016). In Canada, relying on evaporation for fine tailings management is even more challenging due to the colder climate and shorter duration of summer. As evident in Figure 5.2, the combination of freeze-thaw-drying cycles was employed as a dewatering tool and it showed promising results, provided adequate water management (lateral drain, decant structure etc.) is ensured.

## **5.6 Conclusions**

This paper provides an overall study of different mine tailings across the world and how seasonal weathering are employed to support the reclamation outcomes for mine closure. Each of the deposits are different due to the differences in geological origin, weather and site conditions and hence, site specific adaptive management need to be established to limit the accumulation and containment of tailings. The small-scale laboratory test results of the investigated treated oil sands tailings indicate that freeze-thaw dewatering coupled with evaporation and active water

management has a potential to have a substantial impact on developing surface crust (shear strength of >100 kPa). When compared to different tailings (coal, gold, metal), oil sands tailings management proved to be the most challenging due to their extreme slow consolidation rate and the lower hydraulic conductivity of these fine-grained tailings deposit. Apart from climatic factors, subsequent dewatering and transforming the state of the slurry from a viscous liquid to a plastic solid, and then to a brittle solid are highly sensitive to mineralogy. When comparing shear strengths and dewatering as a function of mineralogy under the similar atmospheric conditions, the finer tailings deposits (coal tailings as compared to metal tailings in Australia) recorded lower strength gain due to the atmospheric drying. As expected, similar tailings deposits (coal tailings in Australia vs Canada) that enjoy the benefits of higher evaporation, will experience higher dewatering and shear strength. Based on the laboratory study, the oil sands tailings samples even from the same tailings deposit responded very differently to atmospheric drying when subjected to different frozen temperature gradients. Overall, the results indicate site specific conditions should be a key consideration for the tailings management/ planning team.

## **Acknowledgements**

The authors would like to thank Natural Sciences and Engineering Research Council of Canada (NSERC), Canada's Oil Sands Innovation Alliance (COSIA) and Alberta Innovates-Energy and Environment Solutions for their financial support. Thanks to Dr. Louis Kabwe for writing the French version of the abstract of this paper (the French abstract is not included in the thesis).

## **References**

- Alberta Energy Regulator (AER). 2016. *Alberta's Energy Reserves 2015 & Supply/Demand Outlook 2016-2025* (ST98-2016), Alberta Energy Regulator, Calgary, Alberta.
- Alberta Energy Regulator (AER). 2018. *State of Fluid Tailings Management for Mineable Oil Sands, 2017*. Report, Calgary, Alberta.
- Alberta Energy Regulator (AER). 2020. *State of Fluid Tailings Management for Mineable Oil Sands, 2017*. Report, Calgary, Alberta
- Andersland, O.B. and Ladanyi, B. 2004. *Frozen Ground Engineering*. 2nd Edition, American Society of Civil Engineers & John Wiley & Sons Inc., Hoboken, New Jersey, USA.

- ASTM.2016. Standard Test Methods for Laboratory Miniature Vane Shear Test for Saturated Fine-Grained Clayey Soil. *ASTM Standard D4648/ D4648M-16*. ASTM International, West Conshohocken, PA, 2016.
- Beier, N. A. and Segó, D.C. 2009. Cyclic Freeze-Thaw to Enhance the Stability of Coal Tailings. *Cold Regions Science and Technology*, 55 (3), 278-285.
- Beier, N., Wilson, W., Dunmola, A., & Segó, D., 2013. Impact of flocculation-based dewatering on the shear strength of oil sands fine tailings. *Canadian Geotechnical Journal*, 50 (9), 1001-1007.
- Beier, N., Kabwe, L.K., Scott, J.D., Pham, N.H., and Wilson, G.W. 2016. Modeling the effect of flocculation and desiccation on oil sands tailings. *Geo-Chicago*, Chicago, Illinois, USA, August 14-18, 2016.
- BGC Engineering Inc. (BGC), 2010. *Oil Sands Tailings Technology Review*. Oil Sands Research and Information Network, University of Alberta, School of Energy and the Environment, Edmonton, Alberta. OSRIN Report No. TR-1.
- BGC Engineering Inc. (BGC) and O’Kane Consultants Inc. (OKC). 2014. *Perimeter Ditch Pilot 1 Trial, 2013 Performance Monitoring Update*, Report prepared for Syncrude Canada Ltd., AB, Canada.
- Bussière, B. 2007. Colloquium 2004: Hydrogeotechnical properties of hard rock tailings from metal mines and emerging geoenvironmental disposal approaches. *Canadian Geotechnical Journal*. 44(9), 1019-1052.
- Dunmola, A., and Simms, P. 2010. Solute mass transport and atmospheric drying of high-density gold tailings. In *Proceedings of the Thirteenth International Seminar on Paste and Thickened Tailings*. Australian Centre for Geomechanics. pp. 279-289.
- Dunmola, A., Cote, C., Freeman, G., Kolstad, D., Song, J., and Masala, S. 2013. Dewatering and shear strength performance of in-line flocculated mature fine tailings under different depositional schemes. *Proceedings of Tailings and Mine Waste 2013*, Banff, AB, Canada. pp.5-14.
- Fisseha, B., Bryan, R., & Simms, P. 2010. Evaporation, unsaturated flow, and salt accumulation in multilayer deposits of “paste” gold tailings. *Journal of geotechnical and geoenvironmental engineering*. 136(12), 1703-1712.

- Jeeravipoolvarn, S. 2005. *Compression Behaviour of Thixotropic Oil Sands Tailings*. M.Sc. Thesis, University of Alberta, Edmonton, AB, Canada.
- Johnson, R.L., Pork, P., Allen E.A.D., James, W.H. and Koverny, L. 1993. *Oil Sands Sludge Dewatering by Freeze-Thaw and Evaporation*. Report-RRTAC 93-8, Alberta Conservation and Reclamation Council, AB, Canada.
- Kolstad, D., Borree, B., Song, J., and Mahood, R. 2016. Field Pilot Performance Results for Flocculated Fluid Fine Tailings under Three Depositional Variations. *International Oil Sands Tailings Conference*, Lake Louise, AB, Canada, December 4-7, 2016.
- Lahaie, R., Seto, J T.C., Chapman, D., and Carrier, III, W.D. 2010. Development of accelerated dewatering technology for managing oil sands fine fluid tailings. In *Proceedings of the 63rd Canadian Geotechnical Conference*, Calgary, AB, Canada. pp. 678-685.
- McKenna, G., Mooder, B., Burton, B. and Jamieson, A. 2016. Shear strength and density of oil sands fine tailings for reclamation to a boreal forest landscape. In *proceedings of the 5<sup>th</sup> International Oil sands Tailings Conference*, Lake Louise, Alberta, 4-7 December, 2016.
- Mitchell, J.K. and Soga, K. 2005. *Fundamentals of Soil Behaviour*, 3<sup>rd</sup> ed., John Wiley and Sons, Inc., New York, NY, USA.
- Oil Sands Tailings Consortium (OSTC) and Canada's Oil Sands Innovation Alliance (COSIA). 2012. *Technical Guide for Fluid Fine Tailings Management*, Report, Calgary, Alberta.
- Pham, N.H. and Segoo, D.C. 2014. Modeling Dewatering of Oil Sands Mature Fine Tailings using Freeze Thaw. *International Oil Sands Tailings Conference*, Lake Louise, AB, Canada, December 7-10, 2014.
- Proskin, S.A. 1998. *A Geotechnical Investigation of Freeze-Thaw Dewatering of Oil Sands Fine Tailings*, PhD Thesis. Department of Civil and Environmental Engineering, University of Alberta, Edmonton, AB, Canada.
- Proskin, S., Segoo, D. and Alostaz, M. 2012. Oil Sands MFT Properties and Freeze-Thaw Effects. *Journal of Cold Regions Engineering*, ASCE, 26 (2), 29-54.
- Rima, U.S. and Beier, N. 2018. Evaluation of Temperature and Multiple Freeze-Thaw Effects on the Strength Properties of Centrifuged Tailings. *71st Canadian Geotechnical Conference*, Edmonton, Canada, September 23-26, 2018.

- Rima, U.S. and Beier, N. 2021a. Effects of seasonal weathering on dewatering and strength of an oil sands tailings deposit. *Canadian Geotechnical Journal*, In press. <https://doi.org/10.1139/cgj-2020-0533>.
- Rima, U.S. and Beier, N. 2021b. Effects of multiple freeze-thaw cycles on oil sands tailings behaviour. *Cold Regions Science and Technology*, 192:103404. <https://doi.org/10.1016/j.coldregions.2021.103404>.
- Sanchez Sardon, M.A. 2013. *Combined Evaporation and Freeze-Thaw Effects in Polymer Amended Mature Fine Tailings*. M.A.Sc. Thesis, Department of Civil and Environmental Engineering, Carleton University, Ottawa, ON, Canada.
- Shokouhi, A., Williams, D.J., and Kho, A.K. 2014. Settlement and collapse behavior of coal mine spoil and washery wastes. *Proceedings Tailings and Mine Waste 2014*, Keystone, Colorado, USA, 5-8th October, 2014.
- Simms, P., Soleimani, S., Mizani, S., Daliri, F., Dunmola, A., Rozina, E., and Innocent-Bernard, T. 2017. Cracking, salinity and evaporation in mesoscale experiments on three types of tailings. *Environmental Geotechnics*, 6(1), 3-17.
- Sorta, A.R., Sego, D.C., and Wilson, W. 2012. Effect of thixotropy and segregation on centrifuge modelling, *International Journal of Physical Modeling in Geotechnics*, 12 (4), 143-161.
- Sorta, A.R. Sego, D.C., and Wilson, G.W. 2013. Time domain reflectometry measurements of oil sands tailings water content: A study of influencing parameters. *Canadian Institute of Mining Metallurgy and Petroleum Journal*, 4 (2), 109-119.
- Stahl, R.P., and Sego, D.C. 1995. Freeze-thaw dewatering and structural enhancement of fine coal tails. *Journal of Cold Regions Engineering*, 9 (3), 135-151.
- Vogel, H., Hoffmann, H., Leopold, A., and Roth, K. 2005. Studies of crack dynamics in clay soil II. A physically based model for crack formation. *Geoderma*, 125, 213 - 223.
- Wells, P.S., Revington, A., and Omotoso, O. 2011. Mature fine tailings drying-technology update. *In Proceedings of Paste 2011*. Edited by R.J. Jewel and A.B. Fourie, 5-7 April, 2011. Australian Centre for Geomechanics, Perth, Australia. pp. 155-166.
- Williams, D.J., Paterson, S., Yau, R., and Goddard, D. 2015. Selection of shear strength profile for desiccated tailings to support an upstream raise. *Proceedings of Tailings and Mine waste 2015*, Vancouver, BC, Canada.

Williams, D. J. 2016. Mine site rehabilitation—are we reinventing the wrong wheel?  
In *Proceedings of the 11th International Conference on Mine Closure*. Australian Centre  
for Geomechanics. pp. 595-608.

Williams, D.J, and King, J. 2016. Capping of a surface slurried coal tailings storage facility.  
*Proceedings of the 11<sup>th</sup> International Conference on Mine Closure*, Australian Centre for  
Geomechanics. pp. 263-275.

# 6 MODELING THE EFFECTS OF SEASONAL WEATHERING ON CENTRIFUGED OIL SANDS TAILINGS

## Abstract

The oil sands industry employs different technologies at pilot and commercial demonstration scales in order to improve the dewatering rate of fluid fine tailings. Of these technologies, centrifugation has advanced to the commercial scale and is playing a major role in fluid fine tailings management strategy. However, centrifuge technology on its own may not develop the required strength to ensure fine tailings can be incorporated into dry landform reclamation, which requires water contents close to their plastic limit. Hence, it is paramount to combine more than one technology to maximize post depositional dewatering. Management of the tailings deposit to promote seasonal weathering (freeze-thaw, evaporation and self-weight consolidation) can promote further dewatering. Properly assessing the contributions of the seasonal weathering components is vital to optimize this strategy. Using the geotechnical properties of centrifuged tailings, the effects of seasonal weathering on tailings were modeled under two different freezing temperature gradients. A coupled analysis combining FSConsol and Unsatcon was used to simulate the deposition scenario similar to the laboratory. The modeling results were found to match the laboratory response reasonably well indicating the coupled approach proposed in this manuscript is valid and helps to predict the seasonal weathering effects on dewatering.

## 6.1 Introduction

Alberta, Canada is considered to be the fourth largest proven reserve of crude bitumen in the world (Government of Alberta, 2021a). Most of Alberta's oil is unconventional as it is trapped within oil sands and hence, traditional drilling and pumping methods using the natural pressure differential cannot be employed here (Cossey et al., 2021). Instead, advanced extraction techniques, such as oil sands mining and in-situ development are needed to extract the heavier oil/bitumen. With a

combined estimated reserve of 1.8 trillion barrels of in-place reserves of in-situ crude bitumen, the Athabasca, cold Lake, and Peace River deposits form a massive resource in Alberta. Of these regions, the Athabasca oil sand deposit (situated in northeastern Alberta in Fort McMurray area) is the largest and only one to be shallow enough to allow for surface mining (AER, 2016). Extraction of bitumen from oil sands in a surface mining operation is a water-based process that generates large volumes of byproducts known as tailings. In general, tailings are a warm suspension of sand, fines (clays and silts), residual bitumen and process affected water (Jeeravipoolvarn, 2010). These are temporarily stored above ground in dams referred to as tailings ponds, where the mixtures of coarse streams (primarily sand) form settled sand beaches near the deposition outlet and an aqueous slurry of fines and residual bitumen accumulates in the center of these ponds termed as thin fine tailings (TFT) (Jeeravipoolvarn, 2010; OSTC and COSIA, 2012). When allowed to settle under quiescent conditions (self-weight consolidation under no further loading), TFT forms a material with a solids content (mass of solids divided by the total mass of tailings including bitumen) of around 30-40% by mass referred to as mature fine tailings (MFT) (Spence et al., 2015). Dewatering of fluid fine tailings (collective term for TFT and MFT) to recycle the released water and reduce the environmental footprint is very slow as these materials are highly dispersed, resistant to consolidation and can remain in a soft, fluid state for decades, thus creating a unique fundamental management problem for oil sands industry (AER, 2020). Consequently, the inventory of tailings being stored in the ponds covering a total area of 259 km<sup>2</sup>, has been steadily increasing over time and at present, the total volume of fluid fine tailings (FFT) stored in the pond already exceeded 1302 million m<sup>3</sup> (AER, 2020; Government of Alberta, 2021b). In order to meet regulatory and closure requirements, FFT are needed to be dewatered so that these large volumes of FFT can be accommodated in the development of an environmentally acceptable reclamation plan.

In order to dewater and facilitate the reclamation efforts of the surface mined FFT, different chemical, mechanical and environmental processes have been employed that could have the potential for effective tailings management in the oil sands industry (OSTC and COSIA, 2012). One of these technologies, centrifugation, is currently being used by Syncrude and Canadian Natural Upgrading Ltd. (CNUL) as a key process technology to accelerate dewatering (Spence et al., 2015; AER, 2020). Centrifugation employs dredging FFT from the tailings pond and treating

it with flocculant and/without coagulant prior to feeding to the centrifuge where solids are separated from water via centrifugal force (OSTC and COSIA, 2012). The end product of centrifugation is known as centrifuged tailings. However, the achieved solids content from this technology is typically 50-55% (OSTC and COSIA, 2012), which is not sufficient enough (strength less than 1 kPa, as documented in OSTC and COSIA (2012); Rima and Beier (2021a)) to develop a trafficable surface (atleast 25kPa for mobile equipment trafficability, as documented in OSTC and COSIA (2012)). Additionally, oil sands industry is currently more focused on creating deep deposits (typically > 10-20 meters deep) to eliminate the large footprints typically required for thin layered deposits (OSTC and COSIA, 2012; Hyndman et al., 2018). However, deep deposits of these centrifuged tailings undergo settlement for centuries due to the extremely slow settlement times resulting from decreasing permeability as the deposit densifies (Hyndman et al., 2018).

Since environmental dewatering processes (freeze-thaw dewatering, evaporation, desiccation) are economical and cost-efficient, a combination of these processes can be considered as additional dewatering technologies contributing to creating a reclaimable deposit. Figure 6.1 shows a simplified diagram of the environmental processes contributing to dewatering from the tailings. Freezing process results in the formation of a three-dimensional reticulate ice network surrounding blocks of over-consolidated tailings. Upon thaw, dewatering occurs due to these structural changes within the frozen tailings, which in turn, facilitates water removal from the underlying thawed tailings as ice melts (Proskin et al., 2012). Hence, tailings undergoing freeze-thaw dewatering develop thaw strain ( $\epsilon$ ) (the change in height prior to and after thawing divided by the total frozen height) that further allow for subsequent post thaw consolidation through self-weight consolidation, thereby, causing an increase in effective stress (Proskin et al., 2012). Consequently, solids content increases and void ratio decreases as the tailings material consolidates at a faster rate under self-weight (Proskin, 1998). When evaporation/ drying is incorporated with freeze-thaw dewatering, the thawed tailings further dewater under desiccation process, which is the process of drying and cracking (Jeeravipoolvarn, 2010)). As a result, further dewatering and higher undrained shear strength at the surface can be achieved, enabling reclamation and closure. Among all the environmental processes, the natural process of freeze-thaw dewatering has shown promise as a method to dewater, strengthen and reclaim FFT (as investigated by Dawson and Segó (1993);

Johnson et al., (1993); Proskin (1998); Proskin et al., (2012)). However, much of these works were focused on using thin layered freeze-thaw dewatering but not much on deep deposits. Hence, there is a need to develop a fundamental understanding of the effects of these environmental processes on the dewatering performances of deep deposit tailings.

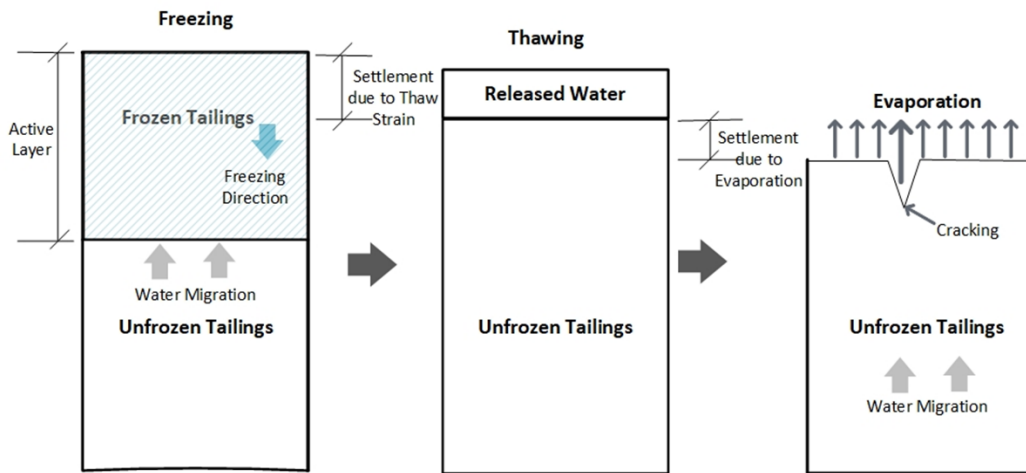


Figure 6.1: Simplified diagram of the seasonal weathering cycles

The objective of the research reported in this paper was to evaluate numerical approaches in order to simulate the dewatering of centrifuged tailings subjected to seasonal weathering under controlled laboratory testing program laboratory results that investigated the effects of seasonal weathering on centrifuged tailings. A coupled analysis methodology was developed here to validate two sequences of laboratory testing under two different freezing temperature gradients.

## 6.2 Tailings Material and Characterization

The centrifuged tailings samples studied in this research were received at the University of Alberta Laboratory in a 200L barrel from Syncrude Canada Ltd. The samples were homogenized thoroughly with a mixer and the mineralogy and geotechnical properties were determined upon delivery (Table 6.1).

Table 6.1: Geotechnical properties of the centrifuged tailings

Property	Value
Water content, w (%)	89
Solids content, s (%)	53
Bitumen content (%)	5.7
Specific gravity, G <sub>s</sub>	2.24
<sup>1</sup> Fines content (%)	87
<sup>2</sup> Clay content (Dispersed hydrometer) (%)	52
<sup>3</sup> Clay content (MBI) (%)	52
<sup>4</sup> D <sub>50</sub> (μm)	1.5
Liquid limit (%)	57
Plastic limit (%)	26
Liquidity index	2

<sup>1</sup> Fines content = Material finer than 0.044 mm

<sup>2</sup> Clay content = Material finer than 0.002 mm

<sup>3</sup> Clay content by Methylene Blue Index (MBI)

<sup>4</sup> Median particle diameter

The initial water content (mass of water divided by the mass of dry solids including bitumen) of the sample was found to be 89% by mass, corresponding to a solids content of 53% by mass. The properties of the as-received centrifuged tailings show a fine-grained tailings material with a higher amount of clay content, high plasticity along with moderate water adsorption onto the clays. These values are influenced by the combined effects of the geologic origin, clay mineralogy, water chemistry and bitumen content (Scott et al., 1985).

### 6.3 Laboratory Setup

Figure 6.2 shows the schematic diagram of the laboratory freeze-thaw test setup. These small-scale freezing tests were carried out in cylindrical freezing cells (10 cm dia x 22 cm height) within a walk-in freezer where the samples were frozen from top to down (one dimensional) under two different temperature gradients of 0.083 and 0.028°C /mm. These two temperature gradients were

applied to the freezing cells through two temperature baths where top boundary temperatures were set at -15 (to achieve  $0.083^{\circ}\text{C}/\text{mm}$ ) and  $-5^{\circ}\text{C}$  (to achieve  $0.028^{\circ}\text{C}/\text{mm}$ ) and bottom boundary temperature was set at  $0^{\circ}\text{C}$  in order to replicate the average temperature of Fort McMurray. The installation of insulation wrap and thermoelectric cooling plate were all applied in order to ensure one dimensional freezing and to represent the freezing process occurred in nature.

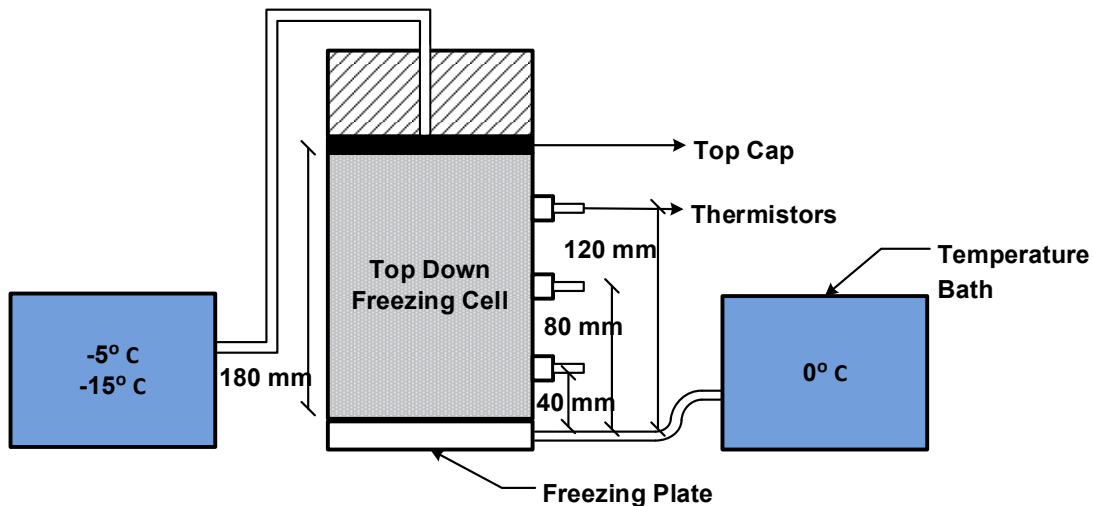


Figure 6.2: Schematic diagram of the freeze-thaw test setup (After Rima and Beier, 2021a and 2021b)

Laboratory investigations were carried out in two phases: 1. First phase that associates with five consecutive freeze-thaw cycles followed by a single cycle of drying-wetting-re-drying after wetting and 2. Second phase that includes five alternate freeze-thaw and drying-wetting cycles to better represent the natural seasonal cycles. For both phases, each of the freeze-thaw cycles took seven days to complete, whereas drying-wetting cycles varied. For the first phase of testing, the centrifuged tailings samples were subjected to a month (dried to a target actual evaporation/potential evaporation (AE/PE) ratio of 0.7 for each test) of drying cycle followed by a single wetting event to simulate the rainfall. After the wetting event, another drying cycle was continued for around twenty days. Further, the second phase of testing included five drying-wetting cycles and hence, each of the drying cycles was run for a shorter duration (seven days) prior to a single wetting event. After wetting event, re-drying cycle was continued for another

seven days. The detailed procedures of the first phase and the second phase testing were documented in Rima and Beier (2021a and 2021b).

## **6.4 Coupled Modeling**

### **6.4.1 Modeling Analysis Development**

A one-dimensional coupled modeling approach was developed to simulate the effects of multiple freeze-thaw and drying-wetting cycles in the laboratory. The modeling exercises were conducted to simulate the laboratory results (water content) of centrifuged tailings samples subjected to seasonal weathering (multiple freeze-thaw consolidation and drying-wetting cycles) under two different temperature gradients (0.083 and 0.028°C /mm), as mentioned in the above section. In this study, a coupled modeling analysis was conducted in two steps. First, the freeze-thaw analysis was coupled with FSConsol model to incorporate the freeze-thaw process into consolidation modeling. Next, the coupled FSConsol model was coupled with the UNSATCON model to further incorporate the evaporation/drying cycles followed by the freeze-thaw cycles. FSConsol is a commercially available one-dimensional consolidation program that incorporates the large strain consolidation theory from Gibson et al. (1967), whereas UNSATCON program developed by Qi and Simms (documented in Qi et al. (2017)) is a research code that simulates tailings dewatering process induced by self-weight consolidation and evaporation while considering stress/desiccation history and hydraulic hysteresis. Since none of these models incorporate the freeze-thaw consolidation directly, the change in water content due to thaw strain was calculated externally in Excel sheet and applied on the active layer (the top layer of the ground that undergoes above (thawing) and below 0°C (freezing) during the year, also known as frost depth (shown in Figure 6.1)) of the deposit (for the laboratory test, the active layer was equal to the total thickness of each of the samples) in FSConsol to account for the freeze-thaw consolidation.

Figure 6.3 shows the flowchart diagram of the coupling analysis. FSConsol was first run where the initial (height and void ratio) and boundary conditions similar to the laboratory were applied. Hydrostatic condition was assumed for the very first run. The boundary conditions at the top were specified as a constant water cap thickness of zero value so that all the fluid will be drained off the top as the tailings consolidates. Similarly, the bottom boundary condition was specified as

impermeable so that no fluid can exit through the bottom of the cell to simulate the laboratory condition.

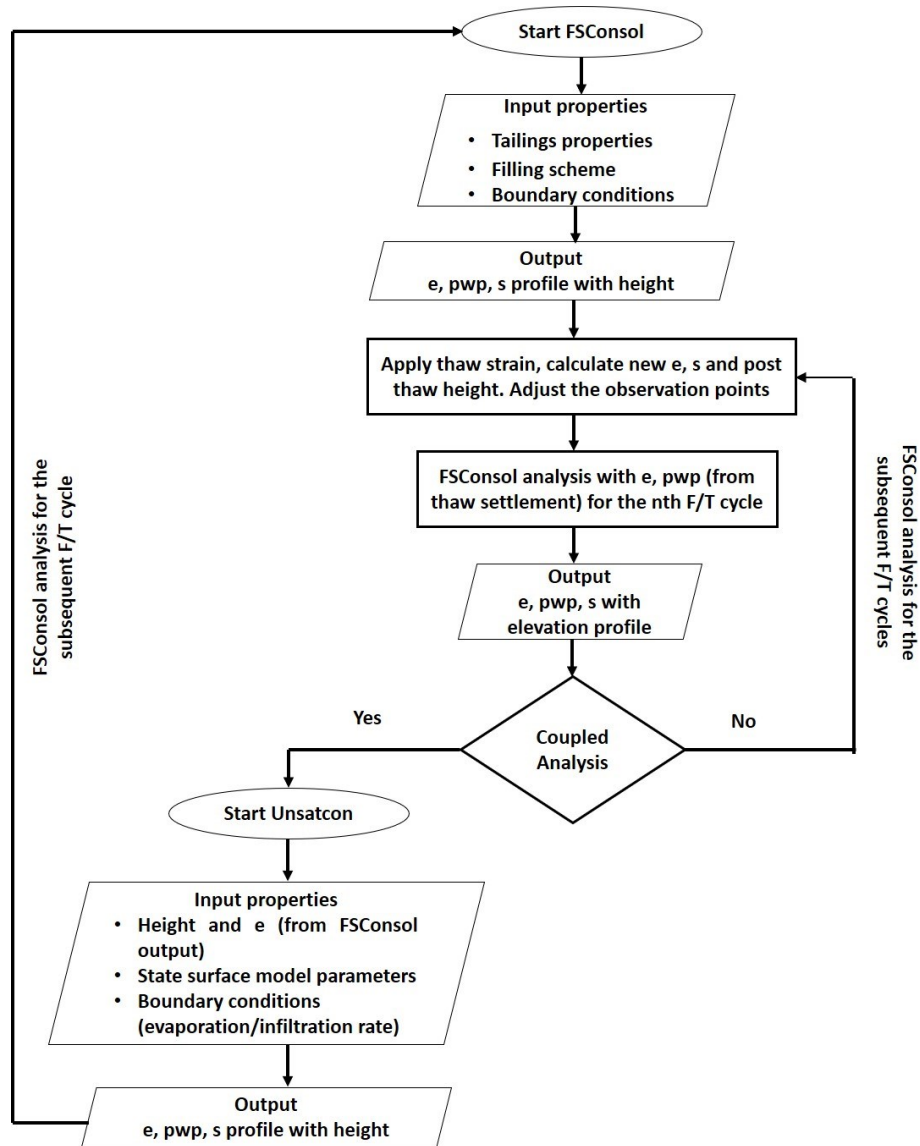


Figure 6.3: Flowchart diagram of coupling analysis

For numerical modeling of the oil sands tailings, large strain consolidation theory is generally adopted (Jeeravipoolvarn, 2010) that requires to input the compressibility (void ratio,  $e$  and effective stress) and saturated hydraulic conductivity ( $K_{sat}$  – void ratio) properties in FSConsol to be obtained from a large strain consolidation test. Using the large strain consolidation apparatus, the material properties of each of the samples were determined. After the consolidation analysis,

the output results such as void ratio ( $e$ ), pore water pressure (pwp) and solids content ( $s$ ) at different pre-sets depths were recorded. Next, solids contents were converted to the bulk density using mass-volume relationship and thaw strain (obtained by fitting laboratory data from  $\varepsilon$ - $\rho$  relationship) was applied into the analysis. The relationship between thaw strain and bulk density for the centrifuged tailings samples under temperature gradients of 0.083 and 0.028 °C /mm is represented below using equation 6.1 and 6.2, respectively:

$$\varepsilon = 0.0684 - 0.079 \ln \rho, \quad [6.1]$$

$$\varepsilon = 0.1887 - 0.276 \ln \rho, \quad [6.2]$$

where,  $\varepsilon$  represents thaw strain (unitless) and  $\rho$  represents bulk density in gm/cm<sup>3</sup>. The above two equations were obtained by fitting the laboratory testing data from  $\varepsilon$ - $\rho$  relationship. The constants of these equations are dependent on the boundary conditions and hence, will be changed based on the available thaw strain data for the particular deposit. Based on the thaw strain, the void ratio and solids content profile from the initial FSConsol run were adjusted. The total height and the heights of all the observation points were adjusted accordingly due to the thaw settlements. Consequently, the input for the next FSConsol run allows incorporating the freeze-thaw consolidation process (denoted as F/T cycle to represent freeze-thaw cycles in the diagram). This was accomplished by changing the initial conditions to reflect the thawed void ratio (based on thaw strain) and pore water pressures (from the previous run) to be applied at the adjusted preset depths in the profile. All these steps prior to coupling with UNSATCON were repeated during consecutive multiple freeze-thaw cycles (for example: first phase testing simulation where FSConsol incorporating thaw strain analysis needs to be repeated for subsequent freeze-thaw cycles).

Whenever drying cycle was introduced, coupled analysis was run by switching from FSConsol to UNSATCON model (for example: second phase testing simulation where alternating analyses were required in each cycle). Hence, the output results (void ratio, elevation) from FSConsol were applied as an initial condition for the UNSATCON model. For modeling the unsaturated soil behaviour, constitutive model (based on state surface modeling approach) was selected, in which the void ratio and water content were expressed as the functions of the net normal and matric

suction in 3D space (Qi, 2017). The parameters of this state surface model for the present study were obtained from the test conducted by Hurtado (2018) on the similar centrifuged tailings. Evaporation rate (in mm/ day) was applied as a top boundary condition obtained from the laboratory tests, whereas no water flux through the bottom was allowed.

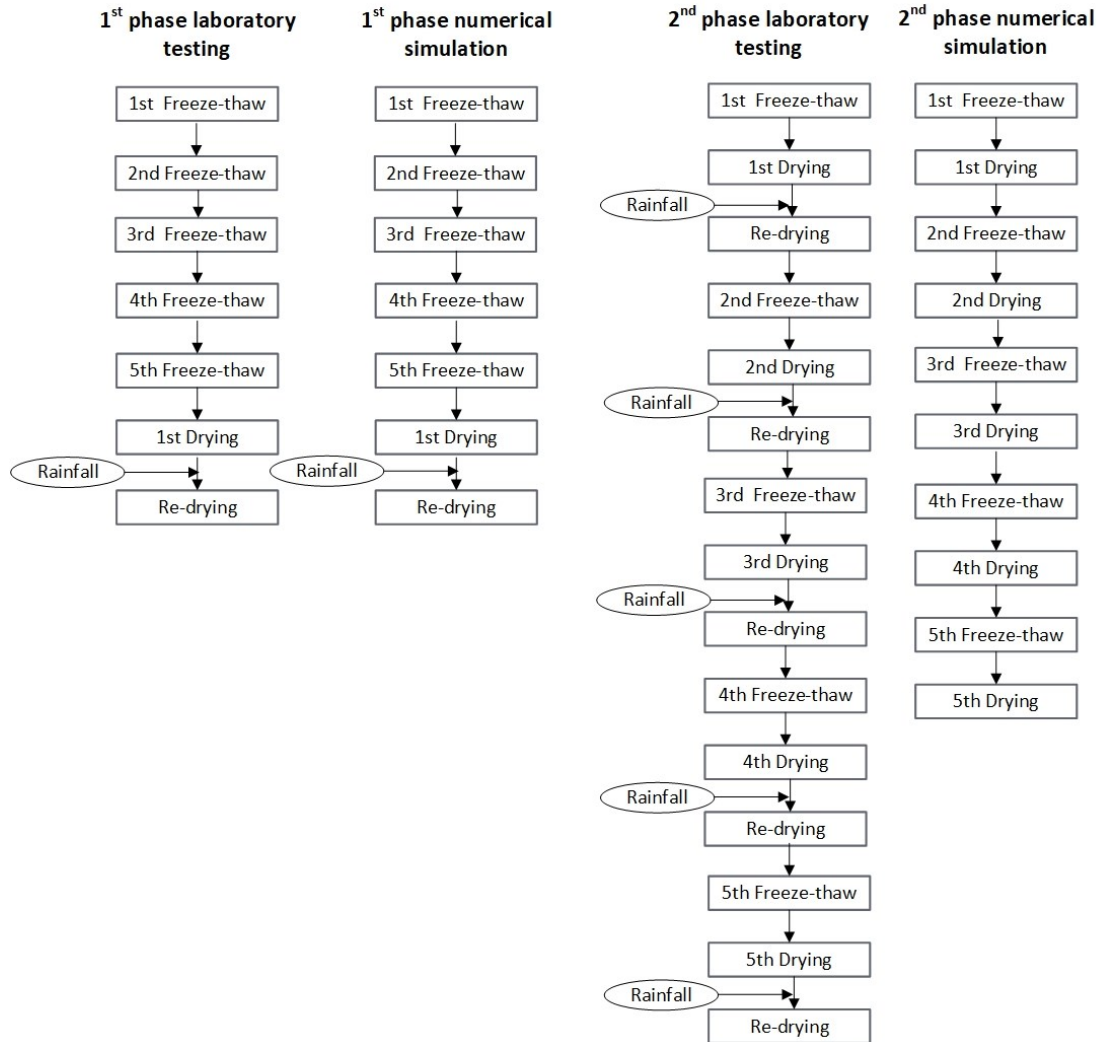


Figure 6.4: First and second phase laboratory testing and numerical simulation sequences

For the numerical modeling, a sequence similar to the laboratory was followed. Figure 6.4 shows the sequences of laboratory and modeling simulation of first and second phase testing. However, due to the complexity of the coupling analysis in second phase testing (five alternate freeze-thaw

and drying- wetting cycles), re-drying after wetting event was not simulated in the numerical model.

#### 6.4.2 Numerical Model Parameters

Tables 6.1, 6.2 and 6.3 show the necessary boundary conditions, initial conditions and summary of material and model parameters for the FSConsol and UNSATCON models, respectively. The initial thickness of each of the sample was 0.18 m similar to the laboratory testing.

Table 6.2: Boundary conditions and summary of parameters for the FSConsol models

Freeze-thaw cycle	Boundary conditions	Material properties				
		Compressibility ( $e = A \cdot \sigma'^B + M$ )*			Permeability ( $k = C \cdot e^D$ )**	
		A	B	M	C	D
0	Top: Constant	5.9548	-0.149	0	2x10-13	15.832
1	water cap:	3.7377	-0.123	0	2x10-12	23.594
2	Thickness 0 m	3.7956	-0.135	0	1x10-10	11.465
3		3.516	-0.146	0	2x10-10	10.723
4	Bottom:	3.516	-0.146	0	2x10-10	10.723
5	Impermeable	3.516	-0.146	0	2x10-10	10.723

\*( $e = A \cdot \sigma'^B + M$ ) Here,  $e$  = Void ratio and  $\sigma'$  = Effective stress in Pascal

\*\* ( $k = C \cdot e^D$ ) Here,  $k$  = Permeability in m/s

To achieve the numerical stability of FSConsol model, a time step of 5 hours was specified. The spatial discretization of this one-dimensional model was a total of 100 nodes, as per the recommendations provided by the manual of FSConsol. The sensitivity analysis was run with different timesteps including an hour and ten hours, and no significant change was observed.

Table 6.3: Boundary conditions and summary of parameters for the UNSATCON models

<b>Property</b>		<b>Value</b>	
Boundary conditions	Top (all cycles)	Desiccation is enabled. Evaporation rate data from laboratory (varied in each cycle)	
	Bottom (all cycles)	No flux	
State surface model parameters (mechanical: void ratio surface)	Plastic	a	2.4
		b	0.33
		c	0.015
		d	0.03
		f	6000
	Elastic	g	5000
		kappa	0.005
State surface model parameters (hydraulic: water content surface)	Primary	C_d0	3
		C_w0	1.35
		lambda_se	0.15
		Lambda_sr	0.17
	Hysteresis	kappa_ss	0.04
Permeability	Multiplier	1 <sup>st</sup> cycle	$2 \times 10^{-13}$
		2 <sup>nd</sup> cycle	$2 \times 10^{-12}$
		3 <sup>rd</sup> cycle	$1 \times 10^{-10}$
		4 <sup>th</sup> cycle	$2 \times 10^{-10}$
		5 <sup>th</sup> cycle	$2 \times 10^{-10}$
	Power	1 <sup>st</sup> cycle	23.594
		2 <sup>nd</sup> cycle	11.465
		3 <sup>rd</sup> cycle	10.723
		4 <sup>th</sup> cycle	10.723
		5 <sup>th</sup> cycle	10.723
M (unsaturation effect)	All cycles	0.75	
Numerical parameters	Number of nodes	10	
	Time step (s)	9	

Please note that the state surface model was developed by Qi (2017), who solved a set of constitutive relationships incorporating volume change and water retention behaviour of unsaturated soils using finite difference techniques. All these in-depth formulations and algorithms were not studied in this paper. Only the parameters applied on similar centrifuged tailings were inputted in the models and these tests were performed by Hurtado (2018).

## 6.5 Modeling Results

### 6.5.1 Numerical Simulation of First Phase Testing

First phase numerical modeling of laboratory testing was run for five consecutive freeze-thaw cycles under two freezing temperature gradients of 0.083 and 0.028 °C /mm followed by a single drying-wetting cycle. Two separate scenarios were modeled here using coupling analysis incorporating the material properties, volume change relationships and the laboratory testing sequences reported above. The model predicted water contents along with the change in elevation after each cycle (denoted as F/T cycle for each freeze-thaw cycles and D-W cycle for drying-wetting cycle in the figures) have been employed in Figures 6.5 and 6.6. Both these figures show that the water contents were consistently decreasing with freeze-thaw cycles and by the fifth cycle, nearly half of the water reduced (44 and 46% reduction in water content for the temperature gradients of 0.083 and 0.028°C /mm, respectively). When drying/evaporation was incorporated in the numerical simulation, both these samples further dewatered to two-fold lower water content (Figure 6.5) for the higher gradient sample and five-fold lower water content (Figure 6.6) for the lower gradient sample, as compared to the initial value.

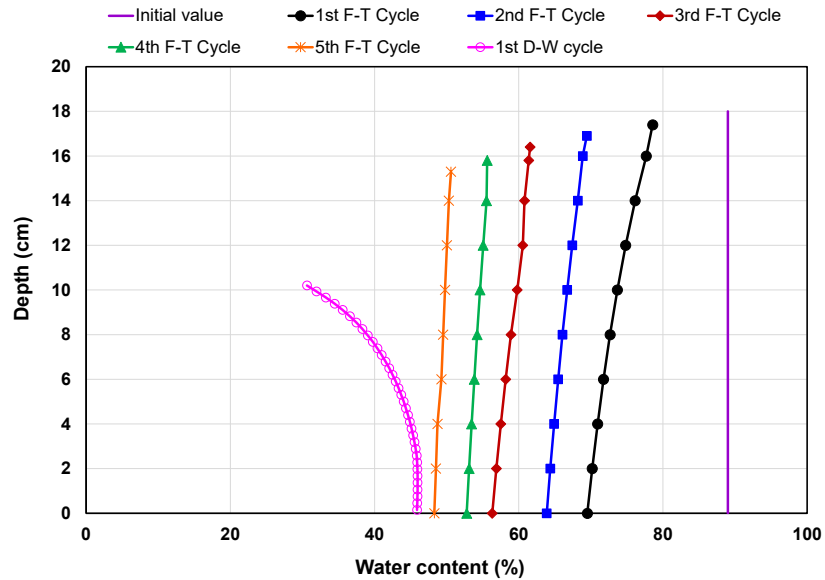


Figure 6.5: Water content profile simulation of centrifuged tailings at a temperature gradient of 0.083 °C /mm

The centrifuged tailings samples at freezing temperature gradients of 0.083 and 0.028°C /mm resulted in water contents of 48.3 and 47.1% at the surface, respectively, after five consecutive freeze-thaw cycles (the initial water content was 89%). Although the reduction in water contents for both the samples did not differ significantly from each other during the freeze-thaw analysis, the drying analysis from UNSATCON model resulted in a higher dewatering on the lower gradient (0.028°C /mm) sample compared to the sample subjected to higher gradient. The lower gradient sample (as shown in Figure 6.6) experienced an average water content of 18.8% throughout the sample with the lowest one observed at the surface (17%). Conversely, the sample subjected to a higher freezing temperature gradient of 0.083°C /mm resulted in an average water content of 42% (shown in Figure 6.5), where the lowest being observed at the surface was 30.6%. The final surface elevations for the higher and lower gradient samples were found to be 10.2 (43% reduction in thickness compared to the initial value) and 9.5 cm (47% reduction in thickness compared to the initial value), respectively, at the end of the model run.

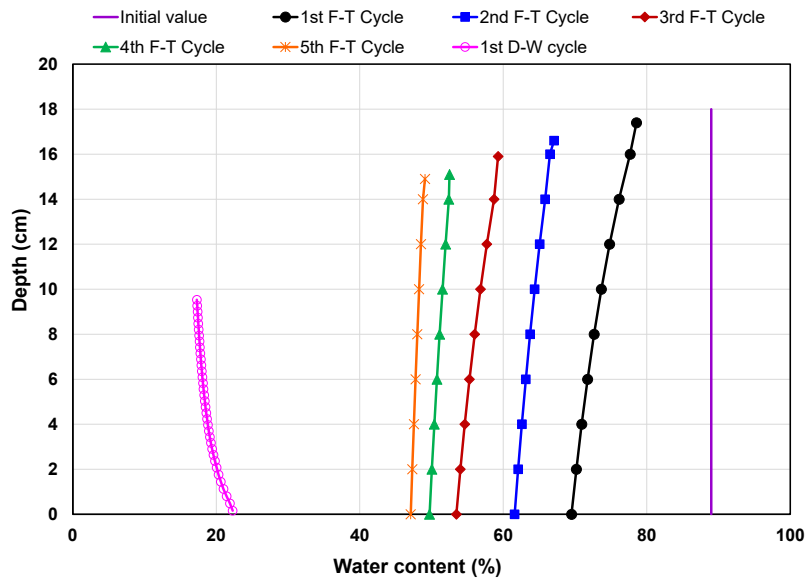


Figure 6.6: Water content profile simulation of centrifuged tailings at a temperature gradient of 0.028 °C /mm

### 6.5.2 Numerical Simulation of Second Phase Testing

Second phase numerical simulations of the laboratory testing were run for five alternate freeze-thaw and drying-wetting cycles where each freeze-thaw cycle was followed by a drying-wetting-re-drying cycle and this sequence was repeated five times per sample to represent five seasonal years in the field. The wetting event per cycle was introduced as a single event in the laboratory to simulate the rainfall where the volume of water evaporated during atmospheric drying/evaporation for that particular cycle was poured back into the cell. As a result, tailings surface was re-wetted, thereby, allowing an increase in water content similar to the pre-drying phase. Upon wetting, the samples went through another drying cycle (with a similar time duration to the pre-wetting drying cycle) to investigate the tailings dewatering behaviour prior to and after the wetting event. The laboratory results suggest that the gain in solids content (or a reduction in water content) achieved during the first seven days of drying period was entirely depreciated by introducing the wetting event (same amount of water was poured back into the cell that was evaporated) (Rima and Beier, 2021a). When the samples were re-dried for another seven days (at the end of fourteen days) upon wetting, an increase in solids content was observed similar to the pre-wetting cycle (within a difference in values of 0-1.4% by mass prior to and post-wetting drying). However, it was the last two cycles (fourth and fifth cycle) where the wetting event does not have any significant impact on increasing the water content of the tailings (particularly significant for lower gradient sample) because of the possible higher suction, thereby, resulting in a further decrease in water content after fourteen days (Rima and Beier, 2021). Nevertheless, incorporating all these components using alternating simulation from FSConsol and UNSATCON in every cycle was very complex and hence, the simulation was simplified by excluding the wetting and re-drying cycles.

Figures 6.7 and 6.8 show the model predicted water content profiles for the two samples after each cycle (freeze-thaw and drying cycles were shown separately and denoted as F/T cycle for each freeze-thaw cycles and D cycle for drying cycle in the figures). The initial water content and elevation were found to be 89% and 0.18 m, respectively. The coupling analysis to simulate second phase of testing shows that the centrifuged tailings samples subjected to temperature gradients of 0.083 and 0.028°C /mm responded quite differently to seasonal weathering. After five alternate freeze-thaw and drying cycles, the samples with higher (0.083°C /mm) and lower temperature gradients (0.028°C /mm) dewatered to nearly four-fold (surficial water content value was 25%, as shown in Figure 6.7) and six-fold (surficial water content value was 16%, as shown in Figure 6.8)

lower water contents, respectively, at the surface when compared to the initial water content value. Both the samples dewatered similarly for the first two seasonal cycles (first freeze-thaw-drying and second freeze-thaw cycles). It was the second drying cycle when dewatering between the two samples started to differ. Evaporation from the lower temperature gradient sample reduced the water content by 29% at the surface compared to the other sample at the end of the second cycle. At the end of the third, fourth and fifth cycle, the sample subjected to a temperature gradient of  $0.028^{\circ}\text{C}/\text{mm}$  resulted in 28, 31 and 36% reduction in water contents at the surface, respectively, compared to the sample under higher freezing temperature gradient ( $0.083^{\circ}\text{C}/\text{mm}$ ). Both the higher and lower temperature gradient samples dewatered considerably after five seasonal cycles with final elevations of 10.2 (43% reduction in thickness from the initial value) and 9.7 cm (46% reduction in thickness from its initial value), respectively. The bottom few hundredths of a meter of the sample were not affected much by the seasonal weathering model run.

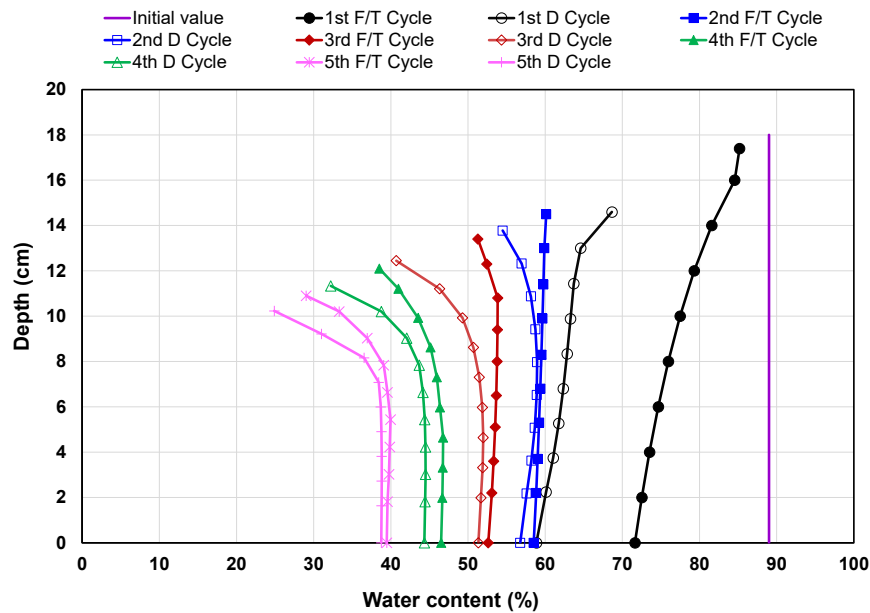


Figure 6.7: Water content profile of centrifuged tailings at a temperature gradient of  $0.083^{\circ}\text{C}/\text{mm}$

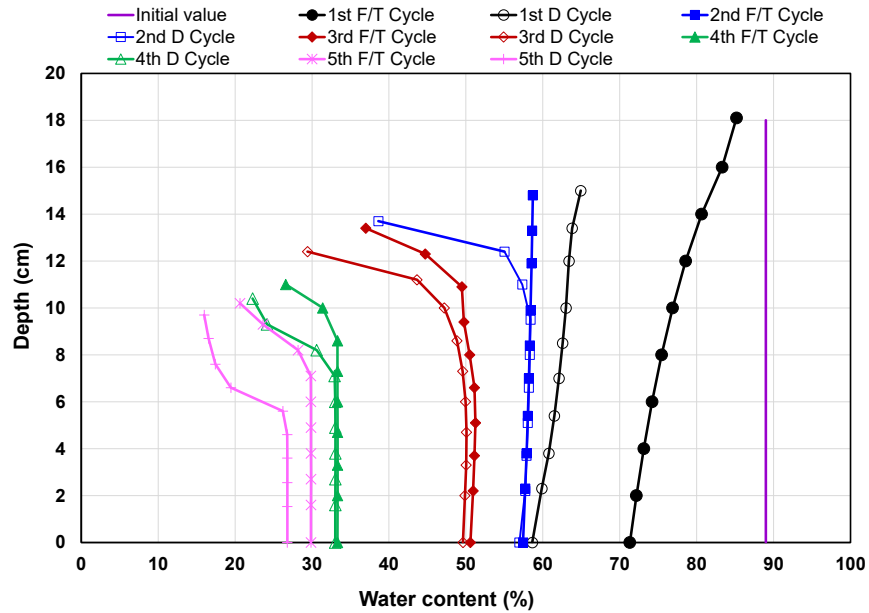
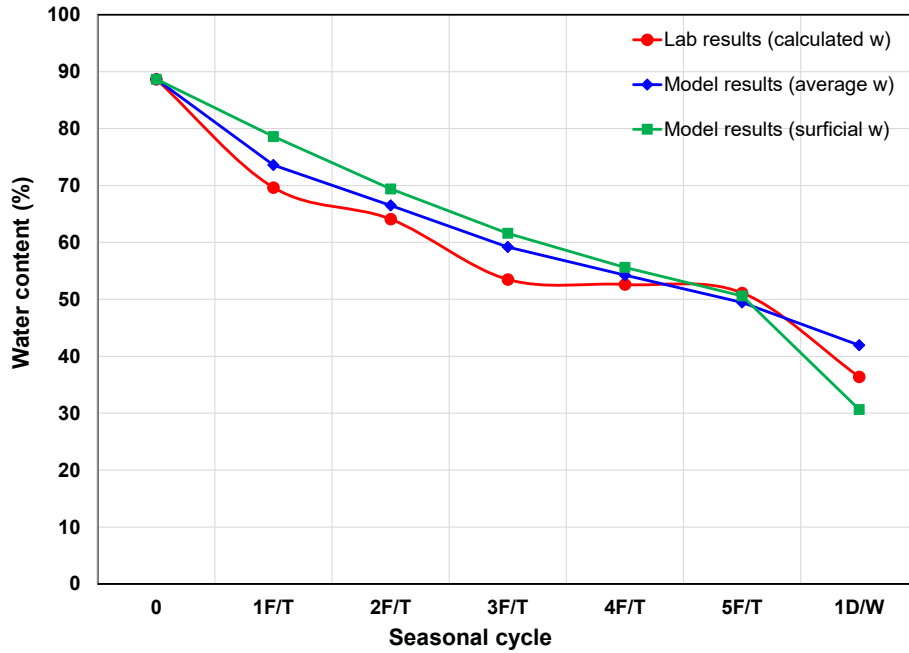


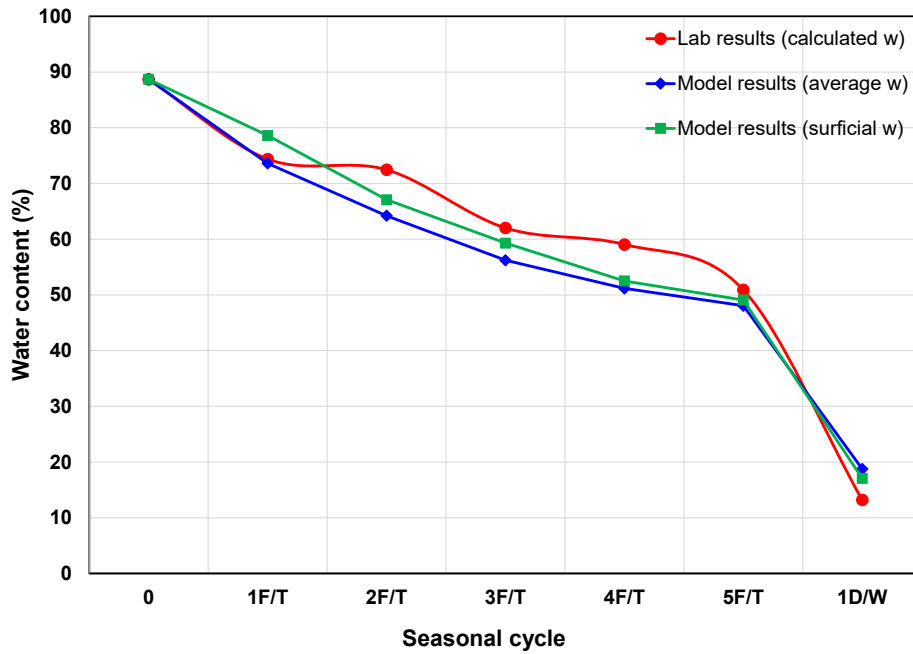
Figure 6.8: Water content profile of centrifuged tailings at a temperature gradient of 0.028 °C /mm

### 6.5.3 Comparison between the Model and Laboratory Results

Figures 6.9 and 6.10 illustrate the cumulative decrease in water content for the two centrifuged tailings samples under the temperature gradients of 0.083 and 0.028°C /mm, respectively, after each seasonal cycle, where Figure 6.9 compares the first phase laboratory testing and modeling results, and Figure 6.10 compares the second phase testing results between laboratory computation and model prediction. The water content obtained from the laboratory after each seasonal cycle was calculated on the basis of thaw strain during freeze-thaw cycles and the changes in weight loss/gain during drying-wetting cycles. Hence, the water content per cycle obtained from the laboratory represents the average water content throughout the depth. In terms of numerical modeling, both the average and surface values were reported on the graph as the deposit surface is expected to dewater the most, given most susceptible to the effects of seasonal weathering.

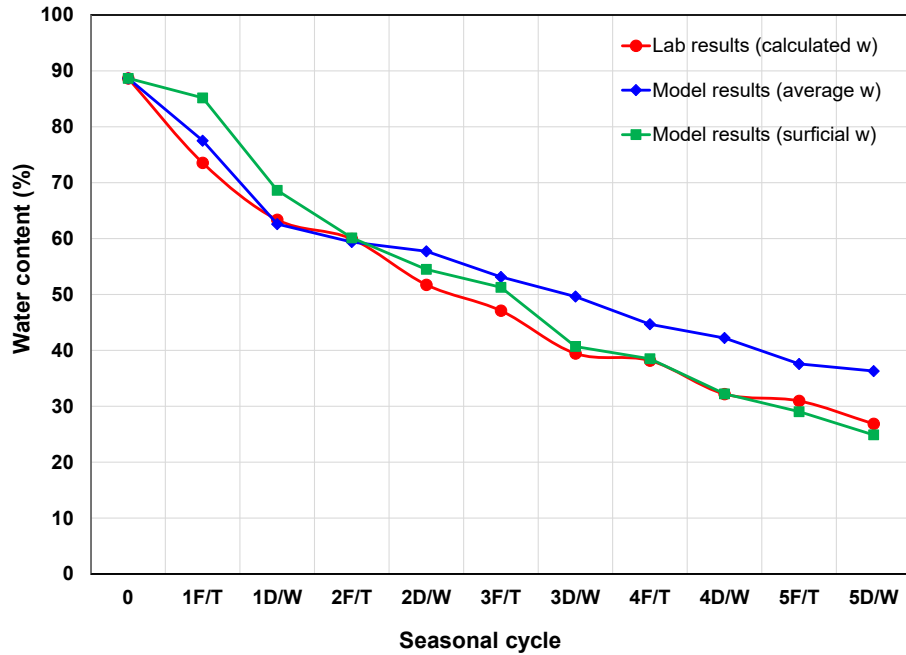


(a)

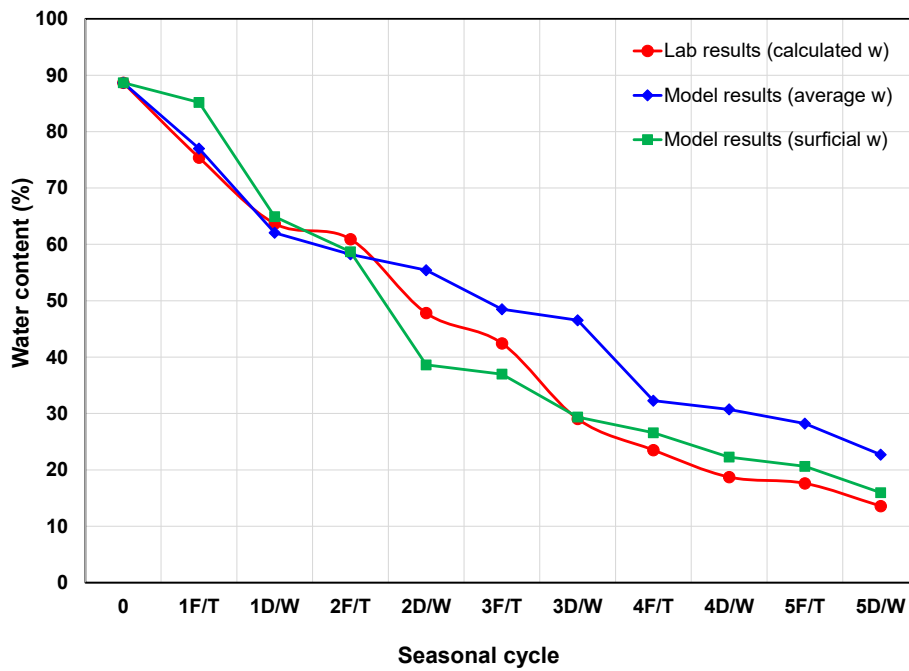


(b)

Figure 6.9: First phase testing comparisons: water content values per seasonal cycle for the centrifuged tailings samples under a temperature gradient of (a)  $0.083^{\circ}\text{C}/\text{mm}$  and (b)  $0.028^{\circ}\text{C}/\text{mm}$



(a)

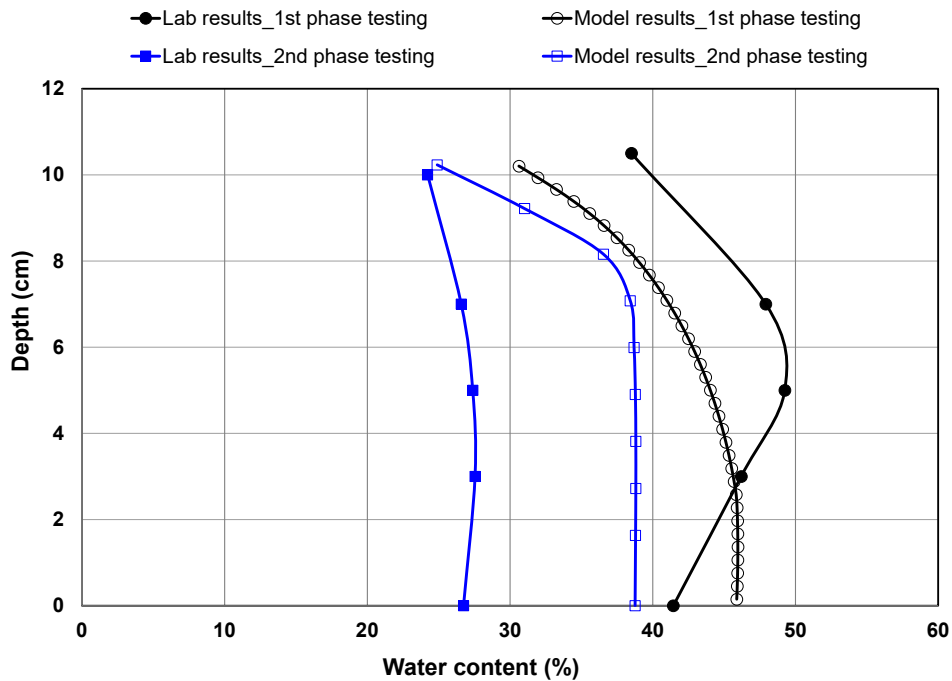


(b)

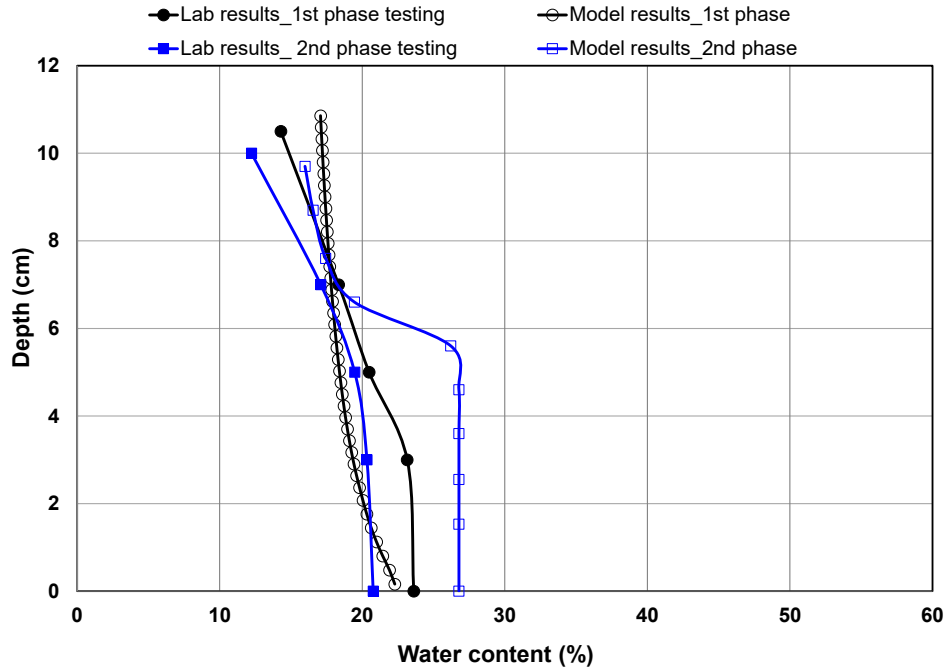
Figure 6.10: Second phase testing comparisons: water content values per seasonal cycle for the centrifuged tailings samples under a temperature gradient of (a) 0.083°C /mm and (b) 0.028°C /mm

As evident in Figure 6.9, the differences between the model prediction and the laboratory computational results were marginal. However, the model overpredicted water content values compared to the laboratory results for the higher temperature gradient sample (Figure 6.9a), while it showed the reversed pattern for the lower temperature gradient sample (Figure 6.9b). The second phase testing, as shown in Figure 6.10, shows a different trend. The laboratory results for both the samples corroborated well with the model predicted water contents at the surface.

Figure 6.11 shows the comparisons between the final (at the end of the tests) laboratory measured and model predicted water content profiles for the two centrifuged tailings samples subjected to temperature gradients of 0.083 and 0.028°C /mm, respectively.



(a)



(b)

Figure 6.11: Laboratory versus model water content profiles of centrifuged tailings at the end of the test under a temperature gradient of (a)  $0.083^{\circ}\text{C}/\text{mm}$  and (b)  $0.028^{\circ}\text{C}/\text{mm}$

As shown in Figure 6.11a, first phase testing results indicate that the simulation for the higher temperature gradient sample overall underpredicted water content values by almost 3% as the average water content values along the depth were found to be 42 and 44.6%, respectively, from the modeling prediction and the laboratory measurement. Likewise, the lowest water content, observed at the surface, were found to be 31 and 39%, respectively, from the modeling and laboratory results (about 8% underprediction of water content compared to the laboratory value). Conversely, the laboratory and model predicted water content profile corroborated quite well for the lower gradient sample (Figure 6.11b). The model overall underpredicted water content values by 1.5% throughout the depth and over predicted this value by about 3% at the surface compared to the laboratory measurement. The model predicted an average water content of 18.6% throughout the depth with a lowest water content of 17% observed at the surface, whereas, the laboratory measured average value was found to be 20% along with the lowest water content of 14.3% observed at the surface. All these values from the lower gradient sample suggest a stiff/ solid

consistency for the tailings, provided these values passed through the plastic limit of 26% (Figure 6.12).

As mentioned above, the numerical model to simulate the second phase testing excluded the wetting event and re-drying cycle after wetting. Hence, the model predictions were expected to achieve higher water contents compared to the laboratory results. However, the laboratory results suggest that the water content reduction/solids content gain just prior to wetting (at the end of seven days of drying cycle prior to wetting event) and post wetting drying phase (at the end of another seven days of drying cycle post wetting) was invariable for the higher temperature gradient sample ( $0.083^{\circ}\text{C}/\text{mm}$ ) and therefore, this sample is not supposed to be impacted much because of these wetting and re-drying event exclusions. It was the lower gradient sample where the water content reduction/solids content gain prior to and after wetting event was not similar at the higher cycles (fourth and fifth cycles). This is due to the possible higher suction values that prevented rainfall to cause any impact on increasing water content upon wetting (Rima and Beier, 2021a). However, the modeling results to simulate the second phase testing (as shown in Figure 6.11) suggest that the model overall overpredicted water content values by about 10 and 5% for the higher (Figure 6.11a) and lower (Figure 6.11b) temperature gradient samples, respectively, as compared to the laboratory results. In contrast to that, the surficial water content values were comparable, given that the model overpredicted water content by almost 1 and 4% for the higher ( $0.083^{\circ}\text{C}/\text{mm}$ ) and lower ( $0.028^{\circ}\text{C}/\text{mm}$ ) temperature gradient samples, respectively. The surface elevation of the higher temperature gradient sample nearly reduced to half of its initial thickness (43 and 44% reduction of its initial thickness from modeling simulation and laboratory results, respectively) at the end of the tests. Likewise, the surface elevation of the lower gradient temperature sample reduced to 46 and 44% of their initial thickness from the numerical modeling and laboratory results, respectively.

Figure 6.12 shows the liquidity index profiles of the coupled analysis models. Similar to the first phase testing, the second phase testing also suggests that the surface of the lower gradient sample was able to pass through the plastic limit. On the contrary, the higher gradient sample was in a relatively softer consistency in the first phase testing (could not reach the plastic limit), while the sample surface just reached to the plastic limit in the second phase of testing. Overall, coupling

analyses were able to predict the laboratory results reasonably well for the centrifuged tailings sample subjected to lower temperature gradient ( $0.028^{\circ}\text{C}/\text{mm}$ ) compared to the higher gradient ( $0.083^{\circ}\text{C}/\text{mm}$ ).

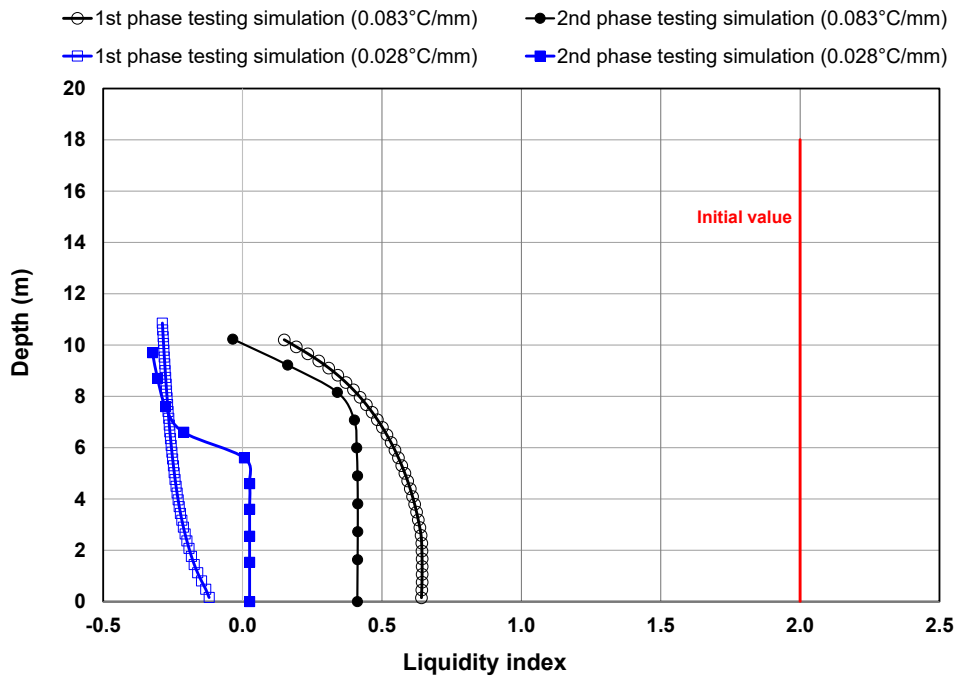


Figure 6.12: Liquidity index profiles of centrifuged tailings from coupled analysis

## 6.6 Discussion

Both the laboratory results and numerical model suggest that the centrifuged tailings samples subjected to seasonal weathering (multiple freeze-thaw and drying cycles) have the potential of improved dewatering compared to the as-received centrifuged tailings. Figure 6.5 and 6.6 show how multiple freeze-thaw cycles at two different freezing temperature gradients contributed to dewatering prior to drying/evaporation. Freeze-thaw process are known to alter the structure of the tailings/soil materials by re-distributing moisture inside the tailings/soil particles that, in turn, improves dewatering upon thaw (Proskin et al., 2012). Consequently, higher dewatering/volume change can be expected during the very first freeze-thaw cycle followed by a gradual decrease in subsequent cycles due to the gradual decrease in available water/moisture inside the tailings materials (Eigenbrod, 1996; Andersland and Ladanyi, 2004). Both of these two figures may look

similar until the drying/wetting cycle has been introduced. Fine grained tailings subjected to freezing likely generates high suction/ negative pore water pressure at the freezing front, thereby, causing water migration upwards to the front (as shown in Figure 6.1) and subsequent reduction in water content and shrinkage crack development in the tailings. The extent of these cracks is predominantly dependent on the temperature gradient, number of freeze-thaw cycles and the physio-chemical interactions among the tailings particles and solutes (Proskin, 1998; Proskin et al., 2012; Pham and Segó, 2014). Apart from the earlier findings (carried out by Segó and Dawson (1992); Proskin (1998); Pham and Segó (2014)), the visual observation from the laboratory testing also suggest that the lower freezing temperature gradient results in higher shrinkage and cracks contributing towards higher evaporation and solids content. Hence, the shrinkage and cracks developed during freeze-thaw cycles facilitated different evaporation rates for the centrifuged tailings under two different gradients, that contributed to the significantly different water content profiles in drying-wetting cycle (as shown in Figure 6.5 and 6.6).

Figures 6.7 and 6.8 show how seasonal weathering in nature can contribute to dewatering of the centrifuged tailings deposit. At the start of the simulation, the tailings are first consolidated at the bottom. With subsequent cycles, the upward water flux due to consolidation becomes less than the applied evaporation at the surface and hence, desiccation occurs. As a result, the tailings surface first becomes unsaturated being exposed to the atmosphere, thereby, reducing water content considerably than the bottom part. However, the void ratio profile (void ratio vs elevation) from the previous freeze-thaw cycle cannot be specified within a single layer deposit in UNSATCON model and hence, an average void ratio was applied than can affect the drying cycle outputs. As shown in Figures 6.7 and 6.8, the water content profiles at the bottom few hundredths of a meter remain almost constant, which can be attributed to the input parameter specified as an average value (void ratio from the previous cycle).

The coupled analysis, as shown in Figure 6.9, correlates well with the first phase laboratory testing results of the centrifuged tailings samples under temperature gradients of 0.083 and 0.028°C /mm. The subsequent cycle has lower impact on the volume changes due to the freeze-thaw cycles, thereby, causing lower dewatering from the sample. Hence, the differences in water content values between the laboratory results and modeling predictions (both average and surficial water content

values) are expected to be marginal. However, the results from the drying model that has a significant impact on dewatering, corroborates well with the laboratory results and validates the efficacy of the coupled analysis model.

Similar to Figure 6.9, Figure 6.10 compares the second phase laboratory testing with the modeling results of the centrifuged tailings under two different temperature gradients (0.083 and 0.028°C /mm). In contrast to the Figure 6.9, the model predicted water contents at the surface correlated well with the laboratory computation for both gradient scenarios of the investigated centrifuged tailings. The model predicted average water content values deviated to an extent upto 18% differences) from the laboratory computed average values and this can be attributed to the limitation of the drying (UNSATCON model) model where input parameter (void ratio) has to be specified as an average value instead of a void ratio profile (varying with depth). The exclusion of wetting and re-drying after wetting events may also have an impact on the variations. However, given the fact that both the samples deviated in their average water content values compared to the laboratory results but correlated well in terms of surficial water content, the limitation of drying model most likely predominantly contributed to these deviations.

Figure 6.11 shows the final water content profiles subjected to first and second phase testing for the investigated two centrifuged tailings under temperature gradients of 0.083 and 0.028°C /mm, respectively. The laboratory results shown on the graph represent the oven measured water content values at the end of the tests. Figure 6.11a shows that the higher gradient centrifuged tailings sample predicted an overall lower water content profile than the laboratory measurement for the first phase testing while the opposite trend was observed in the second phase testing. The higher water content profile predicted in the model for the second phase testing can be attributed to the preclusion of wetting event and re-drying cycle in the model. In addition to that, the limitation of the UNSATCON model to incorporate the void ratio/water content profile from the previous cycle results in the overall differences between the laboratory results and modeling prediction. However, the water content profiles developed to predict the laboratory testing (as shown in Figure 6.11b) supported the laboratory results considerably for the lower gradient tailings sample. Although the drying model could predict the profile for the top few hundredths of a meter of the sample reasonably well following the evaporative flux incorporated in the top boundary, the lower part of

the sample could not be predicted quite well due to the limitation of defining input parameters. Figure 6.12 shows the change in consistency of tailings samples prior to and after seasonal weathering to illustrate the efficacy of these processes that can be applied in the field deposit.

Overall, this study presented coupling three components (incorporating freeze-thaw process into the FSConsol, consolidation from FSConsol and atmospheric drying from UNSATCON) to develop a coupled model. Model predicted dewatering behavior correlated well with the laboratory results that validated this coupling approach. However, the coupling analysis has a few limitations such as: incapability of running under a single program that can incorporate all the seasonal weathering processes (freeze-thaw, consolidation, desiccation etc.) and the limitations of defining input parameters in UNSATCON model such as being unable 1. to define a void ratio profile (varying with depth) instead of an average void ratio per cycle, 2. to define data directly from SWCC curve and compressibility curves instead of fitting data into state surface model and 3. to input separate files for evaporation and infiltration under same cycle. The numerical software available in the industry is yet to develop a program that can simulate the freeze-thaw, consolidation and desiccation of tailings under different boundary conditions and deposition scenarios. Switching between different modeling platforms to address all these seasonal weathering components is cumbersome and time-consuming. Nevertheless, the coupled analysis, in some ways, is able to validate the laboratory analysis based on which field behaviour can be predicted. It may not predict the long-term field behaviour given the complexity related to combining the multiple models for each cycle (Each cycle requires to go through the flowchart each time as shown in Figure 1, that implies the flowchart needs to be repeated 100 times for a prediction of 100 years). However, these analyses can provide insights to predicting dewatering behavior of the future field deposits.

## **6.7 Conclusion**

The coupling modeling methodology presented in this study was able to develop an approach that was validated by comparing it with the laboratory test results of centrifuged tailings under similar boundary conditions. This coupling methodology can assist in tailings management by predicting the short-term behaviour of the dewatering performance of the tailings deposits subjected to the

natural seasonal weathering (freeze-thaw, consolidation and desiccation). Within limited scope, this coupled analysis demonstrated that freeze-thaw cycles can be considered as a part of the tailings management in the region where weather permits. Freeze-thaw process may appear to achieve lower dewatering enhancement compared to atmospheric drying, the shrinkage and/or cracks developed during the freeze-thaw cycles facilitate greater evaporation and desiccation during the subsequent drying cycle, thereby, contributing to overall higher dewatering. The model also confirms the previous research and the present laboratory findings that suggest that lower temperature gradient results in higher solid content/ lower water content in post-thawed tailings. When drying/evaporative component was incorporated, atmospheric drying was shown to significantly (half order of magnitude lower) reduce the water content as compared to the multiple freeze-thaw cycles only. With the combined effects of alternate freeze-thaw and drying-wetting cycles, the tailings could even achieve a water content exceeding the plastic limit (as evident in lower temperature gradient sample), enabling reclamation and closure. While time consuming, this approach can provide insights to predicting dewatering behaviour of future field deposits so that it can be used for planning purposes.

## **Acknowledgements**

The authors would like to thank Natural Sciences and Engineering Research Council of Canada (NSERC), Canada's Oil Sands Innovation Alliance (COSIA) and Alberta Innovates – Energy and Environment Solutions for their financial support. The authors would also like to thank Dr. Louis Kabwe for providing the large strain consolidation parameters.

## **References**

- Alberta Energy Regulator (AER). 2016. *Alberta's Energy Reserves 2015 & Supply/Demand Outlook 2016-2025 (ST98-2016)*, Alberta Energy Regulator, Calgary, Alberta.
- Alberta Energy Regulator (AER), 2020. *State of Fluid Tailings Management for Mineable Oil Sands, 2019*. Report, Calgary, Alberta. See <https://static.aer.ca/prd/2020-09/2019-State-Fluid-Tailings-Management-Mineable-OilSands.pdf> (Accessed 31/07/2021).

- Andersland, O.B. and Ladanyi, B. 2004. *Frozen Ground Engineering*, 2nd Edition, American Society of Civil Engineers & John Wiley & Sons Inc., Hoboken, New Jersey, USA.
- Cossey, H.L., Batycky, A.E., Kaminsky, H., and Ulrich, A.C. 2021. Geochemical Stability of Oil Sands Tailings in Mine Closure Landforms. *Minerals* 2021, 11 (8):830.
- Dawson, R.F. and Segó, D.C. 1993. Design Concepts for Thin Layered Freeze-Thaw Dewatering Systems, *Proceedings of the 46th Canadian Geotechnical Conference*, Saskatoon, SK, Canada: 283-288.
- Eigenbrod, K.D. 1996. Effects of cyclic freezing and thawing on volume changes and permeabilities of soft fine-grained soils, *Canadian Geotechnical Journal*, 33(4): 529-537.
- Gibson, R., England, G., and Hussey, M. 1967. The theory of one-dimensional consolidation of saturated clays. *Geotechnique*, 17: 261-273.
- Government of Alberta. 2021a. *Oil Sands: Facts and Stats. 2021*. Available online: <https://www.alberta.ca/oil-sands-facts-and-statistics.aspx> (accessed on 1st October 2021).
- Government of Alberta. 2021b. Oil Sands Information Portal. Available online: <http://osip.alberta.ca/map/> (Accessed on 1st October, 2021).
- Hurtado, O. 2018. *Desiccation and Consolidation in Centrifuge Cake Oil Sands Tailings*, M.Sc. Thesis, Carleton University, Ottawa, Ontario, Canada.
- Hyndman, A., Sawatsky, L., McKenna, G. and Vandenberg, J. 2018. Fluid Fine Tailings Processes: Disposal, Capping, and Closure Alternatives. In *Proceeding of the 6th International Oil Sands Tailings Conference*, Edmonton, Alberta, Canada. pp. 9-12.
- Jeeravipoolvarn, S. 2010. *Geotechnical Behavior of In-Line Thickened Oil Sands Tailings*. PhD Thesis, University of Alberta, Edmonton, AB, Canada.
- Johnson, R.L., Pork, P., Allen E.A.D., James, W.H. and Koverny, L. 1993. *Oil Sands Sludge Dewatering by Freeze-Thaw and Evaporation*, Report-RRTAC 93-8, Alberta Conservation and Reclamation Council, AB, Canada.
- Oil Sands Tailings Consortium (OSTC) and Canada's Oil Sands Innovation Alliance (COSIA). 2012. *Technical Guide for Fluid Fine Tailings Management*, Report, Calgary, Alberta.
- Pham, N.H. and Segó, D.C. 2014. Modeling Dewatering of Oil Sands Mature Fine Tailings using Freeze Thaw. *International Oil Sands Tailings Conference*, Lake Louise, AB, Canada, December 7-10, 2014.

- Proskin, S.A. 1998. *A Geotechnical Investigation of Freeze-Thaw Dewatering of Oil Sands Fine Tailings*, PhD Thesis. Department of Civil and Environmental Engineering, University of Alberta, Edmonton, AB, Canada.
- Proskin, S., Segó, D. and Alostaz, M. 2012. Oil Sands MFT Properties and Freeze-Thaw Effects, *Journal of Cold Regions Engineering*, ASCE, 26 (2): 29-54.
- Qi, S. 2017. *Numerical Investigation for Slope Stability of Expansive Soils and Large Strain Consolidation of Soft Soils*. PhD Thesis, University of Ottawa, Ottawa, ON, Canada.
- Qi, S.; Simms, P.; Vanapalli, S. 2017. Piecewise-linear formulation of coupled large-strain consolidation and unsaturated flow. I: Model development and implementation. *Journal of Geotechnical and Geoenvironmental Engineering*, 143, 04017018.
- Rima, U.S and Beier N. 2021a. Effects of seasonal weathering on dewatering and strength of an oil sands tailings deposit. *Canadian Geotechnical Journal*, In press. <https://doi.org/10.1139/cgj-2020-0533>.
- Rima, U.S. and Beier, N. 2021b. Effects of multiple freeze-thaw cycles on oil sands tailings behaviour. *Cold Regions Science and Technology*, 192:103404. <https://doi.org/10.1016/j.coldregions.2021.103404>.
- Scott, J.D., Dusseault, M.B. and Carrier, W.D. 1985. Behaviour of the clay/bitumen/water sludge system from oil sands extraction plants. *Applied Clay Science*, 1(1-2): 207-218. [https://doi.org/10.1016/0169-1317\(85\)90574-5](https://doi.org/10.1016/0169-1317(85)90574-5).
- Segó, D. C. and Dawson, R.F. 1992. *Influence of freeze-thaw on behaviour of oil sand fine tails*. Alberta Oil Sands Technology and Research Authority, pp-77.
- Spence, J., Bara, B., Lorentz, J. and Mikula, R. 2015. Development of the Centrifuge Process for Fluid Fine Tailings Treatment at Syncrude Canada Ltd. *In World Heavy Oil Congress 2015*, Edmonton, Alberta, 24-26 March, 2015.

## 7 SUMMARY, CONCLUSIONS AND RECOMMENDATIONS

### 7.1 Summary

This dissertation investigated the mechanisms driving the dewatering and strength behaviour of two types of treated deep tailings deposits (centrifuged tailings and in-line thickened tailings (ILTT)) undergoing seasonal weathering dominated by a) freeze-thaw cycles and b) alternating freeze-thaw and drying-wetting cycles using controlled laboratory experiments. The laboratory experiments were carried out under three temperature gradients of 0.083, 0.056 and 0.028°C/mm to accommodate the average winter temperature (air temperature varies between -8 to -17°C that resulted in a typical ground temperature of -1 to -10°C into the tailings deposit) of Fort McMurray. The laboratory testing carried out on the ILTT samples were compared to the ILTT pilot scale field deposit, while a coupling numerical approach was developed to simulate the laboratory testing performed on the centrifuged tailings samples. Hence, laboratory testing was validated by simulating field conditions and the efficacy of coupled model was validated by simulating the laboratory testing conditions.

The following section summarizes the conclusions of the research program:

#### *7.1.1 Effects of Multiple Freeze-Thaw Cycles on Oil Sands Tailings Behaviour*

Freeze-thaw is considered one of the dewatering technologies that has the potential for reducing water content and increasing the strength of the tailings, thus, contributing to minimize the massive volumes of fine tailings (Proskin, 1998). An improved understanding of the mechanisms involved in freeze-thaw is paramount to assess its effectiveness in the dewatering and strength enhancement of fine tailings. Fluid fine tailings, being predominated by clay minerals, are extremely sensitive to the changes in physico-chemical interactions and hence, the effectiveness of the freeze-thaw cycles was expected to differ by varying the water chemistry. Consequently, the polymer amended treated tailings subjected to freeze-thaw dewatering were expected to behave differently than the untreated FFT. The previous research studies, which were mostly limited to the untreated FFT, suggested that the natural freeze-thaw cycles can be a cost-effective alternative for FFT

management. In order to assess the effectiveness of freeze-thaw process on higher solids content tailings, two polymer amended treated tailings were studied: centrifuged and in-line thickened tailings. The difference in treatment process resulted in higher divalent cations ( $\text{Ca}^{2+}$ ,  $\text{Mg}^{2+}$ ) for centrifuged tailings samples, which, in conjunction with lower clay content contributed to an improved dewatering and strength performance when compared to ILTT samples. Under similar boundary conditions (similar freezing temperature gradient and drying conditions), centrifuged tailings and ILTT samples dewatered to nearly seven-fold and five-fold lower water content at the surface, respectively, compared to their initial values. Similarly, surficial shear strength for the centrifuged tailings sample was found to be three-fold higher than the ILTT sample at the end of the tests (after five cyclic freeze-thaw followed by a single drying-wetting cycle). When compared to the EC values, five consecutive freeze-thaw cycles resulted in a nearly six-fold higher EC value at the surface for centrifuged tailings than the ILTT sample. The higher EC value for the centrifuged tailings suggests an upward migration of increased ion concentrations/solutes to the surface, thereby, causing a double layer suppression and overall volume reduction possibly due to the combined influence of osmotic flow and osmotic compressibility (Barbour and Fredlund, 1989).

The mechanism of water and salt migration during freeze-thaw process was found to be predominantly dependent on the temperature gradient which also controls the dewatering and strength performance. After five consecutive freeze-thaw cycles, lower freezing temperature gradient ( $0.028^{\circ}\text{C}/\text{mm}$ ) resulted in two-folds higher undrained shear strength for centrifuged tailings compared to the other temperature gradients ( $0.083$  and  $0.056^{\circ}\text{C}/\text{mm}$ ). Similarly, EC for the lower gradient temperature gradient was found to be 1.5 times higher than the EC values obtained from the centrifuged tailings samples subjected to other temperature gradients. When incorporated with a cycle of atmospheric drying and wetting, lower temperature gradient sample resulted in nearly 3 times and about 2.5 times higher water content compared to the centrifuged tailings sample subjected to temperature gradients of  $0.083$  and  $0.056^{\circ}\text{C}/\text{mm}$ , respectively. The increase in surficial strength was even significantly higher, where lower temperature gradient sample achieved a shear strength of  $>100\text{kPa}$ , which was found atleast 7 times and 6 times higher than the shear strength measured from the samples with temperature gradients of  $0.083$  and  $0.056^{\circ}\text{C}/\text{mm}$ , respectively. Overall, the first phase testing results concluded that the freezing

temperature gradients coupled with physico-chemical interactions (solids mineralogy and pore water chemistry) can significantly impact the efficacy of the freeze-thaw processes.

### ***7.1.2 Effects of Seasonal Weathering on Dewatering and Strength of Oil Sands Tailings Deposit***

The effects of seasonal weathering on dewatering and strength were investigated by performing five alternating cycles of freeze-thaw and drying-wetting on the polymer amended treated tailings samples (centrifuged tailings and in-line thickened tailing). In other words, this phase of testing (named as second phase testing in this research study) closely resembles the sequences of nature. The effects of seasonal weathering on dewatering and strength performance were evaluated based on a few parameters such as: freezing temperature gradient and physico-chemical interactions to validate the first phase testing results (as summarized in section 7.1.1), number of seasonal cycles and the effects of wetting/rainfall.

Similar to the first phase testing (as illustrated in section 7.1.1), the centrifuged tailings sample subjected to a lower temperature gradient ( $0.028^{\circ}\text{C}/\text{mm}$ ) contributed to an overall lower water content and higher gain in shear strength. The sample with lower temperature gradient at the end of five seasonal cycles resulted in nearly two-fold lower surficial water contents (12.2% by weight) compared to the other two temperature gradient samples (24 and 20.5% by weight for the samples at temperature gradients of 0.083 and  $0.056^{\circ}\text{C}/\text{mm}$ , respectively). As all these three samples exceeded the plastic limit (26%) at the surface, the associated surficial strength was either close to (for higher temperature gradient sample) or already exceeded (for the samples under temperature gradients of 0.056 and  $0.028^{\circ}\text{C}/\text{mm}$ ) 100 kPa (at plastic limit, the tailings has an undrained shear strength of about 100 kPa, as documented in OSTC and COSIA (2012)). Due to the inability of the vane to measure shear strength beyond 100 kPa, the gain in shear strength was compared by the number of cycles each sample took to reach towards plastic limit. The surficial shear strength at the temperature gradient of 0.028 and  $0.056^{\circ}\text{C}/\text{mm}$  exceeded 100 kPa at its fourth and fifth drying cycle, respectively, while it took seven cycles for the higher gradient sample ( $0.083^{\circ}\text{C}/\text{mm}$ ) to achieve around 90 kPa. In addition to this, the formation of a distinguishable desiccated crust layer at the surface confirmed the efficacy of lower temperature gradients on enhanced dewatering

and strength performance. The other two samples at relatively higher gradients were unable to create a desiccated crust at the surface, albeit both samples exceeded plastic limit.

The number of seasonal cycles was found as one of the predominant parameters in this research which has not been investigated much previously. Both the results from the first and second phase testing suggested that the volume changes subsequent to freeze-thaw process was highest in its first cycle and decreased afterwards with subsequent cycles. However, this statement is only implied for the subsequent freeze-thaw cycles as the subsequent drying cycles always contribute to an enhanced dewatering and strength gain. The laboratory testing results also suggested that approximately five seasonal cycles would be adequate to meet a threshold strength ( $>80$  kPa) when water content approached to the plastic limit. These threshold values were confirmed through the wetting behaviour when strength reduction due to rainfall became insignificant.

The effects of rainfall/wetting in increasing the water content or reducing the shear strength was found insignificant at a very low water content (exceeding plastic limit) along with a possibly higher suction. Hence, an increase in number of seasonal cycles is paramount to reach this phase where the contribution of rainfall would not create any significant impact on shear strength reduction. Among two different treated tailings samples (centrifuged tailings at three different temperature gradients and ILTT at a temperature gradient of  $0.028^{\circ}\text{C}/\text{mm}$ ), centrifuged tailings subjected to a lower temperature gradient ( $0.028^{\circ}\text{C}/\text{mm}$ ) was found to be less affected by the rainfall at the higher seasonal cycles, as compared to the ILTT and centrifuged tailings samples at other temperature gradients.

Similar to the first phase testing, the differences in treatment process, solids mineralogy and pore water chemistry led to the changes in dewatering and strength performance between centrifuged tailings and ILTT samples under similar boundary conditions (similar freezing temperature gradient and similar evaporative drying conditions). Centrifuged tailings sample under identical lower temperature gradient ( $0.028^{\circ}\text{C}/\text{mm}$ ) resulted in two-fold lower surficial water content compared to the ILTT sample. When compared to the strength performance, the surficial shear strength for these two samples were comparable as both these tailings achieved a stiff consistency with a surficial shear strength exceeding at least 80 kPa. However, a desiccated and over-

consolidated thin crust layer was developed on a homogeneous underlying centrifuged tailings which was non-existent in ILTT sample subjected to five cycles of seasonal weathering. Overall, the testing results from this study suggested that the increase in seasonal cycles has a potential to transform the soft tailings surface to a solid state, passing through the liquid and plastic limit.

### ***7.1.3 Seasonal Weathering of Oil Sands Tailings Deposit: Comparison of Field and Laboratory Data***

The small-scale laboratory developed methodology (as discussed in Chapter 2 and 3) was evaluated in this research program to investigate whether these laboratory testing could capture what was observed in the field. Seasonal weathering was employed in Syncrude's pilot scale ILTT field deposit, where actual evaporation coupled with freeze-thaw were found to be the predominant dewatering mechanism covering almost three quarters of total dewatering (OKC, 2015). Hence, dewatering (measured by water content) and strength performance in conjunction with salt migration (measured through EC) of the field deposit have been compared with the laboratory testing undergoing seasonal weathering dominated by 1. freeze-thaw cycles and 2. through alternating freeze-thaw and drying-wetting cycles. Although the depth, scale and boundary conditions (controlled laboratory versus uncontrolled field boundary conditions) between field deposit and laboratory simulations were substantially different, the results of the investigated ILTT tailings suggested that the laboratory testing approach was able to bound the field water contents, provided the thermal gradients were kept in the similar range. The water content of the ILTT sample subjected to five freeze-thaw cycles (with no evaporation) reduced by 44% from its initial value. When compared to the field deposit, the average water contents (at a depth from 25 cm to 1.4 m just below the crust) of the underlying tailings from the three different testhole locations TH-03, TH-05 and TH-SB experienced a reduction of about 25.5, 35 and 45%, respectively, from their initial values. During the 5<sup>th</sup> seasonal cycles upon deposition, frost penetrated to a depth of approximately 1.4 m in the field. In addition to this, the absence of deeper surface cracks (less than 5 cm deep) minimized the contribution of evaporation/atmospheric drying at a greater depth from the surface (OKC, 2015). Therefore, freeze-thaw process can be considered as the predominant dewatering mechanism for the underlying softer tailings below the surface crust till a depth of 1.4 m.

When compared to the surficial water contents where evaporation along with freeze-thaw facilitated dewatering, the water contents of the ILTT samples obtained from the small-scale laboratory testing, and field testhole locations TH-03, TH-05 and TH-SB reduced by 79, 96, 89 and 86%, respectively, from their initial values (water contents varying from 120 to 155%) after five seasonal cycles. Hence, the area bounded by a lower limit of water content (representing the worst scenario of seasonal weathering with no evaporation/drying) and an upper limit of water content (representing the combined effects of freeze-thaw-drying) under the controlled laboratory conditions with similar ranges in temperature gradients were found to predict the field water content values.

After five seasonal cycles, a 15 to 20 cm thick crust was formed at the surface of the field deposit, thereby, suggesting a surficial shear strength of over 100 kPa (although the field value was not reported). Although any distinguishable desiccated crust was not formed, the laboratory sample achieved an undrained shear strength of over 80 kPa at the surface with an associated water content of 26% exceeding plastic limit of the sample.

When comparing between field and laboratory results as a function of salt migration (through the measurement of EC values), the laboratory EC values were found gradually increasing with an increase in seasonal cycles, whereas the opposite trend was observed in the field deposit. Five seasonal cycles in the laboratory resulted in two-fold higher EC values compared to the initial, while the field EC values either remained unchanged or decreased (reduced to half) compared to their initial values. The decrease in field EC values/ solute concentration was attributed to the gradual disappearance of the white coated salt crusts due to the weathering of the deposit surface and precipitates/salt runoff from the surface (BGC and OKC, 2014; OKC, 2017). Despite the presence of snow covers and surface weathering affecting the seasonal weathering process in the field, the laboratory testing can provide insights to predicting field behaviour if the boundary conditions can be closely captured.

#### ***7.1.4 Natural Weathering as a Surface Crusting Tool for Tailings Management***

Seasonal weathering has been employed in different mine tailings across the world in order to increase the surface strength to support the reclamation activities for mine closure. However, the success of the environmental dewatering process as a crusting tool depends largely on the types, particle sizes of tailings and climatic factors including geological origin, weather and site conditions. Seasonal weathering (Atmospheric drying and freeze-thaw process) contributes to dewatering by facilitating shrinkage, frost induced cracks (from freeze-thaw process) and desiccation cracks (from evaporation) that propagate more easily through coarser tailings (Morris et al., 1992) compared to the fine tailings. Consequently, oil sands tailings management employing seasonal weathering proved to be the most challenging compared to the other mine tailings (gold, metal) because of their fine-grained particle size, extremely slow consolidation and hydraulic conductivities. When comparing shear strengths and dewatering as a function of particle size distribution/mineralogy under the similar atmospheric conditions (semi arid zone in Australia), the fine-grained tailings deposits (coal tailings) were subjected to lower strength gain as compared to the coarser tailings (metal tailings which is predominantly composed of sand and silt sized particles) deposits. The findings from the research conducted by Williams et al. (2015) and Williams and King (2016) suggested that the coal tailings deposits at New Acland Coal Mine and Ulan Coal Mine in Australia, prior to capping, achieved nearly half to an order of magnitude lower surficial strength compared to the mine tailings deposit from Cannington Metal Mine (silver, lead and zinc) subjected to seasonal weathering.

When comparing shear strength and dewatering improvement as a function of climatic factors, the tailings deposits located in the semi-arid/arid climate zone having longer summer period will undeniably experience higher dewatering and strength improvement than the colder/Arctic climate zone having shorter summer period. Hence, fine-grained tailings like oil sands tailings deposits in Western Canada subjected to atmospheric drying are expected to go through higher challenges because of their material properties combined with the colder climate and shorter drying period. Overall, an adaptive tailings management approach considering site characteristics and tailings properties can ensure the desired improvement in dewatering and strength.

#### ***7.1.5 Modeling the Effects of Seasonal Weathering on Centrifuged Oil Sands Tailings***

A coupled modeling analysis was developed in this research program to simulate the dewatering of centrifuged tailings subjected to seasonal weathering under controlled laboratory testing program (as documented in Chapter 2 and 3). Here, both of the first and second phase laboratory experiments performed on centrifuged tailings were simulated under two temperature gradients (0.083 and 0.028°C/mm) to validate the numerical approach. An integrated modeling software incorporating all the components of seasonal weathering (freeze-thaw, consolidation, evaporation and desiccation) is not commercially available at present. Hence, a coupled model approach was developed, where FSConsol software simulating consolidation and UNSATCON software simulating evaporation and desiccation were combined. In addition to this, thaw strain during freeze-thaw cycle was calculated externally and applied into the FSConsol software to simulate freeze-thaw process coupled with consolidation.

The coupling analysis to simulate the first phase testing (simulating five consecutive freeze-thaw cycles followed by a single cycle of drying-wetting-re-drying after wetting) predicted that by the fifth freeze-thaw cycles, nearly half of the water reduced for both of the high and low temperature gradient samples. When drying/evaporation was incorporated, both these samples further dewatered to two-fold lower water content for the higher gradient sample and five-fold lower water content for the lower gradient sample, as compared to the initial value. When compared with the laboratory first phase testing results, the higher temperature gradient sample (0.083°C/mm) overall overpredicted water content values by almost 3% at the end of the test. The lowest water content was observed at the surface similar to the laboratory results but with an 8% underprediction of the value. Similarly, when compared to the lower temperature gradient sample (0.028°C/mm), the numerical model overall underpredicted water content values by 1.5% throughout the depth and over predicted this value by about 3% at the surface compared to the laboratory measurement.

The numerical model to simulate the second phase testing (five alternating freeze-thaw and drying-wetting cycles) excluded the wetting event and re-drying cycle after wetting for simplicity. Hence, the coupled analysis was expected to predict higher water content compared to the laboratory results, although the water balance prior to wetting and post-wetting drying phase in the laboratory remained equal for the higher temperature gradient sample. After five alternate freeze-thaw and drying cycles, the results from the numerical model predicted that the samples with higher

(0.083°C /mm) and lower temperature gradients (0.028°C /mm) dewatered to nearly four-fold and six-fold lower water contents, respectively, at the surface when compared to the initial water content value. When compared with the second phase testing results, the model overall overpredicted water content values by about 10 and 5% for the higher and lower temperature gradient samples, respectively, as compared to the laboratory results. On the contrary, the surficial water content values were found comparable, as the model overpredicted water content by almost 1 and 4% for the higher (0.083°C /mm) and lower (0.028°C /mm) temperature gradient samples, respectively.

Figures 10.1 and 10.2 show the correlation between the laboratory and model predicted water content values of the centrifuged tailings subjected to temperature gradients of 0.083°C /mm and 0.028°C /mm, respectively.

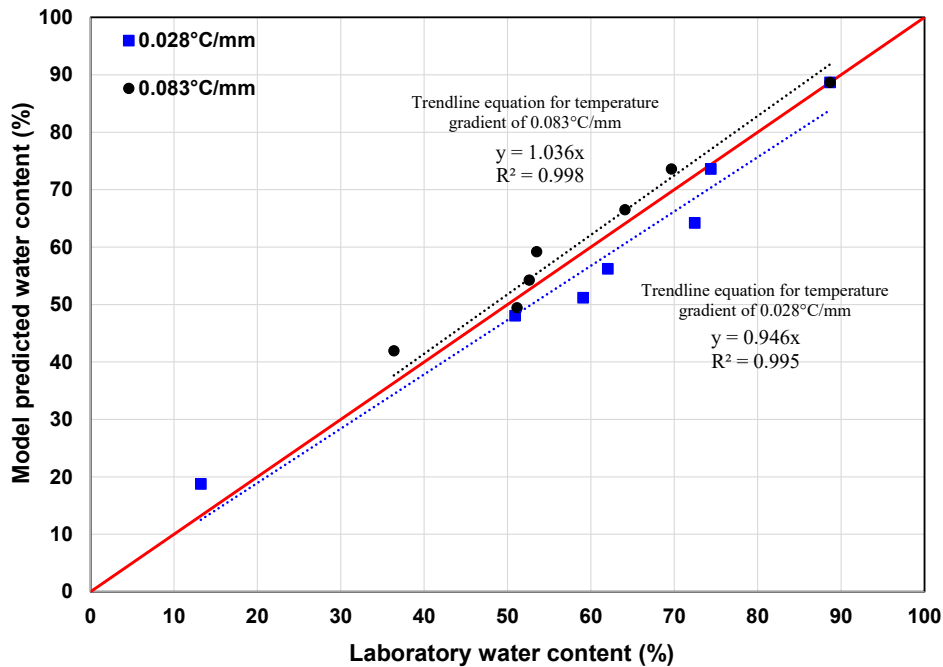


Figure 10.1: First phase testing results- correlation between laboratory and model predicted water content values

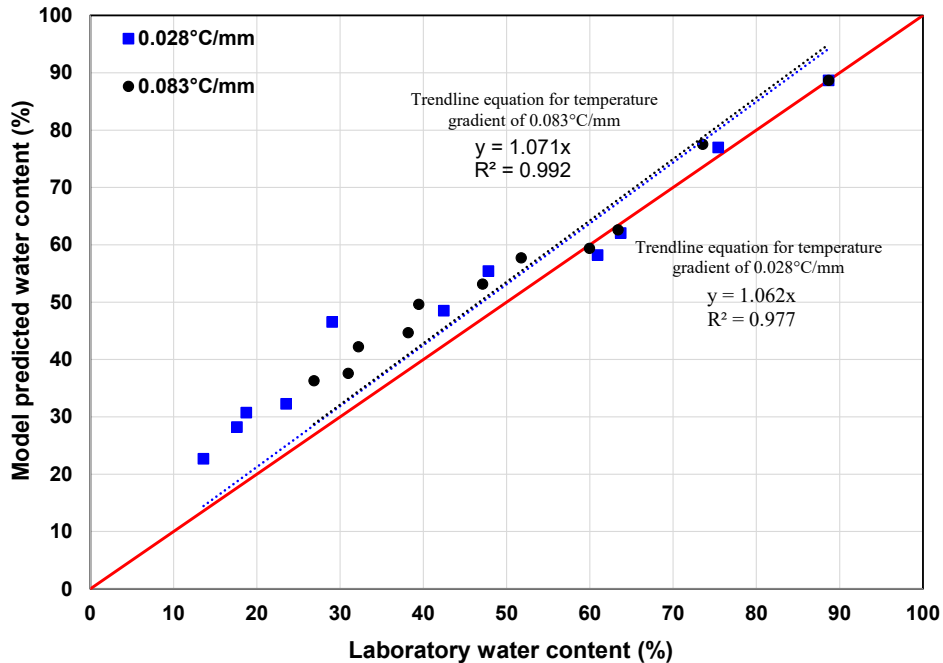


Figure 10.2: Second phase testing results- correlation between laboratory and model predicted water content values

Each of the data point shown in these two figures represents the average water content values obtained from each cycle and the red line represent  $y = x$  line. The best linear fit for each of the samples demonstrates that the coupling modeling approach corroborates pretty well with the laboratory values and has its utility in oil sands dewatering to simulate the attenuation of water content with multiple seasonal cycles.

Similar to the laboratory testing, the coupling model also suggested that the lower temperature gradient overall resulted in higher dewatering compared to the higher gradient sample. The numerical approach to simulate the first and second phase experiments on lower temperature gradient samples predicted that the water content of these samples were able to pass through the plastic limit. In contrast to that, the sample at the higher gradient was found having a liquid/soft consistency in the first phase testing, while the water content of the sample surface almost reached to the plastic limit in the second phase of testing. Although the coupled model could not explicitly predict the bottom few centimeters of the sample due to the limitations of defining a few of the

input parameters as a profile varying with depth, this approach can still provide insights to predicting short term behaviour of the dewatering performance of the future deposits.

## 7.2 Conclusions

From the current research, the following conclusion can be made contributing to the existing knowledge:

- Freeze-thaw process has a significant effect on polymer amended treated tailings properties which enhanced the post-thaw dewatering process. Among different parameters, freezing temperature gradient, freeze-thaw cycles and the effects of physico-chemical interactions (solids mineralogy and pore water chemistry) contributed predominantly to improving the dewatering and strength performances.
- Freeze-thaw process may seem to achieve lower dewatering enhancement compared to atmospheric drying, the shrinkage and/or cracks developed during the freeze-thaw cycles facilitate greater evaporation and desiccation during the subsequent drying cycle, thereby, contributing to overall higher dewatering. The extent of these cracks was found to be predominantly dependent on the temperature gradient, number of freeze-thaw cycles and the physio-chemical interactions among the tailings particles and solutes. Hence, three-fold lower temperature gradient after five freeze-thaw cycles resulted in similar surficial water content (with a difference of 1% higher water content for the lower gradient one) and two times higher surficial strength (8kPa > 4 kPa) compared to its higher gradient. However, when freeze-thaw dewatering was incorporated with a cycle of drying-wetting, this three-fold lower temperature gradient resulted in over 2.5 times lower surficial water content with an associated nearly 8 times higher surficial shear strength (100 kPa > 13.7 kPa) than the higher gradient tailings. Further, five alternating freeze-thaw and drying-wetting cycles representing nature reduced surficial water content by half for three-fold lower temperature gradient tailings with an associated half an order of magnitude higher surficial strength (110 kPa > 35.5 kPa), as compared to the higher gradient one.
- Freeze-thaw dewatering coupled with evaporation increased the surficial strength of the tailings by an order of magnitude higher than the multiple freeze-thaw cycles one. The volume

changes (measured by thaw strain) subsequent to freeze -thaw was always found higher in its first cycle and decreased further with subsequent cycles due to the gradual reduction in available water in tailings. Subsequent cycles had lower impact on volume changes due to freeze-thaw dewatering, not on evaporation/drying. Evaporation/atmospheric drying under similar controlled laboratory boundary conditions contributed to a reduction in water content varying from 4-14% per cycle. The variations in volume changes due to evaporation per cycle were attributed largely to the freezing induced shrinkage and cracks formed in the previous freeze-thaw cycles, thereby, facilitating greater surface area for evaporation.

- The increase in seasonal cycles has a potential to transform the slurry like surface into a desiccated one, regardless of the variations in solids mineralogy, and water chemistry. The polymer amended treated tailings investigated in this research required approximately five seasonal cycles to meet a threshold strength (>80 kPa) when moisture content approaches to the plastic limit. These threshold values were confirmed through the wetting behaviour when strength reduction due to rainfall became insignificant due to very high solids content with a possibly higher suction.

- The effects of physico-chemical interactions (solids mineralogy and pore water chemistry) in dewatering and strength improvement were compared between centrifuged and ILTT tailings. The difference in treatment process (addition of gypsum as a coagulant), solids mineralogy (lower clay content) and pore water chemistry (presence of marginally higher divalent cations and lower SAR value) led centrifuged tailings to contribute to an improved dewatering and strength performance compared to the ILTT under similar laboratory boundary conditions. Multiple freeze-thaw cycles coupled with evaporation resulted in nearly two-fold higher surficial strength (100 kPa vs 60 kPa) for centrifuged tailings compared to ILTT under similar temperature gradient (0.028°C/mm). Furthermore, after five alternate freeze-thaw and drying-wetting cycles, centrifuged tailings sample under similar boundary conditions resulted in two-fold lower surficial water content compared to the ILTT sample. When compared to the strength performance, the surficial shear strength for these two samples were comparable (>100 kPa for centrifuged tailings versus 84 kPa for ILTT) as both these tailings achieved a stiff consistency with a surficial shear

strength exceeding at least 80 kPa. However, a desiccated and over-consolidated thin crust layer was developed at the surface of centrifuged tailings which was non-existent in ILTT sample.

- Upward salt migration mechanism during freeze–thaw was found one of the contributing factors for an increase in ion concentration at the surface. Salt/ion migration additionally facilitated the osmotic suction component that, overall, increased the total suction. Increasing suction during freezing is responsible for attracting unfrozen water towards the freezing zone and overall dewatering. Centrifuged tailings subjected to multiple freeze-thaw cycles resulted in nearly six times higher EC compared to ILTT under similar boundary conditions. The results also suggest that the combined mechanism of volume changes due to freeze–thaw consolidation, osmotic consolidation and osmotically induced consolidation may have possibly contributed to the higher dewatering for centrifuged tailings compared to the ILTT dewatering dominated by the freeze–thaw mechanism only. Furthermore, the water migration along with salt was found, to an extent, influenced by the temperature gradient. A three-fold lower freezing temperature gradient resulted in 1.5 times higher EC values, thus, correlating physico-chemical interactions with dewatering performance being dominated by freezing temperature gradients.

- Laboratory testing approach was able to bound the expected field response, given the thermal gradients were in the similar range. However, the undrained shear strength gain in the field can be largely impacted by the snow covers in winter and surface weathering in summer preventing further propagation of cracks formed at the surface. It is worth mentioning that the formation of surface crust does not ensure a trafficable surface if the depth of the crust is limited and the underlying tailings below the crust are remained too soft. Also, the surface crust that is formed at the surface can be quickly lost once re-wetted. Hence, water management or control of ponded water is paramount in order to fully utilize the benefits of seasonal weathering.

- Laboratory testing results were able to validate the proposed coupled model. The coupled modeling analysis demonstrated the ability to simulate the coupled processes of freeze-thaw, consolidation, evaporation and desiccation. Thus, it can be used in tailings management in the oil sands industry to predict the short-term field response in terms of dewatering. Based on the model

prediction, different scenarios incorporating the sequences of freeze-thaw and evaporation can be maximized in the field.

### **7.3 Recommendations**

- The repeatability and reproducibility could not be employed in this research program due to the limited resources and longer time frames of each experiment. Hence, replicate measurements are recommended for future study.
- Seasonal dewatering was found to increase the strength of the small lab samples under controlled laboratory conditions, but further work is needed to evaluate how deep this seasonal weathering will influence tailings under actual field conditions.
- Further testing should be conducted under large-scale testing setup to validate the reproducibility of these small-scale testing.
- The suction was not measured in this study. It is recommended to measure the suction in order to correlate this with the threshold water content and strength values at which the effects of rainfall will become insignificant on dewatering performance.
- Scanning electron microscope (SEM) is recommended to analyze the changes in microstructure of the samples after each freeze-thaw/ drying -wetting cycle.
- To predict the effects of seasonal weathering on long term dewatering and strength behaviour of the field deposit, the results of the laboratory results are recommended to use in calibrating the thermal properties. Based on the thermal properties, a thermal model should be developed simulating the field conditions.
- An integrated model simulating all the natural dewatering processes (freeze-thaw, consolidation and evaporation) needs to be developed for the different deposition scenarios including multi-layered thin deposit and deep deposits.

## References

- Agarwal, S. 2002. *Efficiency of Shear-Induced Agglomeration of Particulate Suspensions Subjected to Bridging Flocculation*, Ph.D. Thesis, West Virginia University, West Virginia, USA.
- Alberta Energy Regulator (AER). 2016. *Alberta's Energy Reserves 2015 & Supply/Demand Outlook 2016-2025 (ST98-2016)*, Alberta Energy Regulator, Calgary, Alberta.
- Alberta Energy Regulator (AER). 2018 *State of Fluid Tailings Management for Mineable Oil Sands, 2017*. Report, Calgary, Alberta. Available online: [https://static1.squarespace.com/static/52abb9b9e4b0cb06a591754d/t/5bcbdb777817f7df5097c309/1540086655594/Mineable\\_Oil\\_Sands\\_Fluid\\_Tailings\\_Status\\_Rpt\\_2017\\_Sept.28\\_Final.pdf](https://static1.squarespace.com/static/52abb9b9e4b0cb06a591754d/t/5bcbdb777817f7df5097c309/1540086655594/Mineable_Oil_Sands_Fluid_Tailings_Status_Rpt_2017_Sept.28_Final.pdf) (accessed 25/08/2021).
- Alberta Energy Regulator (AER). 2020 *State of Fluid Tailings Management for Mineable Oil Sands, 2019*. Report, Calgary, Alberta. Available online: <https://static.aer.ca/prd/2020-09/2019-State-Fluid-Tailings-Management-Mineable-OilSands.pdf> (accessed 31/07/2021).
- Amoako, K.A. 2020. *Geotechnical Behaviour of Two Novel Polymer Treatments of Oil Sands Fine Tailings*. M.Sc. Thesis, Department of Civil and Environmental Engineering, University of Alberta, Edmonton, AB, Canada.
- Andersland, O.B. and Ladanyi, B. 2004. *Frozen Ground Engineering*, 2nd Edition, American Society of Civil Engineers & John Wiley & Sons Inc., Hoboken, New Jersey, USA.
- ASTM. 2014. Standard Test Methods for Electrical Conductivity and Resistivity of Water. *ASTM Standard D1125-14*. ASTM International, West Conshohocken, PA, 2014. DOI: 10.1520/D1125-14.
- ASTM. 2014. Standard Test Methods for Specific Gravity of Soil Solids by Water Pycnometer. *ASTM Standard D854-14*. ASTM International, West Conshohocken, PA, 2014. DOI: 10.1520/D0854-14.
- ASTM. 2016. Standard Test Methods for Laboratory Miniature Vane Shear Test for Saturated Fine-Grained Clayey Soil. *ASTM Standard D4648/ D4648M-16*. ASTM International, West Conshohocken, PA, 2016. DOI: 10.1520/D4648\_D4648M-16.

- ASTM. 2017. Standard Test Method for Anions in Water by Suppressed Ion Chromatography. *ASTM Standard D4327-17*. ASTM International, West Conshohocken, PA, 2017. DOI: 10.1520/D4327-17
- ASTM. 2017. Standard Test Methods for Liquid Limit, Plastic Limit, and Plasticity Index of Soils. *ASTM Standard D4318-17e1*. ASTM International, West Conshohocken, PA, 2017. DOI: 10.1520/D4318-17E01.
- ASTM. 2017. Standard Test Methods for Particle Size Distribution (Gradation) of Fine-Grained Soils Using the Sedimentation (Hydrometer) Analysis. *ASTM Standard D7928-17*. DOI: 10.1520/D7928-17.
- ASTM. 2019. Standard Test Methods for Laboratory Determination of Water (Moisture) Content of Soil and Rock by Mass. *ASTM D2216-19*. ASTM International, West Conshohocken, PA, 2019. DOI: 10.1520/D2216-19.
- ASTM. 2019. Standard Test Method for Methylene Blue Index of Clay. *ASTM C837-09*. ASTM International, West Conshohocken, PA, 2019. DOI: 10.1520/C0837-09R19.
- ASTM. 2019. Standard Test Methods for pH of Soils. *ASTM D4972-19*. ASTM International, West Conshohocken, PA, 2019. DOI: 10.1520/D4972-19.
- Baker, T. 1976. Transportation, Preparation, and Storage of Freezing Soil Samples for Laboratory Testing, in Sangrey, D., and Mitchell, R. (Eds.), *Soil Specimen Preparation for Laboratory Testing*. ASTM STP 599, ASTM International, West Conshohocken, PA, pp. 88-112. <https://doi.org/10.1520/STP39077S>.
- Barbour, S.L. and Fredlund, D.G. 1989. Mechanism of osmotic flow and volume change in clay soils. *Canadian Geotechnical Journal*, 26 (4):551-562. <https://doi.org/10.1139/t89-068>.
- Barr Engineering Co. (Barr) and O’Kane Consultants (OKC). 2016. *Atmospheric Fines Dryng (AFD) Deposition Optimization: Multi-lift versus Deep Stacking*. Final Report prepared for Shell Canada Energy, Calgary, AB, Canada.
- Bale, B.J.R. 2007. *Freeze Thaw Dewatering of Oil Sands Tailings as Part of a Natural Remediation Strategy*, M.Sc. Thesis, University of Alberta, Edmonton, Canada.
- Beier, N. A and Segó, D.C. 2009. Cyclic Freeze-Thaw to Enhance the Stability of Coal Tailings. *Cold Regions Science and Technology*, 55 (3): 278-285. Doi: 10.1016/j.coldregions.2008.08.006.

- Beier, N. A., Wilson, W., Dunmola, A., & Sege, D., 2013. Impact of flocculation-based dewatering on the shear strength of oil sands fine tailings. *Canadian Geotechnical Journal*, 50 (9):1001-1007. <https://doi.org/10.1139/cgj-2012-0262>.
- Beier, N., Kabwe, L.K., Scott, J.D., Pham, N.H., and Wilson, G.W. 2016. Modeling the effect of flocculation and desiccation on oil sands tailings. *Geo-Chicago*, Chicago, Illinois, USA, August 14-18, 2016.
- BGC Engineering Inc. 2010. *Oil Sands Tailings Technology Review*. Oil Sands Research and Information Network, University of Alberta, School of Energy and the Environment, Edmonton, Alberta, Canada.
- BGC Engineering Inc. (BGC) and O’Kane Consultants Inc. (OKC). 2014. *Perimeter Ditch Pilot 1 Trial, 2013 Performance Monitoring Update*, Report prepared for Syncrude Canada Ltd., AB, Canada.
- Bing, H., He, P. and Zhang, Y. 2015. Cyclic Freeze-Thaw as a Mechanism for Water and Salt Migration in Soil. *Environmental Earth Sciences*, 74 (1): 675-681. <https://doi.org/10.1007/s12665-015-4072-9>.
- Boratynec, D.J. 2003. Fundamentals of rapid dewatering of composite tailings. MSc Thesis, University of Alberta, Edmonton, AB, Canada.
- Bronswijk, J.J.B. 1988. Modelling of water balance, cracking and subsidence of clay soils, *Journal of Hydrology*, 97: 199-212.
- Bussière, B. 2007. Colloquium 2004: Hydrogeotechnical properties of hard rock tailings from metal mines and emerging geoenvironmental disposal approaches. *Canadian Geotechnical Journal*. 44(9), 1019-1052.
- CanmetENERGY, 2009. *Rim ditch dewatering pilot test*. Division Report, Devon 09-80, Alberta.
- Chalaturnyk, R.J., Scott, J., and Özüm, B. 2002. Management of oil sands tailings. *Petroleum Science and Technology*, 20 (9-10): 1025-1046.
- Chamberlain, E.J. 1981. Overconsolidation effects of ground freezing, *Engineering Geology*, 18 (1-4): 97-110. doi:10.1016/0013-7952(81)90050-8.
- Chorom, M. and Rengasamy, P. 1995. Dispersion and zeta potential of pure clays as related to net particle charge under varying pH, electrolyte concentration and cation type. *European Journal of Soil Science*, 46 (4): 657-665.

- Consortium of Oil Sands Tailings Management Consultant (CTMC), 2012. *Oil Sands Tailings Technology Deployment Roadmap*. Project Report, Volume 2, Calgary, Alberta.
- Cossey, H.L., Batycky, A.E., Kaminsky, H., and Ulrich, A.C. 2021. Geochemical Stability of Oil Sands Tailings in Mine Closure Landforms. *Minerals* 2021, 11 (8):830.
- Cowie, B.R., James, B., and Mayer, B. 2105. Distribution of total dissolved solids in McMurray Formation water in the Athabasca oil sands region, Alberta, Canada: Implications for regional hydrogeology and resource development, *AAPG Bulletin*, 99(1): 77-90.
- Darrow, M.M., Guo,R. and Trainor, T.P. 2020. Zeta potential of cation treated soils and its implication on unfrozen water mobility. *Cold Regions Science and Technology*, 173:103029. doi: 10.1016/j.coldregions.2020.103029.
- Das, B.M. 1983. *Advanced Soil Mechanics*. Hemisphere Publishing Corp., New York, NY, USA.
- Dawson, R.F. and Seg0, D.C. 1993. Design Concepts for Thin Layered Freeze-Thaw Dewatering Systems, *Proceedings of the 46th Canadian Geotechnical Conference*, Saskatoon, SK, Canada: 283-288.
- Dawson, R.F., Seg0, D.C., and Pollock, G.W. 1999. Freeze-thaw dewatering of oil sands fine tails. *Canadian Geotechnical Journal*, 36: 587-598. DOI: 10.1139/t99-028.
- Dunmola, A. and Simms, P. 2010. Solute mass transport and atmospheric drying of high density gold tailings. *Proceedings of 13<sup>th</sup> International Seminar on paste and Thickened Tailings*, Toronto, ON, Canada.
- Dunmola, A., Cote, C., Freeman, G., Kolstad, D., Song, J., and Masala, S. 2013. Dewatering and shear strength performance of in-line flocculated mature fine tailings under different depositional schemes. *Proceedings of Tailings and Mine Waste 2013*, Banff, AB, Canada.pp.5-14.
- Eigenbrod, K.D. 1996. Effects of cyclic freezing and thawing on volume changes and permeabilities of soft fine-grained soils, *Canadian Geotechnical Journal*, 33(4): 529-537.
- Fisseha, B., Bryan, R., & Simms, P. 2010. Evaporation, unsaturated flow, and salt accumulation in multilayer deposits of “paste” gold tailings. *Journal of geotechnical and geoenvironmental engineering*. 136(12), 1703-1712.
- Fujiyasu, Y. and Fahey, M. 2000. Experimental study of evaporation from saline tailings. *Journal of Geotechnical and Geoenvironmental Engineering*, 126 (10): 18-27.

- Gibson, R., England, G., and Hussey, M. 1967. The theory of one-dimensional consolidation of saturated clays. *Geotechnique*, 17: 261-273.
- Government of Alberta. 2021a. *Oil Sands: Facts and Stats. 2021*. Available online: <https://www.alberta.ca/oil-sands-facts-and-statistics.aspx> (accessed on 1st October 2021).
- Government of Alberta. 2021b. Oil Sands Information Portal. Available online: <http://osip.alberta.ca/map/> (Accessed on 1st October, 2021).
- Government of Canada. 1981-2010 Canadian Climate Normal station data for Fort McMurray. [https://climate.weather.gc.ca/climate\\_normals/results\\_1981\\_2010\\_e.html?stnID=2519&autofwd=1](https://climate.weather.gc.ca/climate_normals/results_1981_2010_e.html?stnID=2519&autofwd=1) (accessed 13<sup>th</sup> January, 2021).
- Han, Z., and Vanapalli, S.K. 2016. Stiffness and shear strength of unsaturated soils in relation to soil- water characteristic curve. *Geotechnique*, 66 (8): 627-647. <https://doi.org/10.1680/jgeot.15.P.104>.
- Heidarian, P. 2012. *Effect of Initial Water Content and Stress History Water-Retention Behaviour of Mine Tailings*. Ph.D. Thesis, Carleton University, Ottawa, ON, Canada.
- Hendershot, W.H., Lalonde, H. and Duquette, M. 2008. Ion exchange and exchangeable cations, in: Carter, M.R. and Gregorich, E.G., ed. *Soil Sampling and Methods of Analysis*, 2nd edition, Canadian Society of Soil Science, CRC Press, Boca Raton, FL, pp. 197-206.
- Hen-Jones, R.M., Hughes, P.N., Stirling, R.A., Glendinning, S., Chambers, J.E., Gunn, D.A., and Cui, Y.J. 2017. Seasonal effects on geophysical–geotechnical relationships and their implications for electrical resistivity tomography monitoring of slopes. *Acta Geotechnica*, 12: 1159-1173. <https://doi.org/10.1007/s11440-017-0523-7>.
- Henry, H. 2007. Soil freeze–thaw cycle experiments: Trends, methodological weaknesses and suggested improvements, *Soil Biology and Biochemistry*, 39: 977-986. Doi: 10.1016/j.soilbio.2006.11.017.
- Hobbs, P. 1974. *Ice Physics*, Oxford, UK: Clarendon Press.
- Hogg, R. 2000. Flocculation and Dewatering. *International Journal of Mineral Processing*, 58 (1-4): 223-236.
- Hurtado, O. 2018. *Desiccation and Consolidation in Centrifuge Cake Oil Sands Tailings*, M.Sc. Thesis, Carleton University, Ottawa, Ontario, Canada.

- Hyndman, A., Sawatsky, L., McKenna, G. and Vandenberg, J. 2018. Fluid Fine Tailings Processes: Disposal, Capping, and Closure Alternatives. In *Proceeding of the 6th International Oil Sands Tailings Conference*, Edmonton, Alberta, Canada. pp. 9-12.
- Innocent-Bernard, T. 2013. *Evaporation, Cracking, and Salinity in a Thickened Oil Sands Tailings*, M.A.Sc. Thesis, Department of Civil and Environmental Engineering, Carleton University, Ottawa, ON, Canada.
- Jeeravipoolvarn, S. 2005. *Compression Behaviour of Thixotropic Oil Sands Tailings*. M.Sc. Thesis, University of Alberta, Edmonton, AB, Canada.
- Jeeravipoolvarn, S., Scott, J.D., and Chalaturnyk, R.J. 2009. Multi-dimensional Finite Strain Consolidation Theory: Modeling Study. In *Proceedings of the 61st Canadian Geotechnical Conference*, Edmonton, AB, Canada, 22–24 September 2008.
- Jeeravipoolvarn, S. 2010. *Geotechnical Behavior of In-Line Thickened Oil Sands Tailings*. PhD Thesis, University of Alberta, Edmonton, AB, Canada.
- Johnson, R.L., Pork, P., Allen E.A.D., James, W.H. and Koverny, L. 1993. *Oil Sands Sludge Dewatering by Freeze-Thaw and Evaporation*, Report-RRTAC 93-8, Alberta Conservation and Reclamation Council, AB, Canada.
- Kabwe, L.K, Wilson, G.W., Beier, N.A., and Scott, J.D. 2017. Effects of Atmospheric Drying and Consolidation of Flocculated Thickened Tailings and Centrifuged Cake on Near-Surface Shear Strength. *Second Pan-American Conference on Unsaturated Soils*, November 12-15, 2017, Dallas, Texas. <https://doi.org/10.1061/9780784481684.029>
- Kaminsky, H. 2008. *Characterization of an Athabasca Oil Sands Ore and Process Streams*. Ph.D. Thesis, University of Alberta, Edmonton, AB, Canada.
- King, A.P. and Naidus, H. 1969. The Relationship between Emulsion Freeze-Thaw Stability and Polymer Glass Transition Temperature. 1A Study of the Polymers and Copolymers of Methyl Methacrylate and Ethyl Acrylate, *Journal of Polymer Science*, Part C, 27 (1):311-319.
- Knutsson, R., Viklander, P. and Knutsson, S. 2016. Stability Considerations for Thickened Tailings due to Freezing and Thawing, *Proceedings of the 19th International Seminar on Paste and Thickened Tailings*, Santiago, Chile: 567-577.

- Kolstad, D., Borree, B., Song, J., and Mahood, R. 2016. Field Pilot Performance Results for Flocculated Fluid Fine Tailings under Three Depositional Variations. *International Oil Sands Tailings Conference*, Lake Louise, AB, Canada, December 4-7, 2016.
- Konrad, J. and Morgenstern, N.R. 1980. A mechanistic theory of ice lens formation in fine-grained soils. *Canadian Geotechnical Journal*, 17 (4): 473-486.
- Lahaie, R., Seto, J.T.C., Chapman, D., and Carrier III, W.D. 2010. Development of accelerated dewatering technology for managing oil sands fine fluid tailings. In *Proceedings of the 63<sup>rd</sup> Canadian Geotechnical Conference*, Calgary, AB, Canada, pp. 678-685.
- Lal, R., & Shukha, M. K. 2004. *Principles of Soil Physics*. Basel, Switzerland: Marcel Dekker, Inc.
- Locat, J. and Demers, D. 1988. Viscosity, yield stress, remolded strength, and liquidity index relationships for sensitive clays. *Canadian Geotechnical Journal*, 25 (4): 799-806. doi: 10.1139/t88-088.
- Lutenegger, A.J. 1995. Geotechnical Behavior of Over-consolidated Surficial Clay Crusts. Transportation Research Board, No. 1479, pp 61-74.
- MacKay, J.R. 1974. Reticulate ice veins in permafrost, Northern Canada, *Canadian Geotechnical Journal*, 11(2): 230-237.
- Masliyah, J., Zhou, Z.J., Xu, Z., Czarnecki, J., and Hamza, H. 2004. Understanding water-based bitumen extraction from Athabasca oil sands. *The Canadian Journal of Chemical Engineering*, 82(4): 628-654.
- McKenna, G., Mooder, B., Burton, B. and Jamieson, A. 2016. Shear strength and density of oil sands fine tailings for reclamation to a boreal forest landscape. In *proceedings of the 5<sup>th</sup> International Oil sands Tailings Conference*, Lake Louise, Alberta, 4-7 December 2016.
- McKenna, G. 2017. Soft Tailings landform Design. *Tailings and Mine waste Conference*, 2017, Banff, Canada.
- Mikula, R. J., Munoz, V. A. and Omotoso, O. 2008. Centrifuge options for production of “Dry stackable tailings” in surface mined oil sands tailings management. *Canadian International Petroleum Conference*, Calgary, AB, Canada.
- Miller, W.G., Scott, J.D., and Segó, D.C. 2010. Influence of the extraction process on the characteristics of oil sands fine tailings. *Journal of Canadian Institute of Mining, Metallurgy and Petroleum*, 1(2): 93-112.

- Mitchell, J.K. and Soga, K. 2005. *Fundamentals of Soil Behaviour*. 3rd ed., John Wiley and Sons, Inc., New York, NY, USA.
- Morris, P.H., Graham, J. and Williams, D.J. 1992. Cracking in drying soils. *Canadian Geotechnical Journal*, 29 (2): 263-277. <https://doi.org/10.1139/t92-030>.
- Mpofu, P., Addai-Mensah, J. and Ralston, J. 2003. Investigation of the effect of polymer structure type on flocculation, rheology and dewatering behaviour of kaolinite dispersions. *International Journal of Mineral Processing*, 71 (1-4): 247-268.
- Nasser, M. S. and James A.E. 2006. The effect of polyacrylamide charge density and molecular weight on the flocculation and sedimentation behaviour of kaolinite suspensions. *Separation and Purification Technology*, 52 (2): 241-252.
- Newson, T.A., and Fahey, M. 2003. Measurement of evaporation from saline tailings storages. *Engineering Geology*, 70 (3): 217-233.
- Norwest Corporation. 2018. *Fluid Fine Tailings Management Methods- An Analysis of Impacts on Mine Planning, Land, GHGs, Costs, Site Water Balances and Recycle Water Chloride Concentrations*, Report submitted to COSIA, AB, Canada. See [https://www.cosia.ca/sites/default/files/attachments/FFT%20Management%20June%2026\\_0.pdf](https://www.cosia.ca/sites/default/files/attachments/FFT%20Management%20June%2026_0.pdf) (accessed 10/05/2021).
- Oil Sands Tailings Consortium (OSTC) and Canada's Oil Sands Innovation Alliance (COSIA). 2012. *Technical Guide for Fluid Fine Tailings Management*, Report, Calgary, Alberta.
- O'Kane Consultants (OKC). 2015. *Perimeter Ditch Pilot 1 Trial 2014 Performance Monitoring Update*, Report No. 690/91-01, A Report prepared for Syncrude Canada Ltd., Calgary, AB, Canada.
- O'Kane Consultants, 2017. *Perimeter Ditch Pilot 1 Trial 2016 Performance Monitoring Update*, Report prepared for Syncrude Canada Ltd., Calgary, AB, Canada.
- Othman, M.A. and Benson, C.H. 1992. *Effect of Freeze-Thaw on the Hydraulic Conductivity of three Compacted Clays from Wisconsin*, Transportation Research Record, 1369: 118-129.
- Othman, M.A. and Benson, C.H. 1993. Effect of Freeze-Thaw on the Hydraulic Conductivity and Morphology of Compacted Clay, *Canadian Geotechnical Journal*, 30 (2): 236-246. <https://doi.org/10.1139/t93-020>.
- Oztas, T. and Fayetorbay, F. 2003. Effect of freezing and thawing processes on soil aggregate stability. *Catena*, 52 (1):1-8.

- Park, H., Lee, S.R., and Jee S.H. 2010. Bearing Capacity of Surface Footing on Soft Clay Underlying Stiff Nonhomogeneous Desiccated Crust. *International Journal of Offshore and Polar Engineering*, 20 (3): 224-232.
- Pham, N.H. and Segoo, D.C. 2014. Modeling Dewatering of Oil Sands Mature Fine Tailings using Freeze Thaw. *International Oil Sands Tailings Conference*, Lake Louise, AB, Canada, December 7-10, 2014.
- Prasanphan, S. and Nuntiya, A. 2006. Electrokinetic Properties of Kaolins, Sodium Feldspar and Quartz. *Chiang Mai Journal of Science*, 33(2): 183-190.
- Proskin, S.A. 1998. *A Geotechnical Investigation of Freeze-Thaw Dewatering of Oil Sands Fine Tailings*, PhD Thesis. Department of Civil and Environmental Engineering, University of Alberta, Edmonton, AB, Canada.
- Proskin, S., Segoo, D. and Alostaz, M. 2010. Freeze-thaw and consolidation tests on Suncor mature fine tailings (MFT). *Journal of Cold Regions Science and Technology*, 63 (3): 110-120. doi: 10.1016/j.coldregions.2010.05.007.
- Proskin, S., Segoo, D. and Alostaz, M. 2012. Oil Sands MFT Properties and Freeze-Thaw Effects, *Journal of Cold Regions Engineering*, ASCE, 26 (2): 29-54. [https://doi.org/10.1061/\(ASCE\)CR.1943-5495.0000034](https://doi.org/10.1061/(ASCE)CR.1943-5495.0000034).
- Qi, S. 2017. *Numerical Investigation for Slope Stability of Expansive Soils and Large Strain Consolidation of Soft Soils*. PhD Thesis, University of Ottawa, Ottawa, ON, Canada.
- Qi, S.; Simms, P.; Vanapalli, S. 2017. Piecewise-linear formulation of coupled large-strain consolidation and unsaturated flow. I: Model development and implementation. *Journal of Geotechnical and Geoenvironmental Engineering*, 143, 04017018. [https://doi.org/10.1061/\(ASCE\)GT.1943-5606.0001657](https://doi.org/10.1061/(ASCE)GT.1943-5606.0001657).
- Qiu, Y. 2000. *Optimum Deposition for Sub-Aerial Tailings Disposal*, Ph.D. Thesis. University of Alberta, Edmonton, Alberta, Canada.
- Rima, U.S. and Beier, N. 2018. Evaluation of Temperature and Multiple Freeze-Thaw Effects on the Strength Properties of Centrifuged Tailings. *71st Canadian Geotechnical Conference*, Edmonton, Canada, September 23-26, 2018.
- Rima, U.S and Beier N. 2021a. Effects of seasonal weathering on dewatering and strength of an oil sands tailings deposit. *Canadian Geotechnical Journal*, In press. <https://doi.org/10.1139/cgj-2020-0533>.

- Rima, U.S. and Beier, N. 2021b. Effects of multiple freeze-thaw cycles on oil sands tailings behaviour. *Cold Regions Science and Technology*, 192:103404. <https://doi.org/10.1016/j.coldregions.2021.103404>.
- Rozina, E. 2015. *Bearing Capacity of Multilayer deposited In-line Flocculated Oil Sands Tailings*, MAsc. Thesis, Department of Civil and Environmental Engineering, Carleton University, Ottawa, ON, Canada.
- Sanchez Sardon, M.A. 2013. *Combined Evaporation and Freeze-Thaw Effects in Polymer Amended Mature Fine Tailings*. MAsc. Thesis, Department of Civil and Environmental Engineering, Carleton University, Ottawa, ON, Canada.
- Scott, J.D., Dusseault, M.B. and Carrier, W.D. 1985. Behaviour of the clay/bitumen/water sludge system from oil sands extraction plants. *Applied Clay Science*, 1(1-2): 207-218. [https://doi.org/10.1016/0169-1317\(85\)90574-5](https://doi.org/10.1016/0169-1317(85)90574-5).
- Sego, D.C. 1992. *Influence of pore fluid chemistry on freeze-thaw behaviour of Suncor Oil Sand Fine tails (Phase I)*, Report, submitted to Reclamation Research Technical Advisory Committee, Alberta Environment.
- Sego, D. C. and Dawson, R.F. 1992. *Influence of freeze-thaw on behaviour of oil sand fine tails*. Alberta Oil Sands Technology and Research Authority.
- Shokouhi, A., Williams, D.J., and Kho, A.K. 2014. Settlement and collapse behavior of coal mine spoil and washery wastes. *Proceedings Tailings and Mine Waste 2014*, Keystone, Colorado, USA, 5-8th October, 2014.
- Simms, P., Dunmola, A., and Fisseha, B. 2009. Generic Productions of Drying Time in Surface Deposited Thickened Tailings in a “Wet Climate”. *Tailings and Mine Waste '09*, Banff, Canada: 749-758.
- Simms, P., Soleimani, S., Mizani, S., Daliri, F., Dunmola, A., Rozina, E., and Innocent-Bernard, T. 2017. Cracking, salinity, evaporation in mesoscale experiments on three types of tailings. *Environmental Geotechnics*, 6(1): 1-15. DOI: 10.1680/jenge.16.00026.
- Sorta, A.R., and Sego, D.C. 2010. Segregation related to use of Centrifuge in Oil Sands Tailings. *In Proceedings of the 13th International Conference on Tailings and Mine waste*, Banff, AB, Canada. pp. xvii-xli.
- Sorta, A.R., Sego, D.C., and Wilson, W. 2012. Effect of thixotropy and segregation on centrifuge modelling, *International Journal of Physical Modeling in Geotechnics*, 12 (4), 143-161.

- Sorta, A.R., Segó, D.C., and Wilson, G.W. 2013. Time domain reflectometry measurements of oil sands tailings water content: A study of influencing parameters. *Canadian Institute of Mining Metallurgy and Petroleum Journal*, 4 (2), 109-119.
- Sorta, A.R., Segó, D.C., and Wilson, W. 2016. Physical modelling of oil sands tailings consolidation. *Int. J. Phys. Model. Geotech.*, 16 (2): 47–64. <https://doi.org/10.1680/jphmg.15.00006>
- Spence, J., Bara, B., Lorentz, J. and Mikula, R. 2015. Development of the Centrifuge Process for Fluid Fine Tailings Treatment at Syncrude Canada Ltd. *In World Heavy Oil Congress 2015*, Edmonton, Alberta, 24-26 March, 2015.
- Stahl, R.P., and Segó, D.C. 1995. Freeze-thaw dewatering and structural enhancement of fine coal tails. *Journal of Cold Regions Engineering*, 9 (3), 135-151. [https://doi.org/10.1061/\(ASCE\)0887-381X\(1995\)9:3\(135\)](https://doi.org/10.1061/(ASCE)0887-381X(1995)9:3(135)).
- Standard Methods. 2017. 3125 Metals by Inductively Coupled Plasma-Mass Spectrometry. Standard Methods for the Examination of Water and Wastewater. <https://www.standardmethods.org/doi/abs/10.2105/SMWW.2882.048>.
- Stienwand, K.A. 2021. *Accelerating Polymer Degradation to Explore Potential Long Term Geotechnical Behaviour of Oil Sands Fine Tailings*. M.Sc. Thesis, Department of Civil and Environmental Engineering, University of Alberta, Edmonton, AB, Canada.
- Tang, C.S., Cui, Y.J., Shi, B., Tang A.M., and Liu, C. 2011. Desiccation and Cracking Behaviour of Clay Layer from Slurry State under Wetting-Drying Cycles. *Geoderma*, 166 (1): 111-118. doi: 10.1016/j.geoderma.2011.07.018.
- Tang, J. 1997. *Fundamental Behaviour of Composite Tailings*. M.Sc. Thesis, Department of Civil and Environmental Engineering, University of Alberta, Edmonton, AB, Canada.
- Theng, B.K.G. 1982. Clay-Polymer Interactions: Summary and Perspectives. *Clays and Clay Minerals*, 30 (1): 1-10.
- Thurber Engineering Ltd. 2012. *Oil Sands Tailings Technology Deployment Roadmaps*, Project Report-Volume 1, Report prepared for Alberta Innovates-Energy and Environment Solutions, AB, Canada.
- Tripathy, T. and De, B.R. 2006. Flocculation: A New Way to Treat the Waste Water. *Journal of Physical Sciences*, 10:93-127.

- Vogel, H., Hoffmann, H., Leopold, A., and Roth, K. 2005. Studies of crack dynamics in clay soil II. A physically based model for crack formation. *Geoderma*, 125, 213 - 223. <https://doi.org/10.1016/j.geoderma.2004.07.008>.
- Wells, P.S., Revington, A., and Omotoso, O. 2011. Mature fine tailings drying-technology update. *In Proceedings of Paste 2011*. Edited by R.J. Jewel and A.B. Fourie, 5-7 April, 2011. Australian Centre for Geomechanics, Perth, Australia. pp. 155-166.
- Williams, D.J., Paterson, S., Yau, R., and Goddard, D. 2015. Selection of shear strength profile for desiccated tailings to support an upstream raise. *Proceedings of Tailings and Mine waste 2015*, Vancouver, BC, Canada.
- Williams, D. J. 2016. Mine site rehabilitation—are we reinventing the wrong wheel? *In Proceedings of the 11th International Conference on Mine Closure*. Australian Centre for Geomechanics. pp. 595-608.
- Williams, D.J, and King, J. 2016. Capping of a surface slurried coal tailings storage facility. *Proceedings of the 11th International Conference on Mine Closure*, Australian Centre for Geomechanics. pp. 263-275.
- Wilson, G.W., Fredlund, D.G., and Barbour, S.L. 1994. Coupled soil-atmosphere modeling for soil evaporation. *Canadian Geotechnical Journal*, 31(2): 151-161. <https://doi.org/10.1139/t94-021>
- Wilson, G.W., Kabwe, L.K., Beier, N.A., and Scott, J.D. 2017. Effect of various treatments on consolidation of oil sands fluid fine tailing. *Canadian Geotechnical Journal*. 55 (8): 1059–1066. <https://doi.org/10.1139/cgj-2017-0268>.
- Witteveen, P., Ferrari, A., and Laloui, L. 2013. An experimental and constitutive investigation on the chemo-mechanical behaviour of a clay. *Geotechnique*, 63 (3): 244-255. <https://doi.org/10.1680/bcmpge.60531.003>.
- Xia, D; Arenson, L.U., Biggar, K.W., and Seg0, D.C. 2005. Freezing process in Devon silt-using time lapse photography. *In Proceedings of the 58th Canadian Geotechnical Conference 2005*, September 18-21, Saskatoon, SK, Canada.
- Xia, D. 2006. *Frost Heave Studies using Photographic Technique*. MAsc. Thesis, Department of Civil and Environmental Engineering, University of Alberta, Edmonton, AB, Canada.

## Appendix A: Freeze-Thaw Tests Setup

Figures A-1 and A-2 show the freezing cell and the freeze-thaw testing setup in the laboratory. The details of this setup was documented in Chapter 2 and 3.

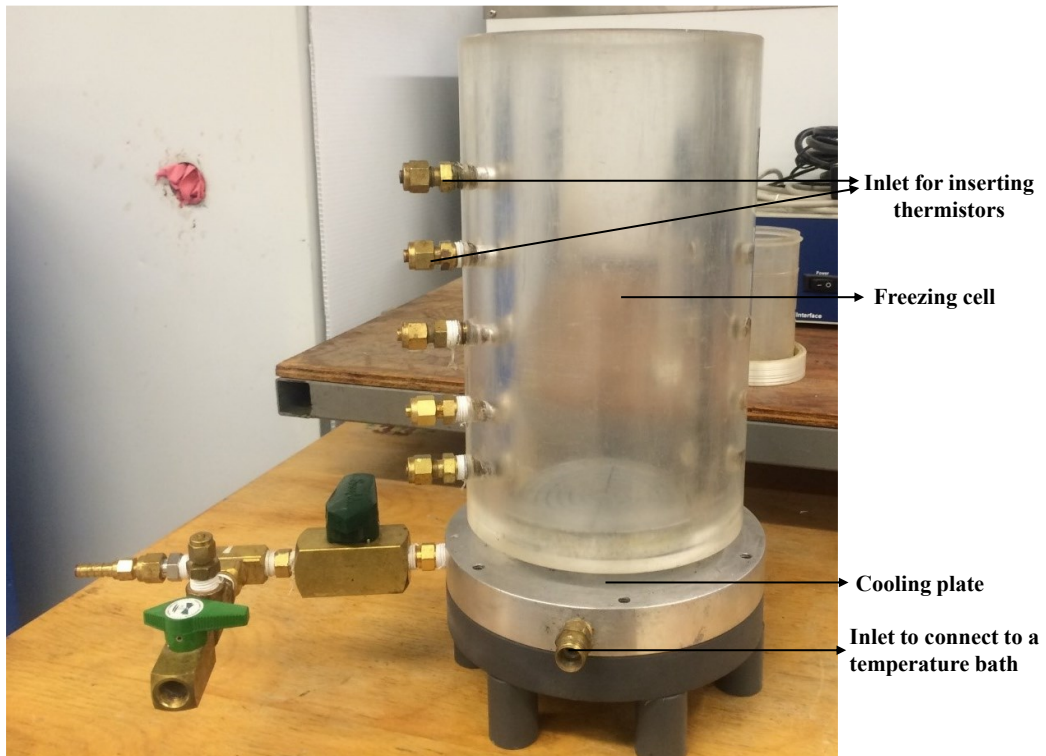


Figure A-1: Freezing cell diagram

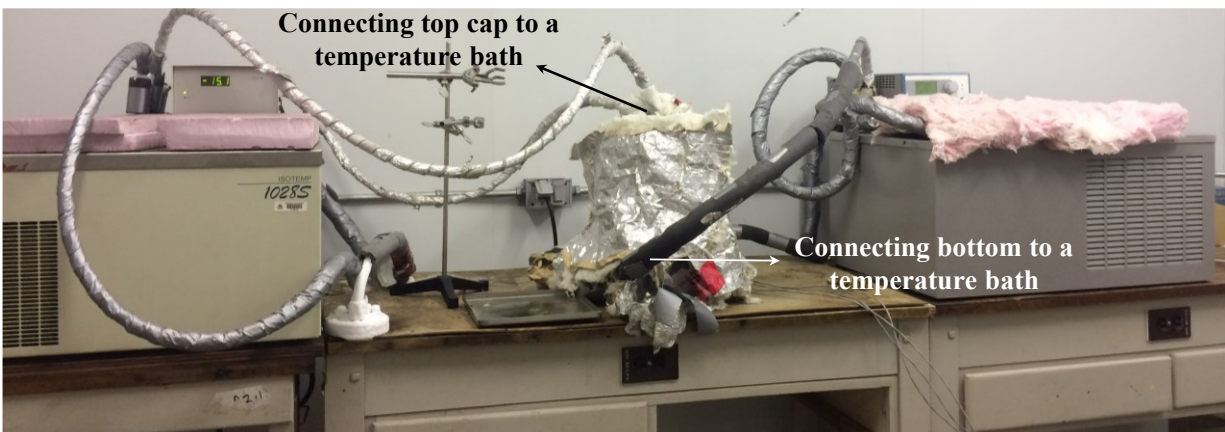


Figure A-2: Freeze-thaw testing setup

## Appendix B: Grain Size Distribution (GSD)

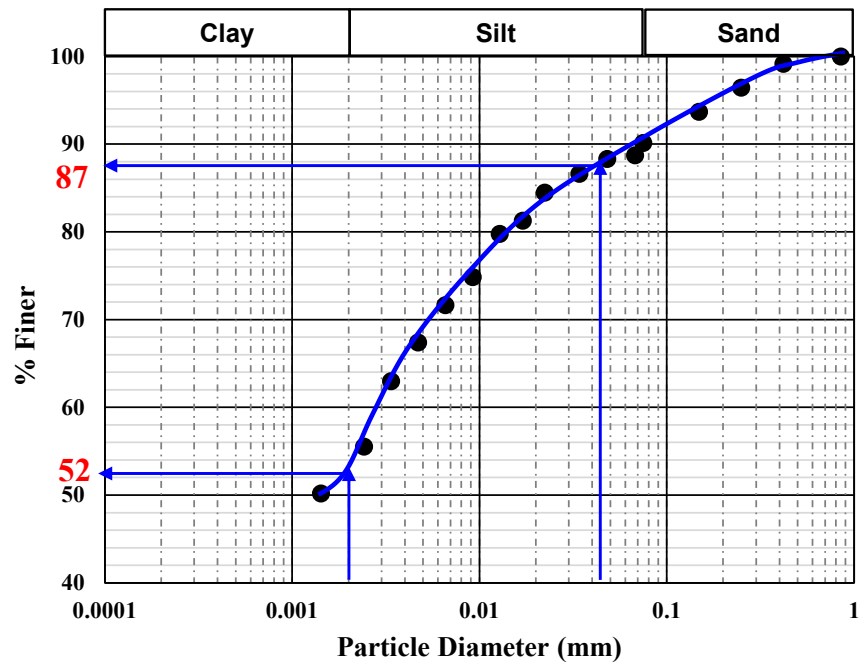


Figure B-1: GSD plot of centrifuged tailings

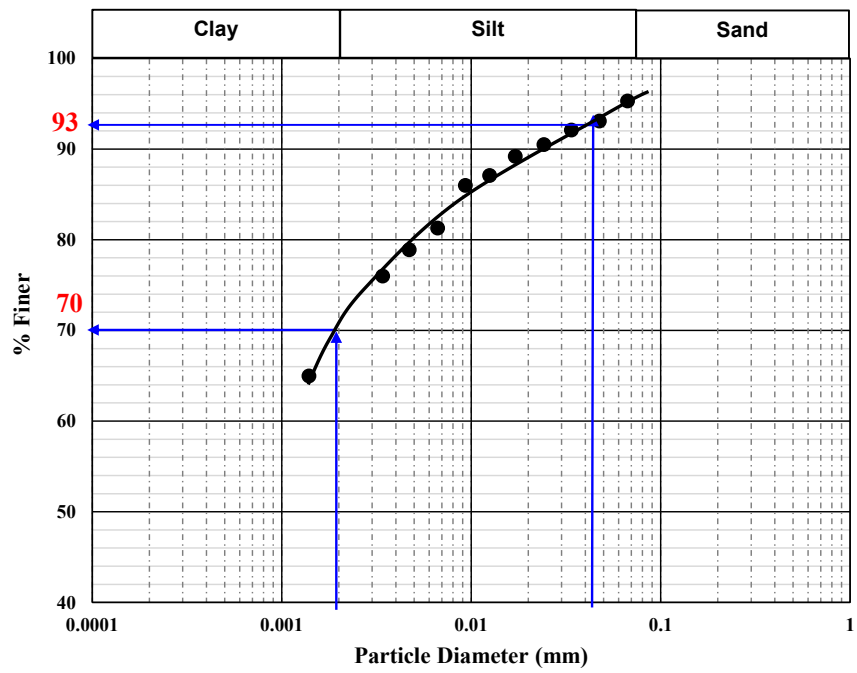


Figure B-1: GSD plot of in-line thickened tailings (ILTT)

## Appendix C: Temperature Plot

Three thermistors were placed along the walls of the freezing cell at fixed distances of 40 mm (Thermistor 3), 80 mm (Thermistor 2) and 120 mm (Thermistor 1) from the bottom plate. These thermistors were calibrated by placing it into the center of the ice bath and reading the temperatures that should read 0°C. Next, the correction factors were applied when the temperatures were deviated from 0°C. The correction factors applied for these three thermistors (Thermistors 1, 2 and 3) were 0, 0.017 and 0.003°C. The room temperature of the walk-in freezer was kept between 0°C to 1°C. Figures A-1 to A-33 show the temperature inside the samples at different depth. Please note that once these samples subjected to multiple freeze-thaw and drying-wetting cycles reduced to a height below than 120 mm, thermistor 1 could no longer be used and hence, two thermistors (Thermistor 2 and 3) were used in those cases to track the temperature within the tailings samples.

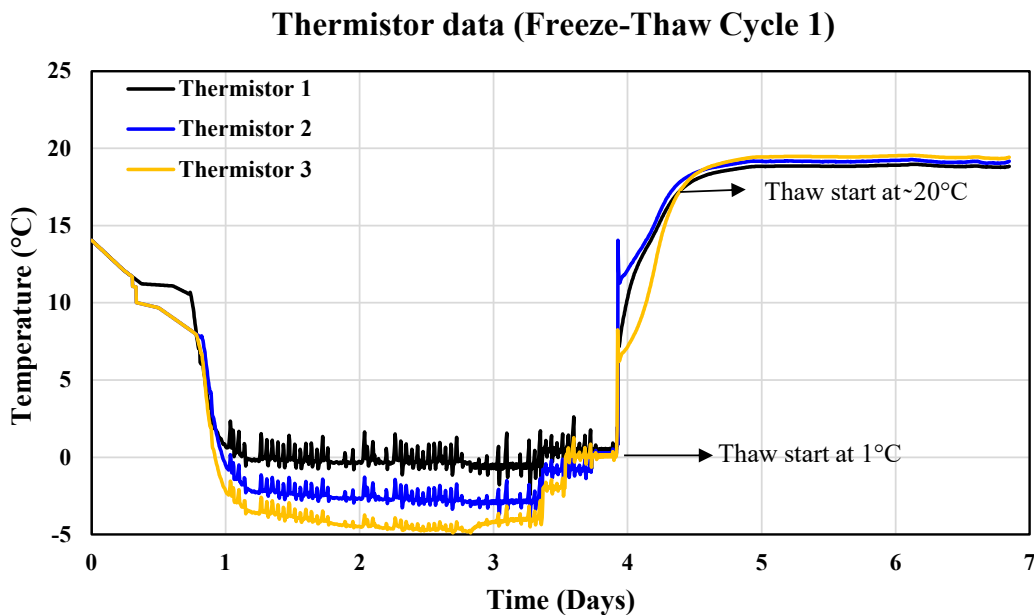


Figure C-1: Temperature plot for centrifuged tailings at a temperature gradient of 0.028°C/mm (first phase testing at 1st cycle)

### Thermistor data (Freeze-Thaw Cycle 2)

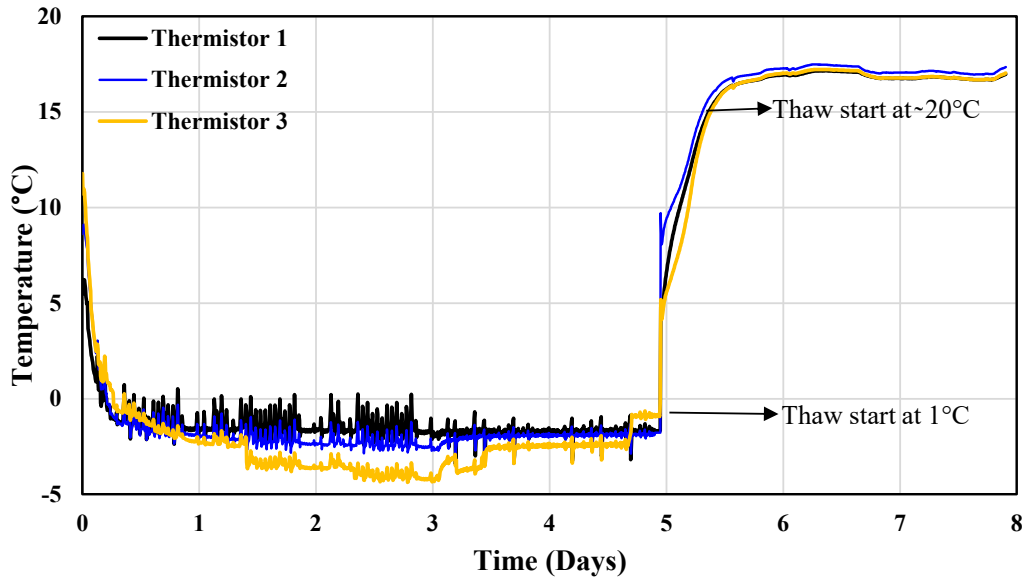


Figure C-2: Temperature plot for centrifuged tailings at a temperature gradient of  $0.028^{\circ}\text{C}/\text{mm}$  (first phase testing at 2nd cycle)

### Thermistor data (Freeze Thaw Cycle 3)

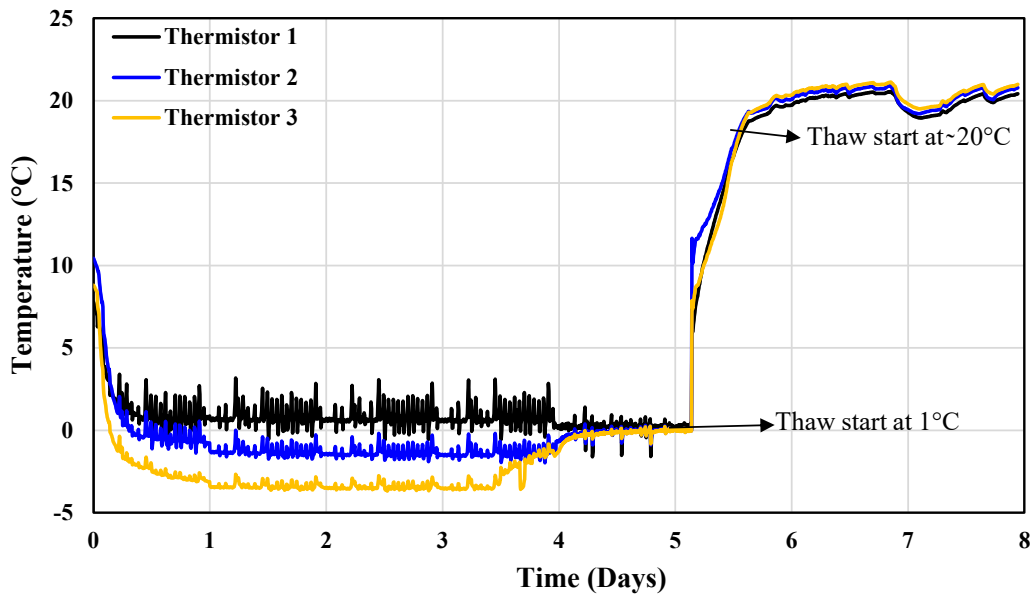


Figure C-3: Temperature plot for centrifuged tailings at a temperature gradient of  $0.028^{\circ}\text{C}/\text{mm}$  (first phase testing at 3rd cycle)

### Thermistor data (Freeze-Thaw Cycle 4)

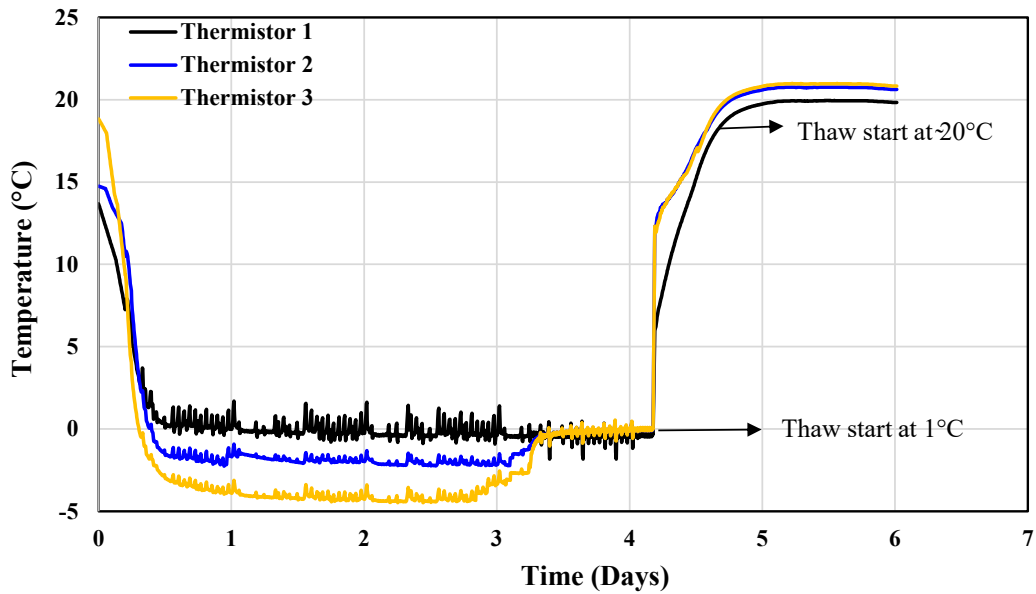


Figure C-4: Temperature plot for centrifuged tailings at a temperature gradient of  $0.028^{\circ}\text{C}/\text{mm}$  (first phase testing at 4th cycle)

### Thermistor data (Freeze-Thaw Cycle 5)

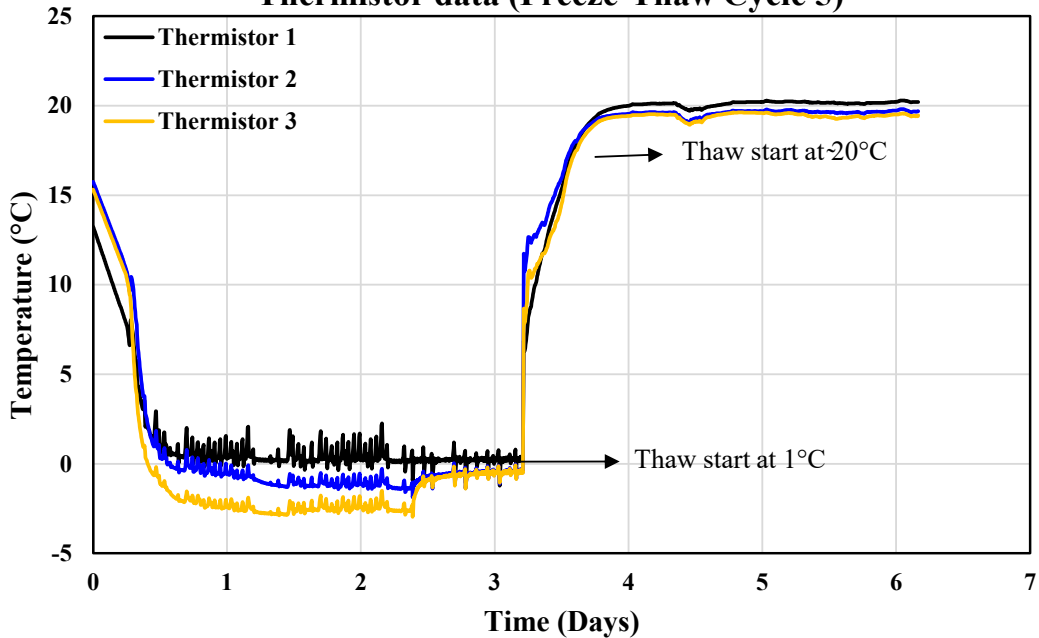


Figure C-5: Temperature plot for centrifuged tailings at a temperature gradient of  $0.028^{\circ}\text{C}/\text{mm}$  (first phase testing at 5th cycle)

### Thermistor data (Freeze-Thaw Cycle 1)

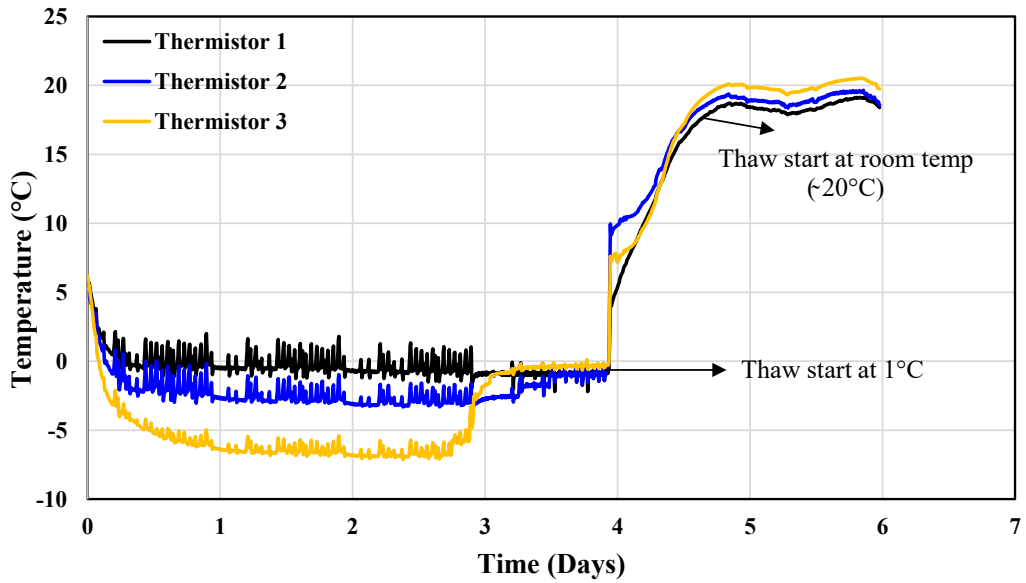


Figure C-6: Temperature plot for centrifuged tailings at a temperature gradient of  $0.056^{\circ}\text{C}/\text{mm}$  (first phase testing at 1st cycle)

### Thermistor data (Freeze Thaw Cycle 2)

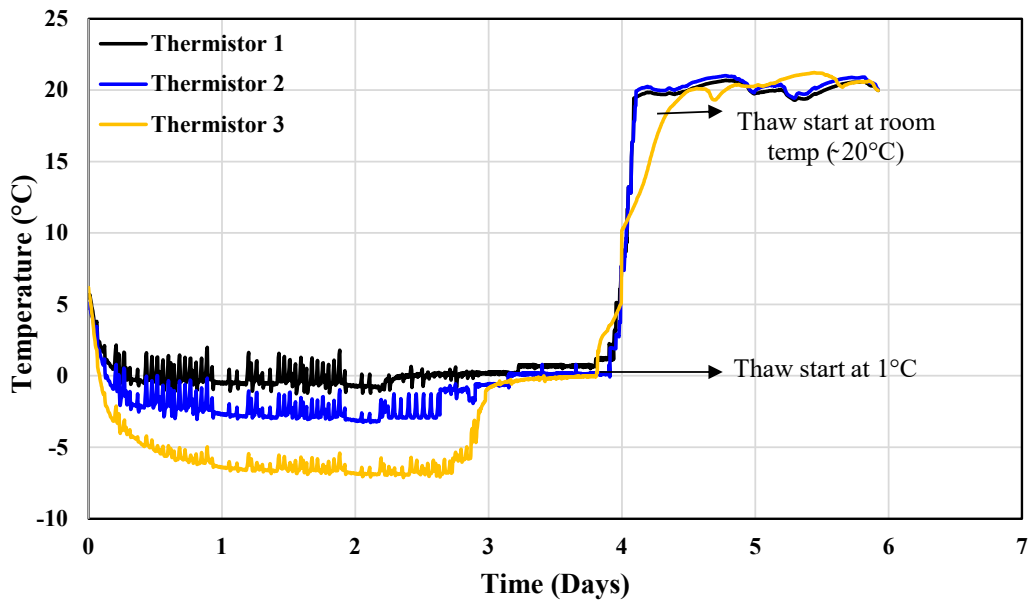


Figure C-7: Temperature plot for centrifuged tailings at a temperature gradient of  $0.056^{\circ}\text{C}/\text{mm}$  (first phase testing at 2nd cycle)

### Thermistor data (Freeze-Thaw Cycle 3)

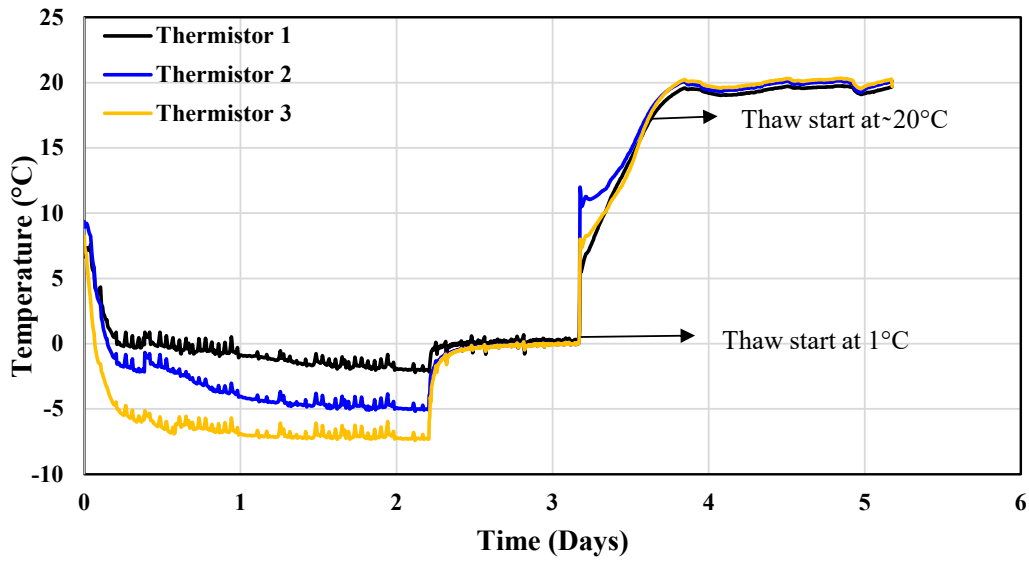


Figure C-8: Temperature plot for centrifuged tailings at a temperature gradient of  $0.056^{\circ}\text{C}/\text{mm}$  (first phase testing at 3rd cycle)

### Thermistor data (Freeze-Thaw Cycle 4)

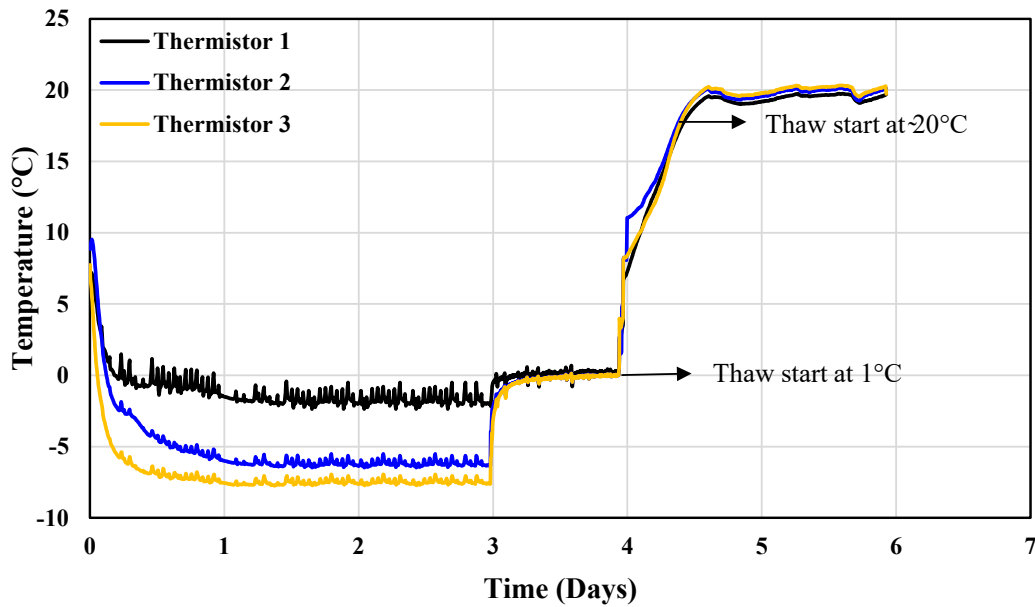


Figure C-9: Temperature plot for centrifuged tailings at a temperature gradient of  $0.056^{\circ}\text{C}/\text{mm}$  (first phase testing at 4th cycle)

### Thermistor data (Freeze-Thaw Cycle 5)

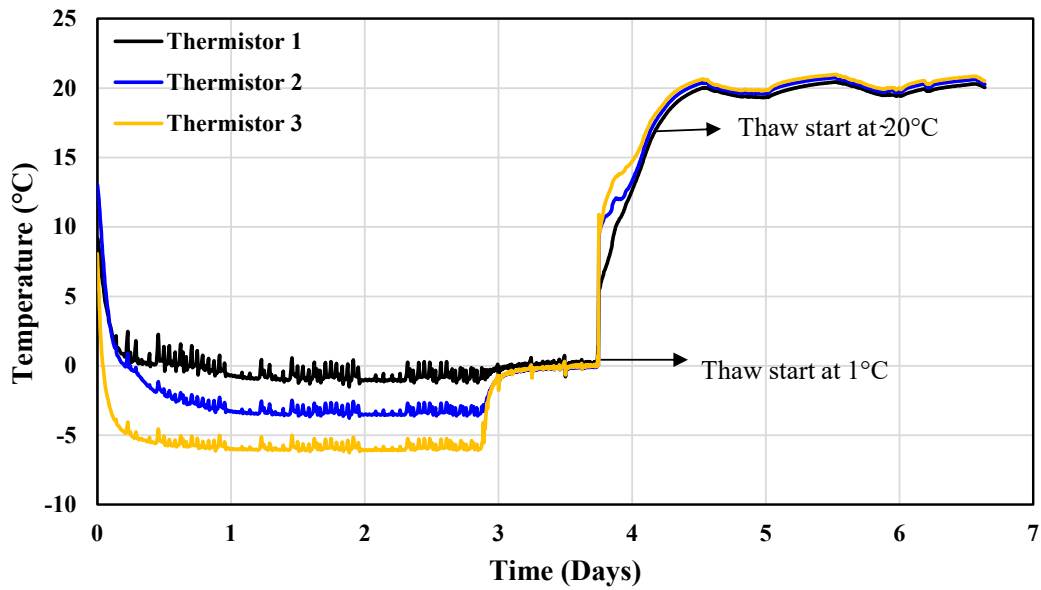


Figure C-10: Temperature plot for centrifuged tailings at a temperature gradient of  $0.056^{\circ}\text{C}/\text{mm}$  (first phase testing at 5th cycle)

### Thermistor data (Freeze-Thaw Cycle 1)

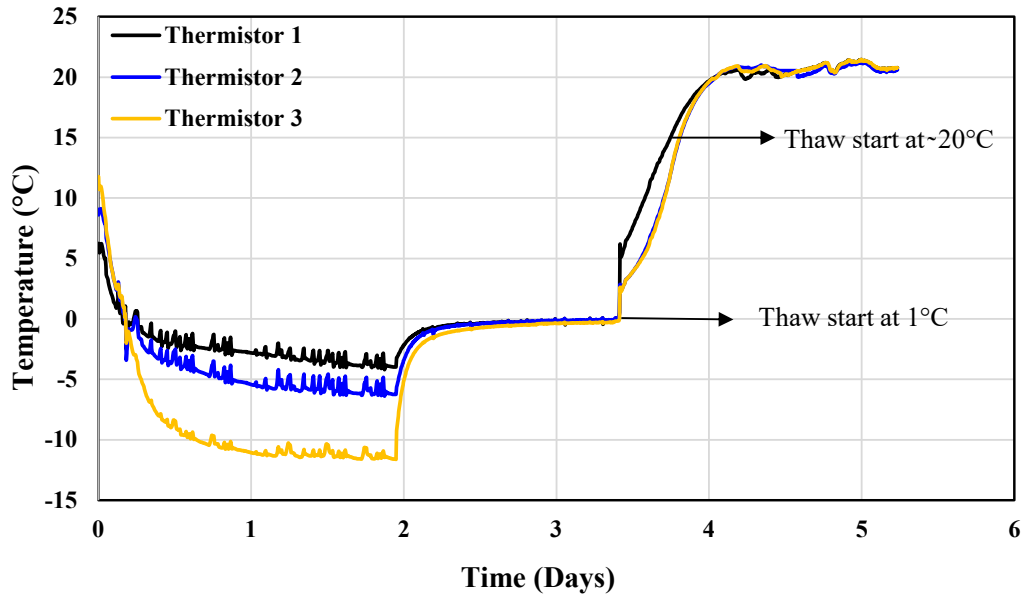


Figure C-11: Temperature plot for centrifuged tailings at a temperature gradient of  $0.083^{\circ}\text{C}/\text{mm}$  (first phase testing at 1st cycle)

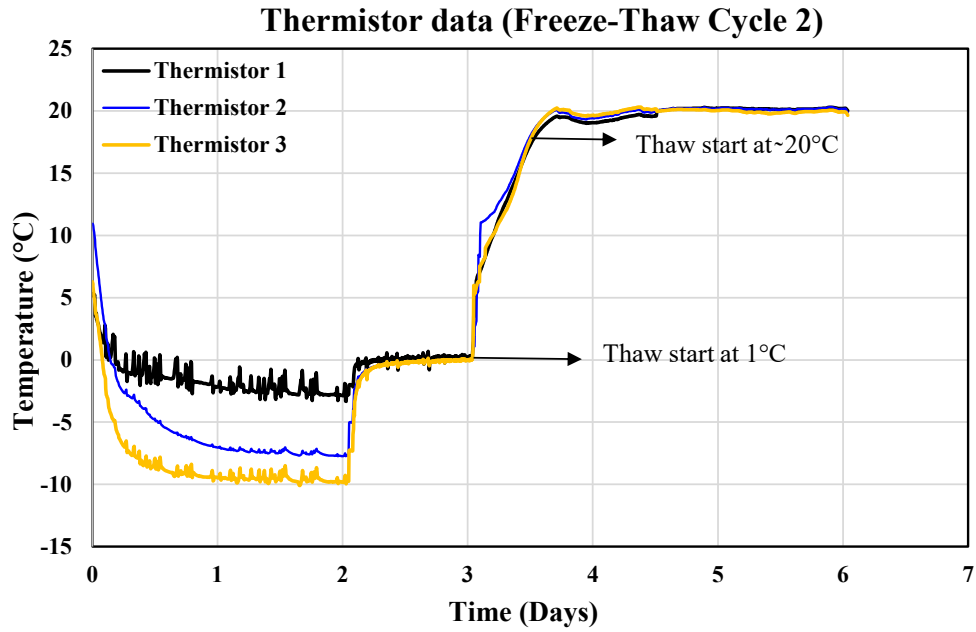


Figure C-12: Temperature plot for centrifuged tailings at a temperature gradient of  $0.083^{\circ}\text{C}/\text{mm}$  (first phase testing at 2nd cycle)

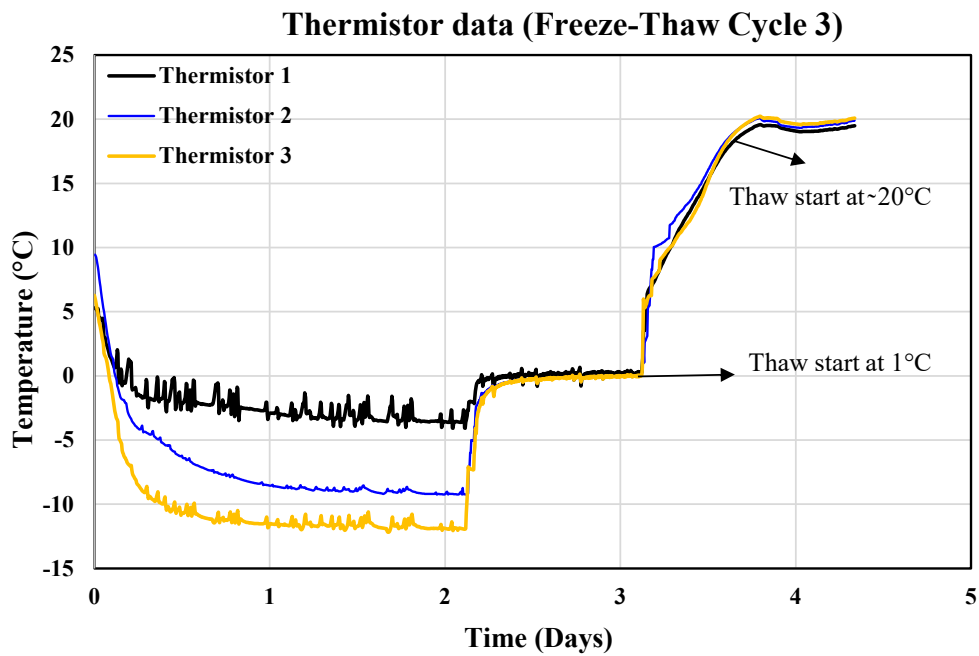


Figure C-13: Temperature plot for centrifuged tailings at a temperature gradient of  $0.083^{\circ}\text{C}/\text{mm}$  (first phase testing at 3rd cycle)

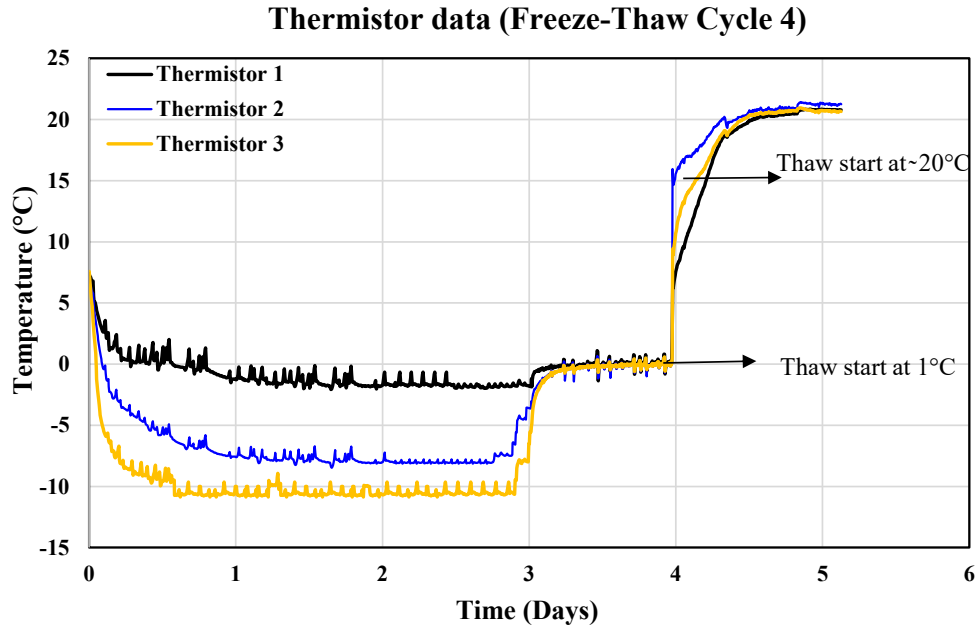


Figure C-14: Temperature plot for centrifuged tailings at a temperature gradient of  $0.083^{\circ}\text{C}/\text{mm}$  (first phase testing at 4th cycle)

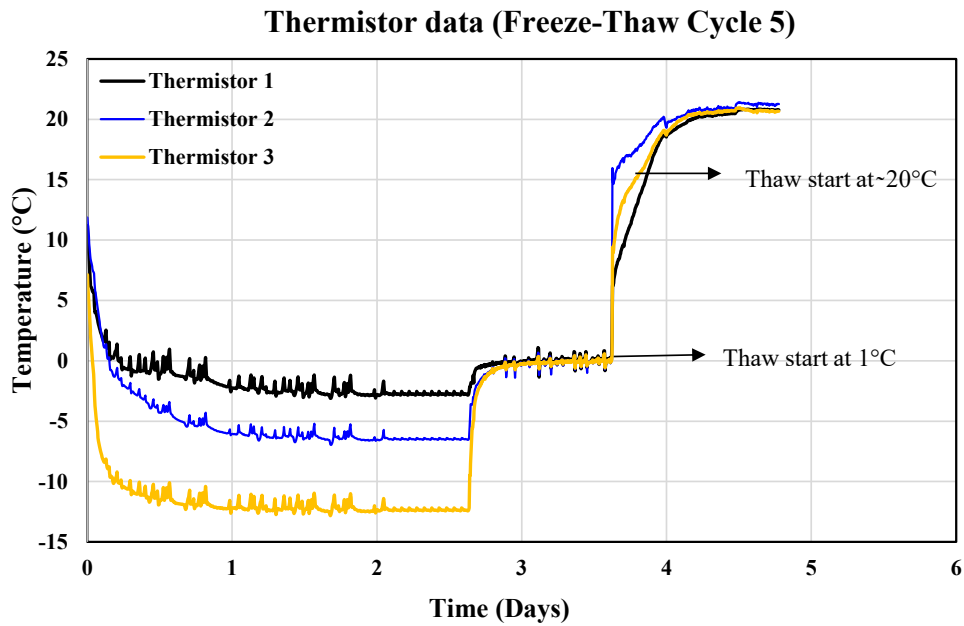


Figure C-15: Temperature plot for centrifuged tailings at a temperature gradient of  $0.083^{\circ}\text{C}/\text{mm}$  (first phase testing at 5th cycle)

### Thermistor data (Freeze-Thaw Cycle 1)

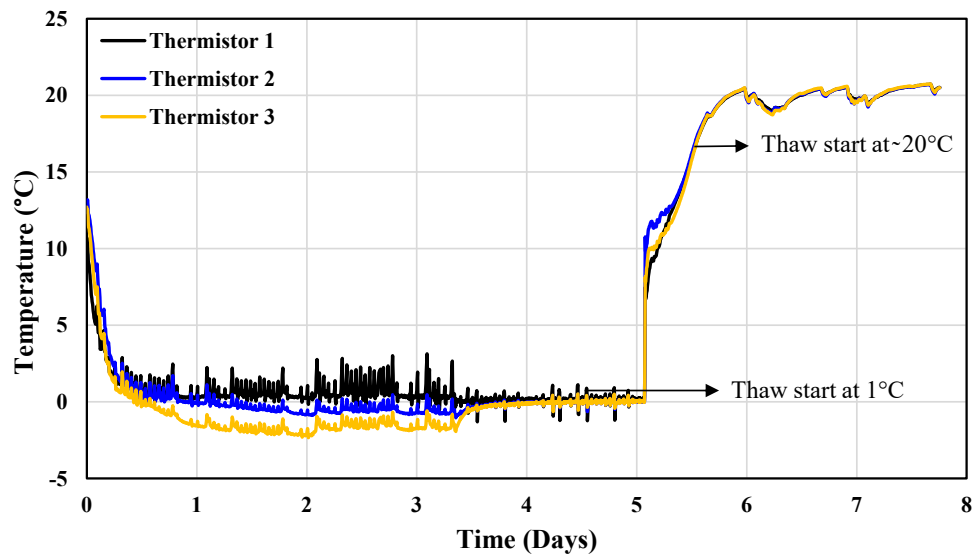


Figure C-16: Temperature plot for centrifuged tailings at a temperature gradient of  $0.028^{\circ}\text{C}/\text{mm}$  (second phase testing at 1st cycle)

### Thermistor data (Freeze-Thaw Cycle 2)

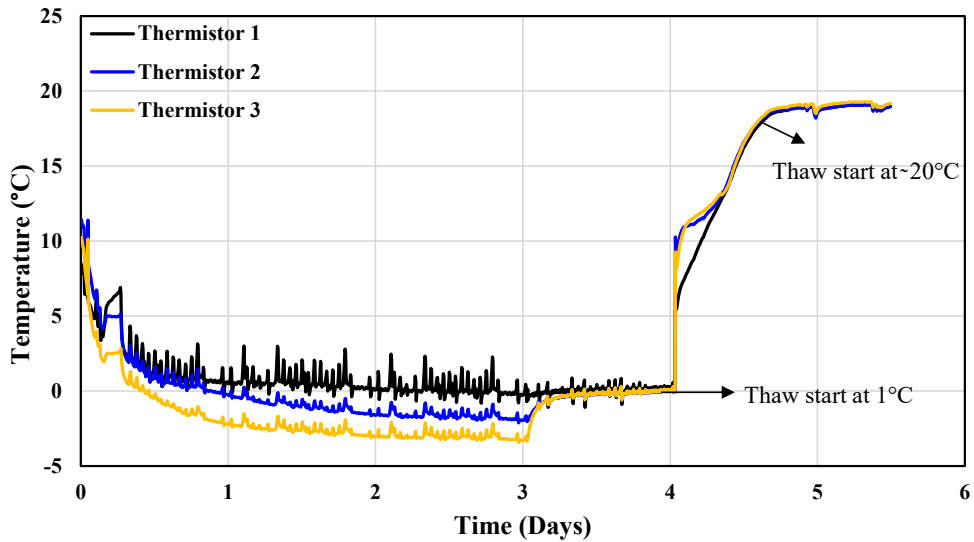


Figure C-17: Temperature plot for centrifuged tailings at a temperature gradient of  $0.028^{\circ}\text{C}/\text{mm}$  (second phase testing at 2nd cycle)

### Thermistor data (Freeze Thaw Cycle 3)

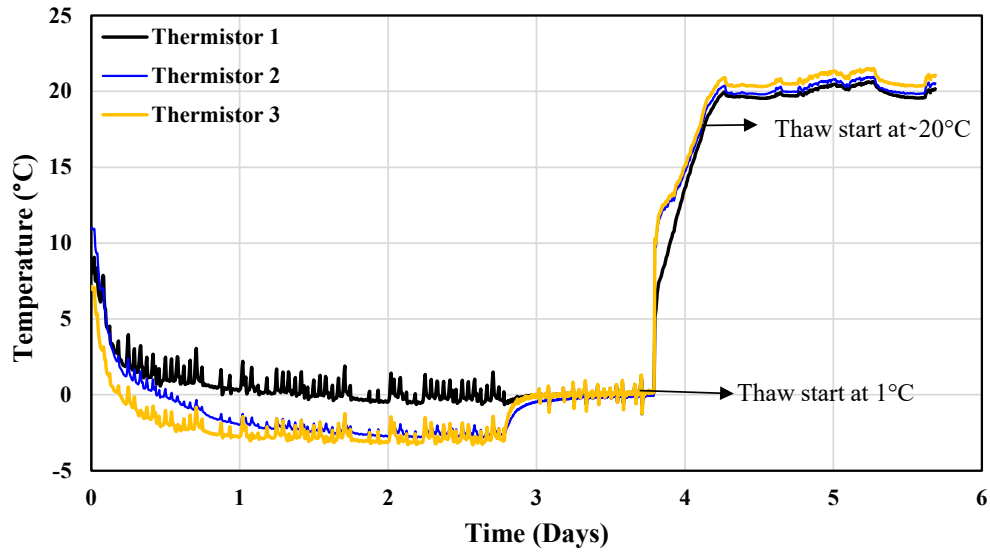


Figure C-18: Temperature plot for centrifuged tailings at a temperature gradient of  $0.028^{\circ}\text{C}/\text{mm}$  (second phase testing at 3rd cycle)

### Thermistor data (Freeze-Thaw Cycle 4)

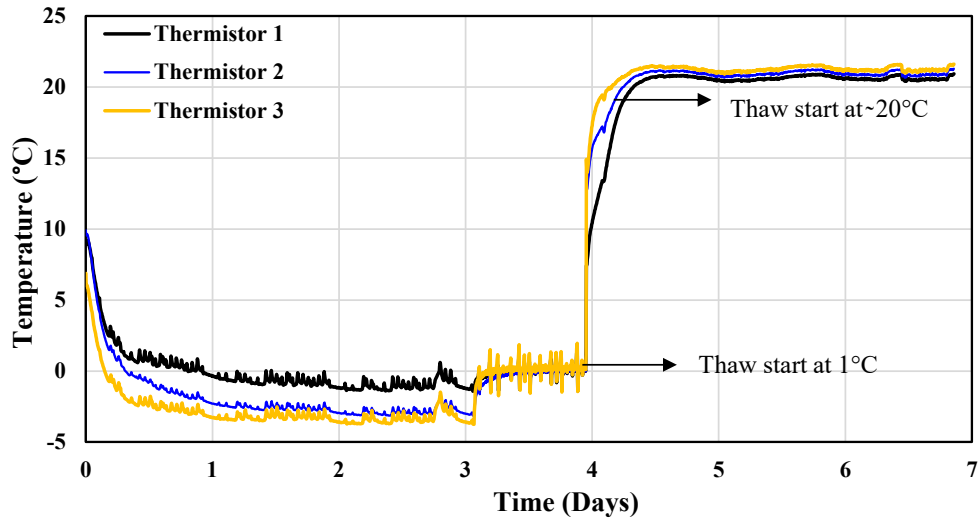


Figure C-19: Temperature plot for centrifuged tailings at a temperature gradient of  $0.028^{\circ}\text{C}/\text{mm}$  (second phase testing at 4th cycle)

### Thermistor data (Freeze-Thaw Cycle 5)

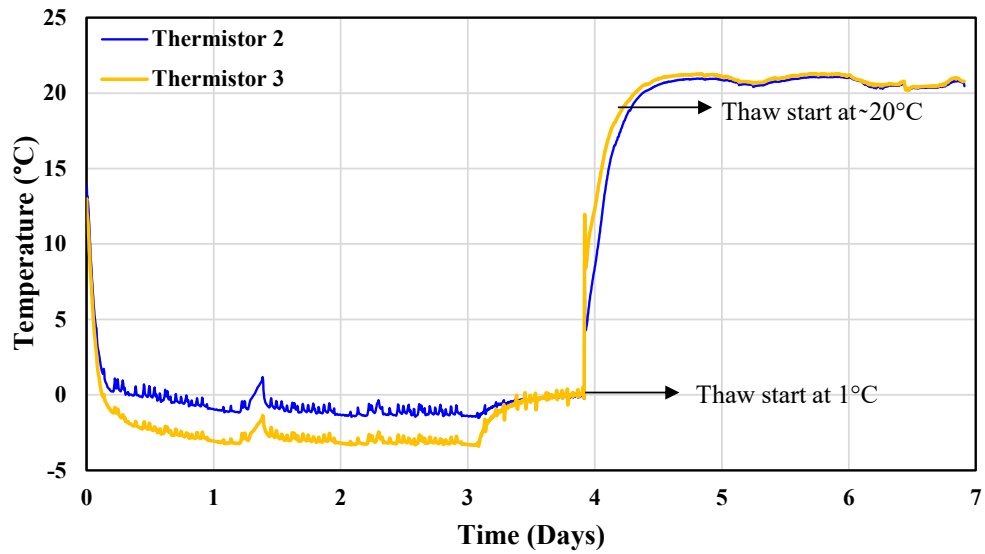


Figure C-20: Temperature plot for centrifuged tailings at a temperature gradient of  $0.028^{\circ}\text{C}/\text{mm}$  (second phase testing at 5th cycle)

### Thermistor data (Freeze-Thaw Cycle 1)

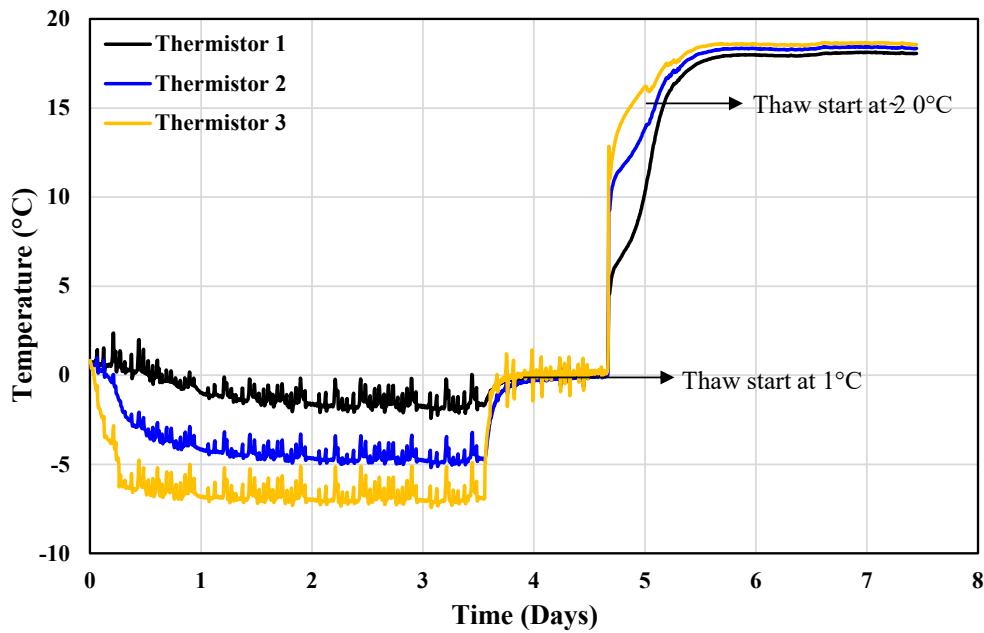


Figure C-21: Temperature plot for centrifuged tailings at a temperature gradient of  $0.056^{\circ}\text{C}/\text{mm}$  (second phase testing at 1st cycle)

### Thermistor data (Freeze-Thaw Cycle 2)

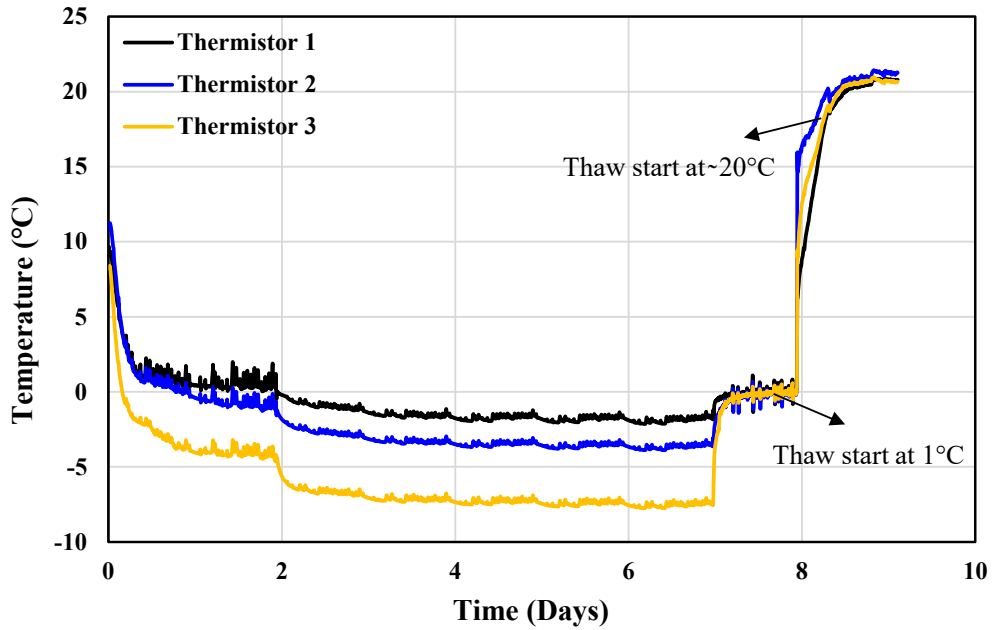


Figure C-22: Temperature plot for centrifuged tailings at a temperature gradient of  $0.056^{\circ}\text{C}/\text{mm}$  (second phase testing at 2nd cycle)

### Thermistor data (Freeze-Thaw Cycle 3)

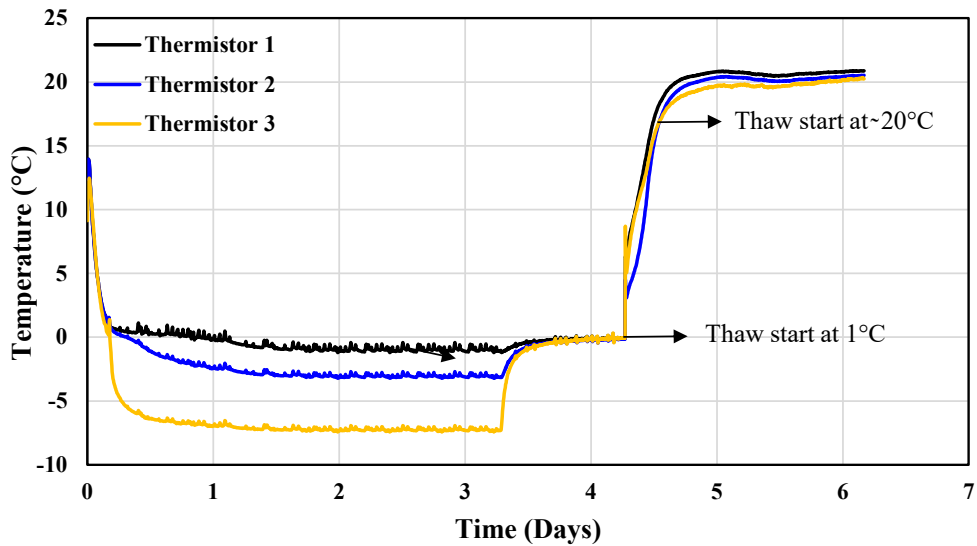


Figure C-23: Temperature plot for centrifuged tailings at a temperature gradient of  $0.056^{\circ}\text{C}/\text{mm}$  (second phase testing at 3rd cycle)

### Thermistor data (Freeze-Thaw Cycle 4)

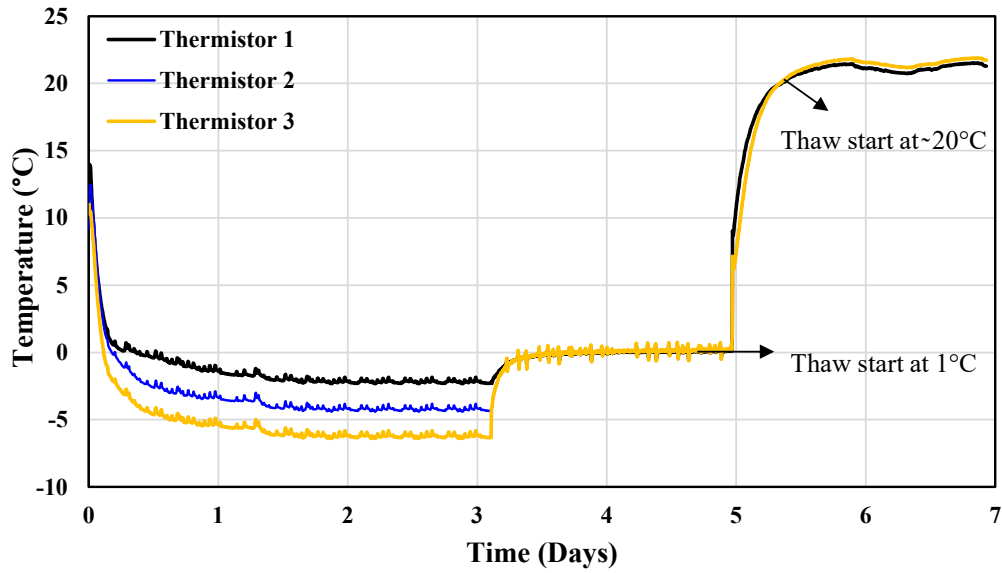


Figure C-24: Temperature plot for centrifuged tailings at a temperature gradient of  $0.056^{\circ}\text{C}/\text{mm}$  (second phase testing at 4th cycle)

### Thermistor data (Freeze-Thaw Cycle 5)

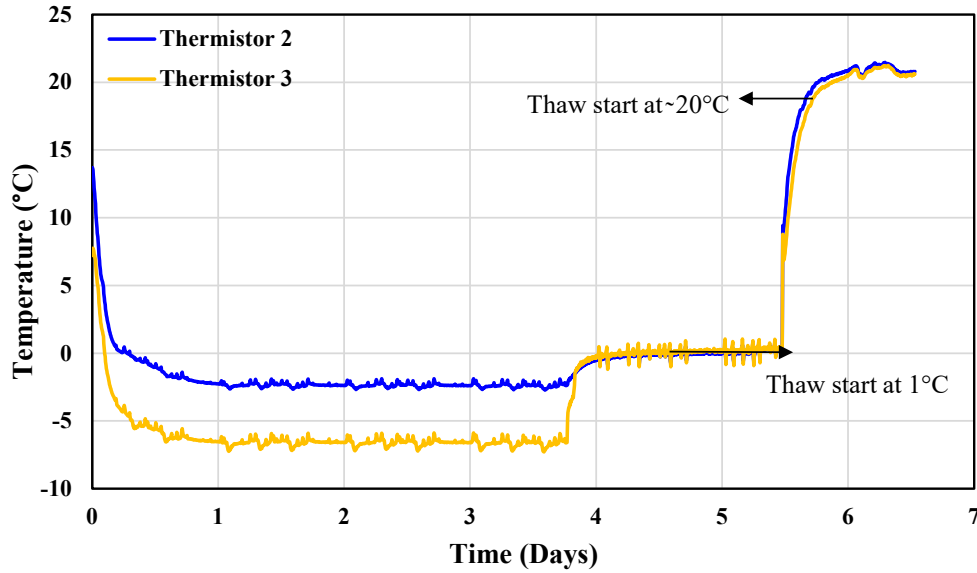


Figure C-25: Temperature plot for centrifuged tailings at a temperature gradient of  $0.056^{\circ}\text{C}/\text{mm}$  (second phase testing at 5th cycle)

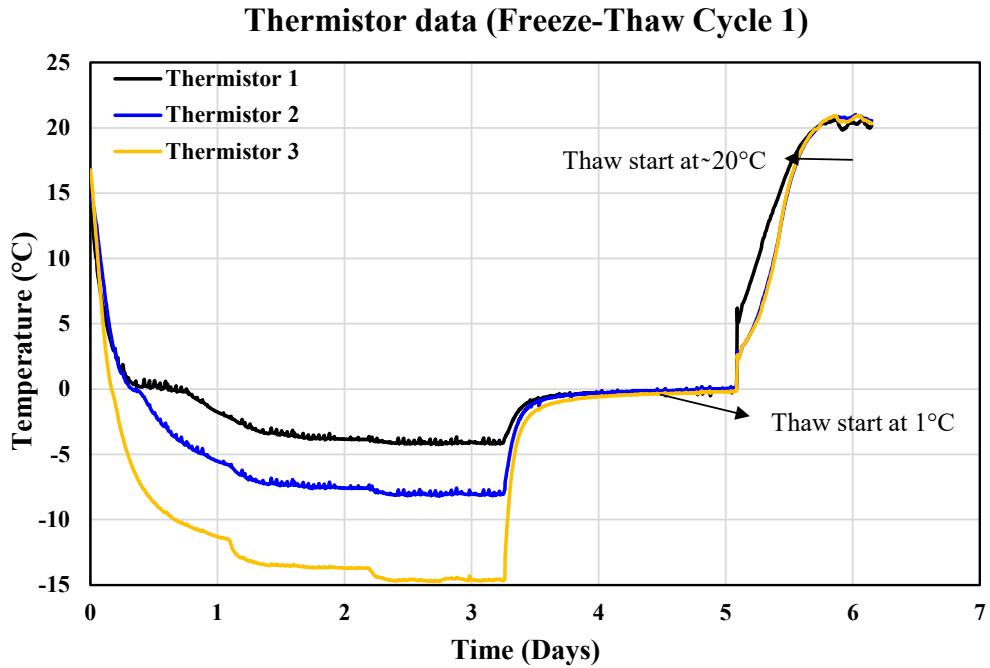


Figure C-26: Temperature plot for centrifuged tailings at a temperature gradient of  $0.083^{\circ}\text{C}/\text{mm}$  (second phase testing at 1st cycle)

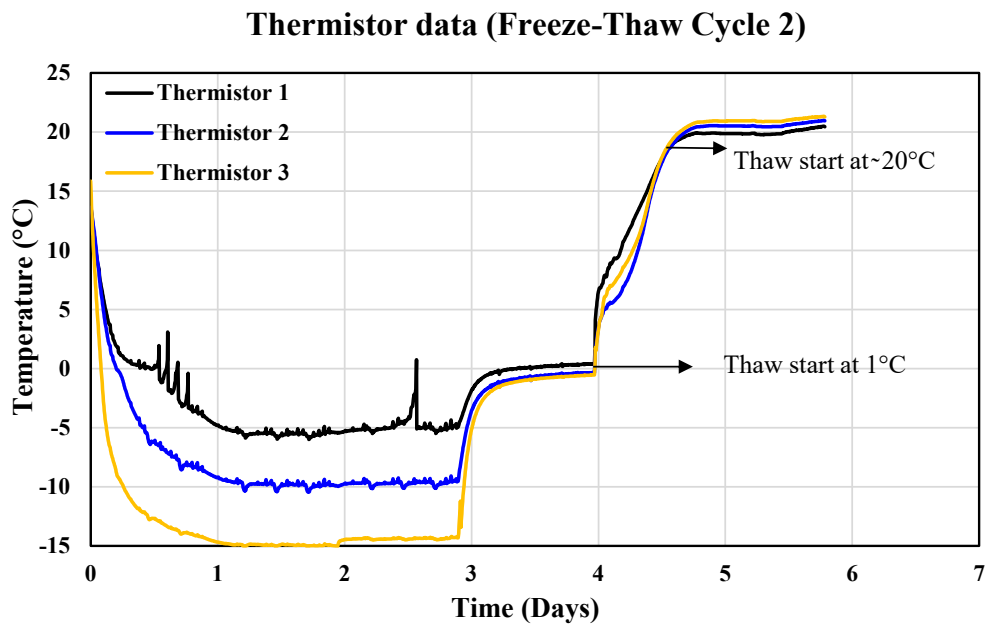


Figure C-27: Temperature plot for centrifuged tailings at a temperature gradient of  $0.083^{\circ}\text{C}/\text{mm}$  (second phase testing at 2nd cycle)

### Thermistor data (Freeze-Thaw Cycle 3)

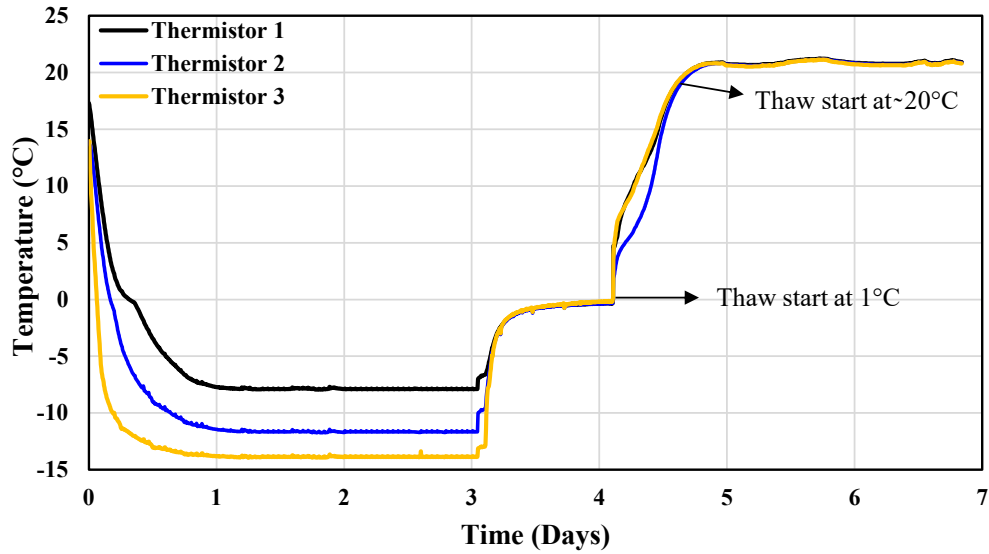


Figure C-28: Temperature plot for centrifuged tailings at a temperature gradient of  $0.083^{\circ}\text{C}/\text{mm}$  (second phase testing at 3rd cycle)

### Thermistor data (Freeze-Thaw Cycle 4)

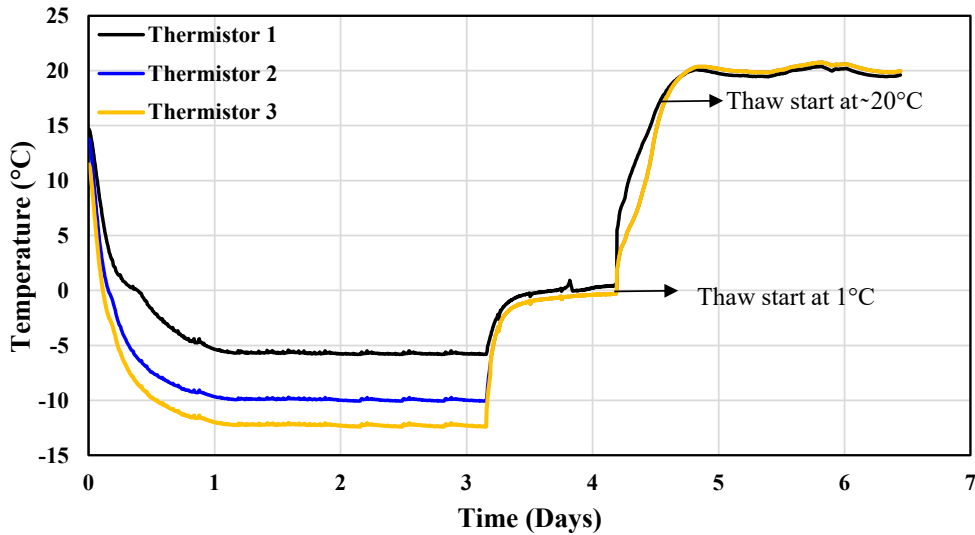


Figure C-29: Temperature plot for centrifuged tailings at a temperature gradient of  $0.083^{\circ}\text{C}/\text{mm}$  (second phase testing at 4th cycle)

### Thermistor data (Freeze-Thaw Cycle 5)

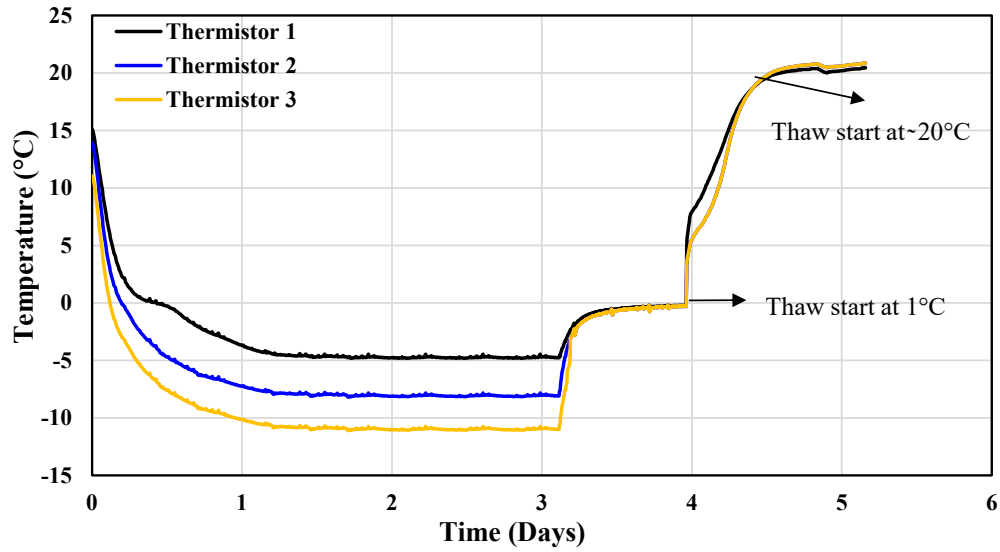


Figure C-30: Temperature plot for centrifuged tailings at a temperature gradient of  $0.083^{\circ}\text{C}/\text{mm}$  (second phase testing at 5th cycle)

### Thermistor data (Freeze Thaw Cycle 6)

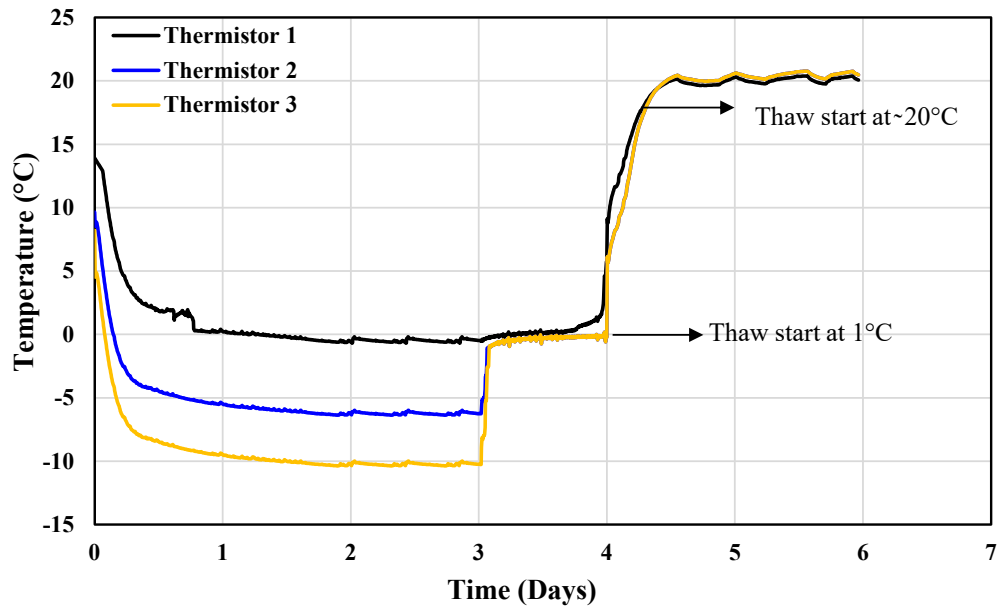


Figure C-31: Temperature plot for centrifuged tailings at a temperature gradient of  $0.083^{\circ}\text{C}/\text{mm}$  (second phase testing at 6th cycle)

**Thermistor Data (Freeze-Thaw Cycle 7)**

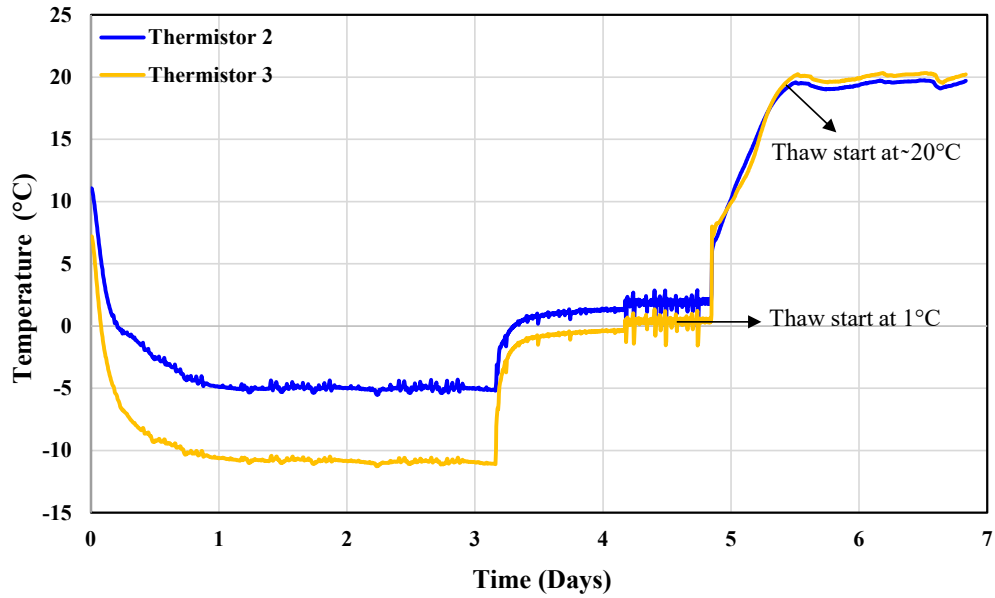


Figure C-32: Temperature plot for centrifuged tailings at a temperature gradient of  $0.083^{\circ}\text{C}/\text{mm}$  (second phase testing at 7th cycle)

**Thermistor data (Freeze-Thaw Cycle 1)**

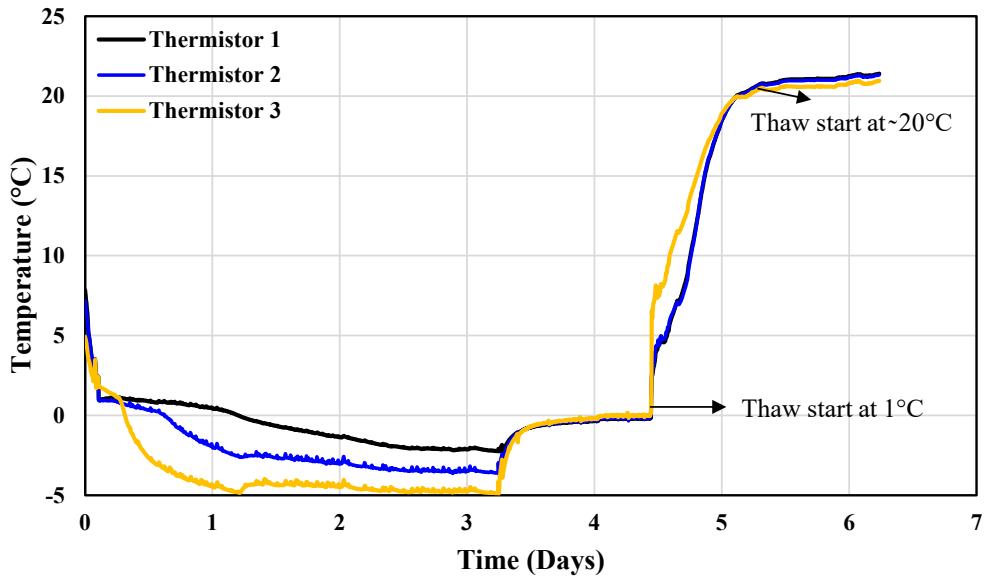


Figure C-33: Temperature plot for ILTT at a temperature gradient of  $0.028^{\circ}\text{C}/\text{mm}$  (first phase testing at 1st cycle)

### Thermistor data (Freeze-Thaw Cycle 2)

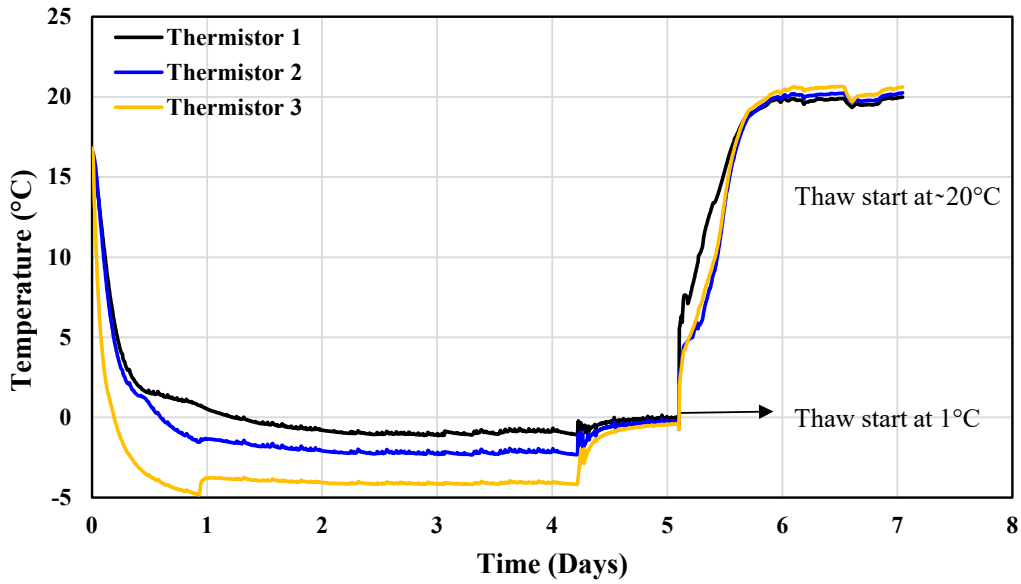


Figure C-34: Temperature plot for ILTT at a temperature gradient of  $0.028^{\circ}\text{C}/\text{mm}$  (first phase testing at 2nd cycle)

### Thermistor data (Freeze-Thaw Cycle 3)

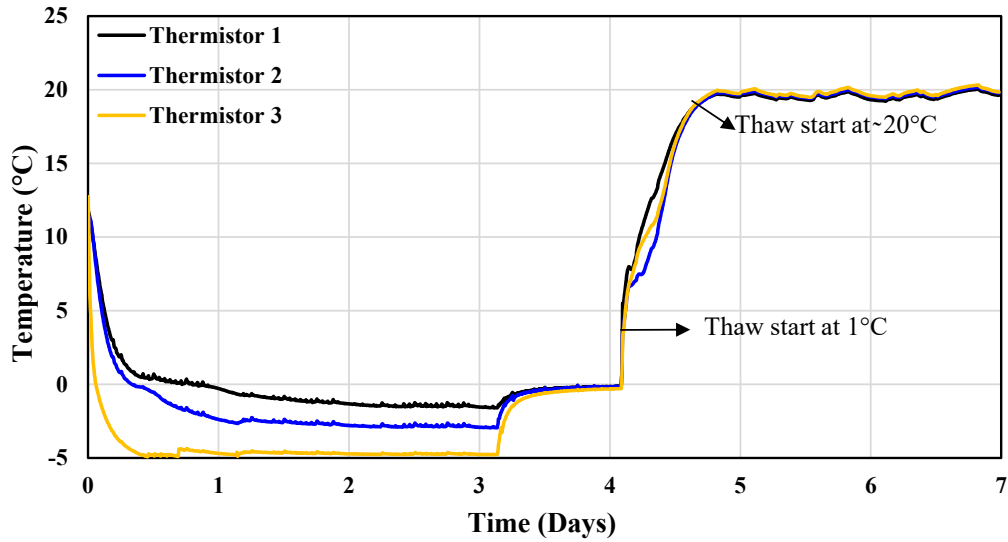


Figure C-35: Temperature plot for ILTT at a temperature gradient of  $0.028^{\circ}\text{C}/\text{mm}$  (first phase testing at 3rd cycle)

### Thermistor data (Freeze-Thaw Cycle 4)

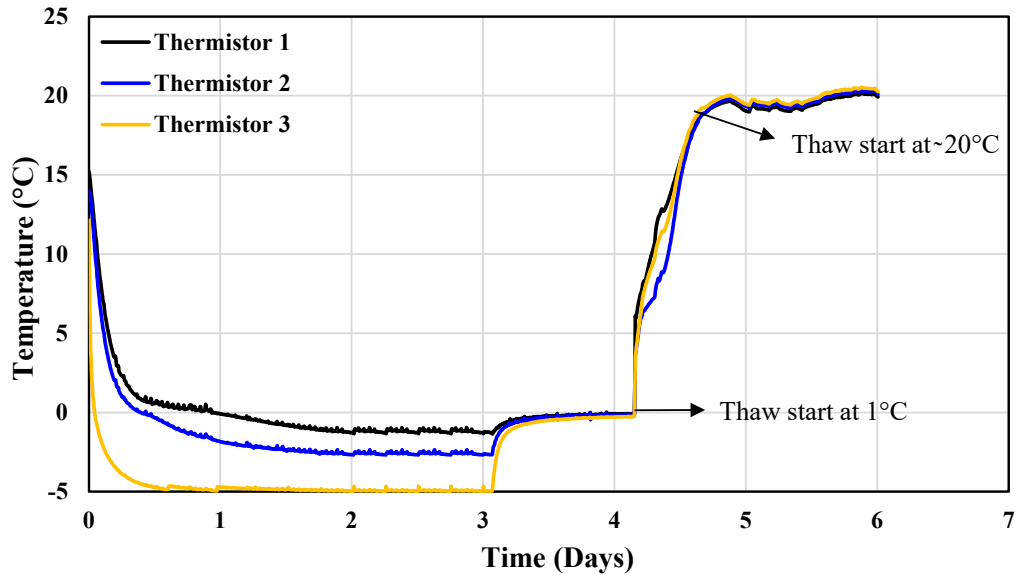


Figure C-36: Temperature plot for ILTT at a temperature gradient of  $0.028^{\circ}\text{C}/\text{mm}$  (first phase testing at 4th cycle)

### Thermistor data (Freeze-Thaw Cycle 5)

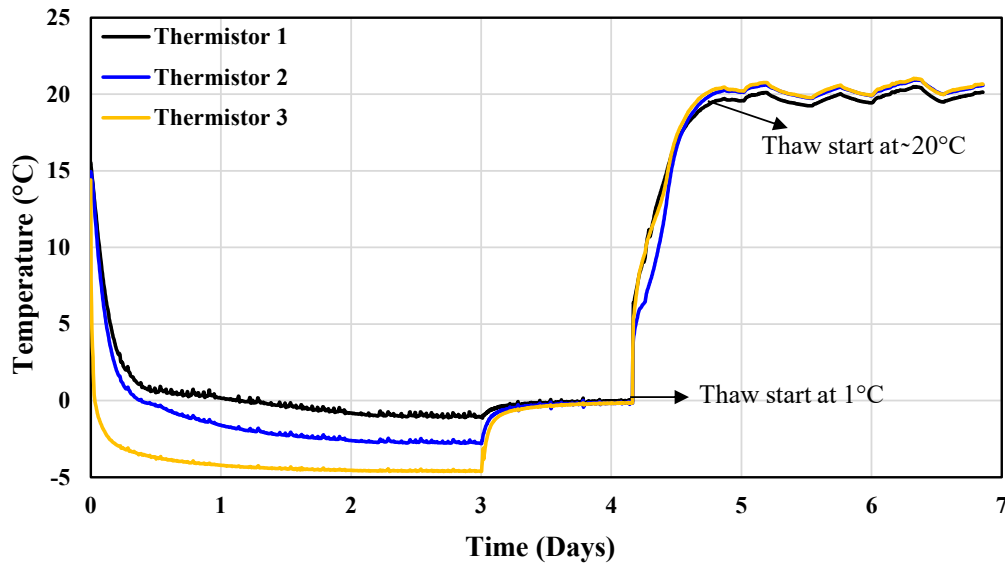


Figure C-37: Temperature plot for ILTT at a temperature gradient of  $0.028^{\circ}\text{C}/\text{mm}$  (first phase testing at 5th cycle)

### Thermistor data (Freeze-Thaw Cycle 1)

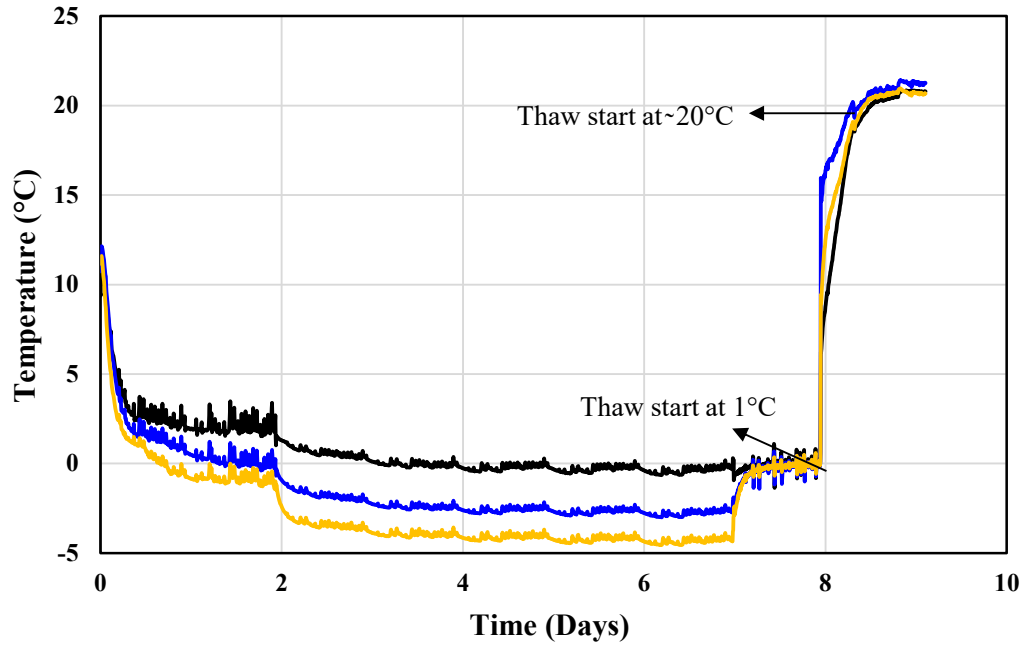


Figure C-38: Temperature plot for ILTT at a temperature gradient of 0.028°C/mm (second phase testing at 1st cycle)

### Thermistor data (Freeze-Thaw Cycle 2)

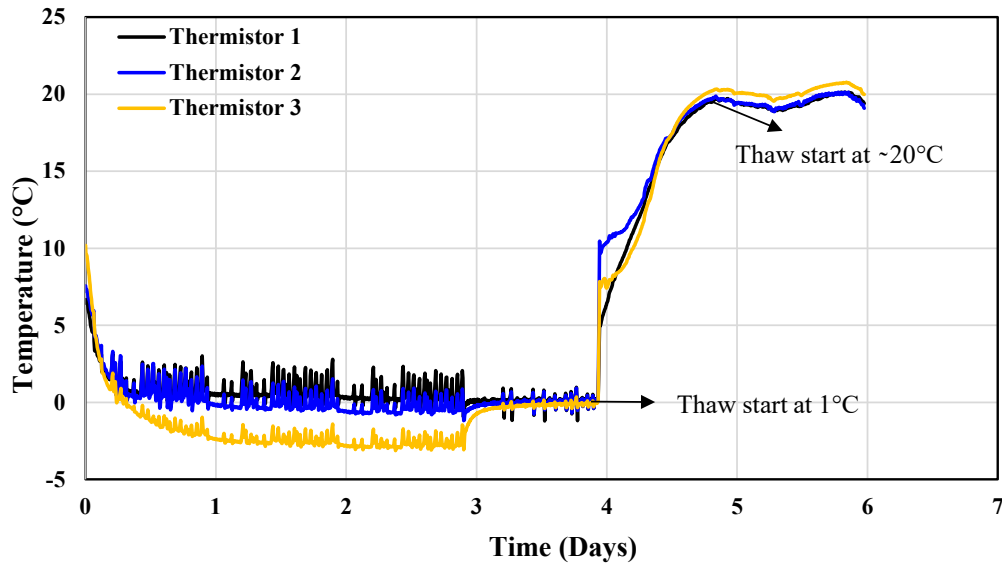


Figure C-39: Temperature plot for ILTT at a temperature gradient of 0.028°C/mm (second phase testing at 2nd cycle)

### Thermistor data (Freeze-Thaw Cycle 3)

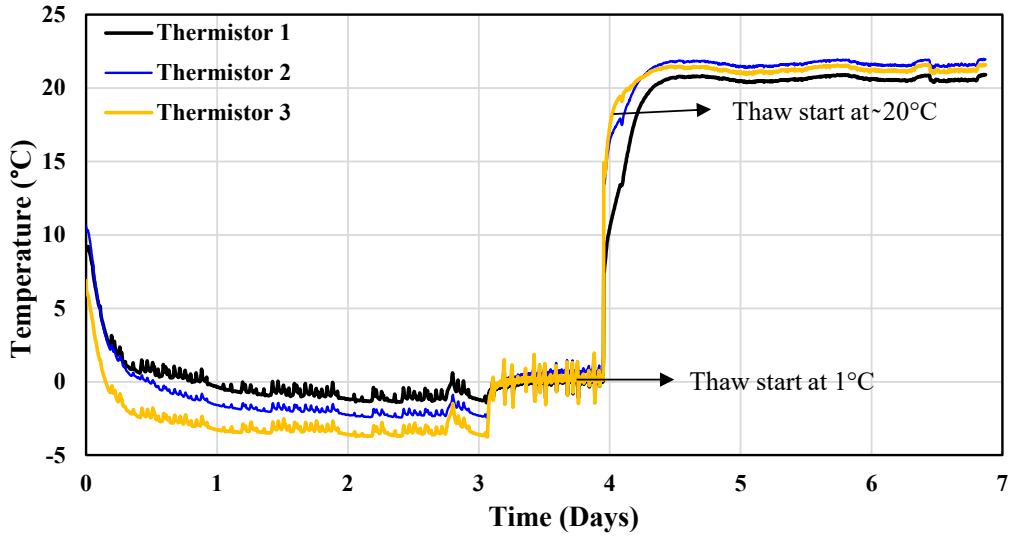


Figure C-40: Temperature plot for ILTT at a temperature gradient of  $0.028^{\circ}\text{C}/\text{mm}$  (second phase testing at 3rd cycle)

### Thermistor data (Freeze Thaw Cycle 4)

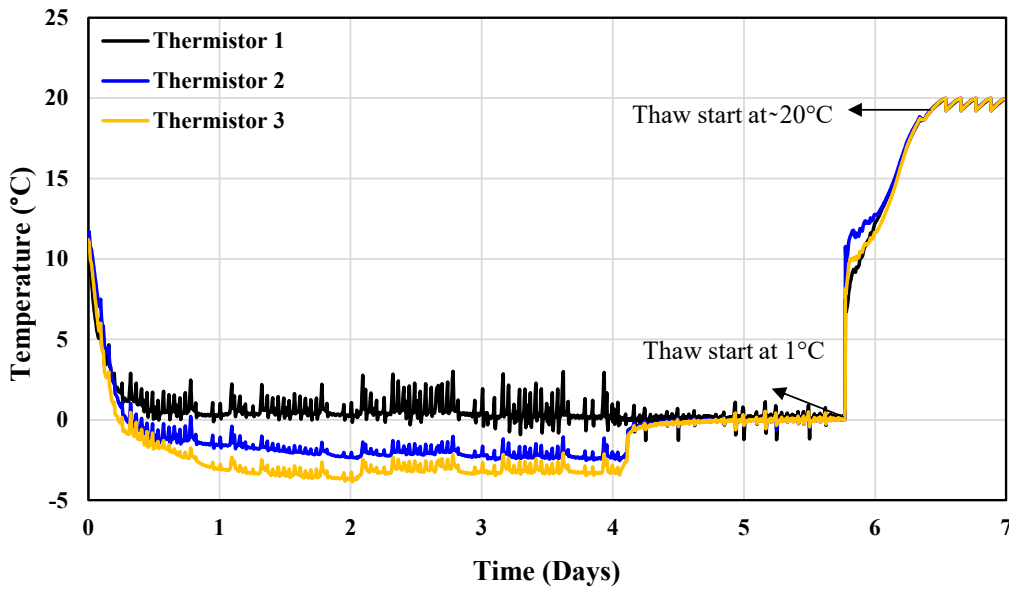


Figure C-41: Temperature plot for ILTT at a temperature gradient of  $0.028^{\circ}\text{C}/\text{mm}$  (second phase testing at 4th cycle)

### Thermistor data (Freeze Cycle 5)

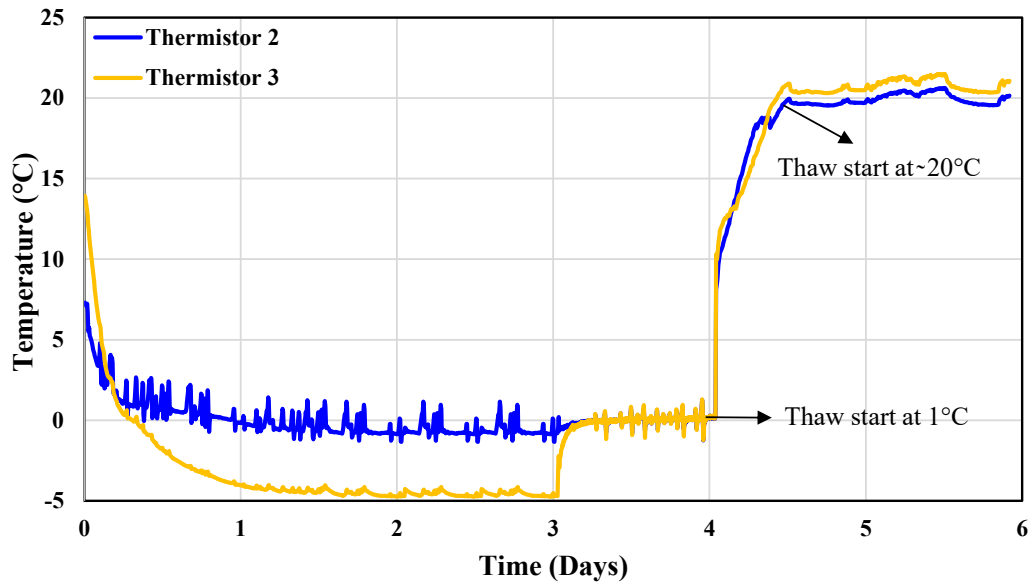


Figure C-42: Temperature plot for ILTT at a temperature gradient of  $0.028^{\circ}\text{C}/\text{mm}$  (second phase testing at 5th cycle)

## Appendix D: Thaw-Strain Diagram

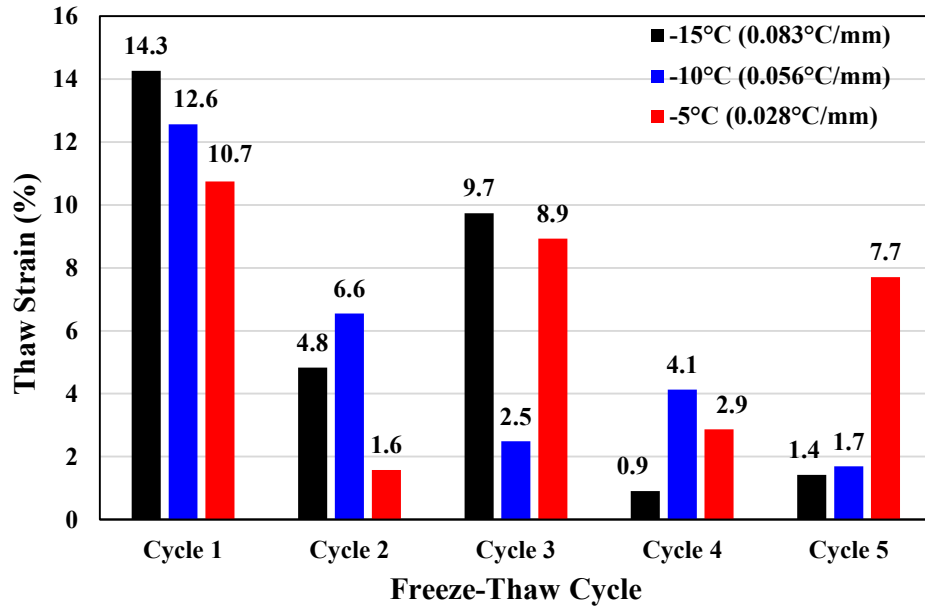


Figure D-1: Thaw strain diagram for the centrifuged tailings samples (first phase testing)

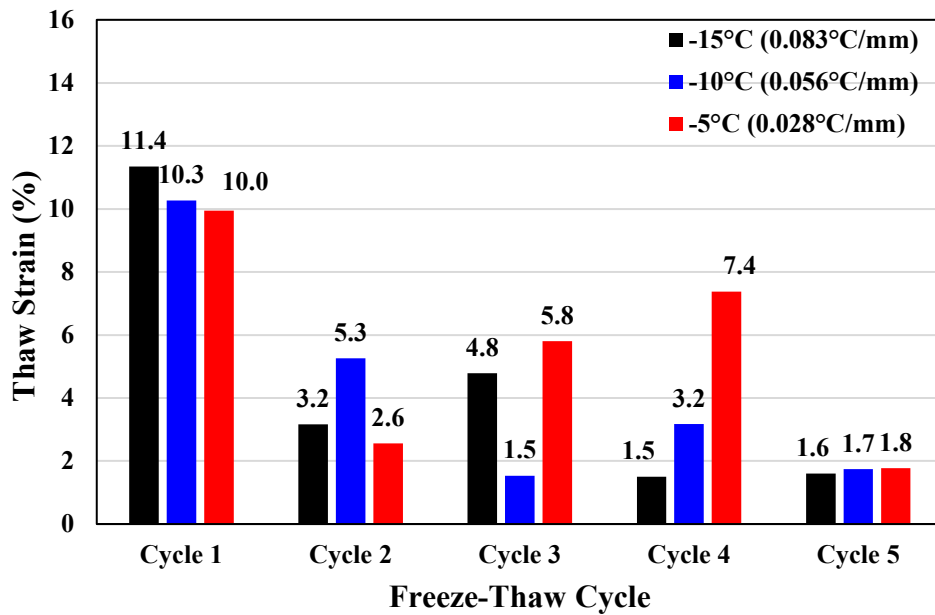


Figure D-2: Thaw strain diagram for the centrifuged tailings samples (second phase testing)

## Appendix E: AE/PE Plot

Figures E-1 to E-8 show the drying curve (Actual evaporation, as a fraction of potential evaporation) for the centrifuged tailings and ILTT samples subjected to first and second phase testing under three different temperature gradients.

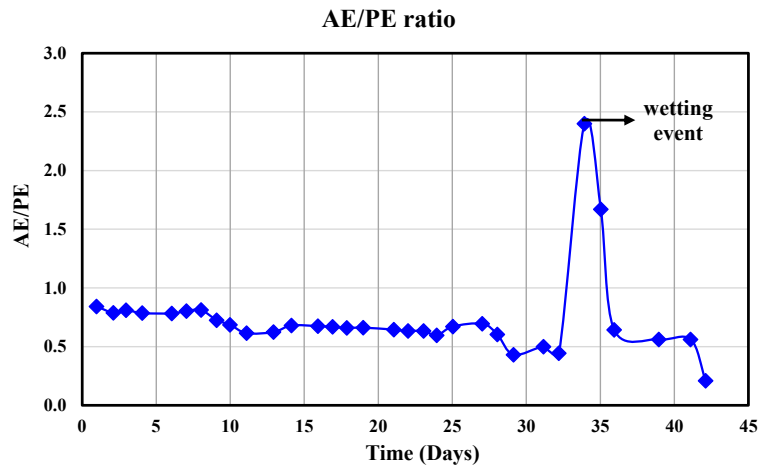


Figure E-1: First phase testing results: normalized evaporation rate (AE/PE) over time for centrifuged tailings under a temperature gradient of  $0.028^{\circ}\text{C}/\text{mm}$

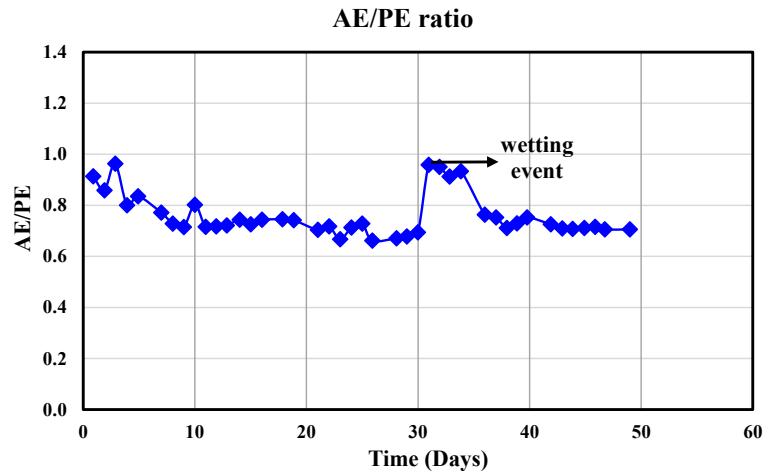


Figure E-2: First phase testing results: normalized evaporation rate (AE/PE) over time for centrifuged tailings under a temperature gradient of  $0.056^{\circ}\text{C}/\text{mm}$

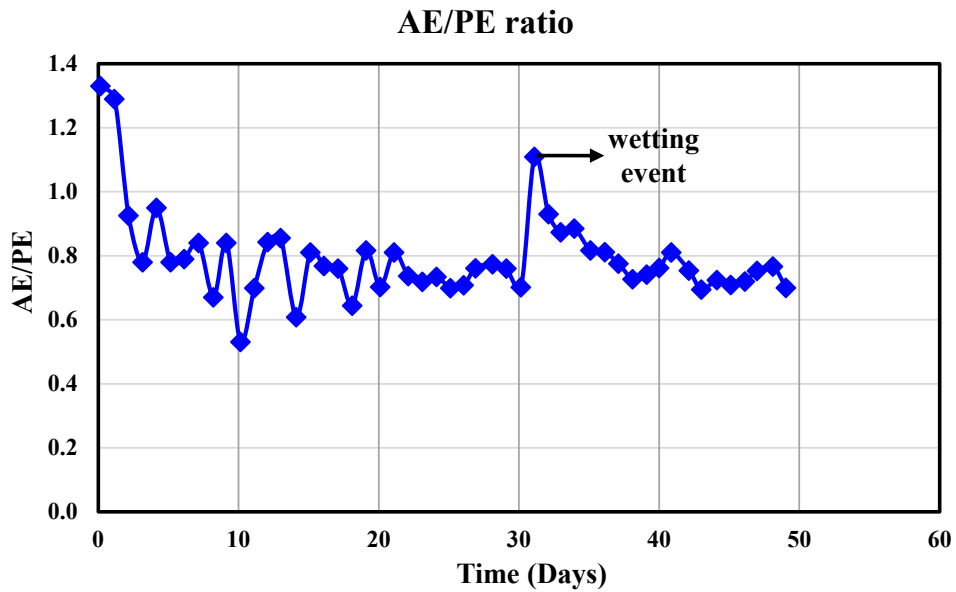


Figure E-3: First phase testing results: normalized evaporation rate (AE/PE) over time for centrifuged tailings under a temperature gradient of 0.083°C/mm

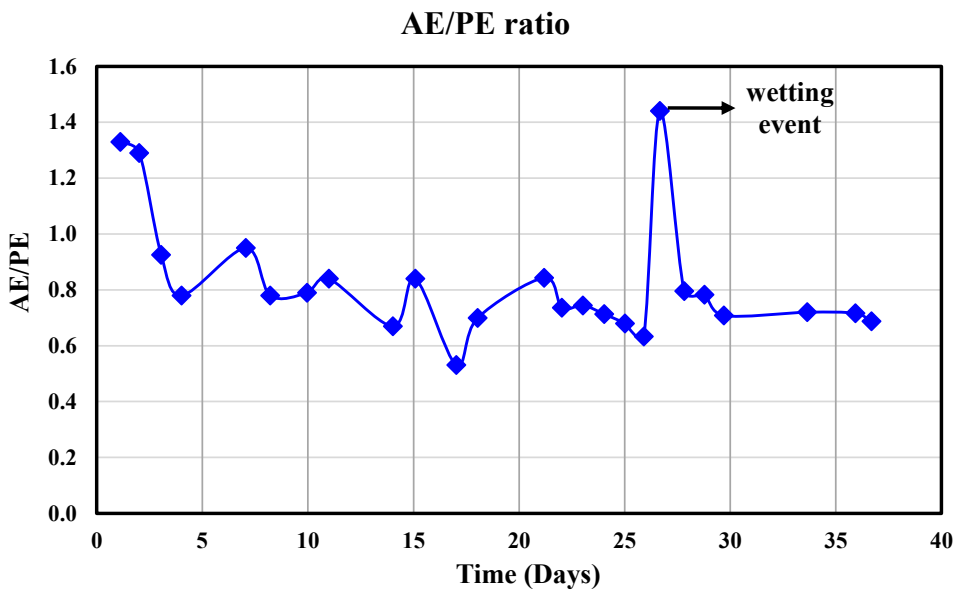


Figure E-4: First phase testing results: normalized evaporation rate (AE/PE) over time for ILTT under a temperature gradient of 0.028°C/mm

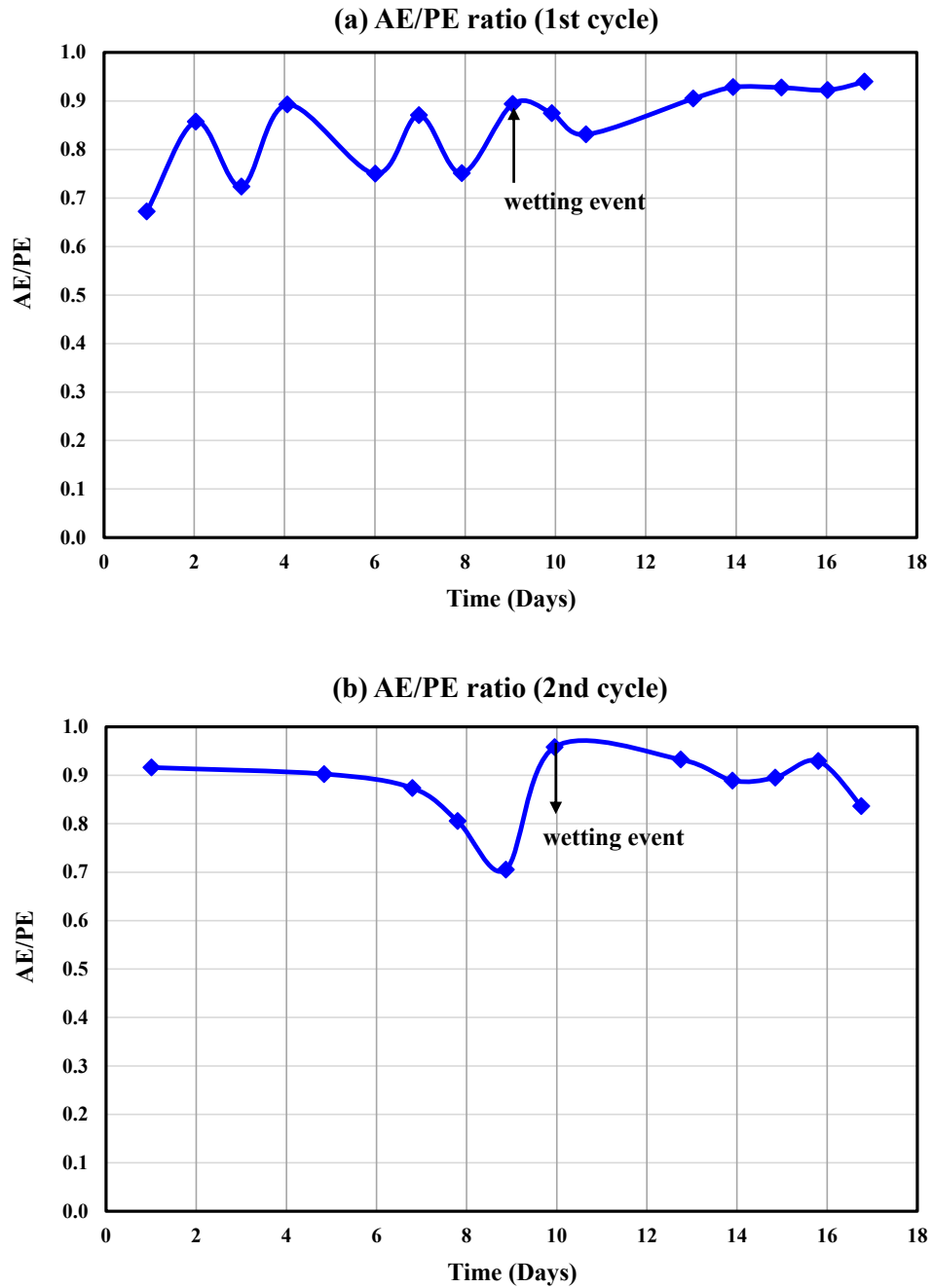


Figure E-5: Second phase testing: normalized evaporation ratio (AE/PE) for the centrifuged tailings under a temperature gradient of 0.028°C/mm at (a) 1st cycle and (b) 2nd cycle

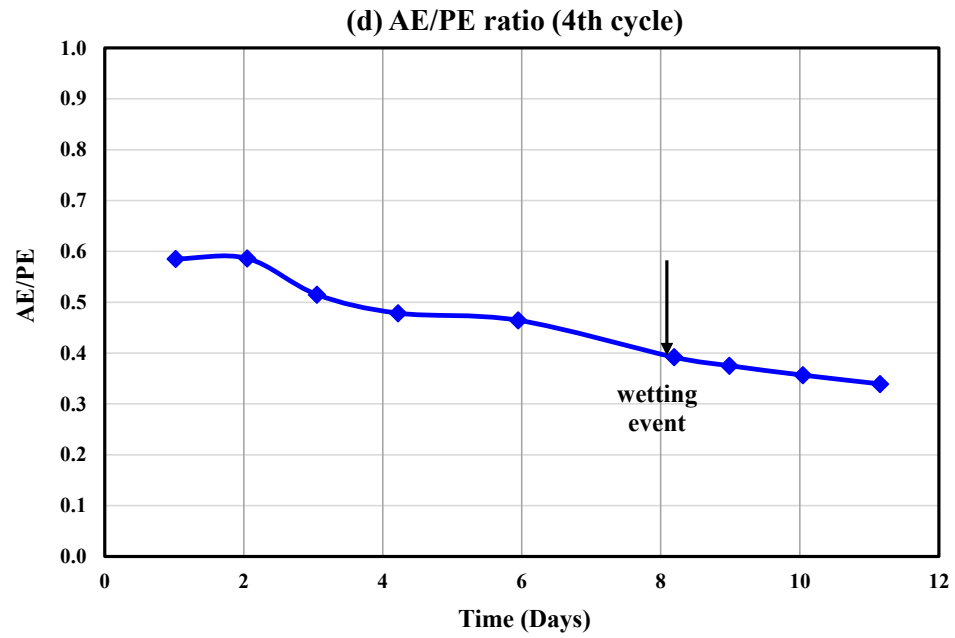
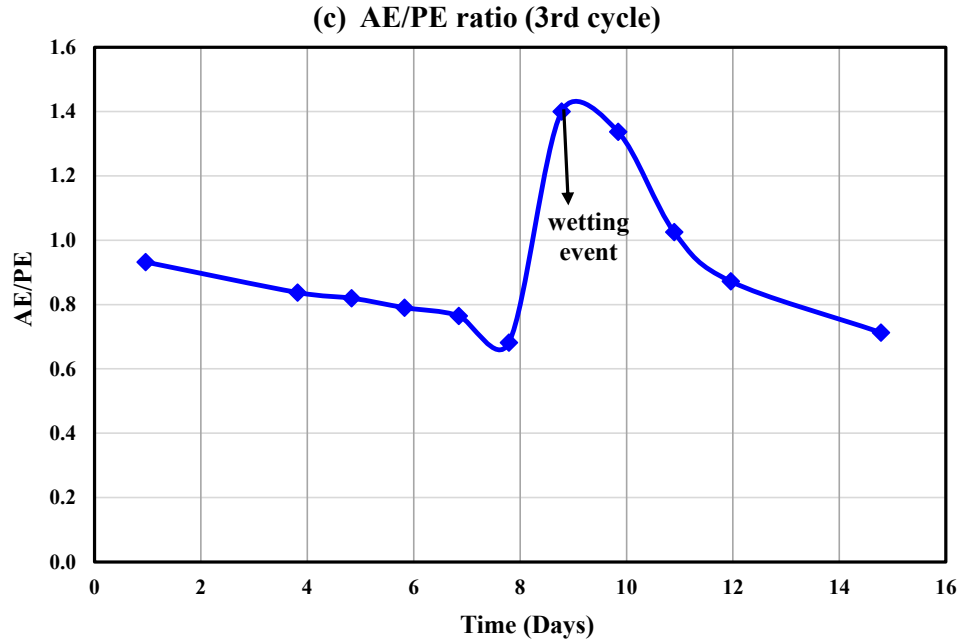


Figure E-5: Second phase testing: normalized evaporation ratio (AE/PE) for the centrifuged tailings under a temperature gradient of  $0.028^{\circ}\text{C}/\text{mm}$  at (c) 3rd cycle and (d) 4th cycle

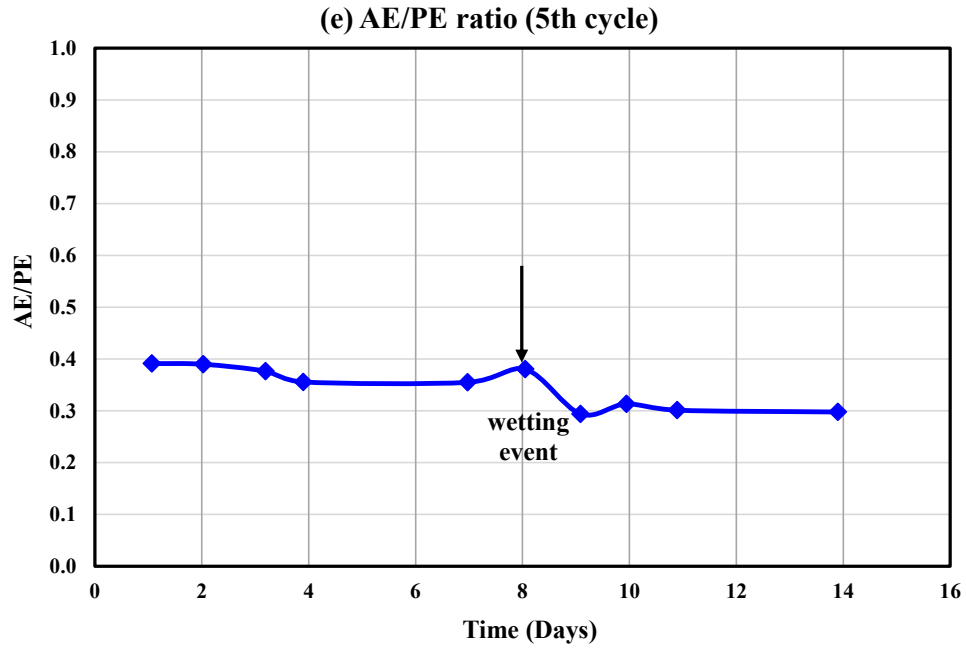


Figure E-5: Second phase testing: normalized evaporation ratio (AE/PE) for the centrifuged tailings under a temperature gradient of  $0.028^{\circ}\text{C}/\text{mm}$  at (e) 5th cycle

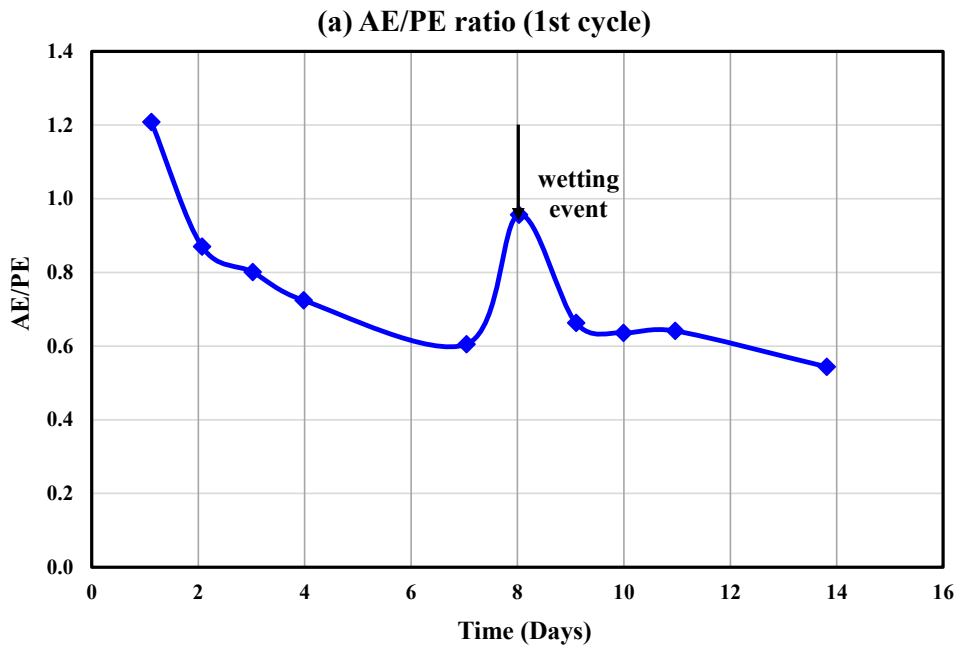


Figure E-6: Second phase testing: normalized evaporation ratio (AE/PE) for the centrifuged tailings under a temperature gradient of  $0.056^{\circ}\text{C}/\text{mm}$  at (a) 1st cycle

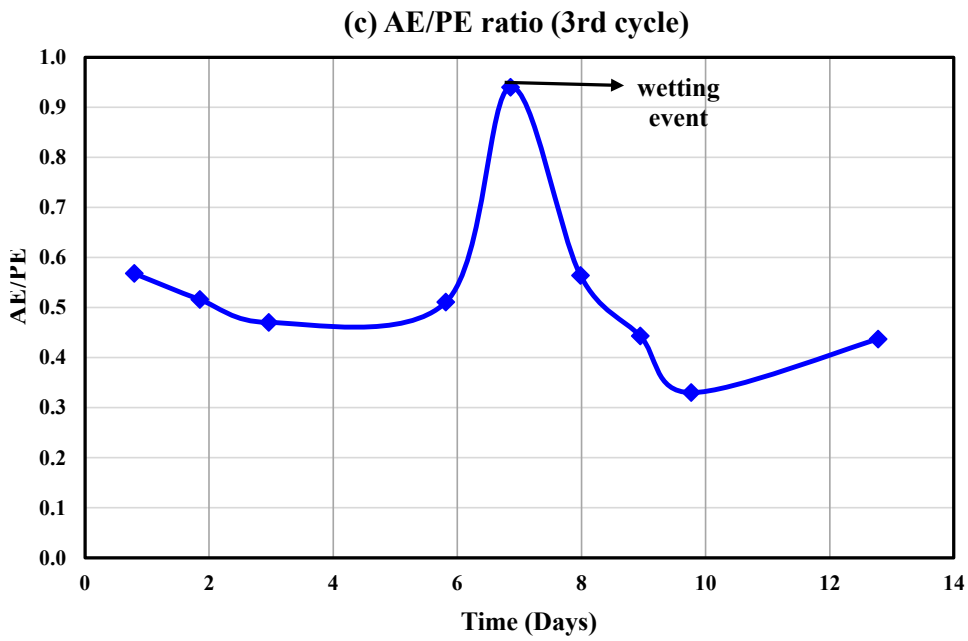
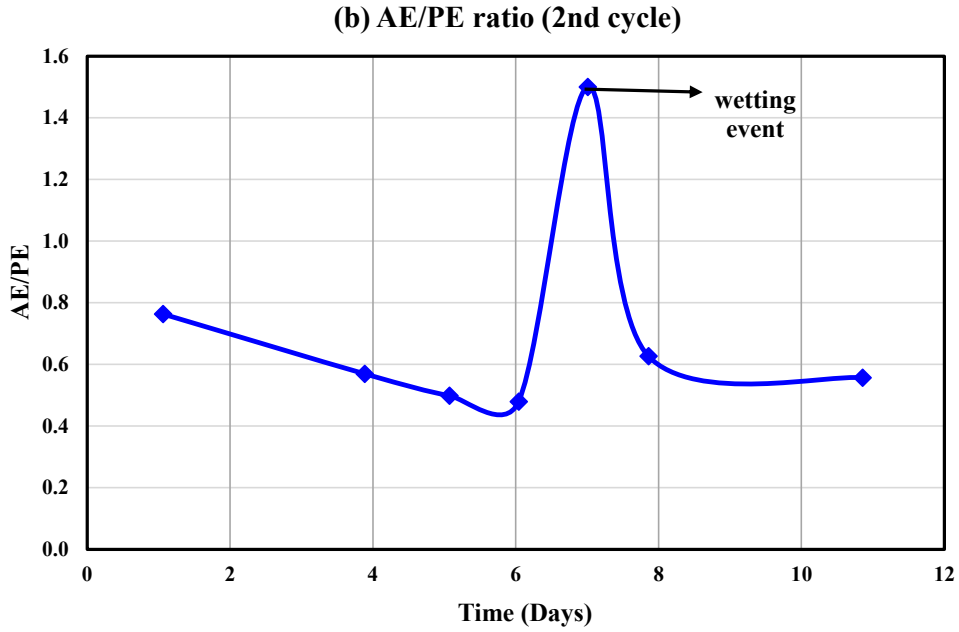
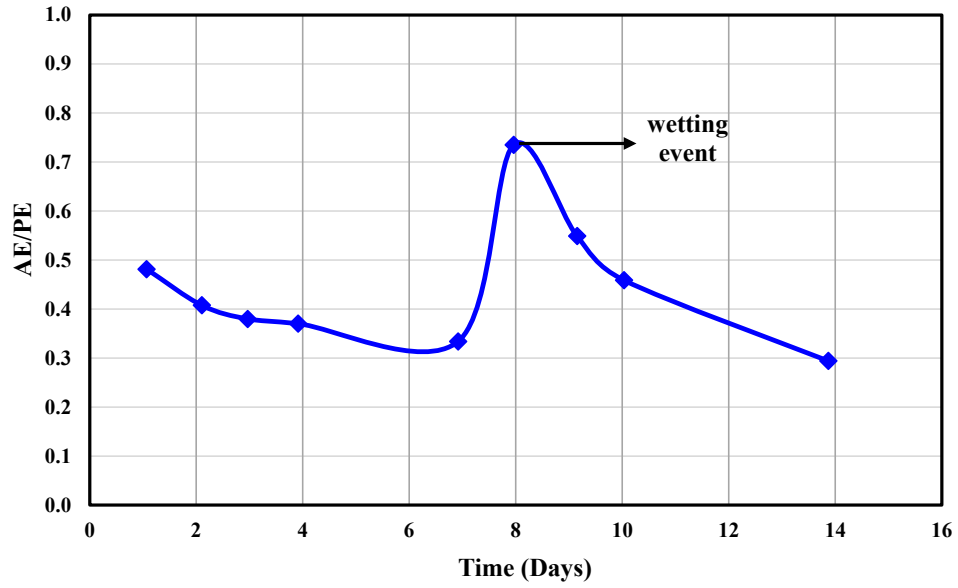


Figure E-6: Second phase testing: normalized evaporation ratio (AE/PE) for the centrifuged tailings under a temperature gradient of  $0.056^{\circ}\text{C}/\text{mm}$  at (b) 2nd cycle and (c) 3rd cycle

(d) AE/PE ratio (4th cycle)



(e) AE/PE ratio (5th cycle)

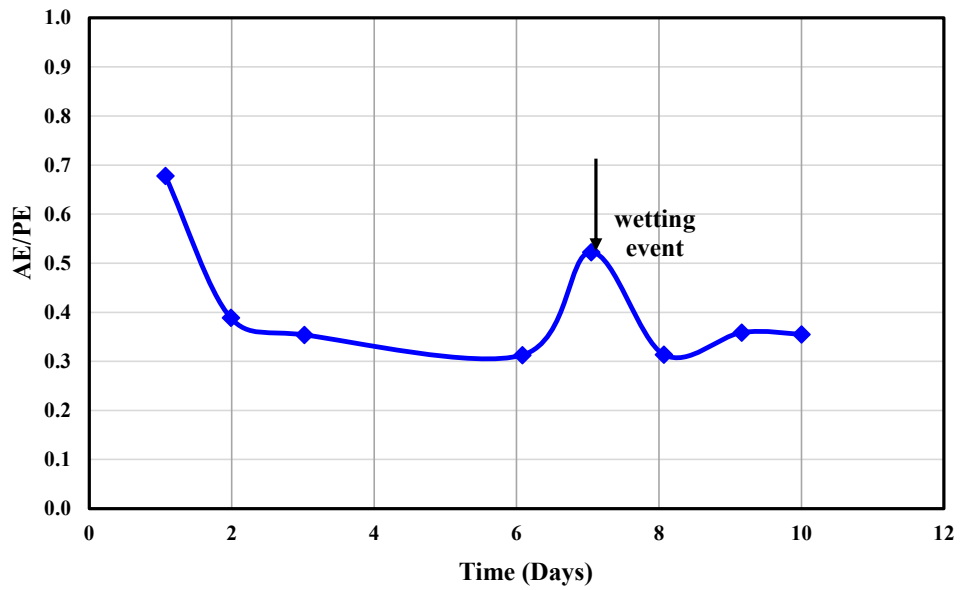


Figure E-6: Second phase testing: normalized evaporation ratio (AE/PE) for the centrifuged tailings under a temperature gradient of  $0.056^{\circ}\text{C}/\text{mm}$  at (c) 4th cycle and (d) 5th cycle

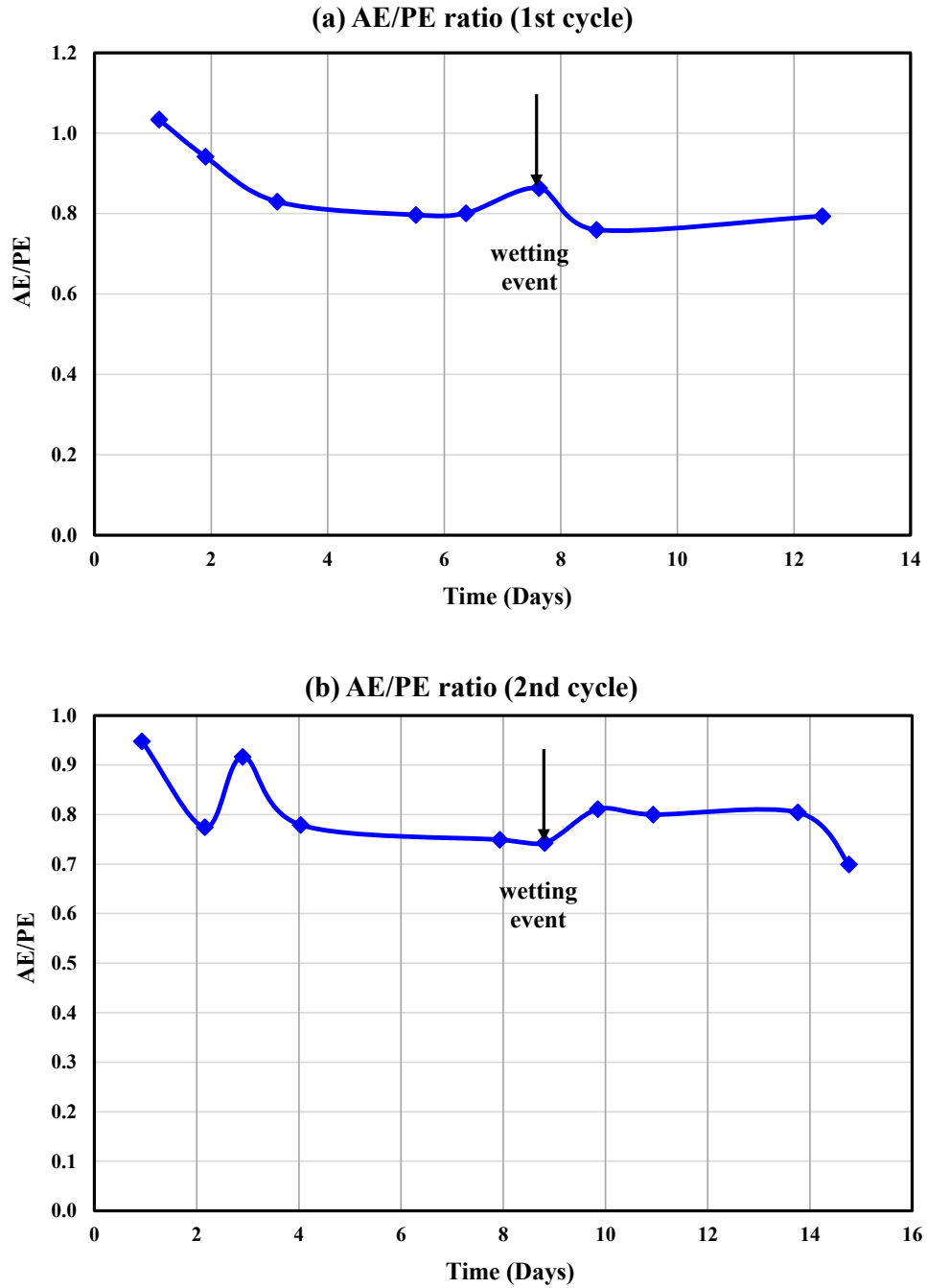


Figure E-7: Second phase testing: normalized evaporation ratio (AE/PE) for the centrifuged tailings under a temperature gradient of 0.083°C/mm at (a) 1st cycle and (b) 2nd cycle

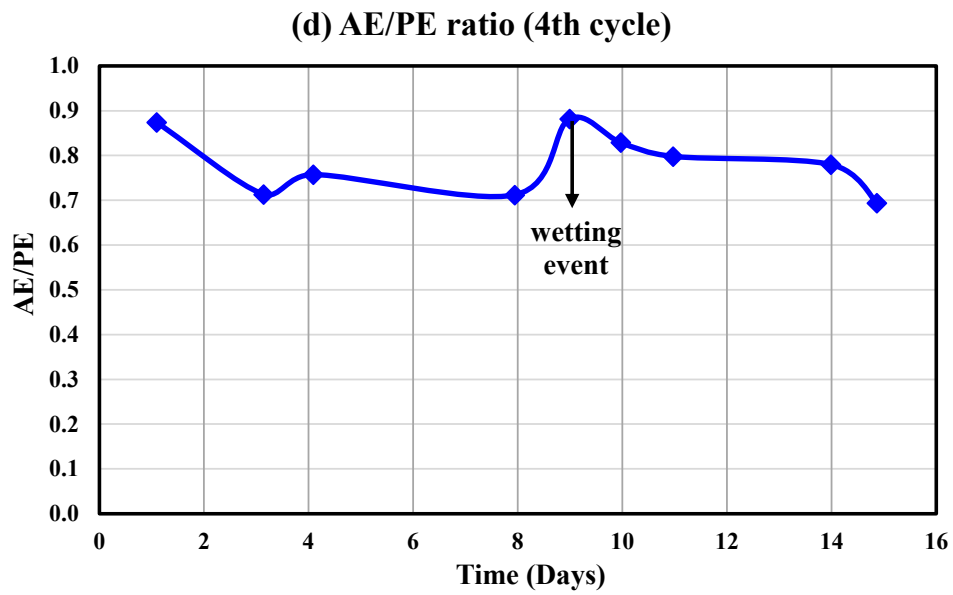
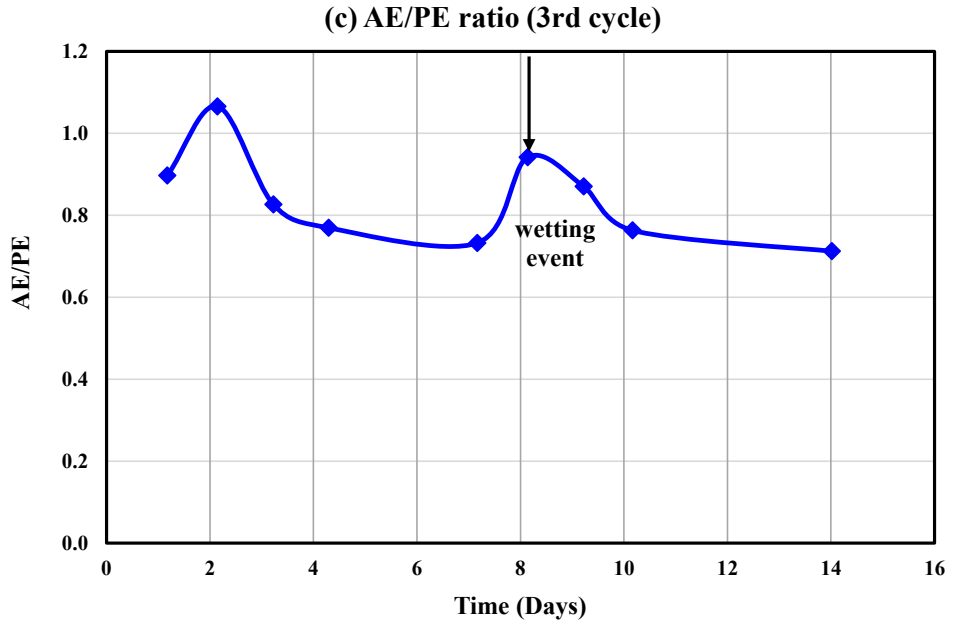
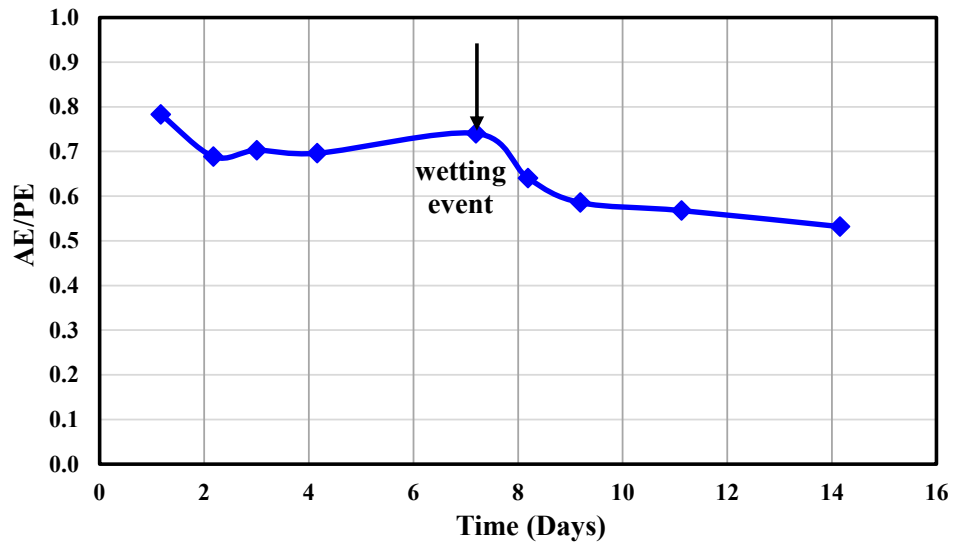


Figure E-7: Second phase testing: normalized evaporation ratio (AE/PE) for the centrifuged tailings under a temperature gradient of  $0.083^{\circ}\text{C}/\text{mm}$  at (c) 3rd cycle and (d) 4th cycle

(e) AE/PE ratio (5th cycle)



(f) AE/PE ratio (6th cycle)

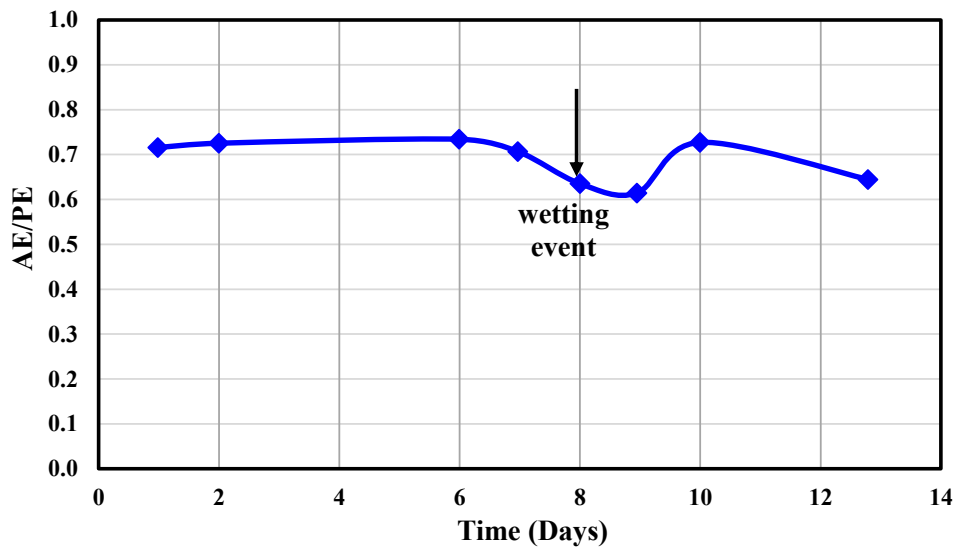


Figure E-7: Second phase testing: normalized evaporation ratio (AE/PE) for the centrifuged tailings under a temperature gradient of  $0.083^{\circ}\text{C}/\text{mm}$  at (e) 5th cycle and (f) 6th cycle

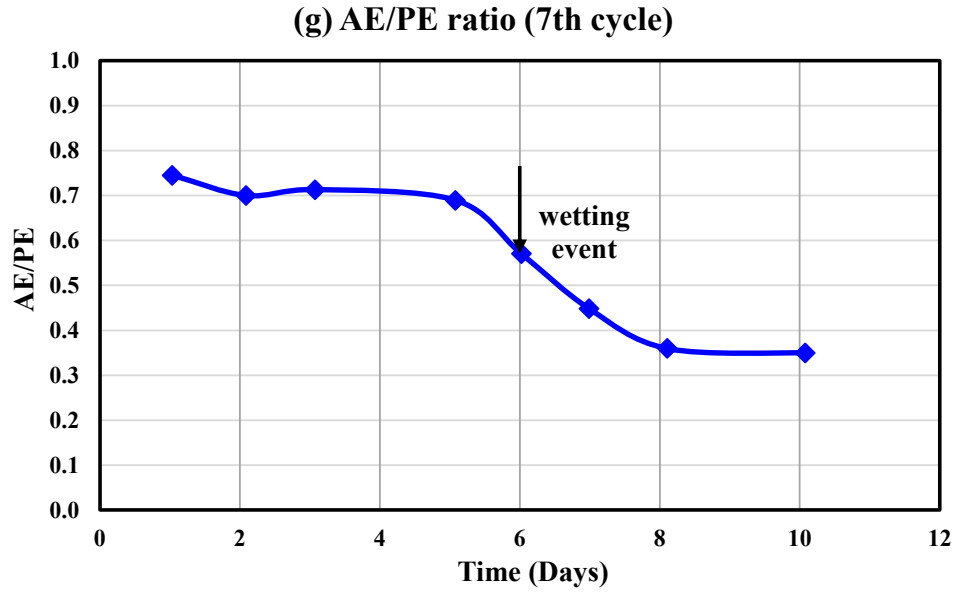


Figure E-7: Second phase testing: normalized evaporation ratio (AE/PE) for the centrifuged tailings under a temperature gradient of  $0.083^{\circ}\text{C}/\text{mm}$  at (g) 7th cycle

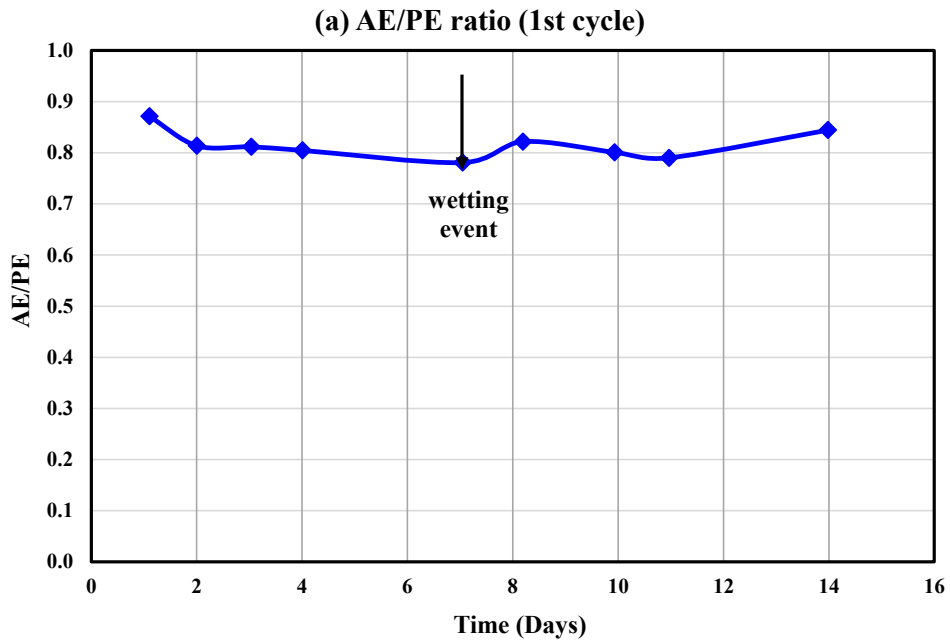


Figure E-8: Second phase testing: normalized evaporation ratio (AE/PE) for the ILTT under a temperature gradient of  $0.028^{\circ}\text{C}/\text{mm}$  at (a) 1st cycle

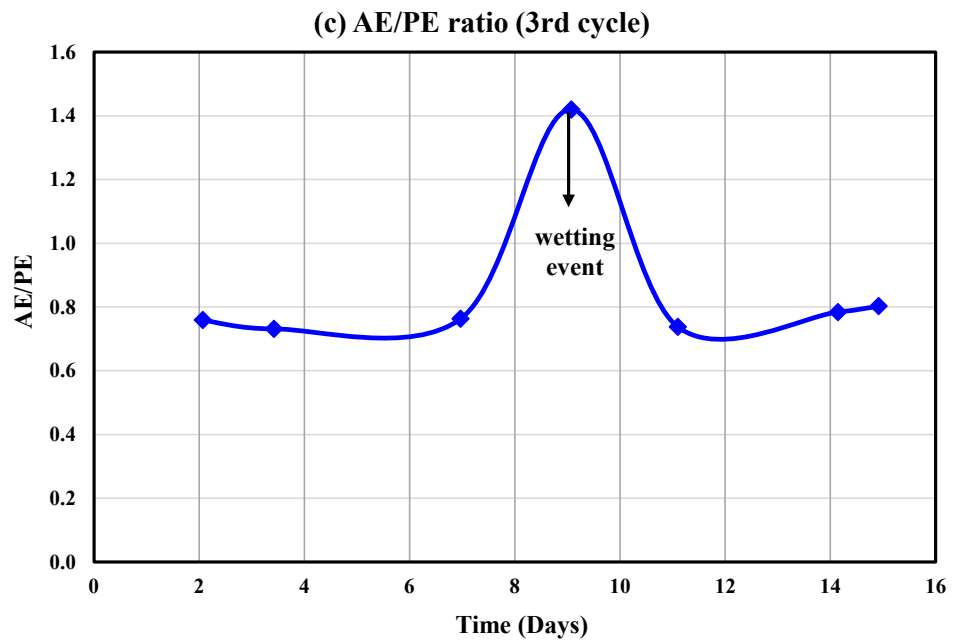
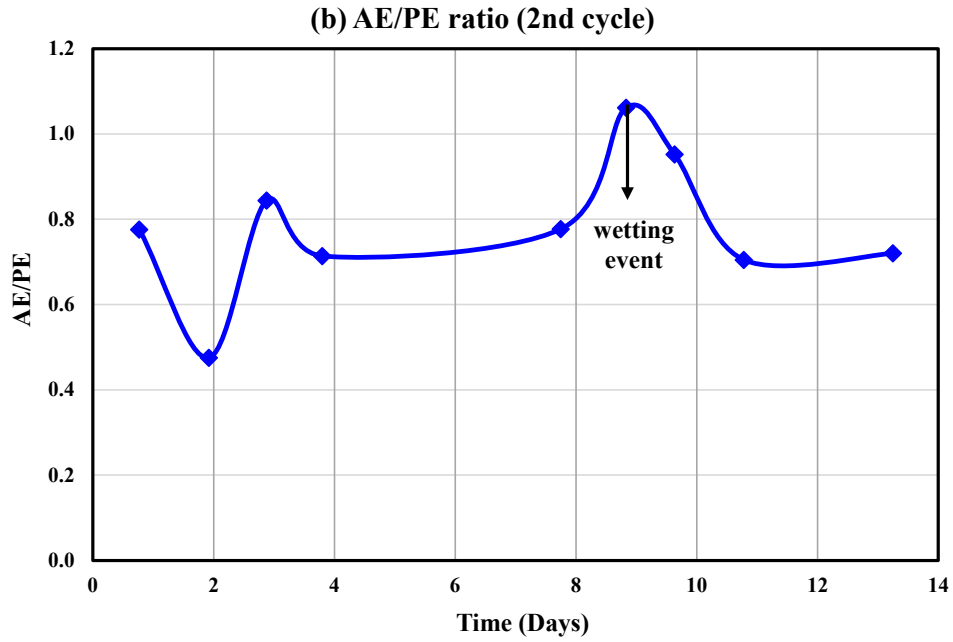


Figure E-8: Second phase testing: normalized evaporation ratio (AE/PE) for the ILTT under a temperature gradient of  $0.028^{\circ}\text{C}/\text{mm}$  at (b) 2nd cycle and (c) 3rd cycle

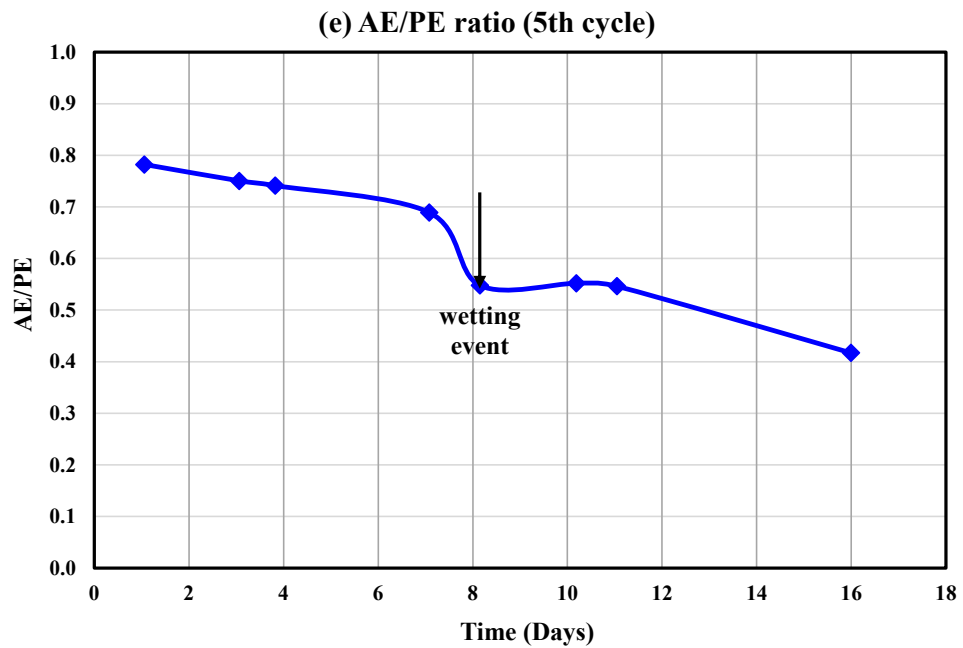
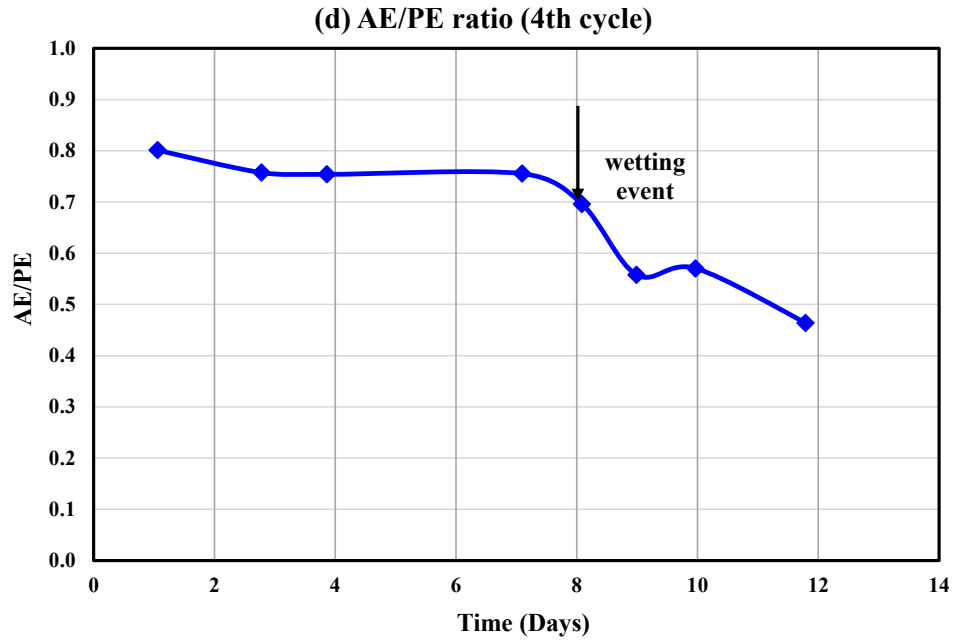


Figure E-8: Second phase testing: normalized evaporation ratio (AE/PE) for the ILTT under a temperature gradient of  $0.028^{\circ}\text{C}/\text{mm}$  at (d) 4th cycle and (e) 5th cycle

## **Appendix F: Precisions of the Laboratory Measurements**

In geotechnical engineering, the most used parameter when discussing the strength behaviour is undrained shear strength. The selection of a representative technique is significant and largely dependent on its application. In field, the undrained shear strength is commonly measured using the field vane shear apparatus. Hence, a desktop manual vane shear apparatus was employed in the laboratory to determine the undrained strength where the key issues were the insertion of the vane to the desired depth with a minimal disturbance of the tailings samples and reproducibility of these measurements. Additionally, errors in measurement can originate from the test procedure, apparatus used and operator. In this case, the disturbance of samples from inserting the vane was minimized by restricting the measurement at the near surface (at a depth of 12.5 mm from the surface) only. Although duplicate samples were not investigated in this study to evaluate the effects of sample disturbance, the duplicate samples tested using the same vane shear apparatus produced similar strength results, as investigated by Amoako (2020) and Stienwand (2021). However, the reported values measured with oil sands tailings samples should not be considered as representative of absolute values, but rather, relative compared to the other samples.

EC and pH measurements are sensitive and can be affected by improper submersion, salt buildup, calibration missteps and leaving bubbles on a probe. In the laboratory, the pH and EC meter was calibrated with different known standard solutions prior to every use. Prior to calibration, probe was rinsed each time with deionized water to prevent contamination. This device has an accuracy of  $\pm 0.1$  in terms of pH and  $\pm 2\%$  in terms of conductivity.

## Appendix G: Numerical Simulation Plots

Figures G-1 to G-13 show the simulation plots of centrifuged tailings samples from the FSConsol and UNSATCON models for first phase testing results. The solids content profiles were shown here as FSConsol does not provide water content profile as an output. Hence, solids content profiles were plotted here to maintain a consistency among the plots extracted from both models. Figures G-14 to G-15 show the simulation plots for the second phase testing results representing each seasonal cycle. Solids content profiles at the end of each cycle (after one freeze-thaw and drying cycle) were presented here.

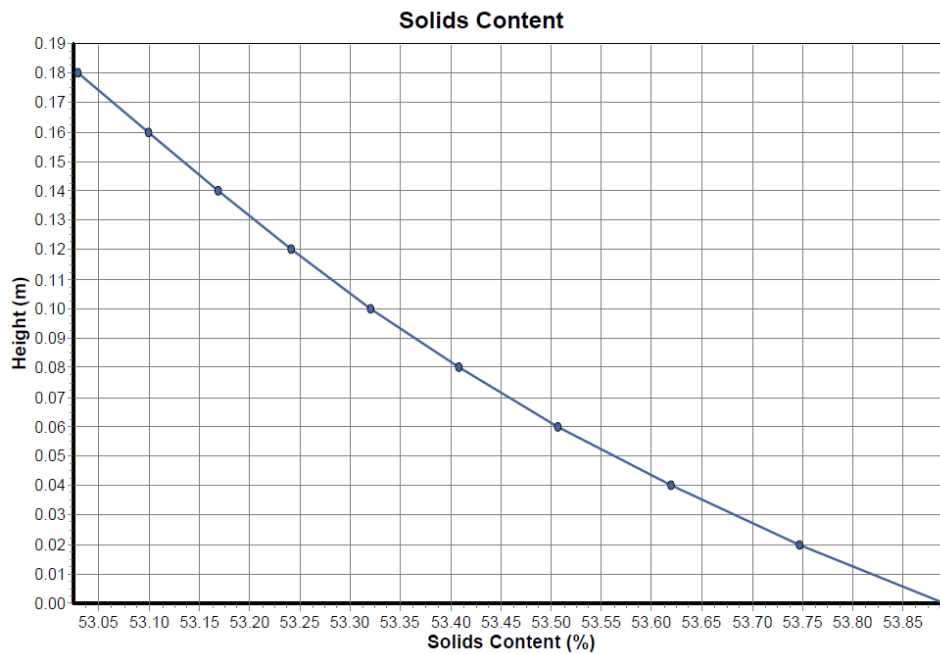


Figure G-1: Solids content results obtained from FSConsol for untreated centrifuged tailings

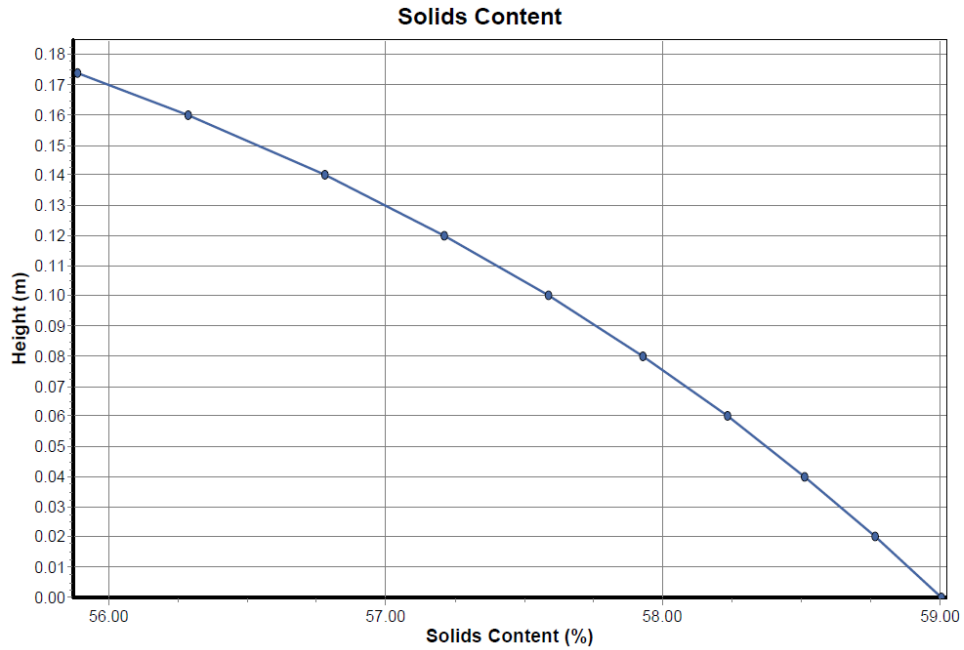


Figure G-2: Solids content results obtained from FSConsol for centrifuged tailings at a temperature gradient of 0.028°C/mm (1st phase testing at 1st freeze-thaw cycle)

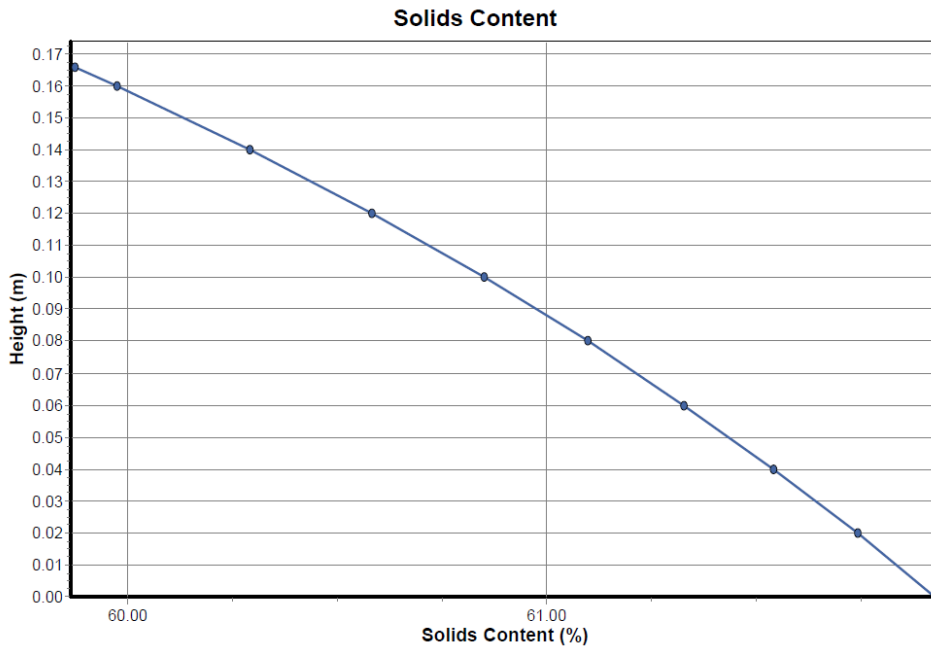


Figure G-3: Solids content results obtained from FSConsol for centrifuged tailings at a temperature gradient of 0.028°C/mm (1st phase testing at 2nd freeze-thaw cycle)

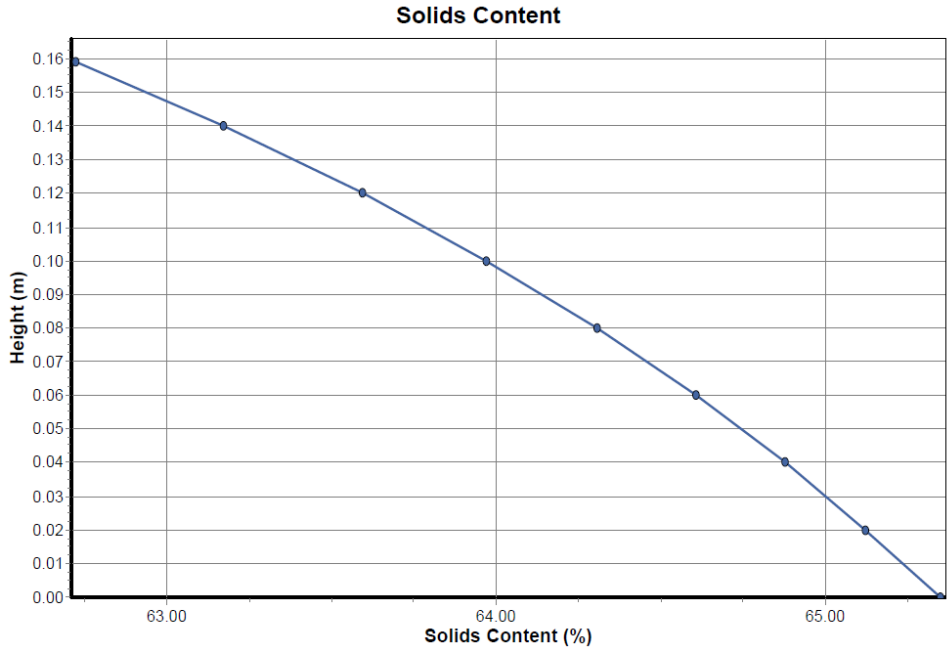


Figure G-4: Solids content results obtained from FSConsol for centrifuged tailings at a temperature gradient of 0.028°C/mm (1st phase testing at 3rd freeze-thaw cycle)

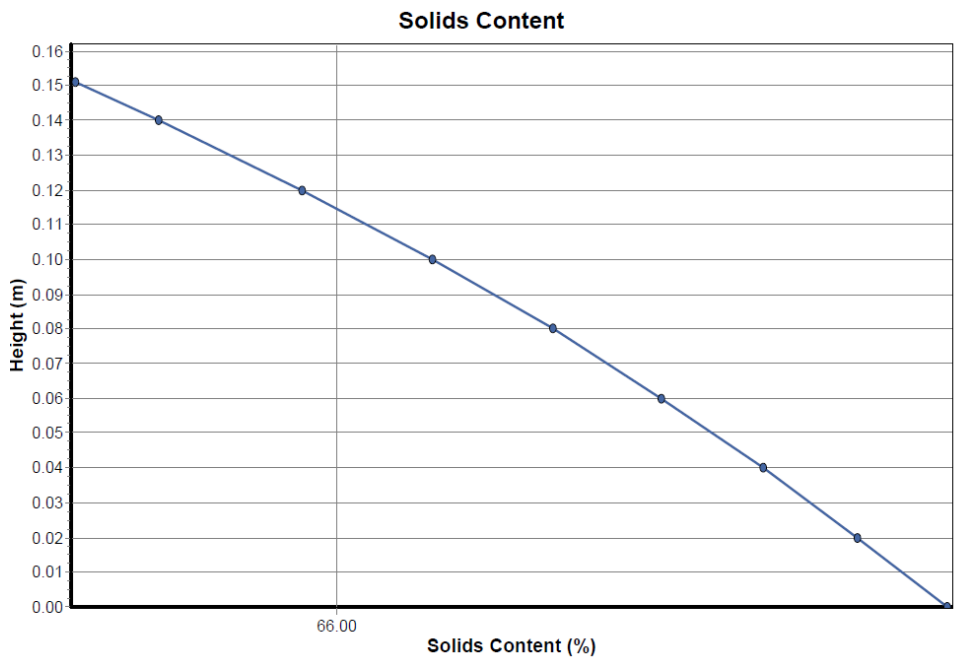


Figure G-5: Solids content results obtained from FSConsol for centrifuged tailings at a temperature gradient of 0.028°C/mm (1st phase testing at 4th freeze-thaw cycle)

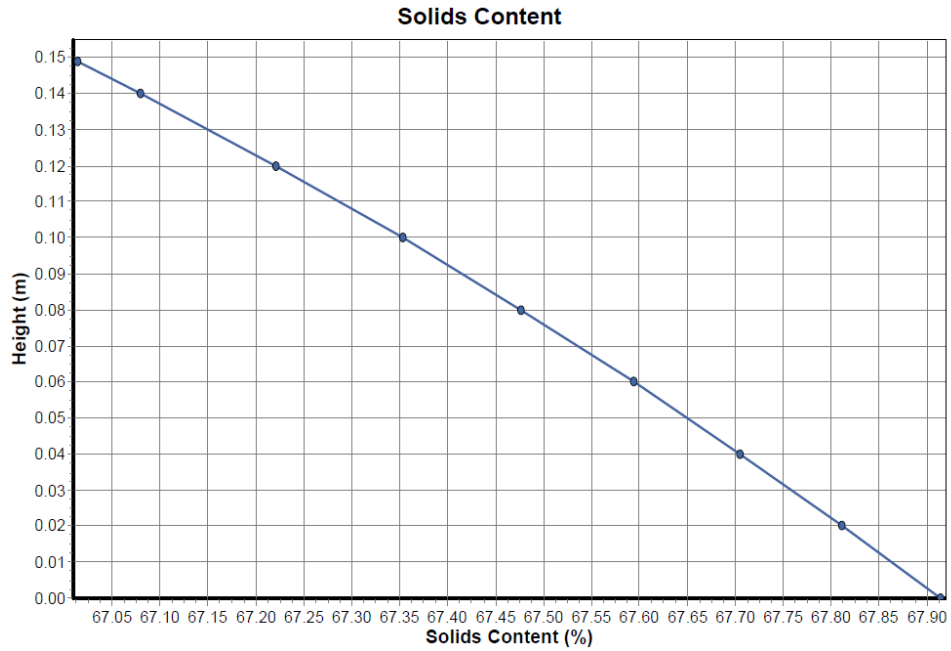


Figure G-6: Solids content results obtained from FSConsol for centrifuged tailings at a temperature gradient of 0.028°C/mm (1st phase testing at 5th freeze-thaw cycle)

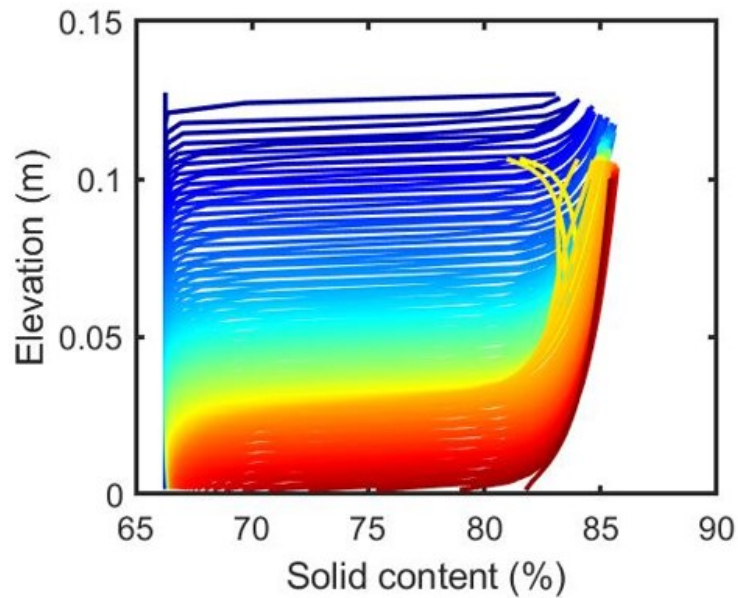


Figure G-7: Solids content results obtained from UNSATCON for centrifuged tailings at a temperature gradient of 0.028°C/mm (1st phase testing after 1st drying-wetting cycle)

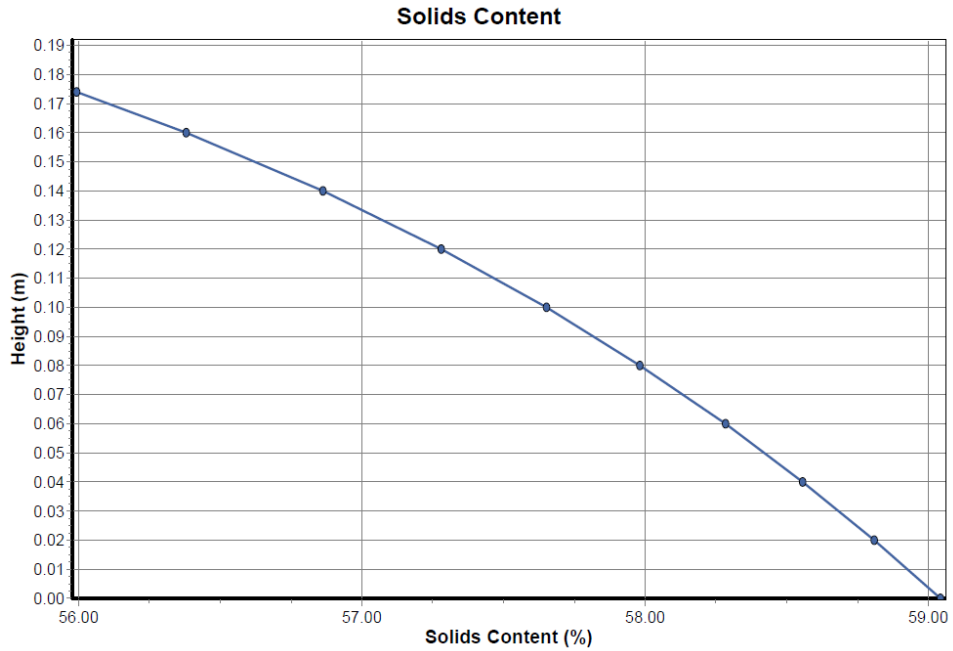


Figure G-8: Solids content results obtained from FSConsol for centrifuged tailings at a temperature gradient of 0.083°C/mm (1st phase testing at 1st freeze-thaw cycle)

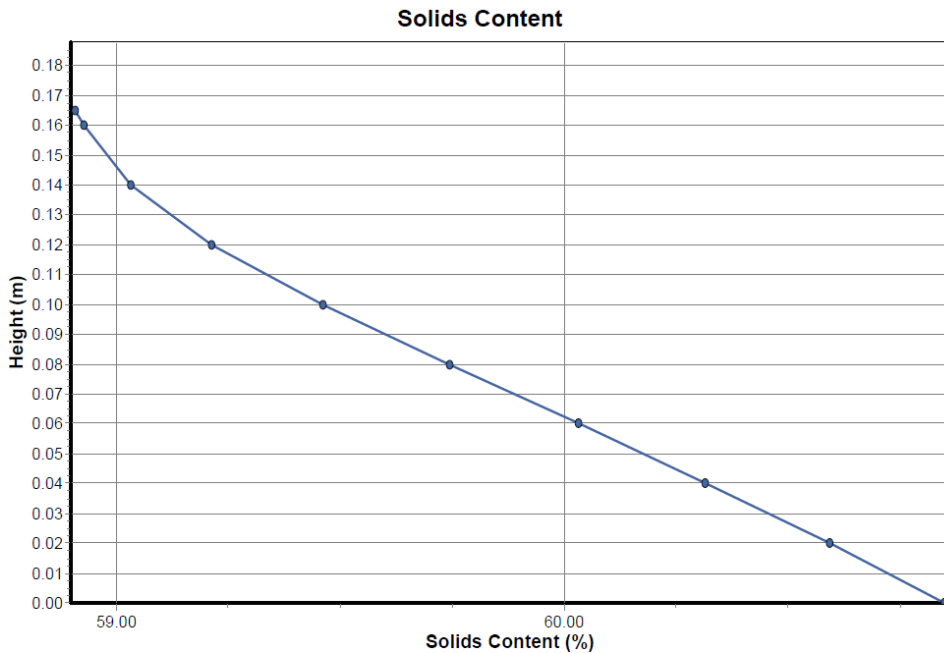


Figure G-9: Solids content results obtained from FSConsol for centrifuged tailings at a temperature gradient of 0.083°C/mm (1st phase testing at 2nd freeze-thaw cycle)

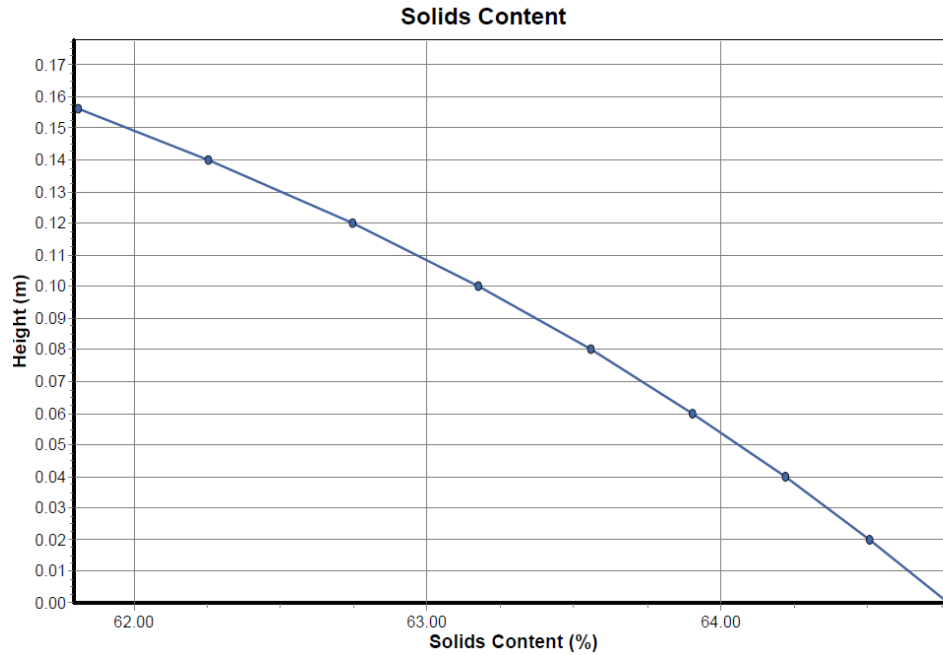


Figure G-10: Solids content results obtained from FSConsol for centrifuged tailings at a temperature gradient of 0.083°C/mm (1st phase testing at 3rd freeze-thaw cycle)

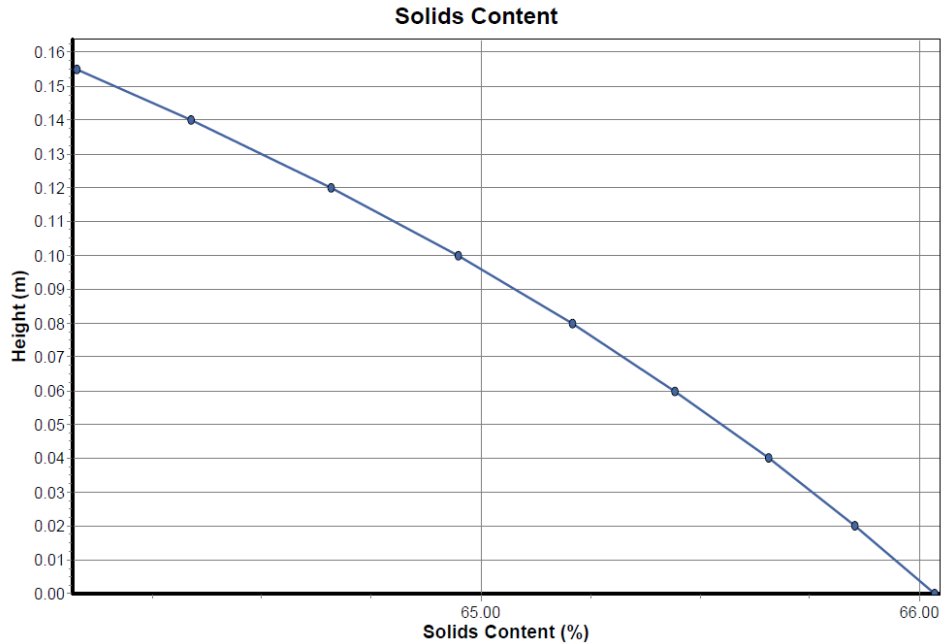


Figure G-11: Solids content results obtained from FSConsol for centrifuged tailings at a temperature gradient of 0.083°C/mm (1st phase testing at 4th freeze-thaw cycle)

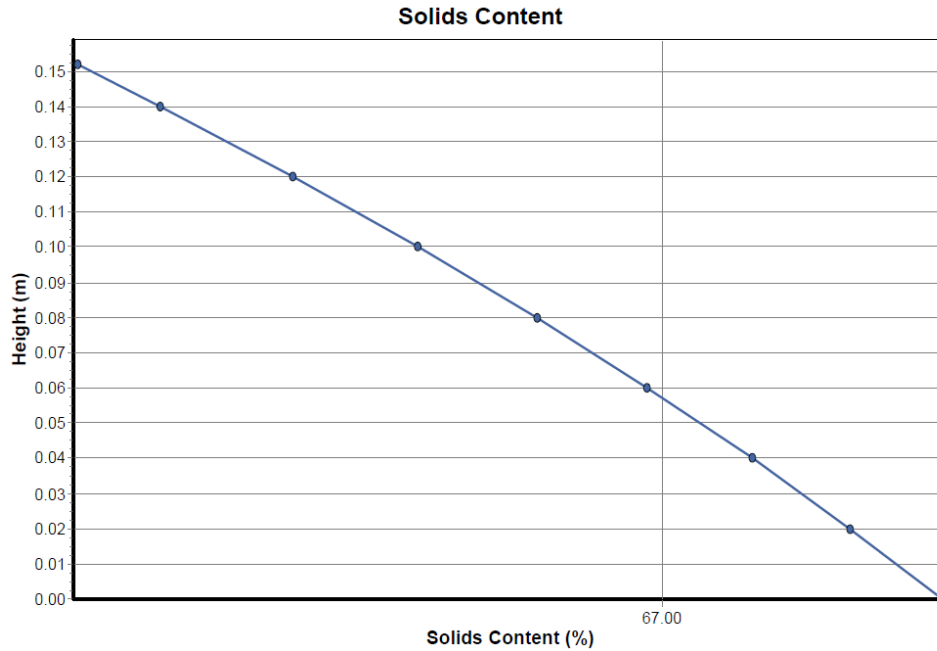


Figure G-12: Solids content results obtained from FSConsol for centrifuged tailings at a temperature gradient of 0.083°C/mm (1st phase testing at 5th freeze-thaw cycle)

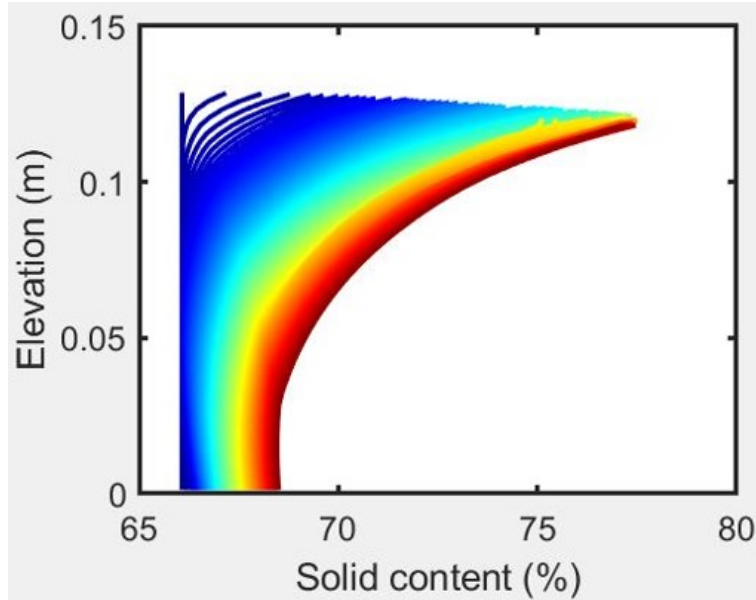


Figure G-13: Solids content results obtained from UNSATCON for centrifuged tailings at a temperature gradient of 0.083°C/mm (1st phase testing after 1st drying-wetting cycle)

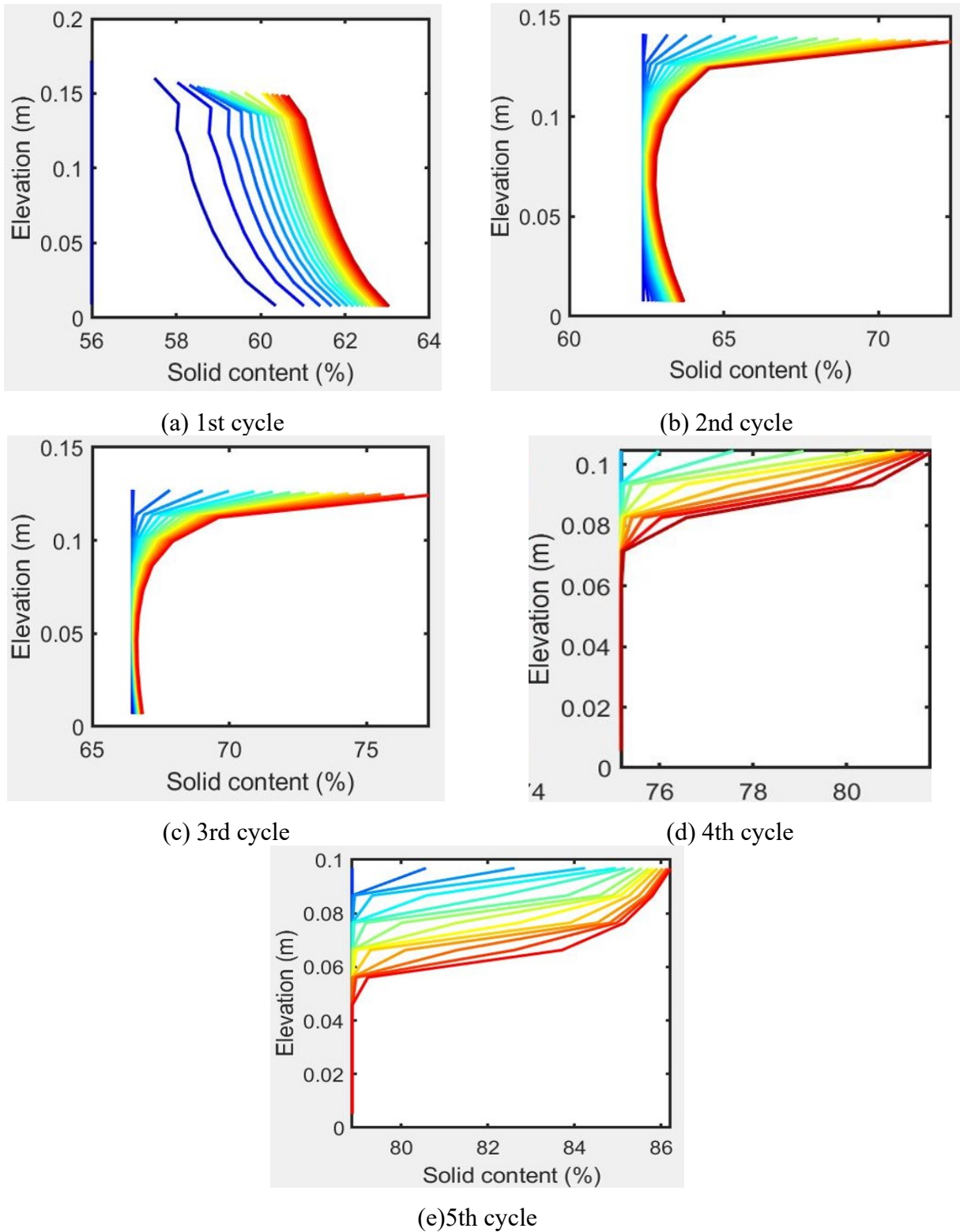
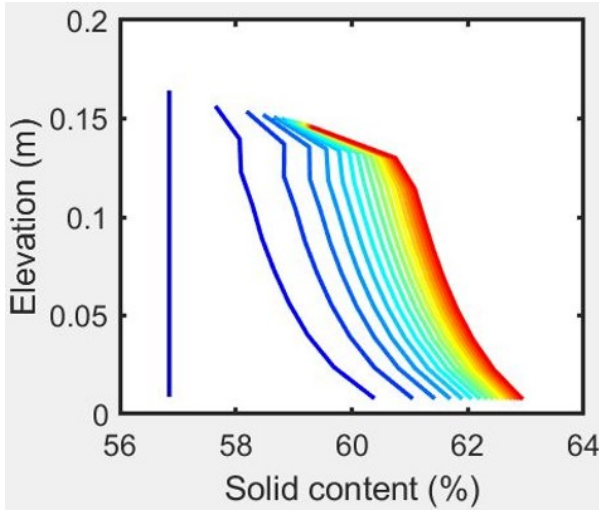
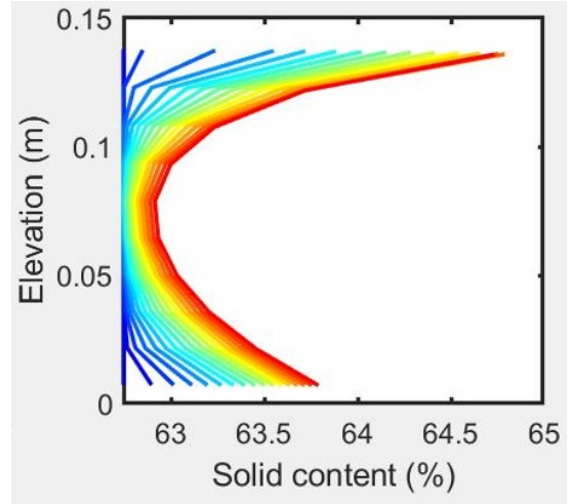


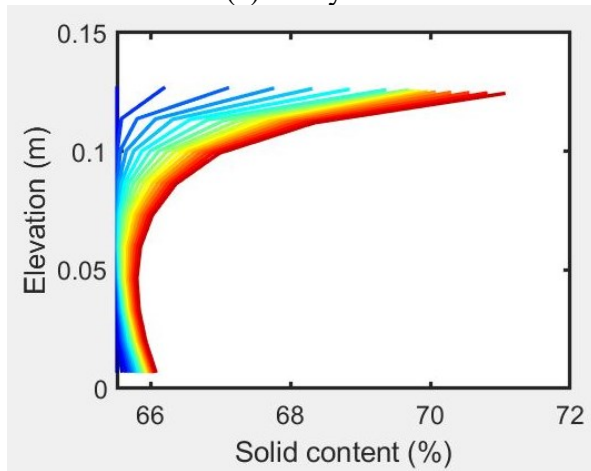
Figure G-14: Second phase testing results: centrifuged tailings at a temperature gradient of  $0.028^{\circ}\text{C}/\text{mm}$  after each seasonal cycle



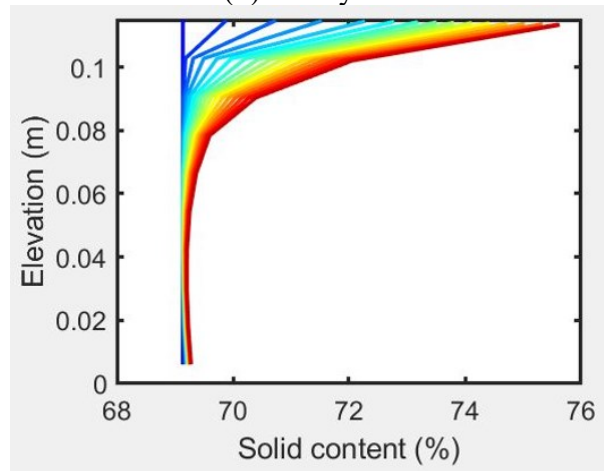
(a) 1st cycle



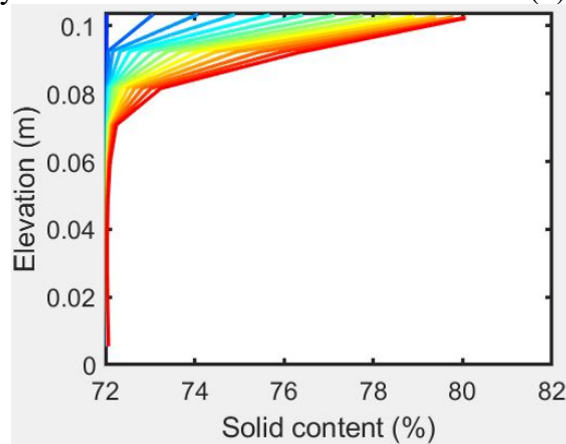
(b) 2nd cycle



(c) 3rd cycle



(d) 4th cycle



(e) 5th cycle

Figure G-15: Second phase testing results: centrifuged tailings at a temperature gradient of  $0.083^{\circ}\text{C}/\text{mm}$  after each seasonal cycle